Synthesis, Characterization and Modeling of Porous Copolymer Particles

Dongyu Fang

A thesis
presented to the University of Waterloo
in fulfillment of the
thesis requirement for the degree of
Doctor of Philosophy
in
Chemical Engineering

Waterloo, Ontario, Canada, 2007

Author’s Declaration

I hereby declare that I am the sole author of this thesis. This is a true copy of the thesis, including any required final revisions, as accepted by my examiners.

I understand that my thesis may be made electronically available to the public.

Abstract

Hydrogels are polymeric materials that have three-dimensional polymeric networks, which are able to absorb and retain a large amount of water within their structures without being dissolved. Among the synthetic hydrogel, poly(2-hydroxylethyl methacrylate) (poly(HEMA)) has been of great interest because of its excellent biocompatibility with the three-dimensional networks. Therefore, poly(HEMA) hydrogels have been widely used in many areas, especially in biomedical and pharmaceutical areas, for such applications as packing materials in chromatography, sorbents in controlled release and drug delivery, implanting materials in tissue engineering. However, the applications of poly(HEMA) are still limited because of its weak mechanical strength and network properties. Therefore, in recent decades, the challenge of how to modify and control the polymer properties and how to build highly porous structures in it has received considerable attention because these modifications could significantly improve the performance of poly(HEMA) hydrogels for more favorable applications. Although HEMA and its polymers have been studied for more than 40 years, few reports about the preparation of micro-/nano-porous poly(HEMA) hydrogel particles and the requirements of their applications have risen. Furthermore, how to control the porous structures and the properties of HEMA copolymers have not been well understood. Accordingly, the objectives of this research were to investigate the synthesis of the porous copolymeric particles of HEMA with various comonomers (MMA, St and NVP), to characterize the porous structures and particle morphology, to simulate the synthesis process and porous characteristics, to explore the effects of the polymer compositions and the porous structures on the swelling properties, and to apply the resultant polymeric particles in the controlled release of the hydrophilic model drug.

In the present studies, HEMA was copolymerized with three different comonomers, methyl methacrylate (MMA), styrene (St) and N-vinyl-2-pyrrolidone (NVP), respectively, to prepare highly porous particles crosslinked using ethylene glycol dimethacrylate (EGDMA) in the presence of 1-octanol used as a porogen by means of suspension copolymerization in an aqueous phase initiated by 2,2-azobisisobutyronitrile (AIBN). Nano-pores were observed in the present studies. The pore size and the swelling properties of these particles can be successfully controlled by changing comonomers or adjusting the crosslinker and porogen concentration. The results indicate that lower crosslinker or porogen concentration favors generating smaller pores, whereas a higher concentration of a hydrophilic comonomer, higher crosslinker concentration and higher porogen volume ratio promote

the generation of larger pores. In addition, the effects of the porous structures and the network properties on the swelling properties were explored. The swelling capacity of the porous particles is reduced with an increase in the EGDMA molar concentration. However, higher porosity in the particles and higher amount of hydrophilic comonomer result in a higher swelling capacity of the particles.

The gel formation and the porous characteristics of HEMA/comonomer/EGDMA systems were simulated using the mathematical models combining the reaction kinetics and the thermodynamics. It was found that the model over-predicted the experimental results of the porosity because the pores and the networks are shrunk or collapsed during the porogen removal. Therefore, the model predicts the maximum porosity that the polymeric particles can reach. If the hydrophobic contents are higher, the model gives better prediction of the porosity.

It is concluded that the microporous structures of HEMA related hydrogels could be controlled by a properly designed process based on the knowledge gained via this research. The output of this research helps with a better understanding for industrial production of micro-porous hydrogels and their applications.

Acknowledgements

I gratefully thank my supervisors, Dr. Garry L. Rempel and Dr. Qinmin Pan, for their support and guidance.

My thanks also go to my friends and labmates Changlin Gan, Dr. Guangwei He, Dr. Xingwang Lin, Jianmin Liu, Chandra Mouli, Dr. Xiaohong Peng, Dr. Zhenli Wei, Dr. Jialong Wu, Hong Yang, and Dr. Lifeng Zhang for their help and support.

Among contributors to this work are Dr. Neil T. McManus, Dr. Jialong Wu and Dr. Guangwei He for many helpful discussions, Dr. Girija for the mercury intrusion porosimetry operation, and Dr. Nina for the SEM operation.

Finally, my greatest thanks go to my family: my wife Mei Wang, my parents and my brother for their love.

Table of Contents

List of Figures

List of Tables

Nomenclature

A:	Absorbance (no units, $A = \log_{10} I_0 / I$, I_0: intensity of incoming light; I: intensity of out coming light)
AIBN:	2,2-Azobisisobutyronitrile
c:	Cohesive energy density, J/m^3
C:	Concentration of the solution, $mol \cdot L^{-1}$
C_0:	Initial drug concentration, $mol \cdot L^{-1}$
C_∞:	Drug concentration at the equilibrium state, $mol \cdot L^{-1}$
C_t:	Drug concentration at time t, $mol \cdot L^{-1}$
D:	Diffusion coefficient of the model drug from polymer to water, cm^2/min
d_0:	Apparent density of particles, g/ml
d_1:	Density of swelling agent, g/ml
d_2:	Density of homogeneous polymers, g/ml
D_{dry}:	Particle diameter of the particle in a dry state
DHPMA:	2,3-dihydroxypropyl methacrylate
DLC:	Drug Loading Capacity
d_M:	Average density of the monomer mixtures, g/ml
d_P:	Density of the homogeneous polymers, g/ml
D_{swell}:	Particle diameter of the particle in a swollen state
$D_v(r)$:	Pore size distribution function, cc/μm/g
f:	Initiation efficiency
FA:	furfuryl acrylate
f_i:	Volume fraction of the monomer i in the monomer mixtures
G_{el}:	Free energy of elastic deformation, $J \cdot mol^{-1}$
G_{mix}:	Gibbs free energy of mixing, $J \cdot mol^{-1}$
HEMA:	2-hydroxyethyl methacrylate
H_{mix}:	Enthalpy for mixing, $J \cdot mol^{-1}$
k:	Constant
k_{cyc}:	Fraction of pendent vinyl groups consumed by cyclization reactions
k_d:	Decomposition rate constant of the initiator AIBN, s^{-1}
k_{pi}:	Rate constant for the propagation, $L \cdot mol^{-1} \cdot s^{-1}$
k_{pji}:	Propagation rate constant between radicals M_j* and monomers M_i, $L \cdot mol^{-1} \cdot s^{-1}$

k_t:	Termination rate constant, $L \cdot mol^{-1} \cdot s^{-1}$
k_{tcij}:	Termination rate constants by coupling between radicals M_i* and M_j*, $L \cdot mol^{-1} \cdot s^{-1}$
k_{tdij}:	Termination rate constants by disproportionation between radicals M_i* and M_j*, $L \cdot mol^{-1} \cdot s^{-1}$
L:	Length of light path, cm
M_∞:	The amount of the drug released at the equilibrium state, mg
M_4:	Structure unit with a pendant vinyl group
$M_{4,j}$:	Crosslinked unit with j structure units
$M_4^s{}_{,j}$:	Unit of the pendent vinyl groups with j structure units or the length of the polymer chain is j in the sol
MA:	methacrylic acid
M_c:	Average molecular weight between two crosslinks, g/mol
M_g:	Weight of the gel polymers, g
M_{inf}:	The amount of the drug released at the equilibrium state, mg
MMA:	Methyl methacrylate
m_p:	Weight of polymers used in the drug loading experiment, g
M_s:	Weight of sol polymer, g
M_t:	Amount of the drug released at time t, mg
M_w:	Molecular weight of the model drug, g/mol
n:	Power law exponent
N:	Average number of segments between two adjacent crosslinking points in the network chains
$n_{comonomer}$:	Number of moles of comonomer, mol
n_{EGDMA}:	Number of moles of EGDMA, mol
n_{HEMA}:	Number of moles of HEMA, mol
n_i:	Number of moles of the species i (1-diluent, 2-network, 3-soluble polymers), mol
NVP:	N-vinyl-2-pyrrolidone
P:	Pressure, kPa
P_j:	Polymer chains with j units
P%:	Porosity
$[P_r^s]$:	Concentrations of active polymers consisting of r structural units in the sol, $mol \cdot L^{-1}$
PVP:	Poly(vinyl pyrrolidone)

Q_n: n^{th} moment of the polymer distribution

$[Q_r^s]$: Concentrations of dead polymers consisting of r structural units in the sol, $mol \cdot L^{-1}$

q_v: Equilibrium volume swelling ratio

q_w: Equilibrium weight swelling ratio

$[R^*]$: Radical concentration, $mol \cdot L^{-1}$

r: Pore radius, μm

$\bar{r}$: Average pore radius, μm

$\bar{r}_{43}$: Effective reactivity ratio

r_μ: Crosslinking reaction rate, $mol \cdot L \cdot s^{-1}$

r_H: HEMA/Comonomer volume ratio, ml/ml

r_{oct}: Porogen volume ratio, ml/ml

r_p: Initial average radius of the particles, μm

SDS: Sodium dodecyl sulfate

S_{mix}: Entropy for mixing, $J \cdot mol^{-1}K^{-1}$

St: Styrene

S_v: Specific porous surface area, m^2/g

t: time, s

T: temperature, °C or K

T_g: Glassy transition temperature, °C or K

U: Molar cohesive energy, $J \cdot mol^{-1}$

V: Volume, L

v_2^0: Volume fraction of the polymer networks in the network phase (gel) at a given degree of polymerization

v_2^{00}: Initial volume fraction of the monomer

$V_{comonomer}$: Volume of each comonomer, ml

V_{dry}: Volumes of a single particle in the dry state, ml

V_{HEMA}: Volume of HEMA, ml

v_g: Volume fraction of the polymeric networks in the whole reaction system at the specific volume conversion

v_i: Volume fraction

V_m: Molar volume, m^3/mol

$V_{m,1}$: Average molar volume of the monomer mixtures, m^3/mol

V_{oct}: Volume of 1-octanol, ml

V_p: Pore volume, ml/g or cm^3/g

$\bar{v}_p$: Volume fraction of the sol and gel polymers in the whole reaction system

V_s: Molar volume of the porogen, m^3/mol

V_{swell}: Volumes of a single particle in the equilibrium swelling state

w: Weight fraction of monomers

W_g: Gel fraction

W_s: Sol fraction

x: Overall reaction conversion of the monomers

$\overline{X}_2$ Weight average molecular weight of the sol polymer

x_j: Instantaneous mole fraction of the radical M_j*

y: Number average of segments of the soluble polymers

Greek symbols

α: Volume conversion

γ: Surface tension of mercury, 4.84mN/m at 25°C

δ_1: Solubility parameter of the solvent, $(Mpa)^{1/2}$

δ_2: Solubility parameter of the polymers, $(Mpa)^{1/2}$

δ_i: Solubility parameter of the monomer i, $(Mpa)^{1/2}$

δ_{pi}: Solubility parameter of the homopolymer synthesized by monomer i, $(Mpa)^{1/2}$

ε: Extinction coefficient, $mol \cdot L^{-1} \cdot cm^{-1}$

ε_c: Contraction factor which is equal to $1-d_M/d_P$

θ: Contact angle, degree (°)

μ_i: Chemical potentials in the separated phase, J

μ_i': Chemical potentials in the network phase, J

v: Crosslink density, g/ml

ξ: Cycle rank (A cycle rank is defined as the number of the independent circuits in the polymer

$\overline{\rho}^s$: Average crosslink density of the sol polymers, g/ml

φ: Volume fraction

φ_c: Critical volume fraction for a phase separation

φ_s:	Radical fraction in the sol
Φ_{sol} :	Volume fraction of the porogen in the reaction mixture
χ:	Flory-Huggins interaction parameter
χ_{ij}:	Flory interaction parameter between species i and j
χ_{12}^{m}:	Monomer-polymer interaction parameter
χ_{12}^{s}:	Porogen-polymer interaction parameter

Chapter 1
Introduction

1.1 Overview

Hydrogels are three-dimensional polymeric networks that can swell in water and retain a significant fraction of water within their structures without being dissolved (Li et al, 2001). Because of their unique properties, hydrogels have been widely used in many areas, especially in the controlled release, the tissue engineering, and so on (Kumar et al, 2002). Among the synthetic hydrogels, HEMA (2-hydroxyethyl methacrylate) related hydrogels are largely used. Homopolymers and copolymers of HEMA can be made using radical initiators or by various methods (γ-rays, UV) (Montheard et al, 1992). The most successful application of poly(HEMA) has been for an ocular device, namely, the hydrophilic soft contact lens. However, there are very few successful clinical trials of implanting with poly(HEMA) in human patients. The reason is probably that the mechanical strength is weak once the polymer is in a swollen state (Montheard et al, 1992). Thus, the synthesis of HEMA copolymers in the presence of different types of comonomers has received considerable attention. As a result, the properties of poly(HEMA) hydrogels can be greatly modified or even controlled for more favorable applications.

The studies on the synthesis of porous polymeric materials have been pursued for more than 40 years. Since a series of the porous copolymer gels were studied, people have found that the porous copolymers have many attractive properties and applications. As crosslinked three-dimensional networks, HEMA polymers and copolymers are essentially the porous materials. However, the mesh size between crosslinks is just several nano-meters. When poly(HEMA) is immersed in water, it swells and becomes very soft and flexible so that this type of poly(HEMA) is always considered non-porous (Chirila et al, 1993). Although a few micro-/macro-porous copolymer gels (Sherrington, 1998; Okay, 2000) and macro-porous poly(HEMA) sponges (Chirila et al, 1993; Liu et al, 2000; Clayton et al, 1997; Dziubla et al, 2001; Gates et al, 2003; Chiellini et al, 2002; Martin et al, 2003; Shapiro et al, 1997) have been synthesized, few micro-porous HEMA copolymers have been reported. Thus, how to produce micro-/nano-porous hydrogels based on HEMA has been of particular interest in the present studies.

Since the first porous polymer gel poly(St-DVB) was synthesized via free radical copolymerization in the presence of organic solvents, the quantitative description of the porous characteristics using mathematical models has become a new topic. Okay (1994 and 1999) first simulated the porosity of porous poly(St-DVB) polymers using kinetic methods. However, up until now, there are almost no model studies on the reaction kinetics and the porous characteristics of porous HEMA copolymers. To fully understand the gel formation and the pore formation in the copolymerization of HEMA and other comonomers which have different properties, the mathematical models should be constructed based on the kinetic mechanisms. In the present studies, HEMA-comonomer-EGDMA systems were simulated by extending the kinetic method proposed by Okay (1999) to the systems combining the gelation kinetics and the thermodynamics in the present work.

1.2 Definition of Porous Materials

With the development of the studies on the porous polymeric materials towards the end of 1950s, it became necessary to distinguish these new materials from the conventional materials and the terms 'macro-porous' and 'micro-porous' were introduced (Okay, 2000). There are different definitions for 'macro-porous' and 'micro-porous'. According to IUPAC, macro-pores refer to the pores which are larger than 50 nm (nanometers) (Okay, 2000). But macro-porous networks usually have a broad pore size distribution ranging from 1nm to 10^3 nm. For instance, if the porous size is beyond 10μm (microns), this type of hydrogel is also called a 'superporous' hydrogel (Kumar et al, 2002). Some literature about the porous poly(HEMA) defines the micropores as pores in the range of 10-100 nm, whereas the macropores are in the range of 100 nm-1 μ m (Chirila et al, 1993). It is well known that nano-scale refers to scales below 100 nm. Therefore, in the present studies, to simplify these definitions, the pores below 100 nm (diameter) were defined as nano- or micro-pores, whereas the pores larger than 100 nm (diameter) were defined as macropores.

1.3 Research Objectives

In the past decade, in order to control the porous structures and the swelling properties of poly(HEMA), a series of comonomers have been introduced. The copolymers of HEMA with various vinyl comonomers have been reported. However, the control of the porous structures and the swelling properties, and the application of the porous HEMA copolymer particles for the controlled release have not been well understood. The modeling of the synthesis of the porous HEMA copolymers has never been studied thoroughly. Therefore, a systematic investigation is needed. Accordingly, the

advantage of the present studies over other published literatures is the connectivity and the systematic approach of the work. Furthermore, the objectives of the present studies are:

- Synthesize micro-/nano-porous HEMA copolymer particles in the presence of hydrophilic and hydrophobic comonomers by a free-radical suspension copolymerization process. Three types of the comonomers of HEMA were studied, including the slightly water soluble MMA (methyl methacrylate), hydrophobic St (styrene) and hydrophilic NVP (N-vinyl-2-pyrrolidone).
- Explore the effects of the various synthesis parameters on the porous structures, including the EGDMA molar concentration, the monomer volume ratio and the porogen volume ratio.
- Simulate the gel formation and the porosity using the mathematical models combining with the gelation kinetics and the thermodynamics.
- Study swelling properties of the highly porous copolymer particles of HEMA and its applications in the controlled release of a hydrophilic model drug.

1.4 Outline of the Thesis

Chapter 1 provides an overview about the background and the objectives of this project. A literature review about the preparation of the porous polymeric materials can be found in Chapter 2. Several preparation techniques were reviewed including suspension polymerization, precipitation polymerization, microemulsion technique, poly HIPE technique and seeded emulsion polymerization. It was found that the presence of the water-insoluble comonomers or solvents could realize the synthesis of the polymer particles in the aqueous phase even though one of the monomers is hydrophilic. It was also found that the suspension polymerization technique is a good way to be used in the preparation of the porous HEMA polymer particles. Chapter 3 introduces the experimental methods used in the project. Because of the hydrophilic properties of HEMA, the solubility properties of the reaction mixture in the aqueous phase are studied in Chapter 4. The synthesis, the characterization and the modeling of the highly porous particles of poly(HEMA-MMA), poly(HEMA-St) and poly(HEMA-NVP) are studied in Chapters 5, 6 and 7, respectively. It was found that the different pore formation mechanisms determine the porous characteristics. The derivation and the theories of the mathematical models are found in Chapter 5. In Chapter 8 and Chapter 9, swelling properties of the porous polymers and their applications in the controlled release are studied. It was found that the swelling properties can be well controlled by the polymer compositions, the network properties and the presence of the porous structures. The controlled release of a model drug

theophylline is found in Chapter 9. The release rate can be well controlled by the porous HEMA copolymeric particles and the release profiles close to zero-order can be obtained depending on the polymer network compositions and the porous structures. The conclusions of this research and recommendations for future research are found in Chapter 10.

Chapter 2
Literature Review

2.1 HEMA and Its Polymers

Polymers and copolymers of HEMA are classified as hydrogels based on hydroxyalkyl methacrylates or acrylates (Mark et al, 1989). The structural formula of HEMA is given by a compound (1).

Compound (1)

Although Woodhouse (1938) first reported both HEMA and its polymer in a patent, he did not notice that the polymer was hydrophilic and capable of swelling by incorporating a large amount of water (Chirila et al, 1993). Since then, many researchers have studied the properties of HEMA and its polymers, as well as the synthesis processes for HEMA related polymers. Homopolymer and copolymers of HEMA can be made by radical initiators or by various methods (γ-rays, UV) (Montheard et al, 1992). For instance, HEMA can be initiated by an organic initiator in a large excess of water, resulting in a coarse and hydrophilic white powder. Because of this unusual manner of polymerization and special properties of poly(HEMA), HEMA has been mentioned in a number of patents regarding its potential use as a co-monomer for a variety of polymeric compositions (Li et al, 2001; Park et al, 2001).

However, the recognition of poly (HEMA) as a valuable biomaterial was entirely the result of the remarkable work reported by a Czechoslovakia group led by Otto Wichterle (Wichterle, 1960; Chirila et al, 1993). The most successful application of poly (HEMA) hydrogels was for an ocular device, the hydrophilic soft contact lens, which has been a successful commodity followed by successful clinical results and a huge commercial industry. Eventually, their potential biomedical applications seemed limitless regarding their great versatility and good performance. However, there are very few successful clinical trials of implanting poly (HEMA) in human patients. The reason is probably that the mechanical strength is weak once the polymer is in a swollen state (Montheard et al, 1992).

Thus, the synthesis of HEMA copolymers in the presence of the different types of comonomers has received considerable attention. By doing so, the properties of poly(HEMA) can be greatly modified or even controlled for more favorable applications.

2.2 Porous Polymeric Materials and Porous Poly(HEMA)

The research of the synthesis of the porous polymers has been pursued for more than 40 years. A typical macro- and micro-porous copolymer gel was prepared by the copolymerization of the styrene and divinylbenzene (DVB). The formation of very small pores (micro-pores) results from the crosslinks of DVB and the styrene at various points (Sherrington, 1998). So the crosslinking helps create pores within the three dimensional matrix. It was found that the pore size at higher crosslinking density is much smaller than that at lower crosslinking density (Sherrington, 1998; Okay, 2000). However, the pores whose formation is only dependent on crosslinking always have random pore size distribution. Therefore, to control the pore size distribution, different kinds of organic diluents, used as porogen, are often introduced to produce more uniform porous copolymer gels (Sherrington, 1998; Okay, 2000). A porogen is an organic solvent or a mixture of several organic solvents that can dissolve monomers but not polymers.

As the crosslinked three-dimensional networks, HEMA copolymers are essentially the porous materials. By the bulk polymerization of HEMA, a glassy and transparent polymer is produced with a pore size of a few nanometers or less (Chirila et al, 1993). When immersed in water, poly(HEMA) swells and becomes very soft and flexible. However, this type of poly(HEMA) is always considered non-porous (Chirila et al, 1993).

It was reported that the poly(HEMA) with the porous structures can be achieved by conventional approaches (Chirila et al, 1993; Sherrington, 1998; Okay, 2000), using crosslink agents and porogens in a free-radical polymerization. When a non-solvent for poly(HEMA) is used as a diluent in a monomer mixture and the maximum swelling capacity of the final polymer is reached in that particular diluent, phase separation occurs resulting in heterogeneous hydrogels that are milky or white materials (Chirila et al, 1993).

Although a few micro-/macro-porous copolymer gels (Sherrington, 1998; Okay, 2000) and macro-porous poly(HEMA) sponges (Chirila et al, 1993; Liu et al, 2000; Clayton et al, 1997; Dziubla et al, 2001; Gates et al, 2003; Chiellini et al, 2002; Martin et al, 2003; Shapiro et al, 1997) have been

synthesized, few micro-porous HEMA copolymers have been reported. How to produce micro-/nano-porous hydrogels based on HEMA has been of particular interest in the present studies.

2.3 Preparation Techniques of Porous Polymeric Materials

According to literature studies, porous polymers could be achieved by the following techniques:

- The use of gases as the void-forming medium. For example, for the thermal initiated crosslinking (co)polymerization, the presence of $NaHCO_3$ which was decomposed by heating can generate gases resulting in porous polymers (Park et al, 2001). Sannino et al also prepared macroporous poly(ethylene glycol) by combining the photocrosslinking reaction with a foaming process recently (Sannino et al, 2006). Many of polymer foams are prepared using this technique (Kiefer et al, 1999).
- The use of polymer emulsions (Kiefer et al, 1999; Okay, 2000; Brown et al, 2005; Joes et al, 2005; Stefanec et al, 2005; Macintyre et al, 2006; Krajnc et al, 2006; Menner et al, 2006;). For this technique, the inner phase consists of volatile solvents or polymeric substances that can be evaporated or decomposed after synthesis, and the outer phase consists of a polymerizable monomer (Kiefer et al, 1999).
- The use of phase separation processes to generate porous structures. For example, the crosslinking (co)polymerization in the presence of the solvents which are good solvents for the monomers, but non-solvents for the formed polymers (Chirila et al, 1993; Okay, 2000; Gao et al, 2005; Arrua et al, 2006).
- Crosslinking (co)polymerization in the presence of the soluble substances (sugars, salts) that are washed out from the polymers after polymerization so that the pores are left behind (Liu et al, 2000; Olah et al, 2006).
- Frost sublimation of the hydrogel swollen in water (Shapiro et al, 1997).
- Supercritical fluid (Wood et al, 2001; Reverchon et al, 2006; Zhang et al, 2007). For example, Wood et al used supercritical CO_2 as a "pressure-adjustable" porogen to prepare nano-porous poly(trimethylolpropane trimethacrylate, TRIM) under a high reaction pressure of 5000~6000 psi (Wood et al, 2001).

- Template or molecularly imprinted polymerization. The polymerization is carried out in the presence of a template material or a template molecule. The pores can be induced by washing out the template. Some porous monolith and porous membranes have been synthesized using this technique (Yan et al, 2004; Bodhibukkana et al, 2006; Sergeyeva et al, 2007)

Among the techniques introduced above, the first, the fourth and the fifth technique can only produce the polymers with large pores at least on the micron scale. For the second technique, in most cases, the pores of a micron size are prepared. However, the micropores can be prepared at the same time by incorporating suitable organic solvents to generate phase separation which is the third techniques. By doing so, the pore size distribution of the polymers prepared by the second technique will be quite broad. By the third technique, micro-porous copolymer gels have been prepared, such as poly(styrene-co-DVB). For the sixth one, a process of utilizing supercritical CO_2 is more favorable to make porous monolith than other polymer morphologies. The porous materials made by the template or the molecularly imprinted polymerization are always only used in the applications related to the template molecules used in the synthesis. Consequently, micro-porous polymers or copolymer particles could be prepared using the phase separation techniques or the polymer emulsion. On the basis of these two techniques, heterogeneous polymerizations or microemulsion polymerization can be applied.

2.3.1 Heterogeneous Polymerization

The polymeric particles can be prepared by the heterogeneous polymerization, including suspension polymerization and precipitation polymerization.

2.3.1.1 Suspension polymerization

Suspension polymerization, consisting of comonomers, initiator, water or other solvents, stabilizer and other additives, is carried out by suspending the monomers as droplets in a continuous phase to prepare polymer beads. The suspension of the droplets is maintained by mechanical agitation and the addition of stabilizers. Various water-insoluble inorganic or organic stabilizers are used to prevent agglomeration of the liquid droplets. The initiators are dissolved in the monomer phase. Theoretically speaking, each droplet in a suspension solution can be treated as a small bulk polymerization system (Odian, 2004). Therefore, the kinetics of polymerization in each droplet is close to the kinetics of the bulk polymerization. Basically, the suspension polymerization is not suitable if the monomers are highly soluble in water. For appreciably water-soluble monomers, polymerization will take place in

solution as well as in the monomer droplets lowering the molecular weight, and the coagulation of the monomer droplets may occur at low conversions if the polymer's T_g is much lower than the polymerization temperature (Odian, 2004). However, note that if a good solvent for the monomers is mixed with the water-soluble monomers, this solvent can extract the monomers from the aqueous phase to the organic phase so that suspension polymerization could be applied. For example, Horak et al (1993) used an aqueous solution of poly(vinyl pyrrolidone) as the water phase and a mixture of high boiling alcohols as the diluents of the monomer phase to synthesize the crosslinked poly(HEMA) beads. They pointed out that the diluents reduce the water solubility of HEMA by extracting HEMA from the aqueous phase to the organic phase.

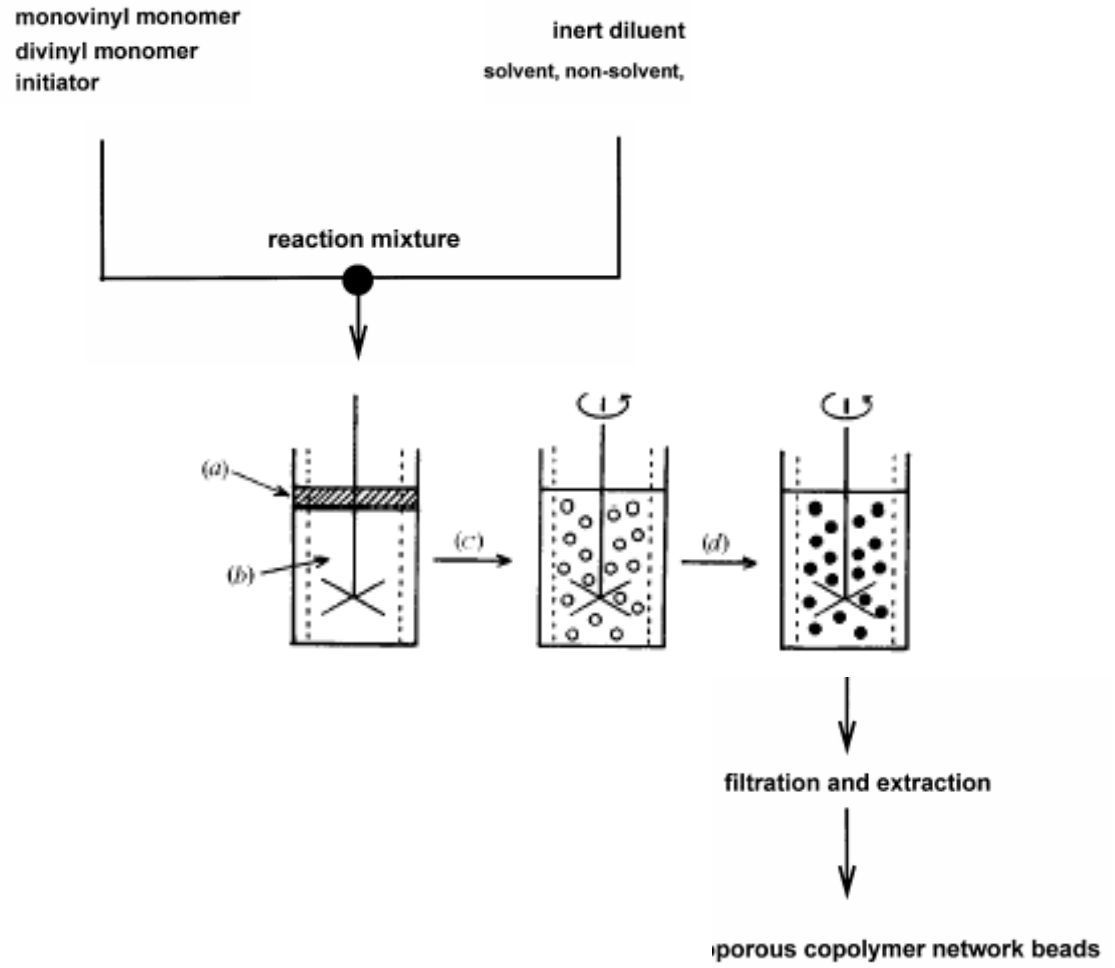

Figure 2-1 Schematic representation of suspension polymerization: (*a*) organic comonomer mixture (with porogen) containing dissolved initiator; (*b*) aqueous continuous phase containing dissolved polymeric suspension stabilizer; (*c*) shearing to form comonomer liquid droplets; (*d*) thermal polymerization to form solid polymer beads (Sherrington, 1998; Okay, 2000).

A synthetic procedure for the suspension polymerization is shown schematically in Figure 2-1. The mixture containing a free-radical initiator, mono-vinyl monomers and a multi-vinyl crosslinker is mixed with an inert diluent (good solvent, non-solvent or a mixture of solvent/non-solvent). The multi-vinyl crosslinker has at least two vinyl groups so that it can create crosslinking points to form polymer networks. The inert diluent must be soluble in the monomer mixture but insoluble in the continuous phase of the suspension polymerization. The reaction mixture is then added into the continuous phase under agitation, so that it is dispersed in the form of droplets in the continuous phase. The copolymerization and crosslinking taking place in the droplets result in the formation of the polymeric beads having a glassy, opaque, or milky appearance depending on the porous morphology. The beads are then extracted with a good solvent to remove the soluble polymers, residual monomers and diluents from the networks. The porous polymer particles are finally obtained after drying.

2.3.1.2 Precipitation Polymerization

The porous polymers can also be obtained by precipitation polymerization. The precipitation polymerization involves the polymerization of the monomers dissolved in bulk or in solution (either aqueous or organic) where the formed polymer is insoluble (Odian, 2004). The hydrophilic crosslinked porous polymeric particles can also be prepared using this technique from water-soluble comonomer systems, such as 2-hydroxyethylmethacrylate–ethylene glycol dimethacrylate (HEMA/ EGDMA) system. For this purpose, various salts are added into the water phase in order to greatly decrease the solubility of the monomers in the aqueous phase. Horak et al (1996), Mueller et al (1978), Scranton et al (1990) and Okay et al (1992) described the synthesis of poly(HEMA) beads in an aqueous phase containing sodium chloride and other additives. The presence of the sodium chloride in the aqueous phase not only reduces the monomer's solubility to allow the formation of the spherical and hydrophilic beads, but also produces the macropores within hydrogels as an inorganic porogen (Martin et al, 2003).

2.3.2 Microemulsion Technique

According to the above descriptions, the organic porogens must be soluble in the organic phase and insoluble in the polymer phase. In contrast, the organized surfactant assemblies such as inverse micelles can be used to capture monomer-insoluble diluents such as the water inside the organic phase (Okay, 2000). This microemulsion can create macro-porous or micro-porous structures since

the nature of the porous structures is largely dependent on the microstructure of the microemulsion (Sasthav, 1992). It has been shown that the water soluble in the reverse micelles can be used as a diluent in the production of the porous Styrene–DVB copolymer beads by suspension polymerization (Okay, 2000). Bennett et al (1995) tried to "trap" microemulsion inside the HEMA polymer matrix to form micropores of a very small diameter. A HEMA or HEMA/water/propanol mixture was used as a continuous phase and methylcyclohexane was used as the discontinuous phase. After the polymerization initialized by UV radiation, the pore size resulting from this type of microemulsion is less than 150nm. These researchers pointed out that increasing the rate of polymerization to impose a kinetic barrier on the agglomeration process would be helpful to produce highly porous polymer by microemulsion. In addition, the preparation of the transparent porous hydrogels from microemulsion systems that consist of MMA, HEMA, EGDMA and different surfactants were investigated as well (Sherrington, 1993; Gan et al, 1994; Liu et al, 1997; Chew et al, 1998). Microporous hydrogels with the pores in around 100 nm were obtained. According to these investigations, although micropores are obtained by microemulsion, a large amount of organic solvent and surfactant is needed, which is bad for the possible applications of poly(HEMA). Moreover, the procedure for preparing the microemulsion is so complicated that it is not practical in the real production. This might be why there have been very few reports about the preparation of the HEMA related polymers using microemulaion polymerization recently.

Another similar preparation technique using the microemulsion for producing porous polymers is called polyHIPE® (HIPE=water-in-oil High Internal Phase Emulsion) (Okay, 2000; Benson, 2003). If water is added slowly to a stirred solution of a surfactant of low hydrophilic–lipophilic balance dissolved in an oil phase, an internal phase volume of water of up to 99% is achieved (Okay, 2000). The crosslinking polymerization results in a solid crosslinked polymer that contains the water droplets. Removal of the water droplets results in a highly porous monolith with extremely low density (about 0.2 g/ml compared to 1.1 g/ml polymer) (Okay, 2000). The average diameter of the water droplets within a HIPE system used to prepare a Styrene–DVB polyHIPE is about 10 mm, and therefore, the surface area of the resulting materials is rather low (about 5 m^2/g) (Sherrington, 1993). In order to increase their surface area, organic diluents such as toluene are added into the oil phase (Okay, 2000; Benson, 2003). In this method, the porous materials with a specific surface area of 350m^2/g were obtained having large pores (water droplets) and the small pores resulting from the phase separation in the oil phase (Okay, 2000). However, a large amount of surfactant is still needed.

Furthermore, two types of pores, generated by water and diluents, make the pore size distribution very broad, which is not good for the applications, such as controlled release and separation.

2.3.3 Seeded Emulsion Polymerization

On the basis of the suspension polymerization and emulsion polymerization technique, an alternatative procedure, namely, seeded emulsion polymerization, which yields uniform porous particles, has been reported. This technique mainly overcomes a relatively broad particle size distribution in the suspension polymerization so that the seeded emulsion polymerization might be used in the initial stage of the suspension polymerization process in order to prepare the shape template particles (Okay, 2000). By introducing an additional inert diluent (a solvent or a nonsolvent) together with monomers to swell the monodisperse polystyrene latex, porous structures within the particles may be obtained upon the removal of the diluent after polymerization (Sherrington, 1998; Cheng et al, 1992). For this purpose, the uniform polystyrene latex in the size range 1.9-6.2μm was used as seeds, which were successively swollen by dibutyl phathalate and a monomer mixture consisting of styrene, HEMA and a crosslinker (EGDMA or DVB) (Tuncel et al, 2002). It was found that HEMA concentration was higher on the particle surface than the interior, which may be caused by the hydrophilicity of HEMA. However, the resultant polymer particles have macropores of several microns. Swelling of the seeds is a crucial step in this technique; therefore a large amount of solvent and a long operation time are needed, which makes this technique impractical.

2.3.4 Summary

In comparison with these techniques introduced in this chapter, the suspension polymerization is relatively better than others because:

- Suspension polymerization is easily operated and controlled, and the reaction time is relatively short.
- Fewer surfactants and organic solvents could be used in the suspension polymerization.
- There are many water-insoluble monomers that can be copolymerized with HEMA to improve characteristics of poly(HEMA) hydrogels.

Although many studies on the suspension polymerization of macro-porous poly (HEMA) have been reported**,** there are few systematic studies on the preparation of micro-porous poly (HEMA) hydrogel

particles, including the effect of synthesis parameters and a quantitative treatment about the porosity, porous size and its distribution depending on the synthesis parameters.

2.4 Modeling of Gel Formation and Porous Characteristics

The studies on the reaction kinetics of free radical crosslinking copolymerization have been carried out for several decades. Different mathematical models have been proposed to simulate the crosslinking process and the polymer gel formation. Flory (1943 and 1953) and Stockmayer (1943 and 1944) first simulated the polymer gel formation using a statistical method which provided the theoretical bases for the further studies on the formation of the polymer gels. However, the main problem of their models, as pointed out by Okay (1994), is that they did not consider the real reaction kinetics. For instance, their models were not directly derived from the elementary kinetic equations involving different types of vinyl groups (Okay, 1994). Consequently, some researchers have proposed different mathematical models derived from real reaction kinetics (Okay, 1994; Li et al., 1989 a, b; Tobita et al., 1989; Mikos et al., 1986 and 1987). Moment methods were used to calculate the polymerization degree to determine the gel point and describe the gelation process in these models. The models derived by Mikos et al (1986 and 1987) could simulate the effective crosslinks. Another model proposed by Tobita and Hamielec (1989) using pseudo-kinetic rate constant method was used to calculate the average chain length of the crosslinked polymers up to the gel point. However, the moment equations derived in their models were so complicated that it was hard to make comparison with experimental results (Okay, 1994). Since then, Okay (1994 and 1999) simplified the moment method being used by Tobita and Hamielec, and obtained good simulation results for the gel formation of the poly(St-DVB) gels.

Since the porous polymers were synthesized in the presence of the organic solvents, how to simulate porous characteristics using mathematical methods has been a new topic. Okay (1994 and 1999) simulated the porosity of the porous poly(St-DVB) polymers based on the gelation model using kinetic methods. The models have shown good simulation results for the gelation of the porous poly(St-DVB) polymers. Although the model over predicted the porosity, the simulation results are still meaningful because the shrinkage of the polymers during solvent removal or drying lowers the porosity in the polymers (Okay, 1994). However, more studies are still needed to extend this method for more polymer or copolymer systems. Up until now, there are almost no model studies on the reaction kinetics and the porous characteristics of porous HEMA copolymers. To fully understand the

gel formation and the pore formation in the copolymerization of HEMA and other comonomers, the mathematical models should be constructed based on the kinetic mechanisms.

2.5 Theoretical Background of Phase Separation

According to the above discussion about the preparation techniques, the porous structures are induced by the phase separation. Typically, the porous polymers can be derived from a phase separation process by carrying out a temperature quench which is also called *thermally induced phase separation* (TIPS) or by carrying out a crosslinking polymerization which is called *chemically induced phase separation* (CIPS) (Kiefer et al, 1999).

For the thermally induced phase separation, a phase separation is initiated by changing the temperature depending on the systems having *upper critical solution temperature* (UCST) or *lower critical solution temperature* (LCST). For instance, PS-cyclohexane system has UCST so that they are miscible above the critical temperature and phase separation occurs by cooling below the binodal or spinodal line (Kiefer et al, 1999). However, it is rarely seen that the porous polymers are produced by this technique although some porous membranes are produced using this technique. Therefore, *chemically induced phase separation* is more efficient to make porous polymers. However, the theoretical backgrounds of TIPS have much in common with CIPS (Kiefer et al, 1999).

To make porous polymers using CIPS, there are two important factors which must be considered. One is the solvent used in the system and the other is the crosslinker content if certain monomers are given. The choice of the solvent is crucial, as it must be a moderately good solvent for the monomers to allow the components to be miscible in the unreacted state, thus giving initially a homogeneous mixture, and the solvent should turn into a non-solvent during the reaction to start the phase separation into discrete liquid domains to induce pores through further crosslinking (Kiefer et al, 1999). If a good solvent and a crosslinker are present in the systems, the three dimensional networks of infinitely large size may start to form (Okay, 2000). According to Flory (1953), ‘infinitely large size’ refers to the polymeric networks having close size to the containing vessel. In the preparation of the porous polymeric particles, this containing vessel could be assumed to be each droplet. If the amount of the crosslinker in the reaction mixture is increased while the amount of the good solvent remains constant, the highly crosslinked network cannot absorb all the diluent molecules present in the reaction mixture, resulting in a phase separation (Okay, 2000). Based on these two cases, Dusek

(1970) proposed *v*-induced syneresis and χ-induced syneresis to describe these two processes. According to the model of *v*-induced syneresis, the microgels (nucleus) are separated because of the high crosslinking and the liquid phase remains a continuous phase. As the polymerization and crosslinking proceed, new nuclei are continuously generated due to the successive separation of the growing polymers, which react with each other through their pendant vinyl groups and radical centers locating at their surfaces to form porous heterogeneous gels by removing the solvent from the systems (Okay, 2000). Therefore, this process is determined by the crosslinking, so it is called *v*-induced syneresis. However, at lower crosslink density, the long network chains slowly relax from swollen state to phase separated state so that their swollen state may become fixed by additional crosslinks and the solvent molecules remain inside the gel in the formation of the droplets (Okay, 2000). Therefore, the *v* refers to the crosslink density of the networks (Okay, 2000). According to the model of χ-induced syneresis, the phase separation is resulted from the presence of the non-solvent. The incompatibility between the network segments and the diluent molecules is responsible for the porosity formation so that this mechanism is called χ-induced syneresis and χ represents the polymer-solvent interation parameter (Okay, 2000). It was found that the pores induced by the *v*-induced syneresis are more ordered and smaller than the latter (Okay, 2000). Therefore, the relative importance of these two processes is determined by the crosslinker contents and the thermodynamic quality of the solvents.

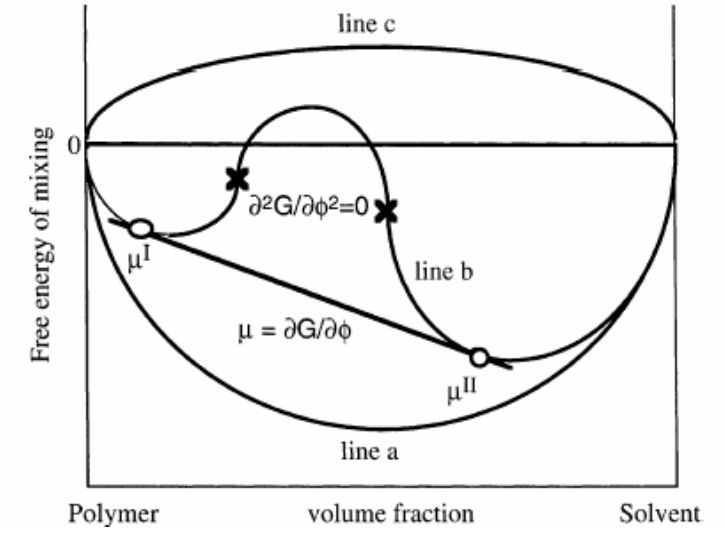

Figure 2-2 Free energy curves corresponding to miscibility (*line a*), phase separation (*line b*), and immiscibility (*line c*) (Kiefer et al, 1999)

The phase separation process can be described from the thermodynamic point of view. It is believed that the phase separation is the result of a change in the free energy of the system. According to Flory-Huggins theory (Flory, 1953), this free energy illustrates the state of the mixing. The Gibbs equation for the mixing is as shown in the equation (2-1).

$$\Delta G_{mix}=\Delta H_{mix}-T\Delta S_{mix} \qquad (2\text{-}1)$$

The ΔG_{mix} is the Gibbs free energy of mixing, the ΔS_{mix} is the change of the entropy for mixing, the ΔH_{mix} is the change of the enthalpy for mixing, and T is the temperature. In polymer systems, the change of the entropy could determine the state of the mixing because of the polymerization. The change in the free energy can be described using Figure 2-2. If the system is fully miscible, the value of the free energy, ΔG, is negative which is shown as *line a* in Figure 2-2. Accordingly, if the system is completely immiscible, the ΔG becomes positive in the whole range of the composition which is shown as *line c*. Hence, a phase separation is equivalent to the transition from the miscible to the immiscible state (Kiefer et al, 1999). The *line b* shows this intermediate state. Thus, the phase separation is illustrated by the change in the curvature of the *line b* mathematically. On the *line b*, the inflection points are given by equation (2-2) which shows the condition of spinodal composition. Any points between these two points will split into two phases to lower the free energy (Kiefer et al, 1999).

$$\frac{\partial^2 \Delta G}{\partial \phi^2} = 0 \qquad (2\text{-}2)$$

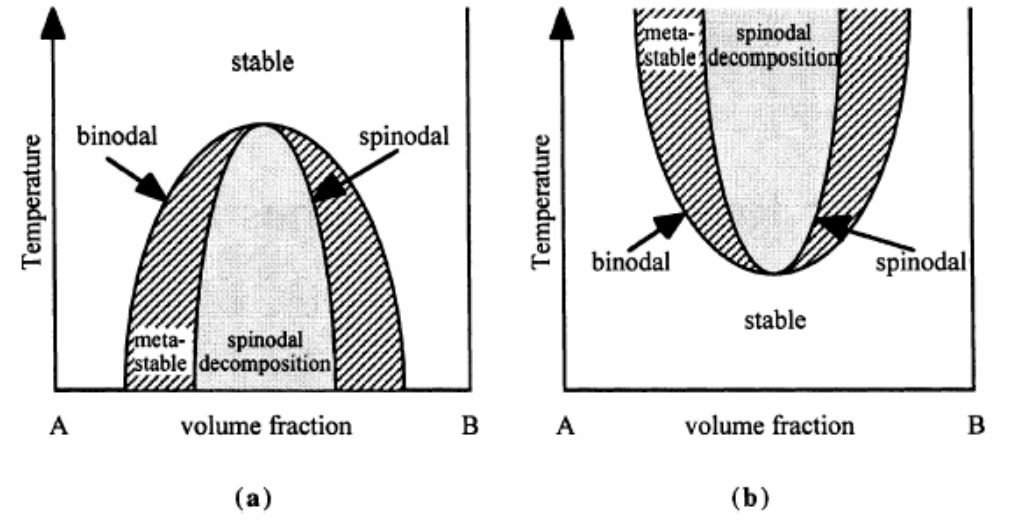

Figure 2-3 Schematic phase diagrams displaying: an upper critical solution temperature (*UCST*) behavior; b lower critical solution temperature (*LCST*) behavior (Kiefer et al, 1999)

On *line b*, the thermodynamic equilibrium states are also shown by the two points which have a common tangent. These points give the composition of a polymer rich phase (I) and a solvent rich phase (II) that can coexist in thermodynamic equilibrium as shown in the equations (2-3) and (2-4), and the summation of such points gives the coexistence curve or binodal line (Kiefer et al, 1999).

$$\mu^{I}_{polymer} = \mu^{II}_{polymer} \qquad (2\text{-}3)$$

$$\mu^{I}_{solvent} = \mu^{II}_{solvent} \qquad (2\text{-}4)$$

Following the procedure described above, the phase diagrams can be made. For the TIPS systems having UCST or LCST, the phase diagrams are shown in Figure 2-3. Similarly, if the temperature axis is changed to conversion, the phase diagram for the CIPS systems is obtained which is similar to the phase diagram having a LCST as shown in Figure 2-4. The φ_c is the critical concentration above which a phase separation would lead to the formation of particles dispersed in a liquid matrix. On a comparision between Figure 2-4 and Figure 2-3, it can be seen that the polymerization and the crosslinking reaction can change the critical temperature so that the phase separation can be induced during the reaction at the reaction temperature with an increase in the polymerization conversion as shown in Figure 2-5 which means the points that are in the miscible region initially could locate in the phase-separated region upon certain polymerization conversion (Hsu et al, 1993).

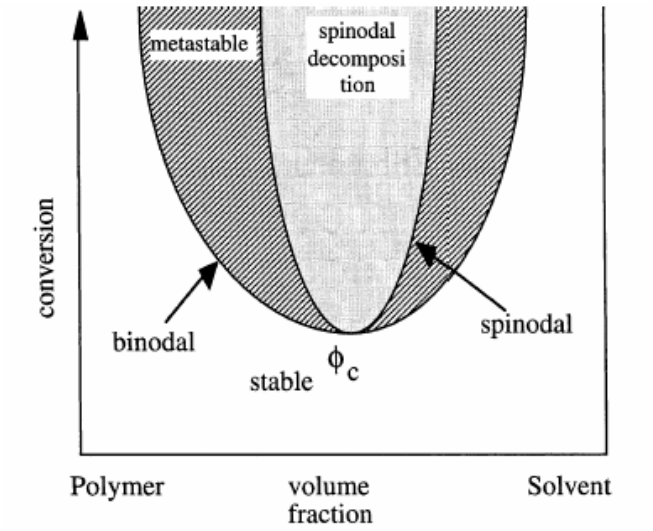

Figure 2-4 Schematic phase diagram for Chemically Induced Phase Separation (CIPS)

For that matter, no matter what polymerization techniques are applied, the synthesis of the porous polymer particles by the phase separation is affected by some common factors including the crosslinking, the comonomers and the solvents (porogens) (Sherrington, 1998). Besides these parameters, the concentration of initiator, the concentration of stabilizer, and the reaction temperature, or even agitation speed are expected to affect the porous structures as well. Accordingly, the properties of the porous structure induced by the phase separation are sensitively dependant on these factors so that one can design tailor-made porous polymers for a specific application (Okay, 2000).

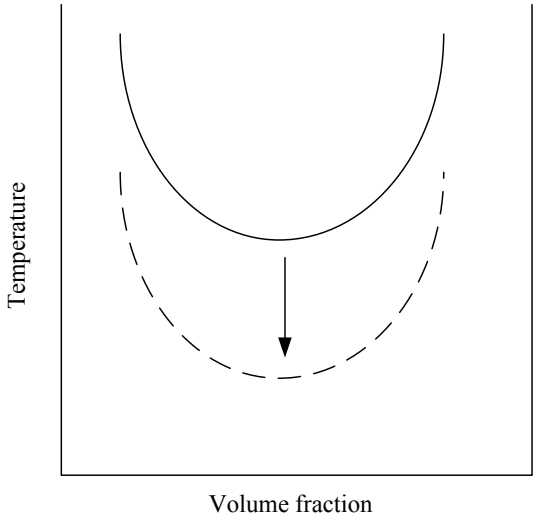

Figure 2-5 Change in the phase diagram as a result of the polymerization and the crosslinking

2.6 Reaction Parameters

2.6.1 Porogens

Obviously, the porogen is one of the most important components in the porous polymeric material preparation. No matter what type of porogen is used, inorganic or organic, the porogen promotes the phase separation, resulting in the porous structures (Okay, 2000). The organic porogens can dissolve monomers and initiators, but not polymers. If the inorganic salts are used as porogens, the phase separation is called enhanced phase separation (Liu et al, 2000). By the enhanced phase separation, macropores are obtained because of the existence of water within the polymer networks (salts are dissolved in water). Hydrogels produced by the enhanced phase separation are often suitable for biomedical applications since lesser amount of organic solvents are used. However, the resulting pores are so large that they have limiting applications.

Porous structures start to form when the amount of the solvent (porogen) and the amount of the crosslinker pass a critical value. The solvating power of the porogen has a key effect on the porous structures of the porous copolymers. Note that the net solvating power of the medium (unreacted monomer mixture + solvent) changes over the course of the reaction as the monomers are consumed. If a good solvent (polymer can be soluble in good solvent) is used as an inert diluent (porogen) in the system, the polymer gel will have a super-coiled structure because of the expansion of polymer chains (Okay, 2000). Therefore, it will have a nonporous in the glassy state. Good solvent cannot cause phase separation until the gel point at certain crosslink density is reached. Thus, polymer chains cannot preserve pore structures during solvent removal. On the other hand, if a non-solvent is used as the porogen, phase separation may occur in the reaction system before the original gel point. This results in the formation of a dispersion of separated discontinuous polymer phase in the continuous "monomer + solvent" phase. As a result of continuing the polymerization, the first separated phase and intra-molecularly crosslinked particles (nuclei) agglomerate into larger clusters called microspheres. Continuing the reaction increases the number of clusters in the reaction system so that a system consisting of a polymer phase and a porogen phase result (Okay, 2000). Removal of the diluent from the gel produces macro- or micro-pores. In the presence of non-solvents, the incompatibility between the network segments and the diluent molecules is responsible for the porosity formation, which is called χ-induced syneresis (Seidl et al, 1963; Okay, 2000). The χ is the polymer–solvent interaction parameter, which relates to $(\delta_1-\delta_2)^2$. The δ_1 is the solubility parameter of the solvent and the δ_2 is the solubility parameter of the polymers.

The research of the porous Styrene-DVB copolymer gel networks revealed that the addition of a solvating diluent (SOL), such as toluene or dichloroethane, produces small average pore diameter and a considerable specific surface area (50–500 m^2/g) and a relatively low pore volume (up to about 0.8 ml/g), whereas addition of a non-solvating diluent (NONSOL), such as *n*-heptane or alcohols, results in a large pore volume (0.6–2.0 ml/g), a relatively large average pore diameter and a specific surface area varying from 10 to 100 m^2/g. (Sherrington, 1998). Figure 2-6 shows the change of the porosity with the solvating power of the solvents summarized by Okay (2000). It can be seen that the porosity is higher in the presence of a non-solvent.

The hydrogels prepared by the copolymerization of MMA and HEMA have micropores if a non-solvent, dodecanol, is used (Vianna-Soares et al, 2003). During the polymerization of HEMA, if the porogen is a good solvent for the polymers, i.e. cyclohexanol; the sizes of polymeric beads are much

smaller than those in the non-solvent of polymers, i.e. 1-octanol (Horak et al, 1993). When the HEMA/EGDMA copolymerization was carried out using cyclohexanol/dodecanol as a SOL/NONSOL mixture, it was found that the porosity of porous poly(HEMA) beads could be readily adjusted by changing the diluent composition (Horak et al, 1996). Accordingly, various combinations of these two diluent types are taken into account to regulate the pore size distribution of the copolymers. In general, increasing the SOL content of a SOL/NONSOL mixture produces smaller pores and thereby increases the internal surface area although the total volume of the pores decreases (Okay, 2000).

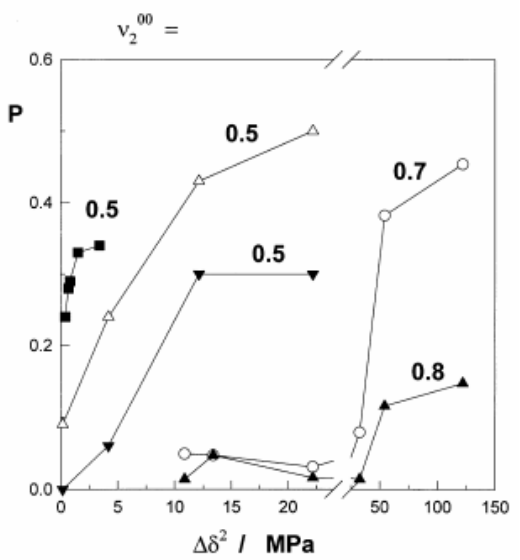

Figure 2-6 The total porosity *P* of S–DVB copolymer networks shown as a function of the diluent quality $\Delta\delta^2=(\delta_1-\delta_2)^2$, where δ_1 and δ_2 are the solubility parameters of the diluent and the polymer, respectively; the initial volume fraction of the monomer v^{00}_2 is shown in the figure (Okay, 2000). Experimental data points are from Seidl et al (1967), Wieczorek et al (1984), and Okay (1986, 1988). The curves only show the trend of the data. Diluent=aliphatic alcohols of various chain length (Seidl et al, 1967), DVB=20%, v^{00}_2=0.70 (○), and 0.80 (▲). Diluent=toluene/cyclohexanol mixtures Okay, 1986 and 1988), v^{00}_2 =0.50; DVB=10 (▼) and 25% (Δ); Diluent=*n*-heptane/toluene mixtures (Wieczorek et al, 1984), v^{00}_2 = 0.50; DVB=50% (■).

2.6.2 Crosslinking

If the amount of the crosslinker in the reaction mixture is increased while the amount of the porogen remains constant, a highly crosslinked network cannot absorb all the diluent molecules present in the reaction mixture, resulting in a phase separation during the gel formation process (Okay, 2000). When the growing gel deswells (or collapses) at the critical point of the phase separation and becomes a microgel (nucleus), the liquid remains as a continuous phase in the reaction mixture. As the

polymerization and crosslinking proceed, successively separated microgels are agglomerated by the reaction of each monomer through their pendant vinyl groups. As a result, the heterogeneous structure, which consists of a gel and a diluent phase, is formed. Voids (pores) of various sizes are created followed by the removal of the diluent from the gel. Therefore, in the presence of a good solvent, the formation of a porous structure is due to the effect of the increased crosslink density so that the solvating power of the monomer mixture is higher than the swelling capacity of the network. This type of porosity formation in polymeric materials is called v-induced syneresis (Seidl et al, 1967; Okay, 2000).

Table 2-1 Solubility Parameter, δ, of the monomers, polymers, and the diluent toluene in HEMA-EGDM copolymerization (Okay, 2000)

Component	δ (MPa)$^{1/2}$
HEMA	23.3
EGDM	18.2
Poly(HEMA)	29.7
Poly(EGDM)	19.2
Toluene	18.2

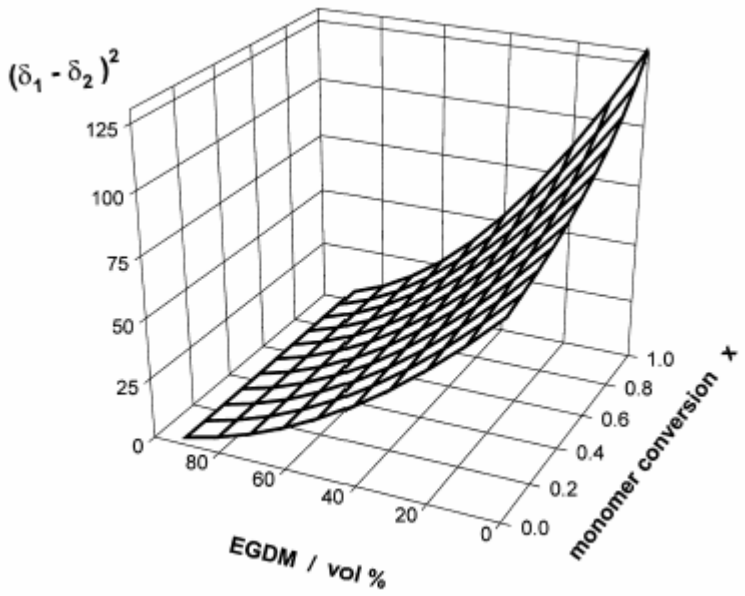

Figure 2-7 Variation of $(\delta_1-\delta_2)^2$ during the course of HEMA–EGDM copolymerization in the presence of toluene as a diluent depending on the initial EGDM concentration and on the monomer conversion (Okay, 2000)

According to the synthesis of styrene-DVB, at a given degree of solvating power of monomers and diluents, the porosity increases on raising the DVB concentration and then remains constant (Okay, 2000). However, not every reaction system follows this relationship, such as methacrylic acid (MA)/DVB, whose porosity is decreased with an increasing amount of DVB. This behavior is probably due to the different reactivity and thermodynamic properties of the monomers (Okay, 2000).

Table 2-2 Comonomer systems for the synthesis of macroporous networks (BAAm=*N*, *N*-methylene (bis)acrylamide; DVB=divinylbenzene; EGDM=Ethylene glycol dimethacrylate; HEMA=2-Hydroxyethyl methacrylate; GMA=Glycidyl methacrylate; MMA= Methyl methacrylate; NIPA=*N*-isopropylacrylamide; TRIM=Trimethylolpropane trimethacrylate) (Okay, 2000)

Comonomer system
Acrylamide/BAAm
Acrylic acid/EGDM
Acrylonitrile/DVB
Acrylonitrile/ethyl or butyl acrylate/DVB
Acrylonitrile/vinyl acetate/DVB
Dimethacrylates with various chain lengths
DVB/1,4-di(methacryloyloxymethyl) naphthalene
2,3-Epithiopropyl methacrylate/EGDM
GMA/EGDM
GMA/2-hydroxypropylene dimethacrylate
HEMA/EGDM
NIPA/dihydroxyethylenebisacrylamide
Maleic anhydride/styrene/DVB
Methacrylic acid/DVB
Methacrylic acid/triethyleneglycol dimethacrylate
Methacrylonitril/DVB
N-methylacrylamide/alkylene(bis)acrylamides
MMA/DVB
MMA/1,4-di(methacryloyloxymethyl) naphthalene
Phenyl methacrylate/DVB
TRIM
TRIM/GMA
TRIM/BAAm
TRIM/MMA
N-vinylcarbazole/DVB
2- or 4-Vinylpyridine/DVB
Vinyl toluene/DVB

With regard to the crosslinking polymerization of HEMA and EGDMA in the presence of toluene as a diluent (Okay et al, 1992), the total volume of the pores first increases with an increase in the crosslinker (EGDMA) concentration up to 20 mol% but then it decreases continuously. This behavior was explained based on the thermodynamic properties of the monomers, toluene or the polymer (Okay, 2000; Okay et al, 1992). As shown in Table 2-1 and Figure 2-7, at low EGDMA content, the residual monomer–toluene mixture is a non-solvent for the growing copolymer chains as $(\delta_1-\delta_2)^2 >> 0$, whereas it becomes a good solvent as the EGDMA concentration increases. At higher EGDMA contents, $(\delta_1-\delta_2)^2$ closely matches such that a phase separation occurs during the copolymerization.

This may only occur as a consequence of the increasing crosslink density (v-induced syneresis), whereas the porous structures formed at low EGDMA content are due to the polymer–(diluent+monomers) incompatibility in the polymerization system (χ-induced syneresis). This is a result of the different solubility parameters of monomers and porogens (Okay, 2000; Okay et al, 1992). Therefore, a different crosslinker concentration could lead to different pore formation mechanisms.

2.6.3 Comonomers

Normally, at least one of the comonomers must be water-insoluble in the suspension polymerization of the porous copolymer particles. All the components are dissolved in the monomer mixture. In addition for the well-known Styrene–DVB comonomers, various comonomer systems synthesized to form macroporous networks are tabulated in Table 2-2. Amongst them, HEMA/EGDMA is a conventional monomer/comonomer to prepare macro-porous sponges. In fact, EGDMA is acting as a crosslinker in the system. But in the system of HEMA/EGDMA, EGDMA is a more water-insoluble monomer. On copolymerizing HEMA with water-insoluble monomers, properties of hydrogels, including hydrophilicity, hydrophobicity, T_g, porous structures, swelling and mechanical intensity, can be improved so that the resultant polymers can be applied in more areas. Very few reports about microporous HEMA copolymers (Vianna-Soares et al, 2003) have appeared, and there is still lack of the systematic research dealing with porous copolymer particles of HEMA.

2.6.4 Reaction Temperature and Initiators

According to the literature, an increase in the reaction temperature shifts the pore size distribution towards smaller pores and the corresponding specific surface area is increased (Svec et al, 1995). The polymerization temperature--porous structure relation is a consequence of the increasing decomposition rate of the initiator on increasing the temperature (Svec et al, 1995). The higher the reaction temperature, the greater the number of free radicals is generated per unit time, so that the greater the number of nuclei and microspheres formed (Okay, 2000). It is easily understood that the increase in the number of nuclei and microspheres decreases their size. The voids after agglomeration are thus smaller. At a low polymerization temperature, the slow polymerization rate makes the transfer of the monomers from solution to the nuclei in relatively sufficient time, which results in the growth of the nuclei of larger sizes due to an increase of monomers in the nuclei (Svec et al, 1995).

Note that increasing the solvating power of the diluent by increasing the temperature may also contribute to the shift of the pore size distribution towards smaller pores (Okay, 2000).

Increasing the decomposition rate of the initiator (e.g. using AIBN as an initiator instead of benzoyl peroxide) decreases the size of the pores at a given polymerization temperature due to the increasing rate of polymerization (Svec et al, 1995; Okay, 2000;). It was also shown that under isothermal polymerization conditions, there is a much narrower distribution of pore sizes than in the nonisothermal polymerization (Okay, 2000; Albright, 1986). Gomez et al (2000) observed that the best products of poly(HEMA-EGDMA) result with 2.44% of the initiator at 70℃ and 0.6% of initiator at 85℃ and higher surface area was obtained in these cases. On the other hand, it has been shown that the concentration and the types of the oil-soluble initiator used in the suspension polymerization for the given monomers has an effect on the polymerization kinetics, the average size and polydispersity of the polymeric beads, and the average pore size (Dowding et al, 1998 and 2000). The average pore size was found to be bigger for benzoyl peroxide-initiated systems than for comparable systems initiated using AIBN (Dowding et al, 1998). However, whether this effect is the same for every system requires further study.

2.7 Applications

HEMA related polymers or copolymers have been mainly applied for bioapplications. For example, several uses concern endovascular occlusion in the case of tumors (Horak et al, 1986), preparation of contact and intraocular lenses, or sorbents for various types of chromatography (Ajzenberg et al, 2001). Porous poly(HEMA) related polymers are one of the most important biomaterials applied in tissue engineering. Poly(HEMA) spongy materials have macropores. The first use of these sponges was studied in the late 1960s for breast augmentation and nasal cartilage replacement (Dziubla et al, 2001). In 1990s, Chirila et al (1993) found that cellular ingrowths and neovascularization occur in poly(HEMA) sponges implanted subcutaneously in rabbits. In vitro assessments have shown a good compatibility of the materials with the maintenance of human fibroblasts in culture. Dziubla et al (2001) applied poly(HEMA) obtained by solution polymerization to long-term implantable drug delivery devices. The materials were attached to the distal end of a 20-gauge catheter tube and implanted subcutaneously and intraperitoneally. After 5 months implantation, insulin was infused into the devices from external pumps and rapid insulin absorption was observed in conjunction with

dramatic lowering of blood glucose levels, which indicated that poly(HEMA) could be used as a long-term implantable drug delivery devices.

Copolymers of HEMA particles can be used as packing materials for chromatography. These packing materials are good for separating or analyzing drugs. At the same time, hydrophilic packing materials are especially useful since they require the use of low toxicity aqueous mobile phases. Vianna-soares et al (2003) applied microporous poly(MMA-HEMA) particles for size exclusion packing materials. The material was used to separate dextran standards (MW 40,000-2,000,000) using deionized and distilled water mobile phase at room temperature.

However, applications of HEMA related polymers are still limited. The development of the controllable micro-porous hydrogels particles will make them have more potential applications, such as separation, catalysis, biosensors, fuel cells, as well as controlled release and tissue engineering.

2.8 Summary

Suspension polymerization is a relatively good method to make micro-porous HEMA related hydrogels. During the preparation of the porous copolymer particles using this technique, how to obtain uniform micro-porous hydrogel particles, how to increase polymerization rate, how to control phase separation and how to control pore size and its distribution are still needed to be studied further. Pores are induced by phase separation in the presence of organic porogen or inorganic salts. In the presence of an organic porogen, micropores can be obtained. The ν-induced syneresis and χ-induced syneresis provide the basic theories regarding pore formation. Several synthesis parameters determine the porous structures.

Although there have been a few reports about macro-porous poly(HEMA) sponges, systematic research involving the preparation of micro-porous HEMA copolymer is still insufficient, especially on how to control the properties of hydrogels and how to obtain a quantitive description of porous structures of HEMA copolymers. Therefore, our research is to prepare highly porous HEMA copolymeric particles. Effects of the monomer ratios, EGDMA concentration, porogen volume ratio on the polymer morphology and related properties will be studied. Mathematical models of porosity combining polymerization kinetics will be constructed to predict the hydrogels' properties. The application of the microporous particles for controlled release will be studied as well.

Chapter 3
Monomer Partitions in Aqueous Phase

Since HEMA is a hydrophilic monomer, poly(HEMA) particles have to be synthesized in an aqueous phase with the help of other solvents that are not soluble in water. The solubility of HEMA in the aqueous phase is up to 80wt% and cyclohexanol can be used to make spherical poly(HEMA) particles by greatly reducing the solubility of HEMA in the aqueous phase to about 40% (Horak et al, 1993). In the present studies, St and MMA are water-insoluble monomers. Although NVP is a strong hydrophilic comonomer, the presence of the water-insoluble 1-octanol still can make suspension copolymerization possible. However, some portions of the hydrophilic content are still dissolved into the aqueous phase even though the suspension copolymerization is possible. Therefore, monomer partition in the reaction system is an important parameter for understanding the polymerization performance and the polymeric particle morphology.

3.1 Materials

Ethylene glycol dimethacrylate (EGDMA, 98%, Aldrich Chemical, Inc.), methyl methacrylate (MMA, 99%, Aldrich Chemical, Inc.), styrene (St, 99%, Aldrich Chemical, Inc.), N-vinyl-2-pyrrolidone (NVP, 99%, Aldrich Chemical, Inc.), 1-octanol (99%, Aldrich Chemical, Inc.), and 2-hydroxyethyl methacrylate (HEMA, 97%, Aldrich Chemical, Inc.) were used without further purification. Methanol was HPLC grade.

3.2 Experimental

The organic mixtures consisting of HEMA, comonomer (HEMA, MMA or NVP), EGDMA and 1-octanol were prepared and then mixed with water at room temperature. The mixtures were shaken for 3 days and maintained still for 1 day before HPLC measurements. The equilibrium concentrations of HEMA, MMA, St, NVP, EGDMA and 1-octanol in the aqueous phase at room temperature were determined by HPLC (Waters 2690 Separations Module) equipped with a UV detector (996 PDA, wavelength 254.0 nm). The mobile phase consists of 60% of methanol and 40% of purified water.

3.3 Results and Discussion

The monomer partitions between the aqueous phase and the organic phase are determined by the solubility of the monomers in the aqueous phase and in the organic phase. This property can be qualitatively described using the solubility parameter, δ ($MPa^{1/2}$).

3.3.1 Solubility Parameter (δ)

The solubility reflects the interactions between the molecules in a mixture. The miscibility of a mixture can be determined by the cohesive energy density *c* as shown in the equation (3-1) (Barton, 1983).

$$c = -\frac{U}{V_m} \qquad (3\text{-}1)$$

where c is the cohesive energy density (J/m^3). U and V_m are the molar cohesive energy (J/mol) and the molar volume (m^3/mol), respectively. According to the cohesive energy density, the solubility parameter (Hildebrand solubility parameter) can be defined as shown in the equation (3-2) (Barton, 1983). If two materials have close δ values between each other, it implies that they have similar cohesive energy so that they could obtain enough energy to disperse sufficiently to permit mixing (Barton, 1983). Basically, the two components, diluent and polymer or diluent and monomer, are miscible if the difference of the solubility values are moderately close, for example $|\delta_1 - \delta_2| < 3$ (Rabelo et al, 1994). In the present studies, the solubility parameter of each reaction component is shown in Table 3-1. The magnitude of these values suggests that the monomer HEMA, comonomer (MMA, St or NVP), and EGDMA are soluble in 1-octanol to make a miscible organic phase since the values of their solubility parameter values do not have much difference. However, 1-octanol is still a non-solvent for the poly(HEMA) (Horak et al, 1993).

$$\delta = c^{1/2} = \left(-\frac{U}{V}\right)^{1/2} \qquad (3\text{-}2)$$

Table 3-1 Values of the solubility parameters in the unit of $MPa^{1/2}$ (Barton, 1983; Brandrup et al, 1999; Okay, 2000)

HEMA	EGDMA	MMA	Styrene	NVP	1-octanol
23.2	18.2	18.9	19.1	23	20.9

3.3.2 Monomer Partitions in Aqueous Phase

Table 3-2 shows the monomer fractions in the aqueous phase. The concentration of 1-octanol in the aqueous phase was too low to be detected. However, it still can be seen that the monomer content in the aqueous phase was reduced at higher 1-octanol concentration in the organic phase, which means that the presence of 1-octanol is helpful to reduce the solubility of the monomers in the aqueous phase.

Table 3-2 Fractions of the monomers soluble in the aqueous phase at room temperature

No.	HEMA/MMA/EGDMA/1-octanol	Fraction (%) in aqueous phase			
		HEMA	MMA	EGDMA	1-octanol
HM-1	2ml /12ml /2.1ml /7ml	49.8%	8.2%	0.59%	-
HM-2	2ml /12ml /2.1ml /14ml	38.2%	6.2%	-	-
HM-3	2ml /12ml /4.9ml /7ml	41.7%	6.7%	0.36%	-
HM-4	2ml /12ml /4.9ml /14ml	41.4%	6.1%	0.36%	-
HM-5	2ml /12ml /7ml /7ml	50.5%	8.3%	0.45%	-
HM-6	2ml /12ml /7ml /14ml	43.1%	5.9%	0.37%	-
No.	HEMA/St/EGDMA/1-octanol	Fraction (%) in aqueous phase			
		HEMA	St	EGDMA	1-octanol
HS-1	2ml /12ml /2.1ml /7ml	18.9%	-	0.26%	-
HS-2	2ml /12ml /2.1ml /14ml	18.7%	0.03%	0.25%	-
HS-3	2ml /12ml /4.9ml /7ml	20.1%	0.02%	0.17%	-
HS-4	2ml /12ml /4.9ml /14ml	19.2%	0.03%	0.17%	-
HS-5	2ml /12ml /7ml /7ml	20.6%	0.03%	0.18%	-
HS-6	2ml /12ml /7ml /14ml	18.0%	-	0.15%	-
No.	HEMA/NVP/EGDMA/1-octanol	Fraction (%) in aqueous phase			
		HEMA	NVP	EGDMA	1-octanol
HN-1	2ml /12ml /2.1ml /7ml	22.9%	43.2%	15.2%	-
HN-2	2ml /12ml /2.1ml /14ml	23.2%	42.2%	10.0%	-
HN-3	2ml /12ml /4.9ml /7ml	23.2%	44.5%	9.2%	-
HN-4	2ml /12ml /4.9ml /14ml	22.4%	46.3%	7.0%	-
HN-5	2ml /12ml /7ml /7ml	23.6%	44.8%	7.1%	-
HN-6	2ml /12ml /7ml /14ml	21.8%	47.0%	5.7%	-

According to Table 3-2, the fraction of HEMA in the aqueous phase is about 40% in the HEMA/MMA system, 20% in the HEMA/St system and 23% in the HEMA/NVP system, respectively, which is very close to or lower than the values reported by Horak et al (1993) even though cyclohexanol, a good solvent for both the monomers and the poly(HEMA), was not used. At the same time, NVP, a hydrophilic component, has lower aqueous solubility as well compared to its solubility in water, whereas it has a good solubility in HEMA and 1-octanol. Therefore, this implies that the introduction of comonomers, together with the organic porogen, can successfully reduce the solvent required.

However, the polymerization happening in the droplets after initiation reduces the solubility of the monomers further because the reaction generates polymer chains that are insoluble in the aqueous phase. Although some monomers are still dissolved in the aqueous phase, the amount should be much less than the data shown in Table 3-2 because the partitions probably can not reach the equilibrium state as described above once the reaction is initiated. Therefore, the discussions in the following chapters will use apparent concentration data of monomers to simplify the problem.

3.4 Conclusions

- The increase in the porogen concentration reduces the solubility of the monomers in the aqueous phase.
- The introduction of comonoers of HEMA can successfully reduce the solvent required in the suspension copolymerization.
- Although some portions of the monomers are soluble in the aqueous phase, to simplify the analysis of the characterization results, original concentration data of each component will be used.

Chapter 4

Preparation Techniques and Characterization Methods for Porous HEMA Copolymer Particles

In this chapter, the synthetic techniques of the porous HEMA copolymer particles and the characterization methods are introduced. The experimental reproducibility of the polymer particle synthesis and characterization are found.

4.1 Synthesis of Porous Polymeric Particles

4.1.1 Materials

Ethylene glycol dimethacrylate (EGDMA, 98%, Aldrich Chemical, Inc.), methyl methacrylate (MMA, 99%, Aldrich Chemical, Inc.), styrene (St, 99%, Aldrich Chemical, Inc.), N-vinyl-2-pyrrolidone (NVP, 99%, Aldrich Chemical, Inc.), 1-octanol (99%, Aldrich Chemical, Inc.), and 2-hydroxyethyl methacrylate (HEMA, 97%, Aldrich Chemical, Inc.) were used without further purification. The structural formula of MMA, St, NVP and EGDMA are shown in the compound (2)-(5), respectively. The initiator was 2,2-azobisisobutyronitrile (AIBN, Polysciences, Inc.). Poly(vinyl-pyrrolidone) (PVP, K90, weight average molecular weight: 360000, Aldrich Chemical, Inc.) and sodium dodecyl sulfate (SDS, 70%, Aldrich Chemical, Inc.) were dissolved in deionized water before using. PVP and SDS were used as a stabilizer and a co-stabilizer, respectively. Petroleum ether (95%, boiling temperature range: 30°C-60°C, Fisher Scientific) and methanol (HPLC grade, Fisher Scientific) were used to wash the polymers after reaction.

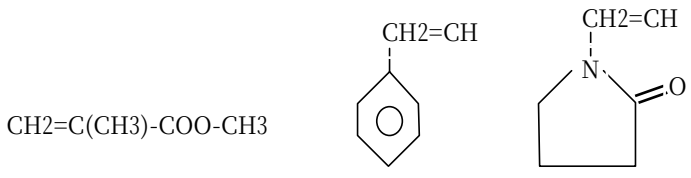

Compound (2) Compound (3) Compound (4)

CH2=C(CH3)-COO-CH2CH2-OOC-C(CH3)=CH2

Compound (5)

4.1.2 Suspension Copolymerization

The reaction process is shown in Figure 4-1. The dispersed organic phase, consisting of HEMA, comonomer (MMA, St or NVP), EGDMA, 1-octanol and AIBN was stirred for 10 minutes using a magnetic stirrer. The dissolved oxygen in the organic phase and stabilizer solution was eliminated by a nitrogen purge. The organic phase was added into the stabilizer solution which consisted of 0.15g SDS and 1.5g PVP in 150ml deionized water. The solution was agitated using a homogenizer for 3 minutes to generate oily droplets. Subsequently, the emulsion was charged into a jacketed steel reactor equipped with a 4-pitched blade agitator at room temperature. The reaction was maintained at 70°C for 4 hours under an agitation speed of 500 rpm followed by a filtration operation to obtain the polymer particles. The particles were washed successively using deionized water and methanol, and then were extracted by ether using a Soxhlet extractor for 24 hours. Finally, the copolymer particles were dried in a vacuum chamber at 35°C for 3 days.

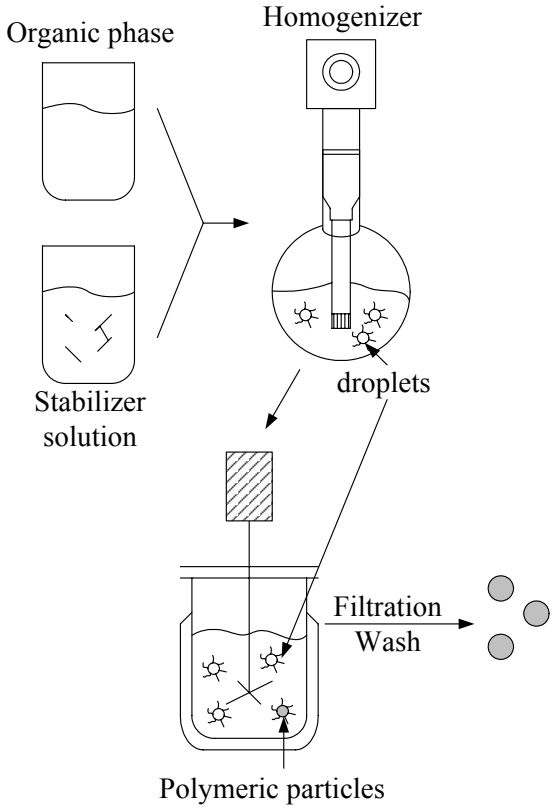

Figure 4-1 Synthesis process of porous HEMA copolymer particles

4.2 Gel Formation Kinetics

4.2.1 Materials

Ethylene glycol dimethacrylate (EGDMA, 98%, Aldrich Chemical, Inc.), methyl methacrylate (MMA, 99%, Aldrich Chemical, Inc.), styrene (St, 99%, Aldrich Chemical, Inc.), and 2-hydroxyethyl methacrylate (HEMA, 97%, Aldrich Chemical, Inc.) were purified using an inhibitor removal column purchased from Aldrich Chemical at room temperature. N-vinyl-2-pyrrolidone (NVP, 99%, Aldrich Chemical, Inc.) was purified by vacuum distillation at 60°C in the presence of sodium hydroxide. 1-octanol (99%, Aldrich Chemical, Inc.) was used without further purification. The initiator, 2,2-azobisisobutyronitrile (AIBN, Polysciences, Inc.), was re-crystallized in methanol of HPLC grade twice and dried in vacuum at room temperature. The purified chemicals were stored in a refrigerator at 1-3°C for future use.

4.2.2 Experimental Methods

HEMA, comonomers (MMA, St or NVP), AIBN and 1-octanol were charged into a series of reaction vials. Oxygen free N_2 was used to eliminate soluble O_2 in each vial. These vials were sealed and put into a water bath at 70ºC. At each predetermined time interval, one of these vials was taken out of the water bath, a small amount of inhibitor (4-Methoxyphenol) was added into the vial, and then the vial was put into ice to stop the reaction. The gels and the reaction mixtures were merged in THF (tetrahydrofuran) and the sample jars were shaken for 3 days during which the fresh THF was added in them. The gels were taken out and dried in vacuum chamber at 70-90ºC for 3 days. The THF solution was evaporated to obtain the *sol* polymers. The gel fraction was then calculated using equation 4-1 (Naghash et al, 1995).

$$W_g = \frac{M_g}{M_g + M_s} \times 100\% \qquad (4\text{-}1)$$

where M_g is the weight of the gels, M_s is the weight of the *sol* polymers, and W_g is the gel fractions.

4.3 Characterization Methods

4.3.1 Reaction Parameters

The following variables are convenient to define the compositions of the reaction mixtures.

1. EGDMA Molar Concentration and EGDMA Volume Concentration

$$\textbf{EGDMA mol\%} = \frac{n_{EGDMA}}{n_{HEMA} + n_{comonomer} + n_{EGDMA}} \times 100\% \quad (4\text{-}2)$$

$$\textbf{EGDMA vol/vol\%} = \frac{V_{EGDMA}}{V_{HEMA} + V_{comonomer}} \times 100\% \quad (4\text{-}3)$$

where n_{HEMA}, n_{EGDMA} and $n_{comonomer}$ are the moles of HEMA, EGDMA and comonomers, respectively.

2. Porogen Volume Ratio, r_{oct}

$$r_{oct} = \frac{V_{oct}}{V_{HEMA} + V_{comonomer}} \quad (4\text{-}4)$$

where V_{oct}, V_{HEMA} and $V_{comonomer}$ are the volume of 1-octanol, HEMA and comonomer, respectively.

3. HEMA/Comonomer Volume Ratio, r_H

$$r_H = \frac{V_{HEMA}}{V_{comonomer}} \quad (4\text{-}5)$$

4.3.2 Mercury Intrusion Porosimetry (MIP)

Porous characteristics, including the porosity (*P%*), the pore volume (V_p), the specific porous surface area (S_v) and the pore size distribution ($D_v(r)$) of the porous particles were obtained using mercury intrusion porosimetry (Poremaster GT-60). As shown in the equation 4-6, the mechanism of the mercury intrusion porosimetry measurement is that the pressure of mercury P is balanced by the surface tension of mercury γ (4.84mN/m) when the mercury enters into the pores with radius of r (Ishizaki et al, 1998). The contact angle, θ, between mercury and the polymers was taken as 140° in the present studies (Vianna-Soares et al, 2003).

$$P \cdot r = -2\gamma \cos\theta \quad (4\text{-}6)$$

The pore volume is measured by the volume of mercury which was intruded into the pores. Therefore, the pore volume between r and r+dr can be described using the equation (4-7):

$$dV_p = -D_v(r)dr \quad (4\text{-}7)$$

If γ and θ are constant, a differential equation is given as follows:

$$Pdr + rdP = 0 \quad (4\text{-}8)$$

From the equations (4-7) and (4-8), the pore size distribution function can be obtained as follows:

$$D_v(r) = P\frac{dV_p}{dP} \cdot \frac{1}{r} \quad (4\text{-}9)$$

In addition, the average pore size can be calculated by integrating the profiles of pore size distribution as shown in the equation (4-10).

$$\bar{r} = \frac{\int r D_v(r) dr}{\int D_v(r) dr} \qquad (4\text{-}10)$$

4.3.3 Scanning Electronic Microscopy (SEM)

LEO 1530 Field-Emission Scanning Electronic Microscopy was used to evaluate the particle morphology and the porous structures. The copolymer particles in a dry state were located on a double-coated electronic tape with a gold coating of 10nm. SEM photos were taken under various magnifications. By measuring a series of the particle sizes in a SEM picture, the average particle size (diameter) and the standard deviation were calculated.

4.3.4 FT-IR

A Bio-Rad Fourier transform spectrometer was used to diagnose chain structures of the resultant polymers. A very small amount of the polymer particles, which was dried in a vacumm chamber at 60°C for 24 hours, was mixed with KBr to make a KBr disk. The FT-IR spectra were recorded on the KBr disks.

4.3.5 Swelling

The equilibrium volume swelling ratio (q_v) was determined by measuring the diameter of single polymeric particles, which were put in a large excess of water for 48 hours at room temperature or at 37°C in an equilibrium swelling state (D_{swell}) and in a dry state (D_{dry}), using an optical microscope equipped with a ruler (0.01mm). The values of q_v were calculated via equation 4-11. V_{swell} and V_{dry} are the volumes of a single particle in the equilibrium swelling state and in the dry state, respectively. Each experiment was repeated three times and the errors were calculated at a 95% confidence interval.

$$\mathbf{q}_v = \frac{V_{swell}}{V_{dry}} = \frac{D_{swell}^{\ 3}}{D_{dry}^{\ 3}} \qquad (4\text{-}11)$$

The equilibrium weight swelling ratio, $q_{w,}$ was calculated via the equation 4-12 (Okay, 2000; Beranova et al, 1969; Galina et al, 1980). In equation (4-12), d_0 is the apparent density of the polymer particles, d_1 is the density of swelling agent (if it is water, d_1=1g/ml) and d_2 is the density of the

homogeneous polymer which is the density for the non-porous polymer synthesized under the same reaction conditions. It was taken as the skeletal density of the porous particles in the present study.

$$\mathbf{q}_w = (\frac{q_v}{d_0} - \frac{1}{d_2}) \cdot d_1 + 1 \qquad (4\text{-}12)$$

4.3.6 Glass Transition Temperature

Since the glass transition temperature of the highly crosslinked polymers is hard to be measured using DSC, the Fox Equation as shown in the equation 4-13 was used to estimate the glass transition temperature of the resultant polymers (Odian, 2004).

$$\frac{1}{T_{g(copolymer)}} = \frac{w_{HEMA}}{T_{gPHEMA}} + \frac{w_{EGDMA}}{T_{gPEGDMA}} + \frac{w_{comonomer}}{T_{gP-comonomer}} \qquad (4\text{-}13)$$

where w is the weight fraction of monomers and T_g is the glass transition temperature in Kelvin. The glass transition temperature of the homopolymers of PHEMA, PMMA, PS, PNVP and PEGDMA are shown in Table 4-1.

Table 4-1 Glass Transition Temperature of Homopolymers

Polymer	PHEMA	PMMA	PS	PNVP	PEGDMA
Tg (°C)	86	105	100	67	130
Reference	Shen et al, 1967	Turner et al, 1987	Brandrup, 1999	Buera et al, 1992	Turner et al, 1987

4.4 Reproducibility of Experimental Methods

4.4.1 Reproducibility of Mercury Intrusion Porosimetry

Table 4-2 Reproducibility of Mercury Intrusion Porosimetry Characterization*

Run	R1	R2	R3	Mean	Error
Porosity (%)	70.2	71.9	75.4	72.5	±3.0
Pore volume(cm^3/g)	1.85	2.0	1.79	1.88	±0.12
Surface area(m^2/g)	16.9	15.5	21.2	17.9	±3.4

*: HEMA/MMA=7ml/7ml; EGDMA=35vol%; AIBN=0.1g; water=150ml; SDS=0.15g; PVP=1.5g; T=70°C; Agi=500rpm

Mercury intrusion porosimetry is one of the most important techniques to characterize the porous structures in the present studies. The accuracy of this measurement is crucial for the research. One sample was selected randomly to be characterized using the mercury intrusion porosimetry. The measurement was repeated 3 times. The average values and the errors at a 95% confidence interval

were calculated as shown in Table 4-2. According to the errors shown in the table, the reproducibility of this measurement method was considered to be acceptable.

4.4.2 Reproducibility of the Synthesis Technique

In the present studies, the porous polymeric particles were synthesized by free radical suspension copolymerization in the aqueous phase. The reproducibility of this technique will be important for the future industrial use and academic studies. A single synthesis experiment was repeated 3 times for each reaction system under the same reaction conditions to test the reproducibility of the free-radical suspension copolymerization process. The average values and the errors at a 95% confidence interval were calculated as shown in Table 4-3. According to the errors shown in Table 4-3, the performance of this process is quite stable for each system. The pore volume is the most accurate parameter measured. This is determined by the mechanism of the mercury intrusion porosimetry because the volume of the intruded mercury is the pore volume which is directly measured by the machine. The surface area and the porosity are calculated based on the intruded volume, but the repeated results do not have much difference. Therefore, the reproducibility of this synthesis technique is acceptable.

Table 4-3 Reproducibility of the Suspension Copolymerization*

	Run	R1	R2	R3	Mean	Error
HEMA-MMA	Porosity (%)	75.4	73.4	70.2	73.0	±3.0
	Pore volume(cm^3/g)	2.22	2.28	1.85	2.12	±0.26
	Surface area(m^2/g)	24.0	24.1	16.9	21.7	±4.7
HEMA-St	Porosity (%)	58.4	46.8	52.5	52.6	±6.6
	Pore volume(cm^3/g)	1.15	0.75	0.84	0.91	±0.24
	Surface area(m^2/g)	10.0	16.5	19.3	15.3	±5.4
HEMA-NVP	Porosity (%)	52.0	60.3	57.5	56.6	±4.8
	Pore volume(cm^3/g)	1.85	2.0	1.79	1.88	±0.12
	Surface area(m^2/g)	70.7	81.3	76.8	76.3	±6.0

*: [EGDMA]=35vol%; AIBN=0.1g; water=150ml; SDS=0.15g; PVP=1.5g; T=70°C; Agi=500rpm; r_H =7ml/7ml

Chapter 5
Synthesis, Characterization, and Modeling of Porous Poly(HEMA-MMA) Particles

5.1 Introduction

The homopolymer of MMA (PMMA) and the copolymers of HEMA and MMA have been studied for decades. PMMA is considered as one of the most useful biomaterials with considerable mechanical strength so that it has been widely used in implanting and in tissue engineering (Almog et al, 1982; Shen et al, 1991; Mabilleau et al, 2006), such as soft contact lens. MMA is always treated as a hydrophobic monomer because PMMA shows almost no swelling (Brannon-Peppas, 1990), which limits its applications as a biomaterial. PHEMA has the excellent biocompatibility but its mechanical strength is weak, especially at the swelling state (Montheard et al, 1992; Clayton et al, 1997). Therefore, the combination of HEMA and MMA will be helpful to control the properties of the resultant polymers for more favorable applications.

Due to the hydrophobic nature of MMA, poly(HEMA-MMA) has a lower degree of swelling than pure crosslinked PHEMA (Fransion et al, 1983). However, the real nature of MMA should be slightly water soluble because it has a slight water solubility of 1.5wt% at 50°C (Ming et al, 1998). Therefore, the nature of poly(HEMA-MMA) should be quite different from the HEMA copolymers copolymerized with other stronger hydrophobic comonomers, such as styrene. For instance, Murphy et al (1988) found that the EWC (equilibrium water content) and water permeability of poly(HEMA-MMA) film is higher than that of poly(HEMA-St). Some researchers have studied the effect of molecular weight, sample thickness and polymer compositions on swelling properties and solute transport in both of PMMA and poly(HEMA-MMA) (Lustig et al, 1986; Turner, 1987).

Many poly(HEMA-MMA) polymers in different polymer morphologies have been synthesized, such as nanoparticles by microemulsion (Ozer et al, 2001; Bhawal et al, 2004), core-shell microspheres (Sivakumar et al, 2002) produced by emulsion polymerization and the tubes formed by the bulk polymerization (Dalton et al, 2002). However, there is still lack of studies on the synthesis of the microporous poly(HEMA-MMA) particles.

How to induce porous structures in poly(HEMA-MMA) is very important nowadays, especially in the areas of separation, tissue engineering and controlled release. For instance, Dalton et al (Dalton et al, 2002) developed macroporous poly(HEMA-MMA) tubes using a small amount of EGDMA as a crosslinker and using water as a non-solvent. The tube could be used in tissue engineering to guide the growth of nerves because of the presence of the pores. Vianna-Soares et al (2003 and 2005) synthesized porous poly(HEMA-MMA) spheres using EGDMA as a crosslinker and AIBN as a initiator in the presence of dodecanol by free radical polymerization in the aqueous phase, and the pore volume (0.018-0.385ml/g) and the specific surface area (20-32m^2/g) were still low. Furthermore, they did not study the formation of the porous structures within the spheres in detail although they tried to use the spheres as absorbents in SEC (size exclusion chromatography) for biomedical applications. All in all, the studies on the porous structures and the particle morphology of the porous poly(HEMA-MMA) particles are still quite insufficient.

The objectives of this chapter were to synthesize the highly porous poly(HEMA-MMA) particles in the presence of an organic porogen (1-octanol), to characterize the particle morphology using SEM, to explore the porous structures and their formation mechanisms, and to simulate the gel formation and the porous characteristics of the porous poly(HEMA-MMA) particles.

5.2 FT-IR

Figure 5-1 shows the FT-IR spectra of HEMA, MMA, EGDMA and one selected polymer sample, and Table 5-1 illustrates the possible spectral band assignments (Perova et al, 1997; Gomez et al, 2000 and 2004). It can be seen that the peaks corresponding to the C=C (the dash line in the figure) in the monomers have almost disappeared in the resultant polymer, resulting from the copolymerization. However, there are still individual C=C bonds in the polymer because of the non-equal concentrations of C=C in the monomers. The pendant C=C bonds left in the networks could affect the particle morphology and the nature of the polymeric particles if they are stored in air for a long time. However, the particles stored in the lab are still quite stable over 2.5 years. On the other hand, according to the characteristic peaks of -OH, they can be found in the resultant polymers, showing the presence of the HEMA monomer.

Table 5-1 Possible Spectral Band Assignments for Poly(HEMA-MMA) Polymers (Perova et al, 1997; Gomez et al, 2000 and 2004)

Wavenumbers (cm^{-1})	Spectral band assignments
3500	Stretching vibration of O-H
2953, 3000	Stretching vibration of C-H
1731	Stretching vibration of C=O
1635	Stretching vibration of C=C
1350-1500	In-plane bending or twist of C-H
1200-1350	Bending vibration of -OH
1000-1200	Stretching vibration of C-O
800-1000	Out-of-plane bending of C-H
750	Out-of-plane bending of C-O

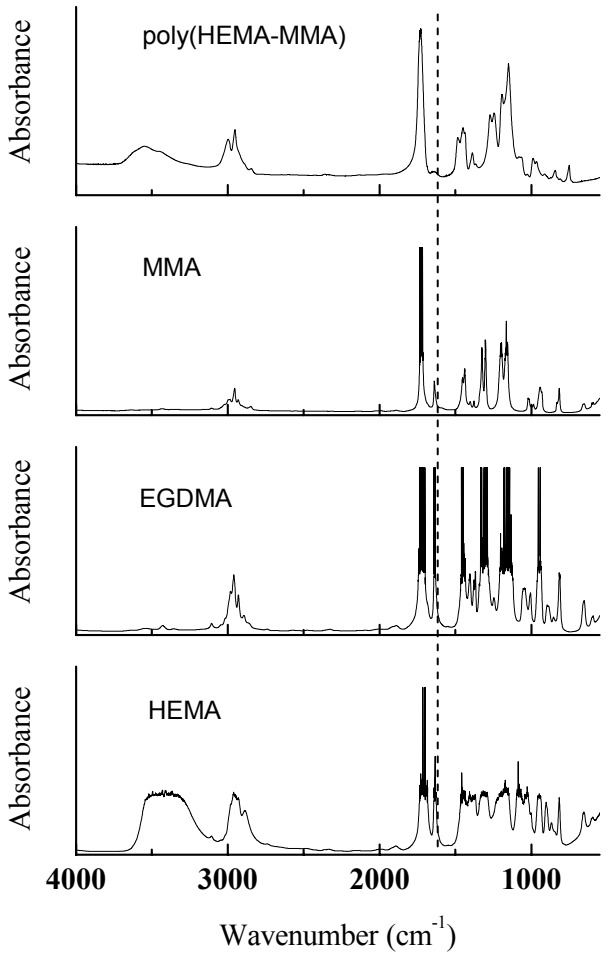

Figure 5-1 FT-IR spectra of poly(HEMA-MMA) polymer synthesized in the present studies. HEMA/MMA=2ml/12ml, EGDMA=2.8mol%.

5.3 Glass Transition Temperature

Table 5-2 shows the estimated glass transition temperature of some selected samples synthesized under different monomer volume ratios and EGDMA molar concentrations using the Fox equation. It can be seen that the glass transition temperature is increased with an increase in the EGDMA molar concentration and the MMA content.

Table 5-2 Glass Transition Temperature of Poly(HEMA-MMA)

HEMA (ml)	MMA (ml)	EGDMA (mol%)	T_g (K)
9.4	4.7	8.4	369.5
9.4	4.7	17.7	374.2
9.4	4.7	23.5	376.9
2	12	7.9	378.7
2	12	16.7	382.4
2	12	22.3	384.5

5.4 Porous Structures and Characterization

According to the present studies, it was found that the EGDMA molar concentration, the porogen volume ratio and the HEMA content play an important role in the particle morphology and the formation of the porous structures of poly(HEMA-MMA) particles.

5.4.1 Effect of EGDMA Molar Concentration

Effect of the crosslinking in terms of the EGDMA molar concentration was studied under a certain porogen volume ratio and certain levels of monomer volume ratios, HEMA/MMA=2ml/12ml and HEMA/MMA=9.4ml/4.7ml. The particles were synthesized at various EGDMA molar concentrations as shown in Table 5-3.

5.4.1.1 Particle Morphology

Particle morphology has a great impact on the end-use properties of porous polymers. For many applications, separated spherical particles with minimized agglomerated particles of irregular shapes are preferred. The average particle diameters and the particle morphology are illustrated in Table 5-3 and Figure 5-2.

As shown in Table 5-3, if the amounts of HEMA and MMA used in the reactions are identical, lower EGDMA molar concentration implies that the overall porogen concentration is higher in the monomer mixtures. It has been observed that higher non-solvent contents for poly(HEMA) result in a smaller

size of the phase-separated droplets (Chirila, 2001). Therefore, the formation of smaller particles is favorable at lower EGDMA molar concentration.

Table 5-3 Reaction compositions and the experimental results of the synthesis of the porous poly (HEMA-MMA) particles at various EGDMA molar concentrations; r_{oct}=1; T=70°C; Agi=500rpm

No.	HEMA (ml)	MMA (ml)	EGDMA (mol%)	Porosity (%)	d_2 (g/cm^3)	d_0 (g/cm^3)	S_v (m^2/g)	Average Pore Size (nm)	Average Particle Size (μm)	Particle Morphology
HM1	2	12	0.6	50.3	1.17	0.86	10.4	7.0	12.0±6.2	p
HM2	2	12	2.8	67.4	1.15	0.74	22.1	9.4	10.2±3.7	p
HM3	2	12	7.9	73.4	1.22	0.67	56.8	32.2	26.0±8.7	p
HM4	2	12	16.7	61.8	1.24	0.81	65.4	23.2	37.5±8.5	p, a
HM5	2	12	22.3	57.1	1.24	0.71	57.7	18.8	45.7±10.8	p, a
HM6	9.4	4.7	0.6	8.9	-	-	-	-	-	i
HM7	9.4	4.7	3.0	25.8	-	-	-	-	-	i
HM8	9.4	4.7	8.4	64.5	1.25	0.85	22.7	46.7	93.6±26.6	p
HM9	9.4	4.7	17.7	52.8	1.32	1.03	42.3	53.1	95.9±11.4	p
HM10	9.4	4.7	23.5	46.6	1.76	0.97	98.3	17.3	24.7±5.84	p, a

p: particle; a: the presence of the aggregated particles; i: the presence of the irregular particles

At higher EGDMA concentration, aggregated particles were observed, such as HM4, HM5 and HM10 because higher MMA and EGDMA concentration result in higher viscosity of the droplets. Another reason might be that more pendent vinyl groups are present at higher EGDMA concentration so that the particles could agglomerate together through the reaction between the pendent vinyl groups on the surface. In addition, the data shown in Table 3-2 implies that some monomers dissolved in the aqueous phase could transfer radicals from the organic phase to the aqueous phase during the reaction, and these radicals can react with other pendant vinyl groups on the surface of the droplets through solution polymerization, resulting in the particle aggregates.

However, under higher HEMA content and at lower EGDMA concentration, the irregular polymer particles were obtained, such as HM6 and HM7. Under higher HEMA content, more HEMA will be lost in the aqueous phase to generate much smaller fine particles in water since water is a non-solvent for poly(HEMA) as well (Dušek et al, 1971). Therefore, the agglomeration of these fine particles and other particles after reaction results in larger irregular particles, whereas a faster crosslinking reaction could lead to increased particle formation to give better particle morphology at higher EGDMA concentration. Figure 5-2 shows the morphology of the selected polymer samples synthesized at different EGDMA concentration. Therefore, the porous poly(HEMA-MMA) particles with good particle morphology were obtained in the present studies.

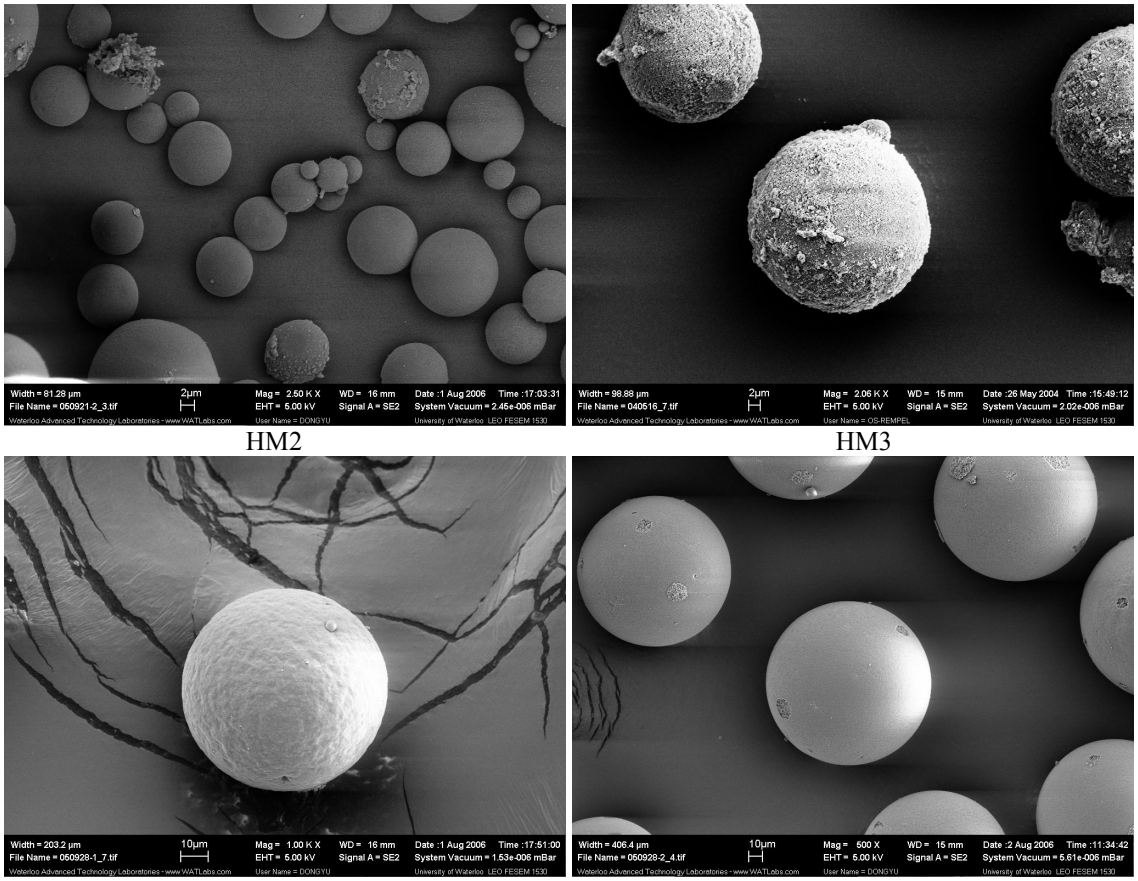

Figure 5-2 Particle morphology of the selected particle samples; HM2: scale bar 2µm, [EGDMA]=2.8mol%, HEMA/MMA=2ml/12ml; HM3: scale bar 2µm, [EGDMA]=7.9mol%, HEMA/MMA=2ml/12ml; HM8: scale bar 10µm, [EGDMA]=8.4mol%, HEMA/MMA=9.4ml/4.7ml; HM9: scale bar 10µm , [EGDMA]=17.7mol%, HEMA/MMA=9.4ml/4.7ml; r_{oct}=1

5.4.1.2 Porous Structures

As shown in Table 5-3 and Figure 5-3, with an increase in the EGDMA molar concentration, the maximums of the porosity and the pore volume were observed. Although the porosity and the pore volume are decreased beyond the maximum values, the specific porous surface area is increased. The apparent density (d_0) is lower at lower EGDMA concentration, whereas it is increased at higher EGDMA concentration. The skeletal density d_2 keeps increasing with an increase in the EGDMA concentration. These imply that the polymer network is more compact and there are more pores generated in the particles.

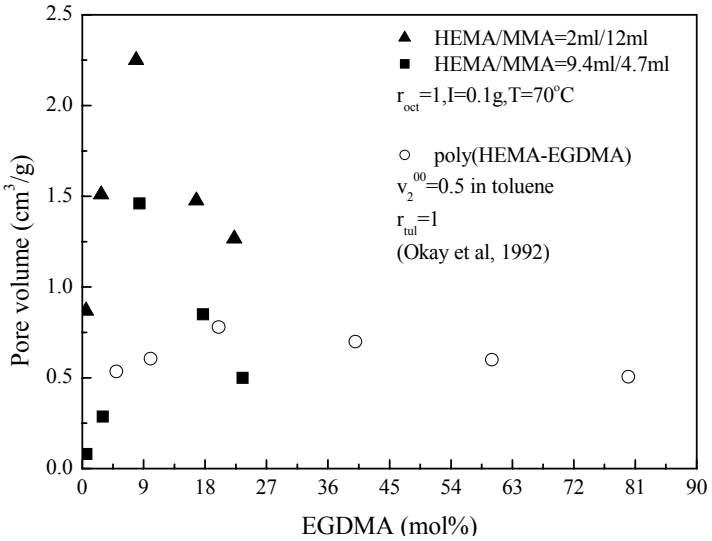

Figure 5-3 Change of the pore volume at various EGDMA concentration for the porous poly(HEMA-MMA) particles; the raw data are shown in Appendix I

It is well known that the formation of the pores is induced by phase separation in the presence of a non-solvent for the polymer. However, the mechanisms of the phase separation, which have been termed χ-induced syneresis and ν-induced synerisis (Okay et al, 1992), are related to the relative amount of the crosslinker and the porogen. At low EGDMA concentration, the residual monomer-porogen mixture is a non-solvent for the growing copolymer chains, whereas it becomes a good one as the EGDMA content increases (Okay, 2000).

At a lower EGDMA concentration, the flexible polymeric networks can be swollen by the solvent-monomer mixtures more easily so that the phase separation occurs at or even later than the original gel point. The porogen phase is separated in the system when the polymer chains grow to a certain extent (Dušek, 1970). Therefore, upon phase separation, there are two phases, including the polymer phase (network phase) and the porogen phase. Since the polymer chains have better solubility in the polymer phase than in the solvent phase (Kwok et al, 2005), this process could also be described by the Gibbs free energy as shown in the equation (2-1). From a thermodynamic point of view, with an increase in the polymerization conversion, ΔS_{mix} is reduced because of the presence of more synthesized polymers so that ΔG_{mix} between polymers and non-solvent is more positive until another steady state is reached which is the phase separation (Kwok et al, 2005). Thus, increasing EGDMA concentration (increasing crosslinking density indeed) results in the separation of more porogen (Dušek, 1970), inducing more pores and leading to higher porosity and higher pore volume.

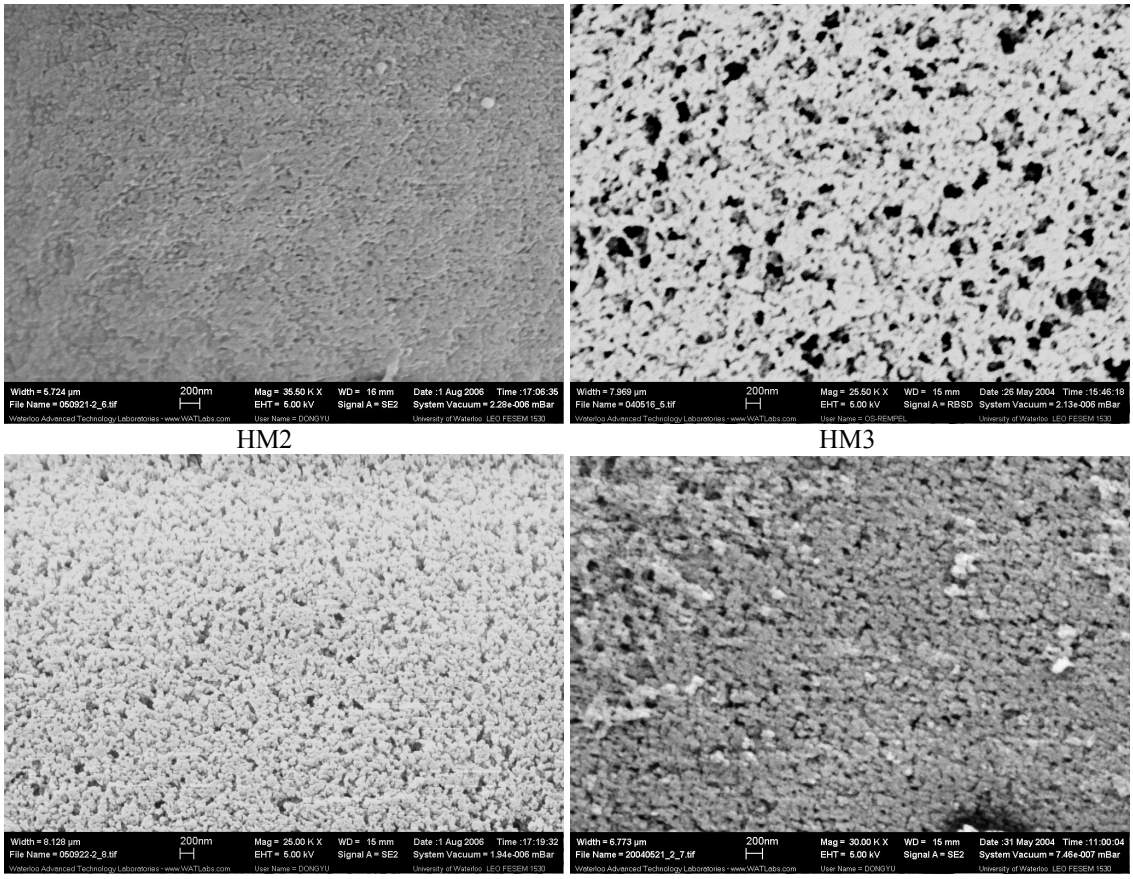

Figure 5-4 Porous structures of poly(HEMA-MMA) particles synthesized at different EGDMA molar concentration; Scale bar: 200nm; HEMA/MMA=2ml/12ml and r_{oct}=1; HM2: [EGDMA]=2.8mol%; HM3: [EGDMA]=7.9mol%; HM4: [EGDMA]=16.7mol%; HM5: [EGDMA]=22.3mol%

However, the pores could be collapsed or shrunk during porogen removal at lower crosslink density because of the flexibility and weak mechanical strength of the polymer chains (Okay, 2000). If the EGDMA concentration keeps increasing, the highly crosslinked microgels which are difficult to swell are separated earlier than the original gel point (Okay, 2000). An increase in crosslinking density induces smaller microgels and shorter polymeric segments between crosslinking points, resulting in much smaller pores. This is why the porosity and the pore volume decrease after the transformation points as shown in Figure 5-3 and Table 5-3. The pore volume data are compared with the pore volume of poly(HEMA-EGDMA) synthesized in the presence of toluene reported by Okay et al (1992). It can be seen that the presence of MMA makes the transformation point occur earlier and the pore volume is much higher. Some data are lower than the reported ones, which may be caused by the lower EGDMA concentration or much smaller microgels at higher EGDMA concentration used in

this study. However, smaller pores generated by more discrete structures could result in higher specific porous surface area as shown in Table 5-3.

The surface porous structures of selected samples are shown in Figure 5-4 and Figure 5-5. It can be seen that the particle surface becomes more heterogeneous with an increase in the EGDMA concentration because of the presence of more discrete microgels separated resulting from the phase separation. At the lowest EGDMA molar concentration, discrete structures are hardly seen. Therefore, these pictures substantiate the transformation from χ-induced syneresis to ν-induced syneresis because ν-induced syneresis generates more discrete structures. As to the particles produced under higher HEMA content, the surface is smoother for various EGDMA concentrations. But it still can be seen that the surface becomes rougher at higher EGDMA concentration as shown by the SEMs of Figure 5-5. At the highest EGDMA molar concentration and higher HEMA contents, such as HM10, the porous surface area is much higher than that under lower HEMA contents, which could be caused by the formation of more pores of a smaller size.

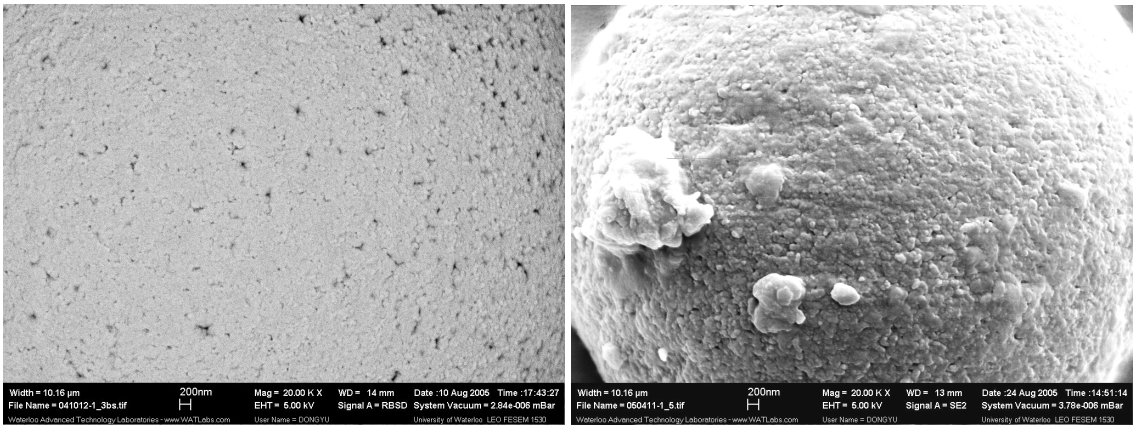

HM8 HM10

Figure 5-5 Porous structures of poly(HEMA-MMA) particles at various EGDMA molar concentrations; Scale bar: 200nm; HEMA/MMA=9.4ml/4.7ml and r_{oct}=1; HM8: [EGDMA]=8.4mol%; HM10: [EGDMA]=23.5mol%

The formation of the pores can also be described by the profiles of the pore size distribution as shown in Figure 5-6 and Figure 5-7. It was found that the pore size distribution has a different behavior at various EGDMA concentrations. As shown in Figure 5-6, the results are consistent with those shown in the SEM pictures of Figure 5-4. Obviously, at lower HEMA content, the pore size becomes larger at the critical point followed by a decrease in the pore size with an increase in the EGDMA concentration, and more pores are generated at higher EGDMA concentration. Under higher HEMA

content, as shown in Figure 5-7, there are much more pores at higher EGDMA concentration. Therefore, higher EGDMA concentration is beneficial in generating more pores and result in good particle morphology.

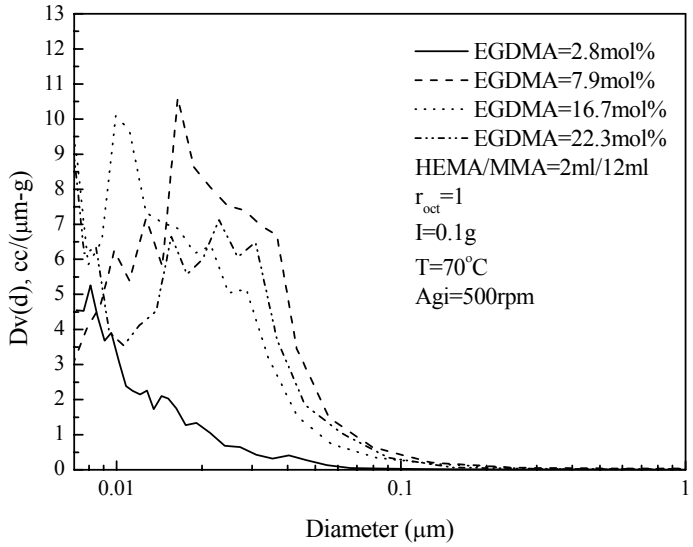

Figure 5-6 Pore size distribution of the porous poly(HEMA-MMA) polymer at various EGDMA concentrations at low monomer ratio

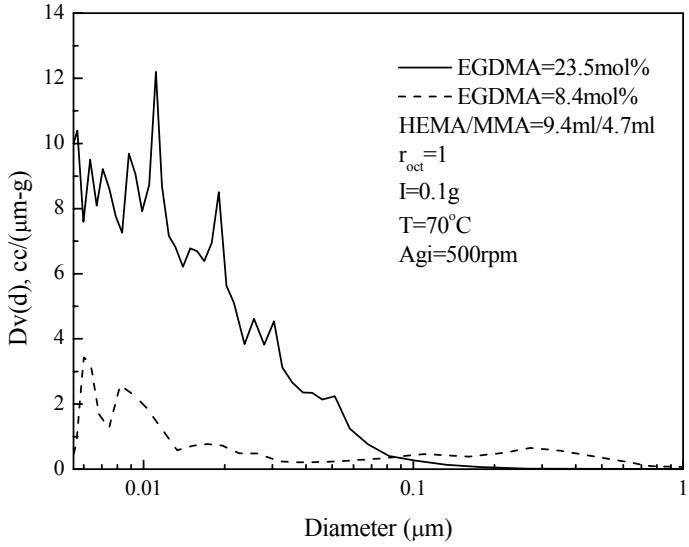

Figure 5-7 Pore size distribution of the porous poly(HEMA-MMA) particles synthesized at various EGDMA molar concentrations at high monomer ratio

5.4.2 Effect of Monomer Ratio

The effect of monomer ratio was studied at higher and lower EGDMA molar concentration. As shown in Table 5-4. The slight difference of the EGDMA molar concentration probably has a negligible effect.

Table 5-4 Reaction compositions and the experimental results of the synthesis of the porous poly (HEMA-MMA) particles at various monomer ratios; r_{oct}=1; T=70°C; Agi=500rpm

No.	HEMA (ml)	MMA (ml)	EGDMA (mol%)	Porosity (%)	d_2 (g/cm^3)	d_0 (g/cm^3)	S_v (m^2/g)	Average Pore Size (nm)	Particle Size (μm)	Particle Morphology
HM2	2	12	2.8	67.4	1.15	0.74	22.1	9.4	10.2±3.7	p
HM11	4.7	9.4	2.8	54.7	1.39	1.32	8.7	11.6	99.8±33.3	p, a
HM12	8.4	5.6	2.9	23.4	1.25	1.04	12.6	16.3	58.8±50.1	p, a
HM7	9.4	4.7	3.0	25.8	-	-	-	-	-	i
HM5	2	12	22.3	57.1	1.24	0.71	57.7	18.8	45.7±10.8	p, a
HM13	4.7	9.4	22.6	77.4	1.28	0.67	72.4	19.7	16.9	p
HM14	8.4	5.6	23.4	45.8	1.71	0.99	80.9	16.5	25.6±16.8	p
HM10	9.4	4.7	23.5	46.6	1.76	0.97	98.3	17.3	24.7±5.84	p, a

p: particle; a: the presence of the aggregated particles; i: the presence of the irregular particles

5.4.2.1 Particle Morphology

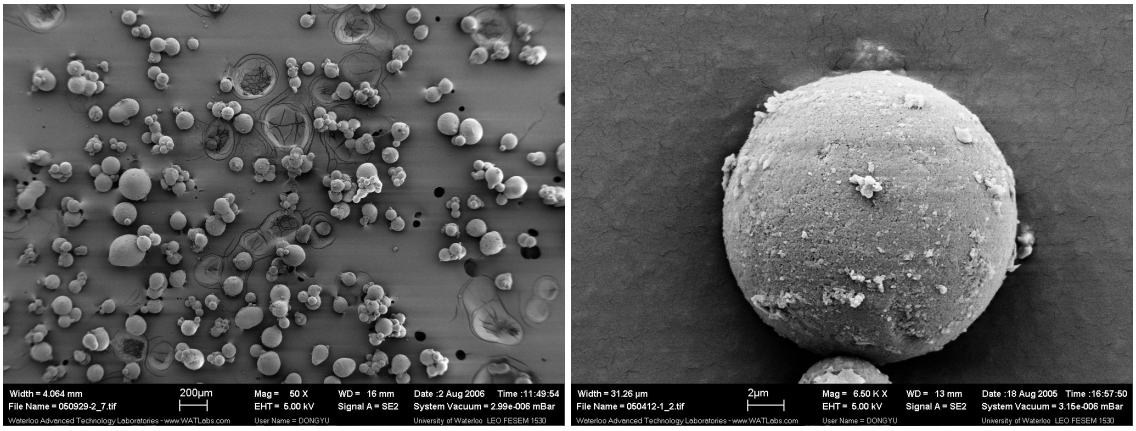

HM11 HM12

Figure 5-8 Particle morphology of the selected samples; HM11: scale bar 200μm, r_H=4.7ml/9.4ml; HM12: scale bar 2μm, r_H=8.4ml/5.6ml; [EGDMA]=~3mol%; r_{oct}=1

Particle morphology is changed with an increase in the HEMA content. At lower EGDMA molar concentration, the increase in the HEMA content results in more particle aggregates or irregular particles. The aggregates make the particle size distribution broader. Under higher HEMA content, the polymers tend to form networks (Bhawal et al, 2004). However, the networks swollen by the

solvent become more rubbery or liquid-like which have been observed in the present studies so that the particles are easily agglomerated to form aggregates or irregular particles. Figure 5-8 shows the particle morphology of the selected polymer samples under different HEMA content at certain EGDMA concentration.

5.4.2.2 Porous Structures

As shown in Table 5-4 and Figure 5-9, the porosity and the pore volume are reduced with an increase in the HEMA content. The polymers which show higher pore volume and porosity have lower apparent density, showing the presence of highly porous structures. However, further increase in the HEMA content does not change the porous volume much more. In addition, as shown in Table 5-4, the specific porous surface area increases with an increase in the monomer ratio at higher EGDMA concentration, whereas it seems to decrease at higher monomer ratios at lower EGDMA concentration. This should result from the different pore formation mechanisms at lower and higher EGDMA concentration as mentioned in the previous section.

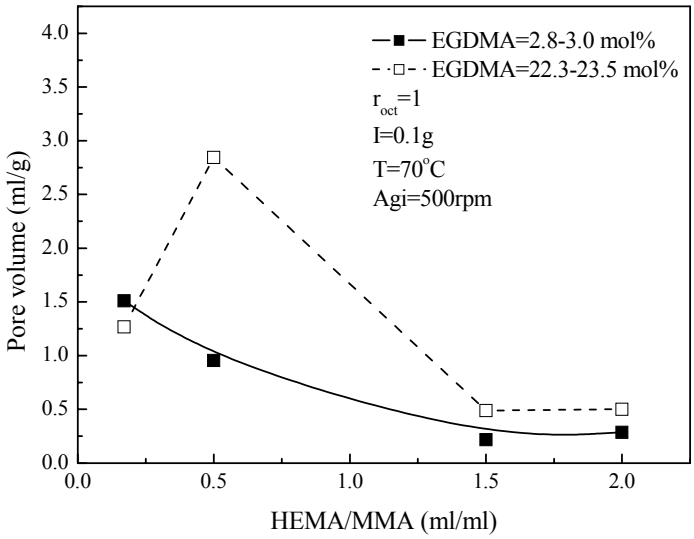

Figure 5-9 Change of the pore volume with monomer ratios of HEMA to MMA; the date are shown in Appendix I

Although 1-octanol is a non-solvent for poly(HEMA), the monomer mixture is a good one for the polymers (Horak, 1993). Therefore, under higher HEMA content and at higher EGDMA concentration, the polymers have better solubility in the reaction mixture. According to Okay et al (1992), good solvents result in lower pore volume and higher specific porous surface area. In the present studies, the same phenomenon was observed as shown in Table 5-4 and Figure 5-9. However,

at lower EGDMA molar concentration, higher HEMA content enhances the formation of the polymeric networks with the separated porogen phase, but the pores are probably collapsed seriously during solvent removal so that the pore volume, the pore size and the specific porous surface area are not changed to a considerable extent. As stated by other researchers, higher MMA content in poly(HEMA-MMA) leads to more discrete structures (Kwok et al, 2005). At lower EGDMA concentration, this structures are fused together easily to form smaller pores and smoother surfaces. Therefore, the polymers with higher HEMA content are less heterogeneous and more rubbery because poly(HEMA) is flexible and rubbery in the swollen state (Montheard, 1992) so that the pores are easily collapsed or even disappeared during porogen removal.

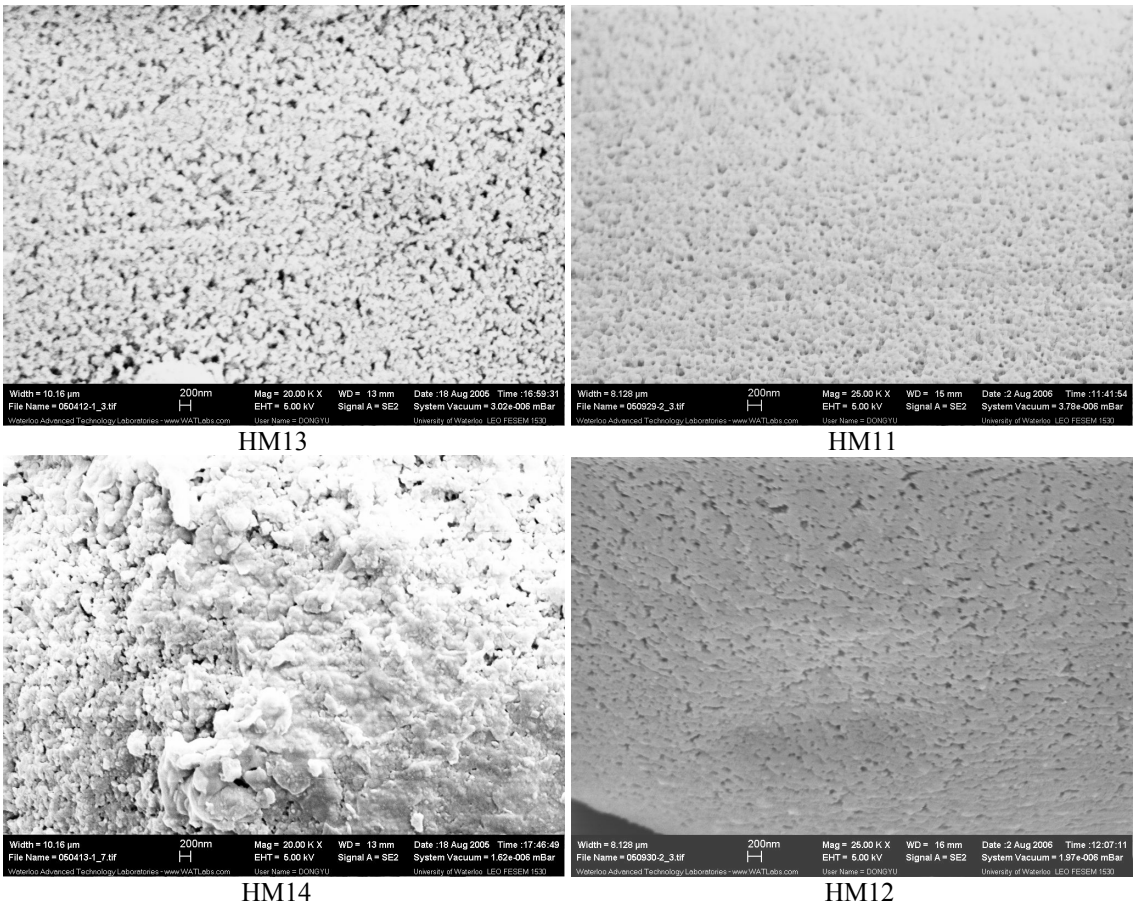

Figure 5-10 The porous structures of the porous poly(HEMA-MMA) particles synthesized at different monomer ratios; Scale bar: 200nm; HM11: r_H=4.7ml/9.4ml, [EGDMA]=~3mol%; HM12: r_H=8.4ml/5.6ml, [EGDMA]=~3mol%; HM13: r_H=4.7ml/9.4ml, [EGDMA]=~23mol%; HM14: r_H=8.4ml/5.6ml, [EGDMA]=~23mol%; r_{oct}=1

The changes of the porous morphology with an increase in the HEMA contents at the high and low levels of EGDMA molar concentration are shown in Figure 5-10. It can be seen that the pore size becomes smaller with an increase in the HEMA content at higher EGDMA concentration, whereas it becomes a little larger with an increase in the HEMA content under lower EGDMA content. According to the particle morphology and porous structures, it seems that the moderate HEMA contents are helpful to form the particles with highly porous structures and good morphology.

To fully understand the change of the porous structures, the pore size distribution profiles have to be studied as shown in Figure 5-11 and Figure 5-12. Figure 5-11 shows the pore size distribution with an increase in the HEMA content at lower EGDMA molar concentration. It can be seen that the pore size distribution is similar but there are more pores at lower HEMA content. Figure 5-12 shows the pore size distribution of the particles synthesized at higher EGDMA molar concentration. With an increase in the HEMA content, the pore size distribution moves toward smaller pores. Since HEMA has large side group and contributes to H-bonding, HEMA is a favorable monomer for forming networks. At lower EGDMA molar concentration, the networks are favored under higher HEMA content so that more porogen is separated, resulting in more pores. However, at higher EGDMA molar concentration, smaller microgels are separated under higher HEMA content to form smaller pores by the agglomeration. Generally speaking, higher HEMA content results in smaller pores.

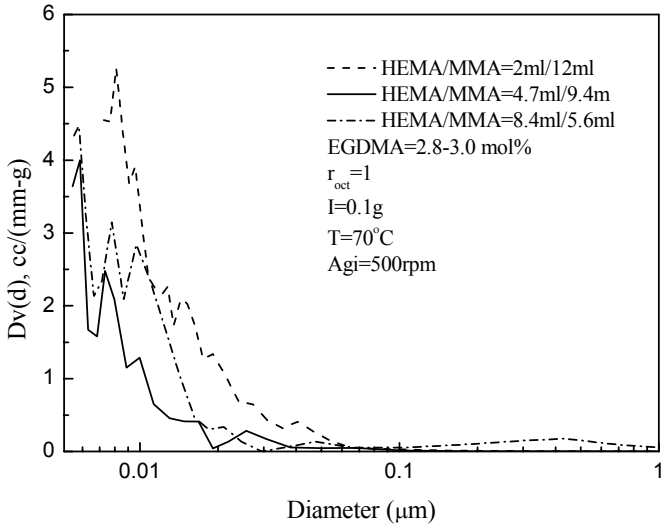

Figure 5-11 Pore size distribution of the porous poly(HEMA-MMA) particles synthesized under various monomer ratios at low EGDMA molar concentration

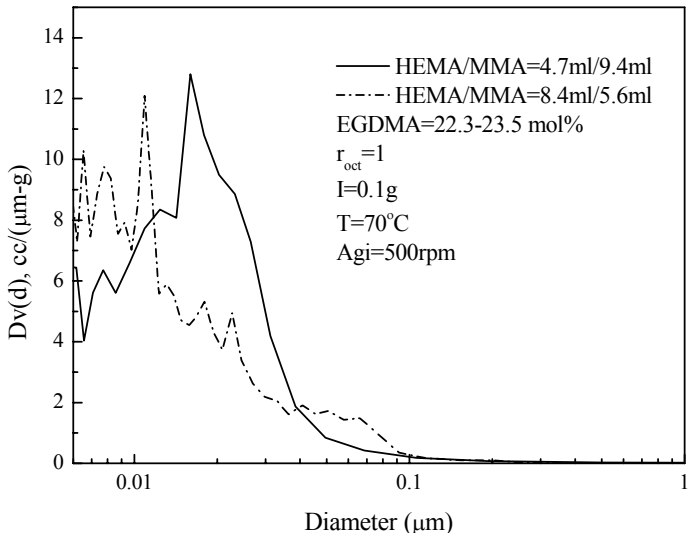

Figure 5-12 Pore size distribution of the porous poly(HEMA-MMA) particles synthesized under various monomer ratios at high EGDMA molar concentration

5.4.3 Effect of Porogen Volume Ratio

Table 5-5 shows the reaction conditions and experimental results for the studies on the effect of the porogen volume ratio on the porous characteristics. According to the results, the particle morphology and the porous structures are quite different at various porogen volume ratios.

Table 5-5 Reaction compositions and the experimental results of the synthesis of the porous poly (HEMA-MMA) particles at various porogen volume ratios; HEMA/MMA=9.4ml/4.7ml; T=70°C; Agi=500rpm

No.	EGDMA (mol%)	r_{oct}	Porosity (%)	d_2 (g/cm^3)	d_0 (g/cm^3)	Average Pore Size (nm)	Particle Size (μm)	Particle Morphology
HM15	3.0	0.5	19.2	-	-	-	-	i
HM16	3.0	0.65	27.1	-	-	-	-	i
HM17	3.0	0.8	48.0	-	-	-	-	i
HM7	3.0	1	25.8	-	-	-	-	i
HM18	23.5	0.5	20.7	1.29	1.11	12.2	15	p, a
HM19	23.5	0.65	66.4	1.60	1.21	17.1	38.7±15.3	p, a
HM20	23.5	0.8	53.1	1.24	0.94	12.1	72.5±11.3	p
HM10	23.5	1	46.6	1.76	0.97	17.3	24.7±5.84	p, a

p: particle; a: the presence of the aggregated particles; i: the presence of the irregular particles

5.4.3.1 Particle morphology

Irregular particles were observed at various porogen volume ratios at lower EGDMA molar concentration. According to the previous discussion, higher HEMA content and lower EGDMA

concentration are the main reasons for the formation of the irregular particles. The morphology of some irregular particles is shown in Figure 5-13. The shrunk particles can be seen in the samples synthesized under higher porogen concentration, such as HM17. Obviously, the networks are collapsed and the rubbery polymers agglomerate together to form irregular particles. At higher EGDMA concentration, as shown in Figure 5-14, good particle morphology was obtained. It was observed that an optimized porogen volume ratio exists to obtain the best particle morphology without any aggregates and the particle distribution is uniform, such as HM20.

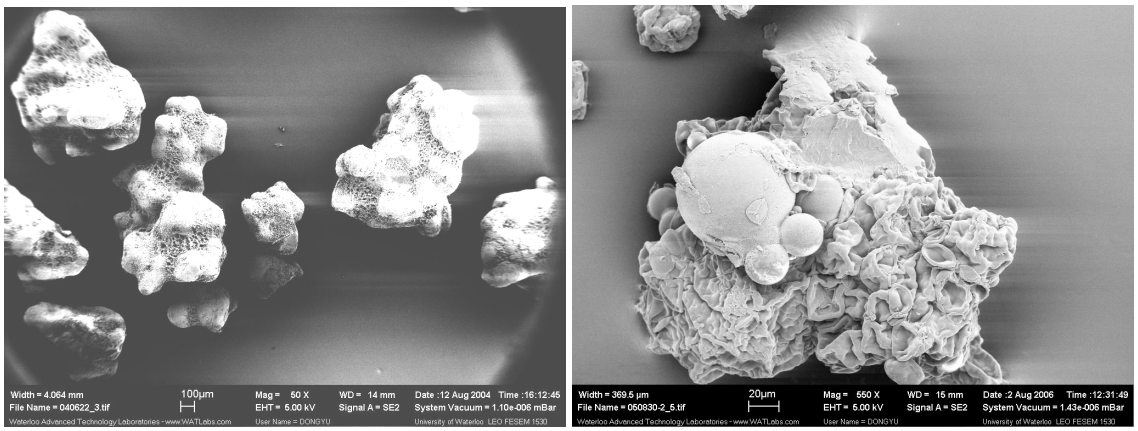

HM15 HM17

Figure 5-13 Irregular particle morphology of the selected particle samples; r_H=9.4ml/4.7ml; [EGDMA]=3mol%; HM15: r_{oct}=0.5, scale bar 100µm; HM17: r_{oct}=0.8, scale bar 20µm

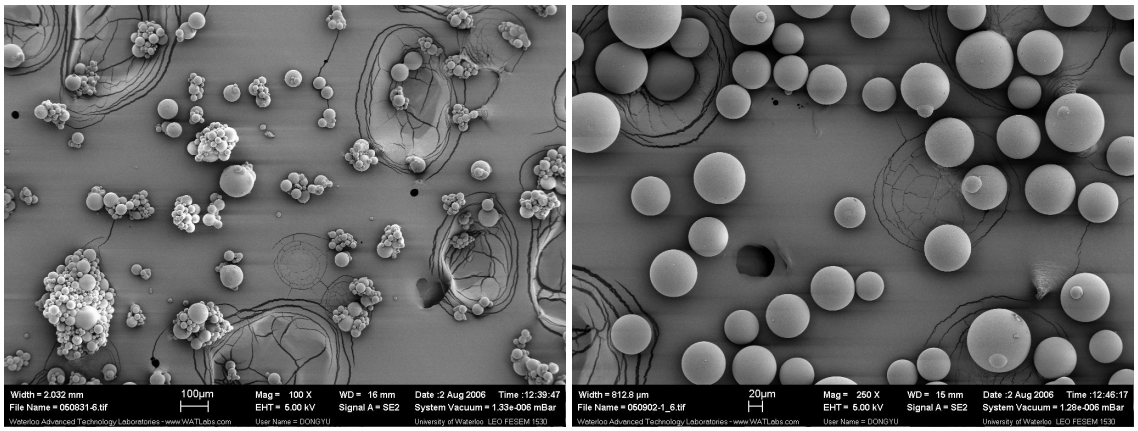

HM19 HM20

Figure 5-14 Particle morphology of the selected particle samples; r_H=9.4ml/4.7ml; [EGDMA]=23.5mol%; HM19: r_{oct}=0.65, scale bar 100µm; HM20: r_{oct}=0.8, scale bar 20µm

5.4.3.2 Porous Structures

As shown in Table 5-5 and Figure 5-15, maximums of the porosity and the pore volume were observed. However, the apparent density decreases a little bit at higher porogen volume ratio, showing the presence of the highly porous structure. This phenomenon is similar with that observed in the synthesis of the porous poly(St-DVB) particles because higher solvent concentration could result in the further dilution of monomer so that isochoric conditions can not be held (Okay, 2000). This implies that the phase separation will be enhanced by higher non-solvent concentration, and the separated phase diminishes in size with the increased non-solvent concentration in the monomer mixture (Dalton et al, 2002). Therefore, the pore size is reduced by the agglomeration of separated phase of smaller size so that the pore volume and the porosity are reduced as well.

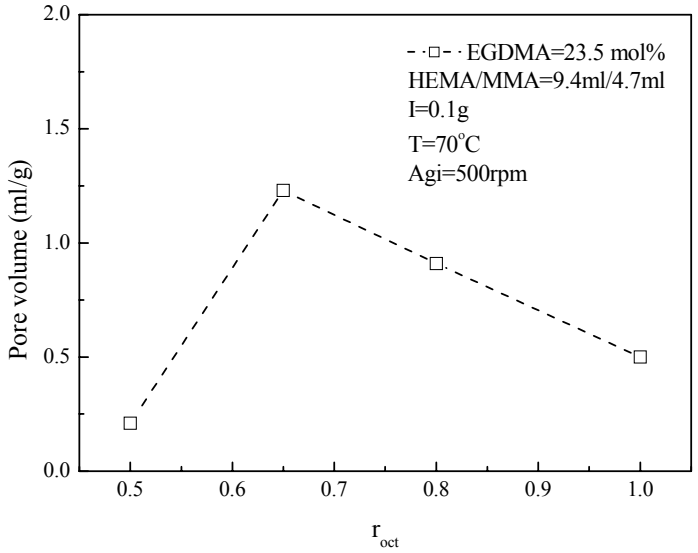

Figure 5-15 Changes of the pore volume at various porogen volume ratios at high EGDMA molar concentration; the data are shown in Appendix I

Smaller microgels lead to higher internal porous surface area as shown in Figure 5-16. In addition, at lower EGDMA concentration, the polymeric networks can absorb more solvent because of the loose networks. However, the network collapse and the agglomeration of the particles are serious. Figure 5-17 shows the morphology of the porous structures at various porogen volume ratios at higher EGDMA concentration. The nano-pores can be clearly seen.

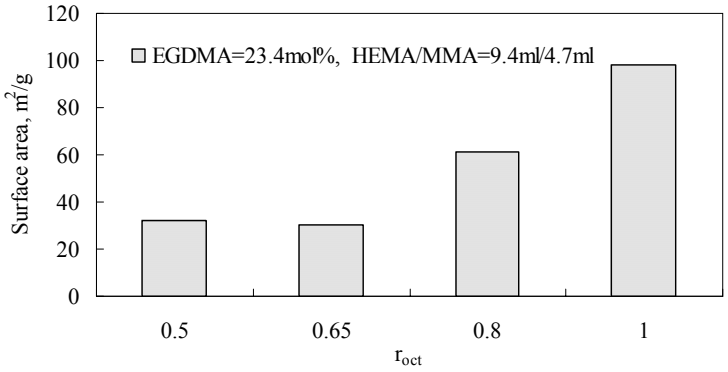

Figure 5-16 Specific porous surface area at various porogen volume ratios; the data are shown in Appendix I

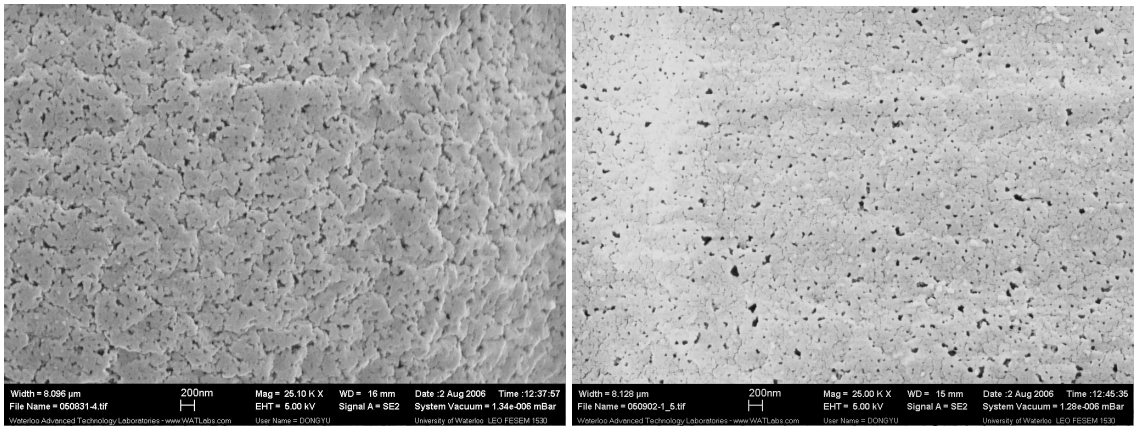

HM19 HM20

Figure 5-17 The porous structures of the porous poly(HEMA-MMA) particles at various porogen volume ratios; Scale bar: 200nm; HM19: r_{oct}=0.65; HM20: r_{oct}=0.8; HEMA/MMA=9.4ml/4.7ml; [EGDMA]=23.5mol%

The pore size distribution as shown in Figure 5-18 demonstrates the change of the pore size with an increase in the porogen volume ratios. The shape of the distribution profiles is quite similar. However, the amount of pores of the various sizes is increased with an increase in the porogen volume ratio according to the height of the peaks. This implies that higher porogen concentration induces more pores. Importantly, the fraction of the pores which are larger than 10 nm is increased greatly as an increase in the porogen concentration, showing the formation of looser polymeric networks. During porogen removal, some pores could be shrunk to form smaller pores so that the fraction of pores whose size is close to 10 nm is greatly increased at higher porogen volume ratio. This results in the rapid increase in the porous surface area as shown in Figure 5-16. Therefore, higher porogen volume ratios contribute more pores in the porous poly(HEMA-MMA) particles.

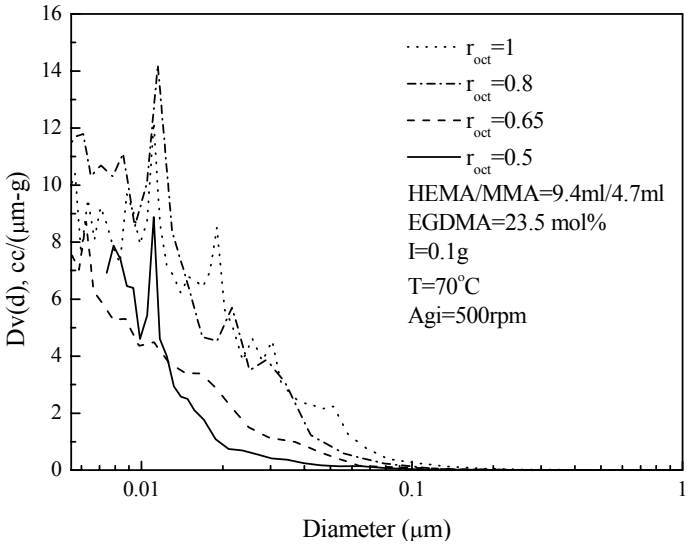

Figure 5-18 Pore size distribution of the porous poly(HEMA-MMA) polymers prepared under various porogen volume ratios

5.4.4 Controllable Pore Size

According to the above discussion, it can be concluded that the pore size of the porous poly(HEMA-MMA) particles can be controlled by combining various EGDMA concentrations, porogen volume ratios and monomer ratios. As shown in the above profiles of the pore size distribution, several peaks can be observed, resulting from the random movement of polymeric chains, the random agglomeration of the microgels and the shrinkage of the pores. Therefore, the average pore size (diameter) calculated using equation (4-10) was used to evaluate the controllable pore size in the porous poly(HEMA-MMA) particles.

As for the pore formation in the porous polymers induced by phase separation, some researchers have used phase diagrams to illustrate the phase changes or the polymer morphology changes during the course of the reaction or in the resultant polymers at the final state (Goh et al, 2002; Gan et al, 1994). However, there are no reports about the controllable pore size in the porous polymers. In the present studies, the diagrams, as shown in Figure 5-19, about the controllable pore size of the porous poly(HEMA-MMA) particles synthesized under the studied reaction conditions were proposed. These diagrams will be helpful to industrial users to synthesize the polymers with favorable pore size.

According to Figure 5-19(A), it can be seen that the average pore size is smaller at lower porogen volume ratios and lower EGDMA concentration. The pore size is larger at moderate EGDMA concentration and higher porogen volume ratios. According to Figure 5-19(B), basically, under

various monomer ratios, the pore size is bigger at moderate EGDMA concentration. If HEMA content is higher, at certain EGDMA concentrations, the pore size is larger. However, below 15vol% of EGDMA concentration, the pore size is the smallest. In a word, the pore size can be controlled in the present studies. By using the diagrams about controllable pore size (Figure 5-19), the porous poly(HEMA-MMA) particles with the designed pore size and the favorable network properties could be synthesized. This will be very significant to the industrial use.

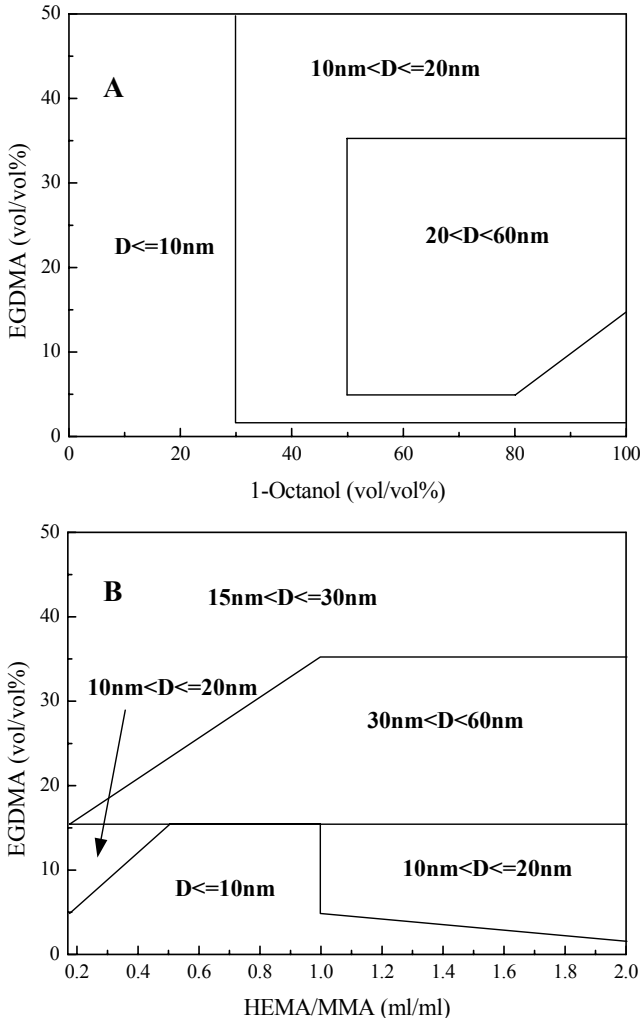

Figure 5-19 Controllable pore size of the porous poly(HEMA-MMA) particles synthesized under various reaction conditions in the present studies

5.5 Modeling of the Porous Poly(HEMA-MMA) Polymer

5.5.1 Model Assumptions

The main assumptions of the model are (Okay, 1994 and 1999): (1) the steady-state approximation is assumed for each of the radical species; (2) thermodynamic equilibrium for every reaction step; (3) polymerization and crosslinking reactions in the network and separated phases are identical; (4) application of Flory-Huggins theory for affine networks, the theory of rubber elasticity and the kinetic theories of gel formation.

5.5.2 Physical Model and Thermodynamics

To predict the porous characteristics, thermodynamic aspects have to be taken into account. According to Okay (1999), a physical model consisting of unreacted monomers, (non)solvent, soluble polymers and polymer networks is used to illustrate the gel and the pores formation beyond the gel point. For the porous polymer particles, the physical model is shown in Figure 5-20.

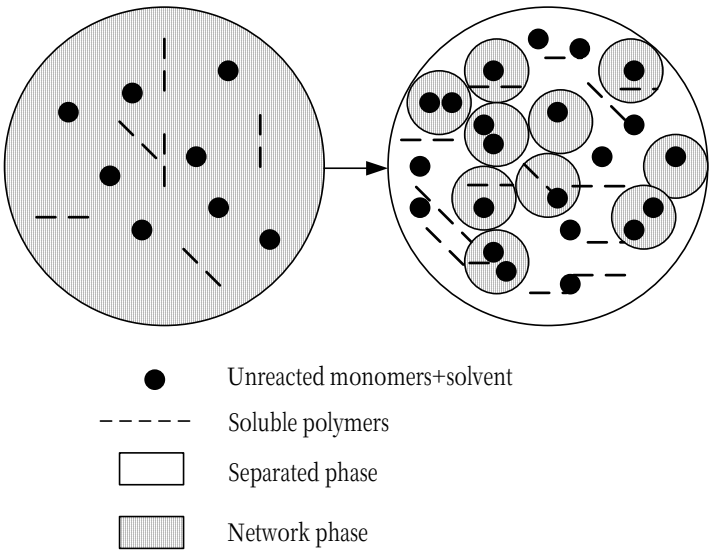

Figure 5-20 A physical model of porous particle synthesis in the state of before (left) and (after) phase separation

There are three components in the system beyond the gel point as described by this physical model, including diluent (unreacted monomers+porogen, Component 1), the networks (Component 2) and soluble polymers (Component 3). Amongst them, the diluent and the soluble polymers compose the

separated phase after the phase separation. Obviously, this whole system can be treated as polymer networks swollen by the separated phase, which implies that this system can be described using swelling thermodynamics. According to Flory and Rehner (1943), the swelling of a nonionic polymer network is governed by two free energy terms, ΔG_{mix}, the free energy of mixing, and ΔG_{el}, the free energy of elastic deformation as shown in the equation (5-1),

$$\Delta G = \Delta G_{mix} + \Delta G_{el} \qquad (5\text{-}1)$$

From Flory-Huggins theory for the affine networks (Flory, 1953), ΔG_{mix} and ΔG_{el} can be calculated using equations (5-2) and (5-3),

$$\Delta G_{mix} = RT(\sum_i n_i \ln v_i + \sum_{i<j} n_i v_j \chi_{ij}) \qquad (5\text{-}2)$$

$$\Delta G_{el} = (3/2)(RT/NV_s)((v_2^0/v_2)^{2/3} - 1 - \ln(v_2^0/v_2)^{1/3}) \qquad (5\text{-}3)$$

where n_i is the number of moles of the species i (1-diluent, 2-network, 3-soluble polymers), v_i is the volume fraction with respect to the whole system, χ_{ij} is the Flory interaction parameter between species i and j, N is the average number of segments between crosslinks in the network chains, v_2^0 is the volume fraction of the polymer networks in the network phase (gel) at a given degree of polymerization, and V_s is the molar volume of the porogen. Substitution of equations (5-2) and (5-3) into equation (5-1) and differentiating with respect to the number of moles of the diluent n_1 and the soluble polymer n_3 for both of the network phase (gel) and the separated phase (sol) provide the equations of chemical potentials μ_i for the diluent and the soluble polymers in the different phases. From the thermodynamic point of view, at the equilibrium swelling state, the chemical potentials of the diluent and the soluble polymers in the separated phase and in the network phase should be equal so that equations (5-4) and (5-5) are obtained,

$$\Delta\mu_1 - \Delta\mu_1' = 0 \qquad (5\text{-}4)$$

$$\Delta\mu_3 - \Delta\mu_3' = 0 \qquad (5\text{-}5)$$

where μ_i' and μ_i represent the chemical potentials in the network phase and in the separated phase, respectively.

It has been shown that the pores are induced by the phase separation. This implies that the degree of dilution ($v_2^{0\,-1}$) can not be higher than the swelling capacity of the network (v_2^{-1}) during the course of the reaction (Dušek, 1965 and 1967), which means $v_2^{0\,-1}$ and v_2^{-1} are equal at the incipient phase separation so that equation (5-6) is given,

$$v_2 = v_2^0 \qquad (5\text{-}6)$$

Consequently, equations (5-7) and (5-8) are obtained for the swelling system in 1-octanol for the present studies. The derivation of these two equations can be found in Appendix II.

$$0.5N^{-1}v_2^0 + \ln\left(\frac{v_1}{v_1^{'}}\right) + (1 - v_1 - v_3^{'}) - (v_3 - v_3^{'})/y + \chi_{12}v_2^{0\,2} + \chi_{13}(v_3^2 - v_3^{'\,2}) + (\chi_{12} + \chi_{13} - \chi_{23})v_2^0 v_3 = 0 \qquad (5\text{-}7)$$

$$-\ln\left(\frac{v_1}{v_1^{'}}\right) + (1/y)\ln\left(\frac{v_3}{v_3^{'}}\right) + 2\chi_{13}(v_3^{'} - v_3) + (\chi_{23} - \chi_{12} - \chi_{13})v_2^0 = 0 \qquad (5\text{-}8)$$

In equations (5-7) and (5-8), v_3 and $v_3^{'}$ are the volume fractions of soluble polymers in the gel and in the sol, respectively. v_1 and $v_1^{'}$ are the volume fractions of diluent in the gel and in the sol, respectively. The parameters χ_{12}, χ_{13} and χ_{23} are the Flory-Huggins interaction parameters between each component. N is the number of the repeat units or the segments between crosslinks, and y is the number of segments for the soluble polymers.

In addition to the above equations showing the thermodynamic balance, the material balance between the gel phase and the sol phase are shown in equations (5-9), (5-10) and (5-11).

$$v_1 + v_2^0 + v_3 = 1 \qquad (5\text{-}9)$$

$$v_1^{'} + v_3^{'} = 1 \qquad (5\text{-}10)$$

$$v_2^0 = \bar{v}_p W_g / v_g \qquad (5\text{-}11)$$

where v_g is the volume fraction of the polymeric networks in the whole reaction system at the specific volume conversion α, and $\bar{v}_p$ is the volume fraction of the sol and gel polymers in the whole reaction system. W_g is the gel fraction. $\bar{v}_p$ can be calculated using the equation (5-12) (Okay, 1999).

$$\bar{v}_p = \frac{\alpha v_2^{00}(1 - \varepsilon_c)}{(1 - \alpha v_2^{00}\varepsilon_c)} \qquad (5\text{-}12)$$

where v_2^{00} is the initial volume fraction of the monomers in the reaction mixtures, and ε_c is defined as the contraction factor (Okay, 1994) which is equal to $1\text{-}d_M/d_P$. In the present studies, d_M was used as the average density of the monomer mixtures and d_P was the density of the homogeneous polymers. The derivation of equations (5-11) and (5-12) can be seen in Appendix III.

With regard to the Flory interaction parameters, it can be assumed that $\chi_{12}=\chi_{13}$ and $\chi_{23}=0$ because the gel and the sol polymers are assumed to have the same chemical compositions (Okay, 1999). The interaction parameter between the diluent and the polymers can be calculated using the following equation (Okay, 1994),

$$\chi_{12} = \chi_{12}^{m} + (\chi_{12}^{s} - \chi_{12}^{m})\Phi_{sol} \qquad (5\text{-}13)$$

Where χ_{12}^{m} is the monomer-polymer interaction parameter and χ_{12}^{s} is the porogen-polymer interaction parameter. Φ_{sol} is the volume fraction of the porogen in the reaction mixture at certain reaction time related with the volume conversion, i.e.,

$$\Phi_{sol} = \frac{1 - v_2^{00}}{1 - \alpha v_2^{00}} \qquad (5\text{-}14)$$

Since the monomer mixtures consisting of HEMA, EGDMA and various comonomers are present in the reaction systems, the average interaction parameter is used. According to Barton (1983), the Flory interaction parameter can be estimated using the solubility parameters as shown in equation (5-15),

$$\chi_{12}^{m} \approx 0.34 + \frac{V_{m,1}}{RT}(\delta_1 - \delta_2)^2 \qquad (5\text{-}15)$$

where $V_{m,1}$ is the average molar volume of the monomer mixture, and T is the reaction temperature, and R is the gas constant. The solubility parameters of the monomer mixtures (δ_1) can be calculated from the solubility parameters of each monomer as shown in equation (5-16) (Okay et al., 1992),

$$\delta_1 = \frac{v_2^{00}(1-x)\sum_{i=1}^{3} f_i \delta_{mi}}{1 - x v_2^{00}} \qquad (5\text{-}16)$$

where x is the overall conversion of the monomers and δ_{mi} is the solubility parameter of the monomer i. f_i is the volume fraction of the monomer i in the monomer mixtures. The solubility parameters of the copolymers (δ_2) can be estimated using equation (5-17) (Okay et al., 1992),

$$\delta_2 = \sum_{i=1}^{3} f_i \delta_{pi} \qquad (5\text{-}17)$$

where δ_{pi} is the solubility parameter of the homopolymer synthesized from monomer i. The interaction parameter χ_{12}^{s} is one of the independent variables in the model to represent the thermodynamic aspect of the porogen used in the synthesis of the porous polymeric particles which can also be calculated using equation (5-15) with corresponding parameters.

To solve equations (5-7) through (5-12), the kinetic parameters, including W_g, N, y and α, have to be obtained from the output of the gelation kinetic model.

5.5.3 Gelation Kinetic Model

In the reaction kinetic part, the additional assumptions which are similar with those made by Okay (1999) have to be made: i) every pendent vinyl group has the same reactivity; ii) chain transfer reactions are ignored; iii) the polymerization is terminated mainly by coupling.

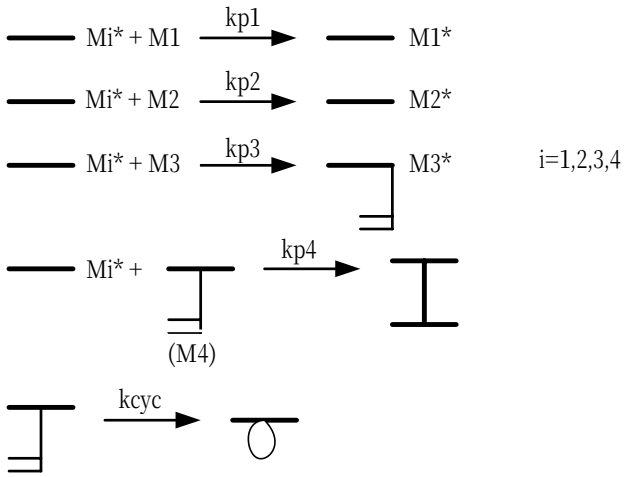

Scheme 1 Monomer reactions and radical types in the reaction system.

Compared to the simulation for porous poly(St-DVB) polymers, the systems in the present studies are much more complicated because of the presence of one more comonomer. However, the kinetic method used by Tobita et al (1989) and Okay (1994) is still applicable. According to this method, four types of radicals are taken into account in the reactions as shown in Scheme 1. These four types of radicals include those ended with M_1 (HEMA), those ended with M_2 (MMA, St or NVP), those ended with M_3 (EGDMA) and pendent vinyl groups M_4. If the pendent vinyl groups connect two polymeric chains as shown in Scheme 1, crosslinked structures are formed. The last step illustrated in Scheme 1 shows the self-cyclization of pendent vinyl groups, which has been found in many crosslinking polymerizations (Elliott et al, 1999 and 2001; Ward et al, 2000). The reaction rate equations for each monomer can be derived accordingly as shown in equations (5-18)-(5-24):

$$r_I = -k_d[I] \tag{5-18}$$

$$r_{M_1} = -k_{p1}[R^*][M_1] \tag{5-19}$$

$$r_{M_2} = -k_{p2}[R^*][M_2] \tag{5-20}$$

$$r_{M_3} = -2k_{p3}[R^*][M_3] \tag{5-21}$$

$$r_{M_4} = k_{p3}[R^*][M_3] - k_{cyc}k_{p3}[R^*][M_3] - k_{p4}[R^*][M_4] \tag{5-22}$$

$$r_{\mu} = k_{p4}[R^*][M_4] \tag{5-23}$$

$$[R^*] = (2fk_d[I]/k_t)^{0.5} \tag{5-24}$$

In the above equations, M_4 is the structure unit with a pendant vinyl group, and r_{μ} is the reaction rate for the crosslinks. [R*] is the radical concentration calculated from psudo-steady assumption (Odian, 2004). Among the parameters shown in the above equations, f is the initiator efficiency, k_d is the decomposition rate constant of the initiator, k_{cyc} is the fraction of pendent vinyl groups consumed by cyclization reactions, k_{pi} is the rate constant for the propagation and k_t is the termination rate constant. Since there are four different types of radicals, the propagation rate constants and the termination rate constants are defined in equations (5-25)-(5-28) according to the psudo-kinetic rate constants (Tobita et al., 1989; Okay 1994):

$$k_{pi} = \sum_{j=1}^{4} k_{pji}x_j \tag{5-25}$$

$$k_{tc} = \sum_{i=1}^{4}\sum_{j=1}^{i} k_{tcij}x_i x_j \tag{5-26}$$

$$k_{td} = \sum_{i=1}^{4}\sum_{j=1}^{i} k_{tdij}x_i x_j \tag{5-27}$$

$$k_t = k_{tc} + k_{td} \tag{5-28}$$

where k_{pji} is the propagation rate constant between radicals M_j* and monomers M_i. k_{tcij} and k_{tdij} are the termination rate constants for coupling and disproportionation between radicals M_i* and M_j*. x_j is the instantaneous mole fraction of the radical M_j* as shown in equation (5-29). [R*] is the same as that derived from psudo-steady state assumption.

$$x_j = \frac{[M_j^*]}{[R^*]} \quad j=1, 2, 3, 4 \tag{5-29}$$

$$[R^*] = \sum_{j=1}^{4}[M_j^*] \tag{5-30}$$

Okay et al (1994) and Tobita et al (1989) have pointed out that x_j is related with the instantaneous composition of the copolymers. Researchers have been very familiar with the composition equations

for 2-monomer and 3-monomer copolymerization systems. However, for tetrapolymer compositions, the equations become very complicated. Walling et al (1945) extended the copolymerization theory developed by Alfrey et al (1944 and 1946) and Mayo et al (1944) to n-monomer systems. However, this theory is too complicated to be used practically. Hocking et al (1996) derived the composition equation for terpolymerization and extended it to the system with four monomers. This equation as shown in the equation (5-31) is relatively simple and generated acceptable errors compared to the other models.

$$d[M_1]:d[M_2]:d[M_3]:d[M_4]=$$
$$[M_1]\left\{[M_1]+\frac{[M_2]}{r_{12}}+\frac{[M_3]}{r_{13}}+\frac{[M_4]}{r_{14}}\right\}:[M_2]\frac{r_{21}}{r_{12}}\left\{\frac{[M_1]}{r_{21}}+[M_2]+\frac{[M_3]}{r_{23}}+\frac{[M_4]}{r_{24}}\right\}: \qquad (5\text{-}31)$$
$$[M_3]\frac{r_{31}}{r_{13}}\left\{\frac{[M_1]}{r_{31}}+\frac{[M_2]}{r_{32}}+[M_3]+\frac{[M_4]}{r_{34}}\right\}:[M_4]\frac{r_{41}}{r_{14}}\left\{\frac{[M_1]}{r_{41}}+\frac{[M_2]}{r_{42}}+\frac{[M_3]}{r_{43}}+[M_4]\right\}$$

In the free radical crosslinking copolymerization, the propagation rate constant was found to be reaction-controlled up to 80% conversions (Okay, 1999), so k_{pi} is assumed to be constant in the present studies. In addition, basically, k_t will decrease beyond the gelation because the reaction turns from being a chemical-controlled one to a diffusion-controlled one (Okay, 1999). There are some empirical relations available to estimate the values of k_t during the post-gelation period (Li et al., 1989; Tobita et al., 1989). Equation (5-32), which was used in the modeling of the synthesis of poly(St-DVB) (Okay, 1999), was used to estimate the k_t during the post-gelation time in the present studies. In the equation (5-32), A is an adjustable parameter which could be obtained by fitting the experimental data under certain reaction conditions, and x is the overall reaction conversion. x_c is the critical conversion at the gel point. When the overall conversion is less than the critical conversion, the termination rate constant $k_t=k_{t0}$.

$$k_t / k_{t0} = \exp[-A(x - x_c)] \quad (x>x_c) \qquad (5\text{-}32)$$

The polymerization mechanisms including initiation, propagation, crosslinking and termination in the sol are proposed as shown in Scheme 2. The *s* and the *g* represent the polymers in the sol and in the gel, respectively. The terms without *s* and *g* are referred to the polymers belonging to the whole reaction systems. To characterize the gel formation and determine the gel point, the molecular weight of soluble polymers is calculated using the method of moments as shown in equations (5-33) and (5-34). With the proceeding of the polymerization, the soluble polymers in the sol are consumed to become branched or crosslinked polymers in the gel. To differentiate the soluble polymers and the

crosslinked ones, the symbols with a dot '•' relate to the linear polymer chains which are called primary polymers by Mikos et al (1986 and 1987) and Okay (1994), whereas those without this dot relate to branched or crosslinked molecules.

Initiation:	$I \xrightarrow{k_d} 2R$	
	$R + M_i^s \xrightarrow{k_I} P_1^s$	*i=1, 2, 3, 4*
Propagation:	$P_j^s + M_i^s \xrightarrow{k_{pi}} P_{j+1}^s$	*i=1, 2, 3, 4 and j≥1*
Crosslinking:	$P_j^s + M_{4,j}^s \xrightarrow{k_{p4}} P_j^g$	*j≥1*
Termination:	$P_j^s + P_k \xrightarrow{k_t} Q_{j+k}$ *or* $Q_r^s + Q_k$	*r, k≥1*

Scheme 2 Polymerization mechanisms

$$Q_n = \sum_{r=1}^{\infty} r^n ([D_r^s] + [P_r^s]) \quad \text{n=0, 1, 2…} \tag{5-33}$$

$$\bar{X}_n = \frac{Q_n}{Q_{n-1}} \quad \text{n=1, 2, 3…} \tag{5-34}$$

In equations (5-33) and (5-34), $[D_r^s]$ and $[P_r^s]$ are the concentrations of dead polymers and active polymers (radicals) consisting of *r* structural units. Q_n represents the nth moment of the polymer distribution. The nth average polymerization degree is shown in equation (5-34). Similarly, the moment equation for the active polymer chains or the polymer radicals is shown in equation (5-35).

$$\lambda_n = \sum_{r=1}^{\infty} r^n [P_r^s] \quad \text{n=0, 1, 2…} \tag{5-35}$$

The radicals of the linear polymers in the sol. According to Scheme 2, the reaction rate equations for the radicals of the linear polymers can be derived as shown in equations (5-36) and (5-37):

$$r_{P_1^{s\bullet}} = \sum_{i=1}^{4} k_i [R][M_i^s] - \sum_{i=1}^{4} k_{pi} [M_i^s][P_1^{s\bullet}] - k_t [R][P_1^{s\bullet}] \approx 0 \tag{5-36}$$

$$r_{P_j^{s\bullet}} = \sum_{i=1}^{4} k_{pi} [P_j^{s\bullet} - P_{j-1}^{s\bullet}][M_i^s] - k_{p4} [M_4^g][P_j^{s\bullet}] - k_t [R][P_j^{s\bullet}] \approx 0 \quad \text{j≥2} \tag{5-37}$$

To derive the rate equations in terms of the moments, equation (5-36) is multiplied by *j* and added with equation (5-37) which is multiplied by j^n and summed up from *j=2 to* ∞. Consequently, the nth

instantaneous moment equation for the radicals in the sol is obtained as shown in equation (5-38). In the equations, [R]=[R*].

$$r_{\lambda_n^{s\bullet}} = k_t[R]^2 + \sum_{i=1}^{4} k_{pi}[M_i^s] \sum_{v=0}^{n-1} \binom{n}{v} \lambda_v^{s\bullet} - (k_{p4}[M_4^g] + k_t[R])\lambda_n^{s\bullet} \approx 0 \ (*) \quad n \geq 0 \qquad (5\text{-}38)$$

According to other researchers (Flory, 1953; Dušek, 1982; Okay, 1994), the decrease in the crosslink density in the sol beyond the gel point is very rapid, and over a wide conversion range, the average chain length of the sol polymers remains almost constant. This has been shown by the experimental data in various systems (Hild et al., 1981; Hild et al., 1985; Naghash et al., 1995). Therefore, this statement implies that the reaction rate for the sol polymers is close to zero during the course of the reaction beyond the gelation point. According to these findings, the steady-state assumption can be made on the sol polymers so that the 0, 1st, and nth moments of the radicals belonging to the primary polymer chains are figured out as shown in equations (5-39) through (5-41).

$$\lambda_0^{s\bullet} = \varphi_s[R] \qquad (5\text{-}39)$$

$$\lambda_1^{s\bullet} = \varphi_s^2 \sum_i k_{pi}[M_i^s] / k_t \qquad (5\text{-}40)$$

$$\lambda_n^{s\bullet} = n!(\lambda_1^{s\bullet} / \lambda_0^{s\bullet})^n \lambda_0^{s\bullet} \qquad (5\text{-}41)$$

$$\varphi_s = \frac{k_t[R]}{k_t[R] + k_{p4}[M_4^g]} = \frac{k_t[R]}{k_t[R] + k_{p4}[M_4]W_g} \qquad (5\text{-}42)$$

where φ_s, as shown in equation (5-42), is defined as the fraction of the radicals in the sol with respect to the whole reaction systems.

The linear polymers in the sol. According to Scheme 2, the rate equation of the linear polymers in the sol can be derived:

$$r_{Q_j^{s\bullet}} = k_{td}[R][P_j^{s\bullet}] + 0.5k_{tc} \sum_{n=1}^{j-1} [P_n^{s\bullet}][P_{j-n}^{s\bullet}] \qquad (5\text{-}43)$$

By combining the moment equations for the radicals and assuming (Okay, 1994):

$$\lambda_n^{s\bullet} >> \lambda_{n-1}^{s\bullet} \qquad (5\text{-}44)$$

$$\sum_{i=1}^{4} k_{pi}[M_i^s] = \sum_{i=1}^{4} k_{pi}[M_i] \qquad (5\text{-}45)$$

The moment equation for the linear polymers in the sol is:

$$r_{Q_n^{s\bullet}} = (k_{td}/\phi_s + \frac{n+1}{2}k_{tc})\lambda_0^{s\bullet}\lambda_n^{s\bullet} \qquad n\geq 0 \qquad (5\text{-}46)$$

The radicals of the branched polymers in the sol. Similarly, by applying the mass balance, the rate equations for the radicals belonging to the branched or crosslinked polymers are:

$$r_{P_1^{s\bullet}} = \sum_{i=1}^{4} k_i[R][M_i^s] - \sum_{i=1}^{4} k_{pi}[M_i^s][P_1^{s\bullet}] - k_t[R][P_1^{s\bullet}] \approx 0 \qquad (5\text{-}47)$$

$$r_{P_j^{s\bullet}} = k_{i4}[R][M_{4,j-1}^s] + \sum_{i=1}^{3} k_{pi}[M_i][P_{j-1}^s - P_j^s] + \sum_{r=1}^{j-1} k_{p4}[M_{4,r}^s][P_{j-r-1}^s] - (k_{p4}[M_4] + k_t[R])[P_j^s] \approx 0 \qquad (5\text{-}48)$$

where $M_4^s{}_{,j}$ is the unit of the pendent vinyl groups with j structure units or the length of the polymer chain is j. According to Okay (1994), $[M_4^s{}_j]$ can be estimated using equation (5-49) assuming the crosslinks are distributed homogeneously along the branched polymer chains,

$$[M_{4,j}^s] = \frac{[M_4^s]}{Q_1} jP_j^s \qquad (5\text{-}49)$$

Through a similar steady-state assumption on the radicals, the generalized moment equation for the radicals of the branched polymers is:

$$\lambda_n^s = n\left(\frac{\lambda_1^{s\bullet}}{\lambda_0^s}\right)\lambda_{n-1}^s + \frac{k_{p4}[M_4^s]}{k_t\lambda_0^s Q_1^s}\varphi_s^2 \sum_{v=0}^{n-1}\binom{n}{v}\lambda_v^s Q_{n+1-v}^s \qquad n\geq 0 \qquad (5\text{-}50)$$

The branched polymers in the sol. According to the mass balance on the branched or the crosslinked polymers, equations (5-51) and (5-52) are obtained,

$$r_{P_j^s} = k_{td}[R][P_j^s] + 0.5\sum_{r=1}^{j-1} k_{tc}[P_r^s][P_{j-r}^s] - k_{p4}[M_{4,j}^s][R] \qquad (5\text{-}51)$$

$$r_{Q_n^s} = k_{td}[R]\lambda_n^s + 0.5k_{tc}\sum_{v=0}^{n}\binom{n}{v}\lambda_v^s\lambda_{n-v}^s - k_{p4}[M_4^s]\lambda_0^s\frac{Q_{n+1}^s}{Q_1^s} \qquad (5\text{-}52)$$

Prior to the gel point, the radical fraction in the sol (φ_s) and the sol fraction (W_s=*1-*W_g) are equal to 1, so the 0, 1st, and 2nd instantaneous moments equations for the branched polymers prior to the gel point are,

$$r_{Q_0^s} = r_{Q_0^{s\bullet}} - k_{p4}[M_4]\lambda_0^{s\bullet}W_s \qquad (5\text{-}53)$$

$$r_{Q_1^s} = r_{Q_1^{s\bullet}} \tag{5-54}$$

$$r_{Q_2^s} = 2(k_{td} / \varphi_s + 1.5k_{tc})(\lambda_1^s)^2 \tag{5-55}$$

$$\lambda_1^s = \lambda_1^{s\bullet} + \varphi_s{}^2 (k_{p4}[M_4]W_s / k_t)\,\bar{X}_2^{\,s} \tag{5-56}$$

Although φ_s=1 corresponds to the conditions prior to the gel point, the values calculated at φ_s=1 also represents the average values for the whole reaction systems during the reaction (Okay, 1994). Therefore, W_s can be defined using equation (5-57) (Okay, 1994),

$$W_s = \frac{Q_1^{s\bullet}}{Q_{1,\varphi_s=1}^{s\bullet}} \tag{5-57}$$

According to Okay (1994), the number of branched units per weight-average linear polymer chain in the *sol*, $\bar{\varepsilon}^s$ and the average crosslink density of the *sol* polymers, $\bar{\rho}^s$, can be defined using equations (5-58) and (5-59),

$$\bar{\rho}^s = \frac{2[\mu^s]}{Q_1^{s\bullet}} \tag{5-58}$$

$$\bar{\varepsilon}^s = \bar{\rho}^s \bar{X}_2^{s\bullet} \tag{5-59}$$

As mentioned above, beyond the gelation, the average crosslink density and the average number of the branched units per weight-average polymer for the whole system can be calculated as shown in equations (5-60) and (5-61) (Okay, 1994),

$$\bar{\rho} = \frac{2[\mu]}{Q_{1,\varphi_s=1}^{s\bullet}} \tag{5-60}$$

$$\bar{\varepsilon} = \bar{\rho}\bar{X}_{2,\varphi_s=1}^{s\bullet} \tag{5-61}$$

Gelation. At the gel point, $\bar{X}_2^s$ becomes infinite as shown in equation (5-62) (Flory, 1953; Okay, 1994). According to Flory (1953) and Stockmayer (1944), the average molecular weight of the branched polymer can be described by equation (5-63). This equation implies that the average molecular weight of the *sol* polymers becomes infinite which corresponds to the gel point when the number of the branched units per weight-average linear polymer chain in the sol $\bar{\varepsilon}^s$ is equal to 1.

$$\lim_{t \to tc} \bar{X}_2^s = \infty \tag{5-62}$$

$$\overline{X}_2^s = \frac{\overline{X}_2^{s\bullet}}{1-\overline{\varepsilon}^s} \tag{5-63}$$

Network properties. The average number of the segments (N) between crosslinks and the average molecular weight between two crosslinks (M_c) are very important network properties which can be calculated from the cycle rank of the networks. A cycle rank is defined as the number of the independent circuits in the polymer gel (Flory, 1953). Okay (1994) calculated the number of the segments based on this definition. Prior to the gel point, the networks do not consist of closed circuits so that the cycle rank ξ=0 (Okay, 1994). So the average number of active crosslinks of each polymer chain at the gel point is (Okay, 1994),

$$\frac{[\mu_1^g]}{Q_1^{g\bullet}} = \left(2\overline{X}_{2,\varphi_s=1}^{s\bullet}\right)^{-1} \tag{5-64}$$

Beyond the gel point, the additional crosslinks are added to the polymers because of intermolecular crosslinks (Okay, 1994). Therefore, the average crosslinks per polymer chain in the gel phase is,

$$\frac{[\mu^g]}{Q_1^{g\bullet}} = \frac{[\mu](1+W_s)}{Q_{1,\varphi_s=1}^{s\bullet}} \tag{5-65}$$

The derivation of equations (5-64) and (5-65) are shown in Appendix IV. Thus, the cycle-rank density of the network which is generated by the gelation can be calculated using equations (5-64) and (5-65),

$$\frac{\xi}{Q_1^{g\bullet}} = \frac{[\mu](1+W_s)}{Q_{1,\varphi_s=1}^{s\bullet}} - \frac{1}{2\cdot\overline{X}_{2,\varphi_s=1}^{s\bullet}} \tag{5-66}$$

Therefore, the number of the repeat units or the number of segments between crosslinks is derived from equation (5-66) (Okay, 1994),

$$N = \left(\frac{[\mu](1+W_s)}{Q_{1,\varphi_s=1}^{s\bullet}} - \frac{1}{2\cdot\overline{X}_{2,\varphi_s=1}^{s\bullet}}\right)^{-1} \tag{5-67}$$

Furthermore, by using equation (5-66), the number average molecular weight between two crosslinks can be estimated,

$$M_c = \frac{\overline{X}_1^{g\bullet}}{\xi} = \frac{N}{Q_0^{g\bullet}} = \frac{N}{Q_0^{s\bullet}W_g} \tag{5-68}$$

To predict the gel point, equations (5-18)-(5-24), (5-36), (5-37), (5-51), (5-53), (5-54), (5-58), (5-59) and (5-63) can be solved (φ_s=1 and W_s=1) together until equation (5-62) is achieved. Beyond the gel point, φ_s and W_s are not equal to 1 since *sol* and gel coexist in the system.

5.5.4 Calculation

For an isothermal copolymerization, the reaction volume changes with the reaction due to the different densities of the monomers and the polymers so that a balance equation (5-69) was used to include this volume effect during the calculation (Okay, 1994 and 1999).

$$r_S = \frac{d(VS)}{Vdt} = \frac{dS}{dt} + \frac{S}{V}\frac{dV}{dt} \qquad (5\text{-}69)$$

where S represents the concentration of species I, M_i, and the moments of the polymer distributions. The dV/dt is the rate of the volume change. If the reaction mixtures are assumed to be ideal solutions which means the volume is additive, the dV/dt is,

$$\frac{dV}{dt} = V\sum_{i=1}^{3} r_{M_i}\left(\frac{1}{d_{M_i}} - \frac{1}{d_p}\right)Mw_i \qquad (5\text{-}70)$$

where r_{Mi} is the polymerization rate of monomer i, d_{Mi} is the density of the monomer i and Mw_i is the molecular weight of monomer i.

In addition, for the solution of the kinetic model, to simplify the treatment of the model, additional approximations were made during the course of the computation. First of all, the propagation, the crosslinking and the termination rate constants are assumed to be independent of the type of radicals. This assumption is the same as the one made by Okay (1999) for the poly(St-DVB) syntem. Although the reaction systems in the present studies are more complicated, this assumption is still reasonable because the mobility of the radicals is extremely low beyond the gel point so that the radicals tend to react with other surrounding radicals. Another approximation is that the pendent vinyl group reactivity is ten to hundredfold smaller than the reactivity of the vinyl groups on the divinyl monomers (Okay, 1999), which means,

$$k_{p4} = 0.1k_{p3} \qquad (5\text{-}71)$$

On the other hand, the soluble polymers are consumed very quickly in the gel formation under crosslinking which implies that $v_3=v_3'=0$ can be assumed in the thermodynamic equations. To figure out v_1, v_2^0 *and* v_g, the thermodynamic equations have to be solved together with the reaction kinetic equations from which W_g and N are obtained. Since v_g is the volume fraction of the polymeric

networks with respect to the whole reaction system, the porosity (*P%*) of the resultant porous polymeric particles of poly(HEMA-MMA), poly(HEMA-St) and poly(HEMA-NVP) can be simulated using equation (5-72),

$$P\% = (1 - v_g)\% \qquad (5\text{-}72)$$

Table 5-6 Kinetic Constants and Parameters for the Porous poly(HEMA-MMA) Particle Synthesized at 70°C Using AIBN as an Initiator (1-HEMA; 2-MMA; 3-EGDMA)

Constants and Parameters	References
f=0.59	Li et al, 1989 (b)
$k_d(s^{-1})=3.4\times10^{-5}$	Li et al, 1989 (b)
k_{p1}=116.7 L/(mol·s)	Estimated from reactivity ratios
k_{p2}=461.7 L/(mol·s)	Li et al, 1989 (b)
k_{p3}=941.8 L/(mol·s)	Li et al, 1989 (b)
$\overline{r_{43}}$ =0.1	Okay, 1999
$k_{tc}^0=3.50\times10^7$ L/(mol·s)	Tefera et al., 1997
k_{td}^0=0 L/(mol·s)	Okay, 1999
k_{cyc}=0.3	Okay, 1999
r_{12}=0.110	Ajzenberg et al, 2001
r_{21}=0.814	Ajzenberg et al, 2001
r_{13}=0.811	Ajzenberg et al, 2001
r_{31}=6.548	Ajzenberg et al, 2001
r_{23}=0.67	Li et al, 1989 (a)
r_{32}=1.49	Li et al, 1989 (a)
d_1=1.073 g/ml	
d_2=0.936 g/ml	
d3=1.051 g/ml	
dp, g/ml	equal to d_2
$\delta_1=23.2$ (Mpa)$^{1/2}$	Okay, 2000
$\delta_2=18.9$ (Mpa)$^{1/2}$	Brandrup et al., 1999
$\delta_3=18.2$ (Mpa)$^{1/2}$	Okay, 2000
$\delta_{oct}=20.9$ (Mpa)$^{1/2}$	Brandrup et al., 1999
$\delta_{PHEMA}=29.7$ (Mpa)$^{1/2}$	Okay, 2000
$\delta_{PMMA}=18.0$ (Mpa)$^{1/2}$	Barton, 1983
$\delta_{PEGDMA}=19.2$ (Mpa)$^{1/2}$	Okay, 2000
M_{w1}=130.14 g/mol	
M_{w2}=100.12 g/mol	
M_{w3}=198.22 g/mol	
A	11

5.5.5 Simulation of Porous Poly(HEMA-MMA) Polymer

Although many poly(HEMA-MMA) polymers of different polymer morphology have been synthesized, there is almost no research on the modeling of the gel formation and the porous characteristics of the porous poly(HEMA-MMA) polymers. The modeling studies will be very helpful to guide the synthesis of the porous poly(HEMA-MMA) polymers with the favorable porous

structures and network properties. Li et al (1989a) used mathematical models to study the synthesis of poly(MMA-EGDMA). The polymers they studied were non-porous polymer and they only studied the polymer reactions upon the gelation. Naghash et al (1995) simulated the gel fractions of poly(MMA-EGDMA) at 70°C but they did not study the network properties. Scranton et al (1990) used the statistical models to simulate the gel properties and the molecular weight of poly(HEMA-EGDMA) polymers. However, their studies were not based on the real reaction kinetics and were not focused on the porous structures either. In the present studies, the synthesis of the porous poly(HEMA-MMA) polymers and their properties are simulated using the mathematical models introduced in the previous section. The model parameters being used in the simulation are shown in Table 5-6. These parameters were collected from the various reports. Some reaction constants are hard to come by, such as k_{p1}, so that they are estimated from the available reactivity ratios.

5.5.5.1 Reaction Kinetic Behavior and Gel Point Determination

According to equations (5-62) and (5-63), the gel point can be determined when the number of the branched units per weight-average linear polymer chain in the sol is equal to 1 or the weight average molecular weight becomes infinite. Figure 5-21 shows the change in the average molecular weight of the branched polymers in the *sol* and the crosslink density in terms of $\bar{\varepsilon}^s$ under certain reaction conditions. It can be seen that the gel point determined by $\overline{X}_2^s$ and $\bar{\varepsilon}^s$ are identical. Accordingly, the gelation time and the critical conversion at gel point can be found out. The reaction conversion at different reaction time is shown in Figure 5-22. The gelation happens at a certain reaction conversion followed by the acceleration of the reaction rate. As studied by many researchers, the s shape curve results from the dramatic decrease in k_t relative to k_p (Flory, 1953). Beyond the gel point, the polymer chains form the networks by crosslinking so that the gel fraction (W_g) increases to 1 with an increase in the amount of polymers in the network phase after a certain reaction conversion as shown in Figure 5-23. During this course, as shown in Figure 5-24, the number of the segments between the crosslinks (N) and the number average molecular weight between the successive crosslinks (M_c) decrease rapidly beyond the gel point with increasing crosslinking.

Figure 5-25 shows a comparison between the experimental results and the model prediction. At the intermediate stage of the reaction, the experimental values are greater than the predicted values. The reaction parameters were collected from other papers so that the deviations are introduced in the simulation. To obtain the perfect simulation results, the experiments have to be conducted to measure

the real reaction constants in the copolymerization. On the other hand, during the kinetic experiments, the reaction was probably not stopped right away at each time interval so that it proceeded a little longer resulting in a little higher W_g values than that expected. Thirdly, the model assumptions also introduce errors into the model. However, the model still gives a relatively good prediction of the gel point, the early stage of the gelation and the final stage of the gelation.

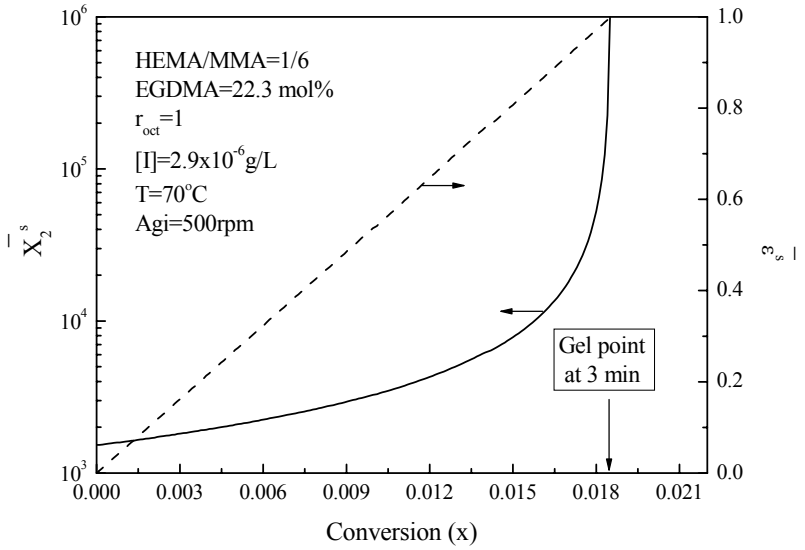

Figure 5-21 Average molecular weight of the branched polymers in the *sol* and the crosslink density in terms of $\bar{\varepsilon}^s$

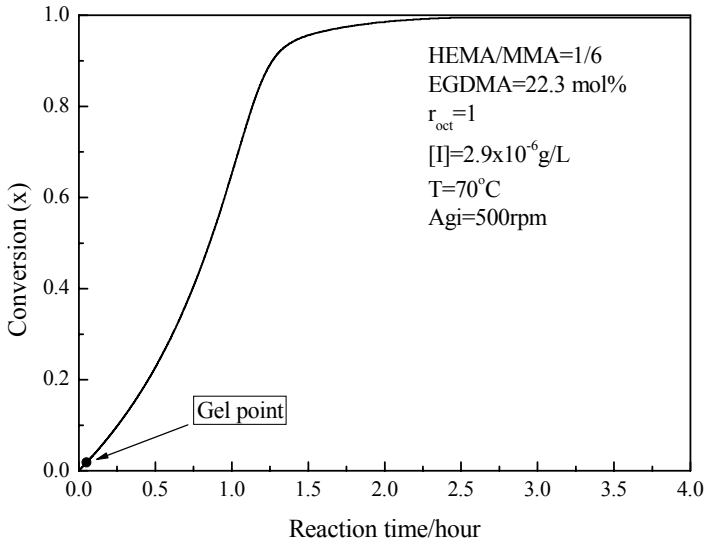

Figure 5-22 Change of the overall monomer conversion *x* with the reaction time in HEMA-MMA copolymerization with the crosslinking of EGDMA. The gel point is shown as a filled circle

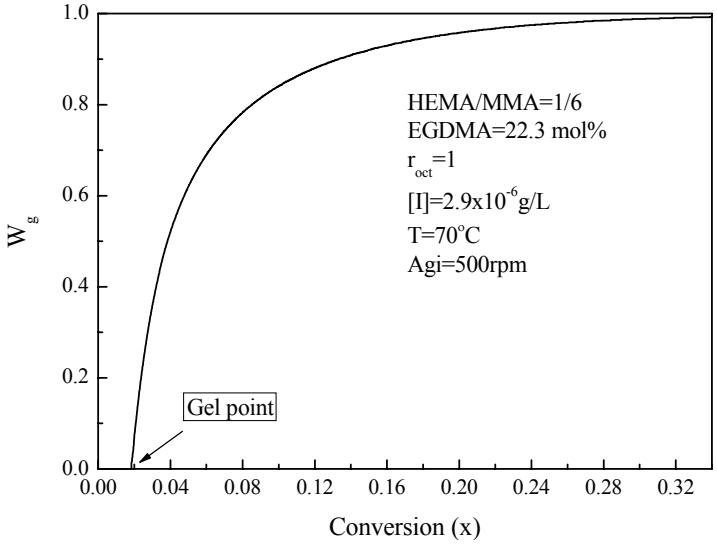

Figure 5-23 Change of the gel fraction W_g with reaction conversion

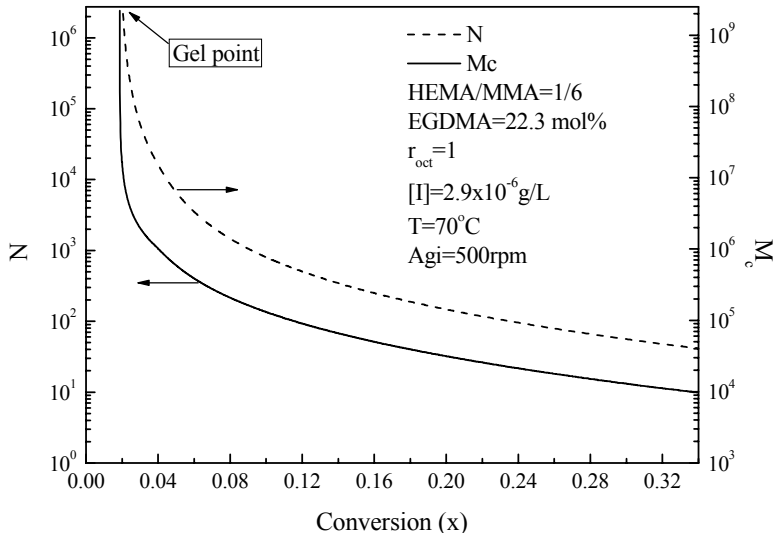

Figure 5-24 Change of the number of segments and the number average molecular weight between successive crosslinks

Generally speaking, the properties shown in Figure 5-21 through Figure 5-25 are similar with the well-known features for the free radical crosslinking copolymerization of PMMA (Flory, 1953; Li et al, 1989) and poly(HEMA-MMA) (Scranton et al, 1990).

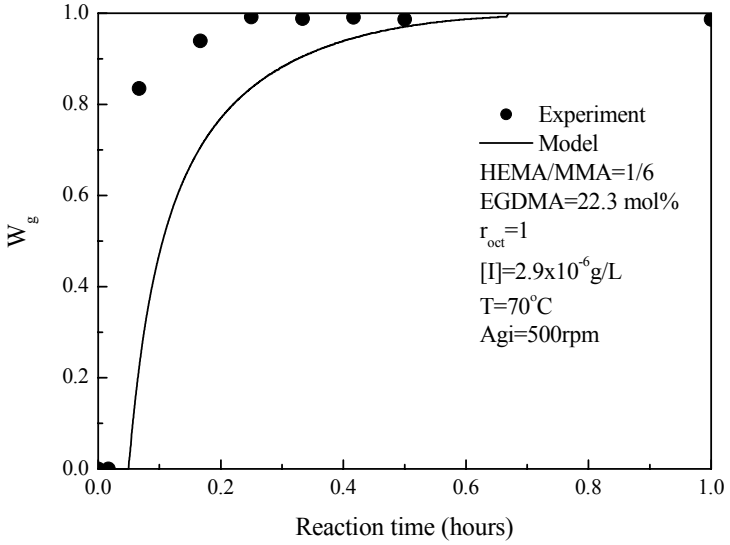

Figure 5-25 Comparison between the experimental results and the model prediction

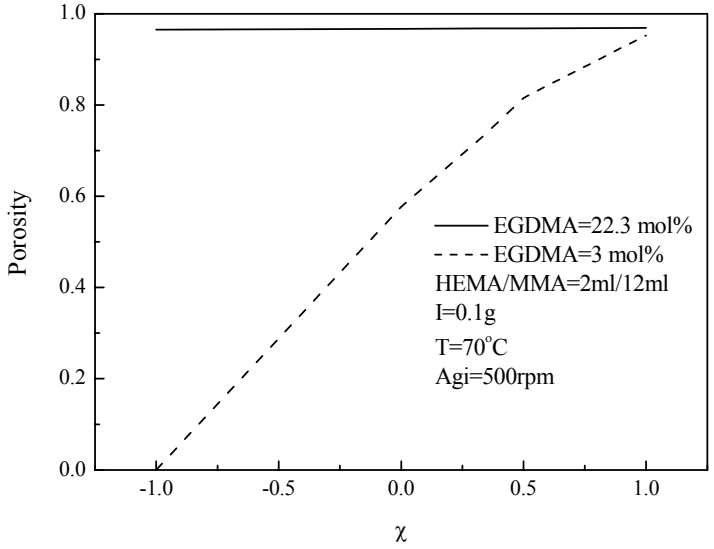

Figure 5-26 Change of the porosity with an increase in the interaction parameter; r_{oct}=1

5.5.5.2 Effect of Solvent

The effect of the thermodynamic quality of the solvent at the high and low levels of the EGDMA concentration is shown in Figure 5-26. With an increase in the interaction parameters, which means the solvents become poorer for the polymers, the porosity of the resultant polymers is increased. At lower EGDMA concentration, the porosity is greatly increased if the solvent changes from a good solvent to a non-solvent. It has been known that the porous structures are generated by the phase separation (Dušek, 1965 and 1967; Okay, 2000). Although the resultant polymers are easy to be

swollen under lower EGDMA concentration, the presence of a non-solvent will enhance the phase separation resulting in higher porosity because more solvent is separated, which corresponds to χ-induced syneresis.

However, it seems that the solvent thermodynamic quality has little effect on the porosity at higher EGDMA concentration. The effect of the thermodynamic quality of the solvent at higher EGDMA concentration is shown in Figure 5-27. The porosity becomes quite close between each other at full reaction conversion. It can be seen that the porosity decreases sharply at the beginning and increases again in a good solvent which has low values of the interaction parameters. The decrease in the porosity results from the increase in the gel fraction (W_g) for the network phase beyond the gel point. With the proceeding of the crosslinking, the polymer volume is reduced (Okay, 1999) and the phase separation occurs so that the porosity starts to increase. Therefore, the point from which the porosity starts to increase corresponds to the phase separation point. This implies that the reaction system undergoes phase separation beyond the gel point due to an increase in the crosslink density in a good solvent (Okay, 1999), which corresponds to *v*-induced syneresis. At the same time, from Figure 5-27, it also can be seen that the phase separation occurs later at lower values of the interaction parameters (good solvent). In a non-solvent, the porosity decreases from the gel point which means the system has been discontinuous at the gel point because the phase separation has happened prior to the gel point. Therefore, a strong non-solvent enhances the phase separation prior to the gel point (Okay, 1999). Thus, the porous structures can be generated either in a good solvent or in a non-solvent at certain crosslinker concentrations. This is consistent with the statement of Okay (1999) that the porous networks can be prepared even in the presence of good solvents.

Figure 5-28 and Figure 5-29 show the effect of the solvent on the volume swelling ratio of the resultant polymers in different solvents with different thermodynamic quality after 4 hours reaction. Firstly, it can be seen that the q_v keeps decreasing with an increase in the values of the interaction parameter. It has been mentioned that a high interaction parameter value implies that the solvent is a non-solvent for the polymers, and a non-solvent can not swell the polymer greatly compared to a better solvent having a low interaction parameter value. Secondly, the solvents' thermodynamic quality has a greater effect on the q_v values at lower crosslinker concentration, and furthermore, the polymers synthesized at a lower crosslinker concentration can be swollen much more. Similar experimental results were shown in the poly(HEMA-EGDMA) reaction systems as well (Okay, 1992; Horak et al, 1993).

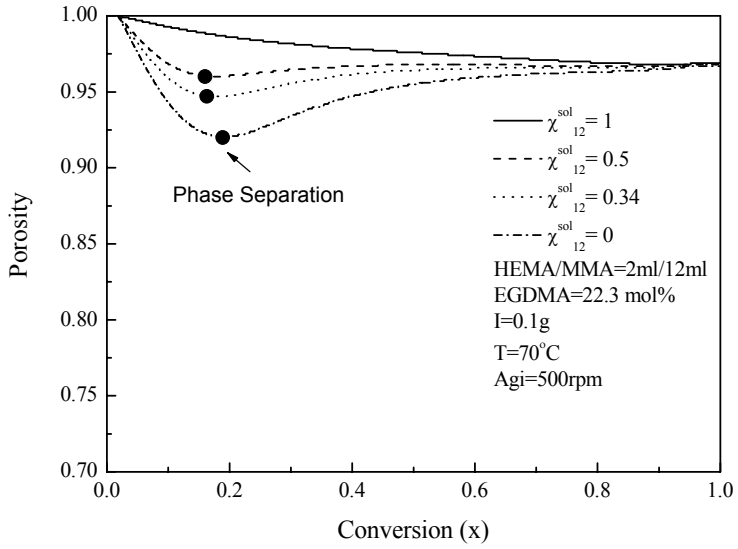

Figure 5-27 Variation of the total porosity of the porous poly(HEMA-MMA) networks with the monomer conversion in the presence of various solvents; r_{oct}=1

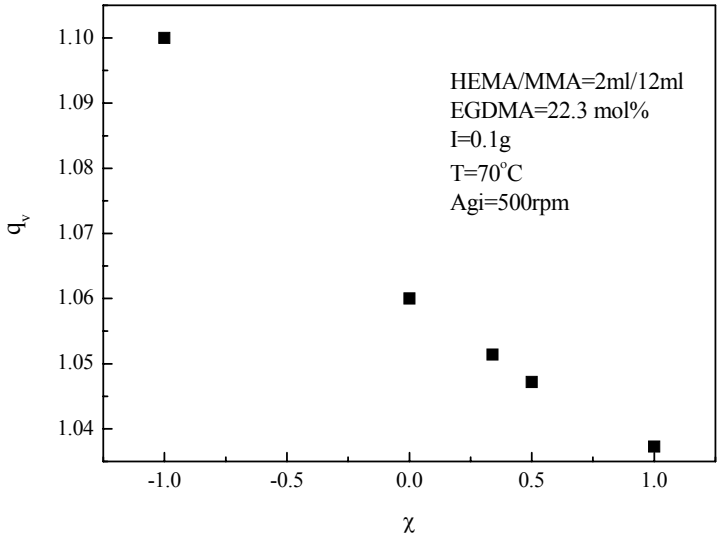

Figure 5-28 Change of volume swelling ratio of the polymer in 1-octanol during the reaction; r_{oct}=1

The volume of the porogen also has an effect on the porous structures. The more porogen that is present, the higher the porosity is. Figure 5-30 shows the change of the porosity with an increase in the porogen volume in the reaction systems. It can be seen that the porosity increases with an increase in the porogen volume ratio because the separated porogen occupies more spaces in the network phase. However, the increase in the porosity becomes slow at higher porogen volume ratio. This is caused by the relatively small fraction of monomer contents at higher porogen volume ratios so that

the systems could not hold the isochoric condition due to the loose networks (Okay, 2000). On the other hand, the change of the porosity is not that much at higher crosslinker concentration because the crosslink density is so high that more pores of much smaller size are generated. These pores, which are of smaller size, do not have a significant effect on the porosity.

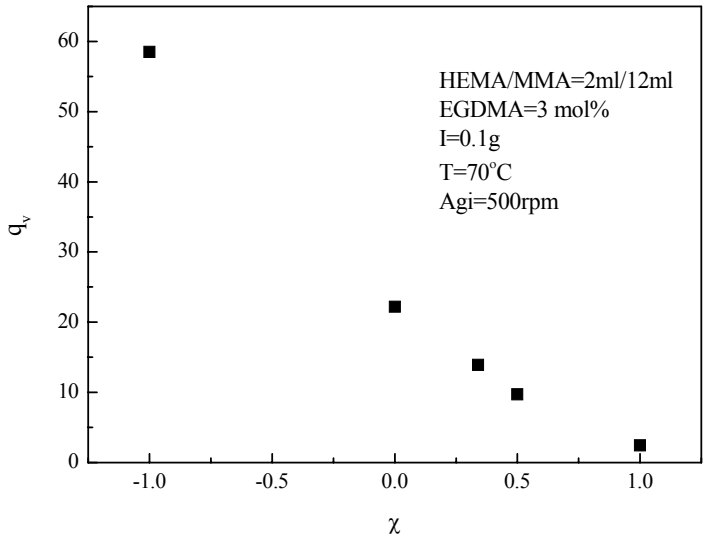

Figure 5-29 Change of volume swelling ratio of the polymer in 1-octanol during the reaction; r_{oct}=1

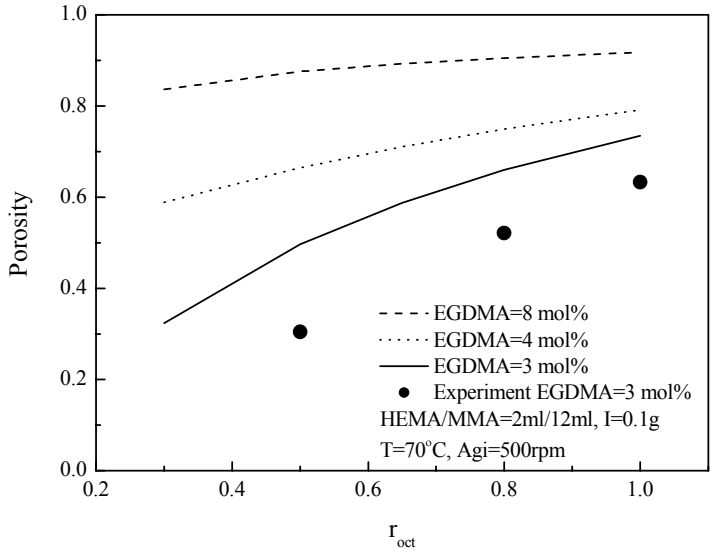

Figure 5-30 Effect of porogen (1-octanol) volume ratio on the porosity of the resultant polymers

The experimental values and the simulated values are compared in Figure 5-30 as well. The experimental results have the same trend as the simulated ones. The difference between them is

probably caused by the porous collapse during porogen removal and drying. Therefore, the model predicts the maximum porosity of the resultant polymers (Okay, 1999).

5.5.5.3 Effect of EGDMA Molar Concentration

The effect of the EGDMA concentration on the kinetics of HEMA-MMA-EGDMA copolymerization and the porosity at 70°C is simulated as shown in Figure 5-31 through Figure 5-36.

The filled circles shown in Figure 5-31 represent the gel points at different EGDMA concentrations at certain monomer ratios, porogen volume ratios and initial initiator concentration. As the EGDMA concentration in the reaction systems increases from 3mol% to 22mol%, the critical conversion at the gel point decreases from 0.110 to 0.018. Beyond the gel point, the reaction conversion increases significantly because of the gel effect (Flory, 1953; Okay, 1999). However, at lower EGDMA concentration, the reaction is slower than those at higher EGDMA concentrations.

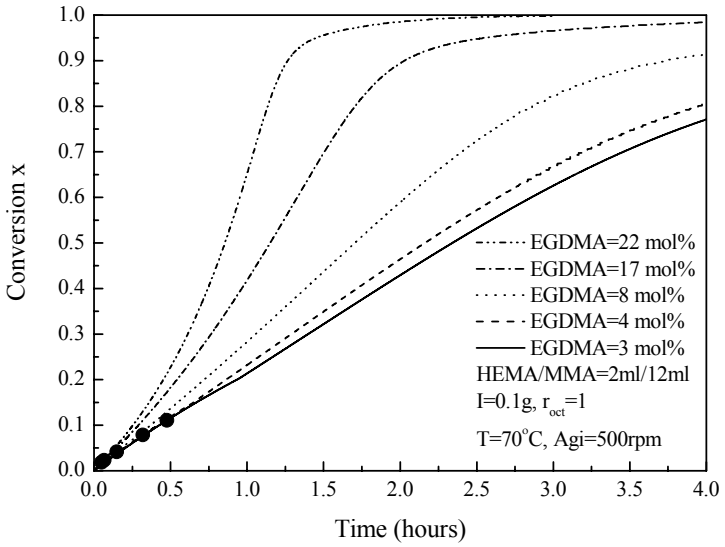

Figure 5-31 Reaction conversion and gel points at different EGDMA molar concentration

Figure 5-32 clearly shows the gel points from the change of the average molecular weight for the branched polymers in the *sol*. At the gel point, the average molecular weight of the branched polymers in the sol becomes infinite. At higher EGDMA concentration, the average molecular weight of the branched polymers increases faster than for those at lower EGDMA concentration because of an increased rate of crosslinking.

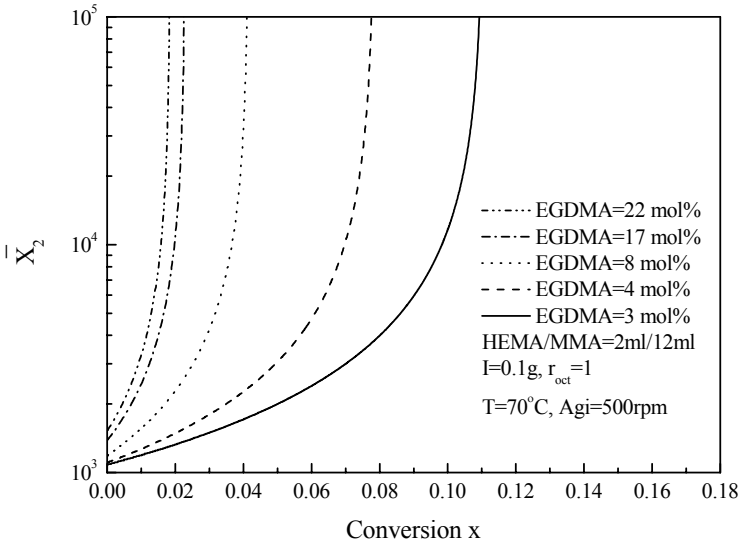

Figure 5-32 Change of the average molecular weight of the branched polymers in the sol until the gelation

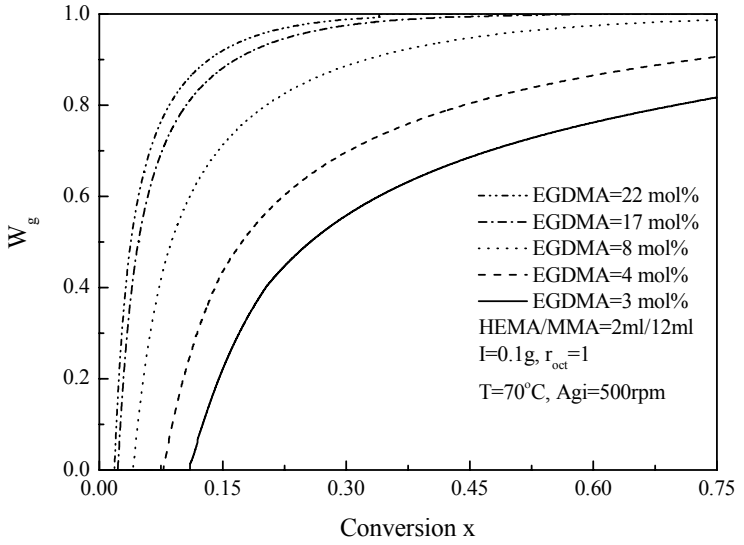

Figure 5-33 Changes of the gel fraction W_g with the reaction conversion at different EGDMA molar concentration

The increase in the EGDMA concentration also makes the increasing rate of W_g faster as shown in Figure 5-33. At higher EGDMA concentration, the concentration of the pendent vinyl groups is increased, resulting in a higher growth rate of W_g. On the other hand, higher concentration of the pendent vinyl groups leads to small segment numbers and lower molecular weight between successive crosslinks as shown in Figure 5-34 and Figure 5-35.

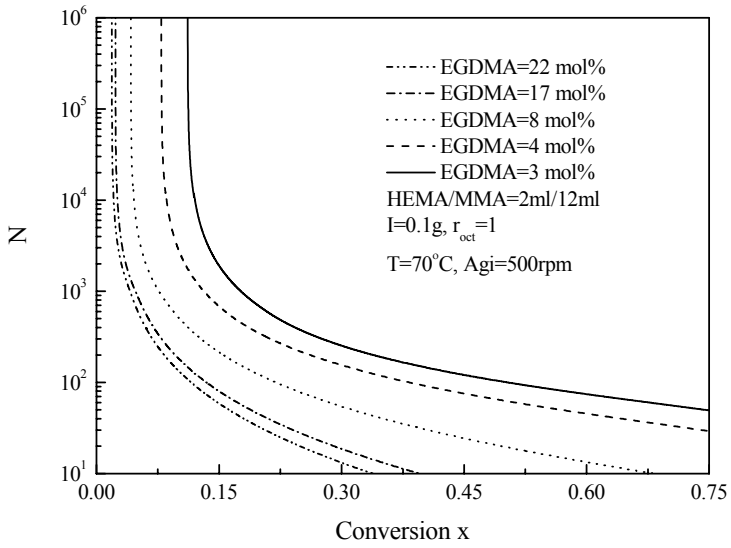

Figure 5-34 Changes of N with reaction conversion at different EGDMA concentration

The change of the q_v and M_c is shown in Figure 5-35. It can be seen that the q_v values keep decreasing with an increase in the EGDMA concentration. At higher EGDMA concentration, the polymeric networks are difficult to become swollen because they are more compact. The less the M_c values, the more compact the networks are. Therefore, both M_c and q_v are decreased with an increase in the EGDMA molar concentration.

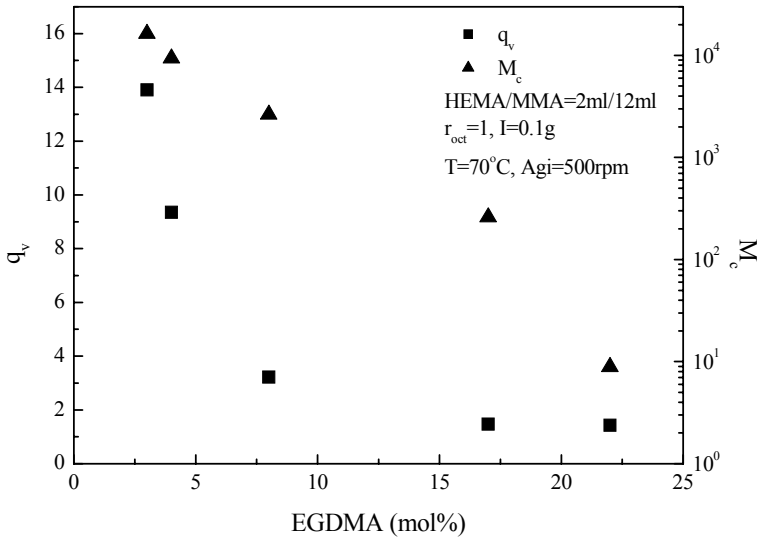

Figure 5-35 Changes of the q_v and M_c at different EGDMA concentration

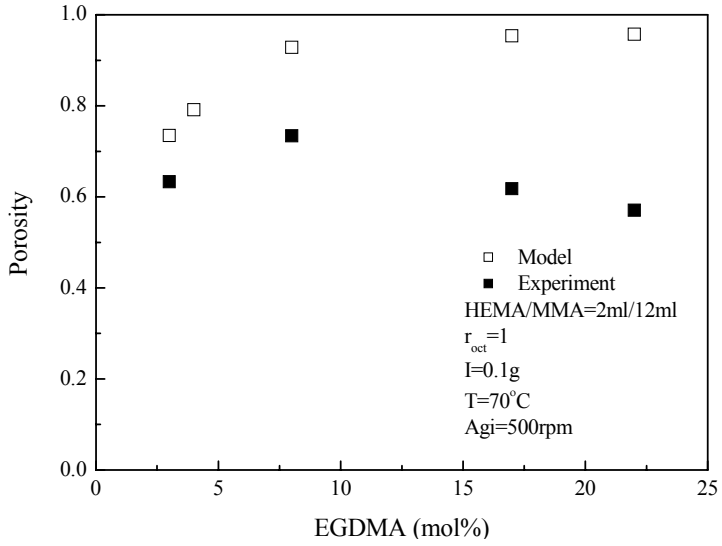

Figure 5-36 Changes of the porosity at different EGDMA concentration

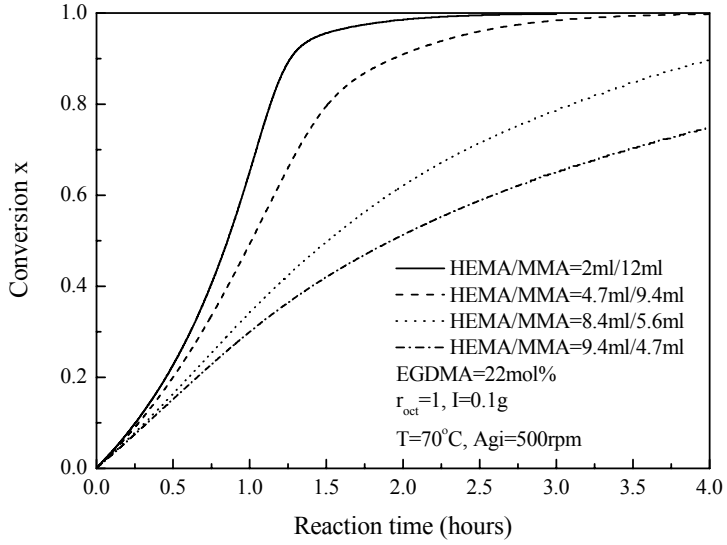

Figure 5-37 Polymerization conversions at various monomer ratios of HEMA to MMA

Figure 5-36 shows the variation of the porosity at the various EGDMA molar concentrations. The simulation results illustrate that the porosity increases at first up to an EGDMA concentration of 8mol% and then levels off. This is consistent with the experimental results as shown in Figure 5-36. Compared to the simulation results, the porosity is decreased at higher EGDMA concentration in the experimental results. This could be caused by the damage of the pores under higher intrusion pressure during measurements and the pore collapse during the porogen removal. The results demonstrate that porous structures can be formed even at lower crosslink density in the presence of a non-solvent.

Although higher EGDMA concentration leads to higher porsosity (Okay, 1999), the further increase in the EGDMA concentration does not change the porosity that much because of higher conversion, resulting in more compact networks and shorter segments between successive crosslink points. Therefore, the model predicts the highest porosity during the synthesis of the porous polymers. However, it predicts the critical point accurately.

5.5.5.4 Effect of the Monomer Ratio HEMA/MMA

The effect of the monomer volume ratio of HEMA to MMA was simulated using the present model. According to the experimental results, the higher the HEMA content, the smaller the porosity and the pore volume are. However, from the simulation results shown in this part, it could be seen that the decrease in the porosity under higher HEMA content results from the shrinkage of the polymeric networks.

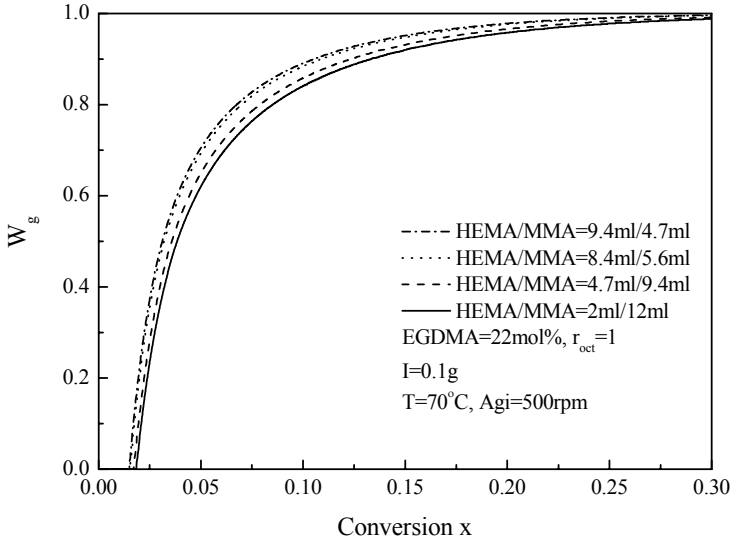

Figure 5-38 Change of the gel fractions with reaction conversion at various monomer ratios

The behaviors of the reaction kinetics are shown in Figure 5-37 through Figure 5-39. The reaction time is 4 hours. As shown in Figure 5-37, the reaction rate is faster at lower HEMA content than those under higher HEMA content. However, according to Figure 5-38, the gelation occurs a little earlier under higher HEMA content than those under lower HEMA content. This could be explained using Figure 5-39. Prior to a certain reaction conversion, the average molecular weight for the polymers synthesized under lower HEMA content is higher because of the fast reaction rate. However, the increasing rate of $\overline{X}_2$ under higher HEMA content is faster because of the higher molecular weight of

HEMA. On the other hand, HEMA has a big side group and the –OH groups contribute to stronger interactions between the polymeric chains. All of these possible reasons could lower the mobility of the polymeric chains under higher HEMA content with the proceeding of the reactions so that the gel point occurs a little bit earlier under higher HEMA content as shown in Figure 5-38 and Figure 5-39. Therefore, it substantiates that higher HEMA content can accelerate the network formation.

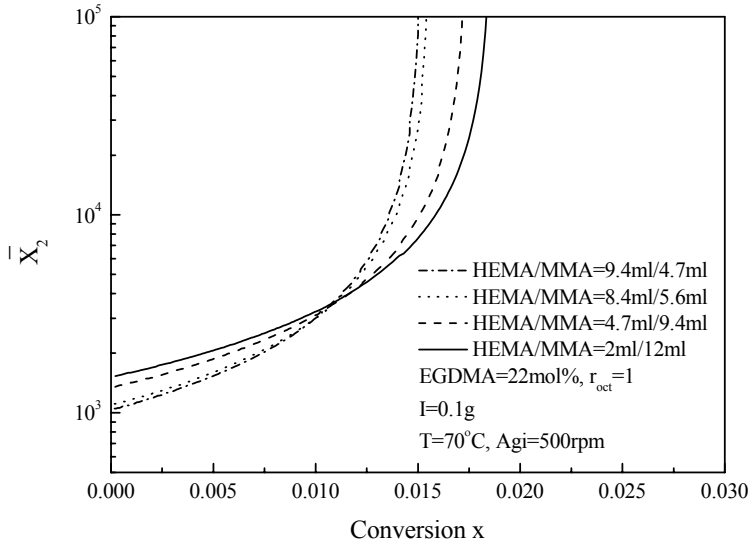

Figure 5-39 Changes of the average molecular weight of the branched polymers at various monomer ratios of HEMA to MMA

Figure 5-40 shows the change of the q_v in the porogen 1-octanol with the various monomer ratios of HEMA to MMA. As studied by Horak (1993), 1-octanol is a non-solvent for the poly(HEMA-EGDMA). Therefore, 1-octanol will enhance the phase separation under higher HEMA content so that the q_v values are decreased with an increase in the monomer ratios of HEMA to MMA. At higher EGDMA concentration, the q_v values do not have much difference since the highly crosslinked networks are difficult to become swollen.

Figure 5-41 shows the simulation results for the porosity under various monomer ratios of HEMA to MMA. The porosity increases with an increase in the HEMA content because more porogen is separated under higher HEMA content. According to the comparison between the experimental results and the simulation results shown in Figure 5-41, the porosity is decreased with an increase in the monomer ratios for the experimental results, whereas the simulation results show the increasing porosity at various monomer ratios.

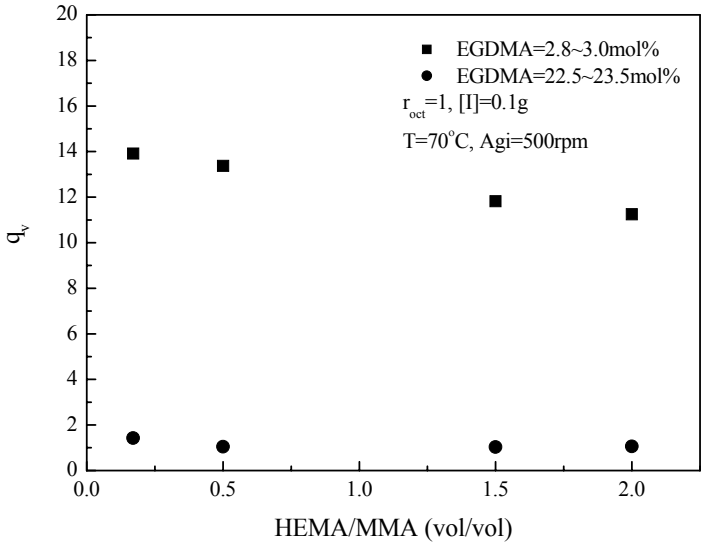

Figure 5-40 Change of q_v values with the various monomer ratios of HEMA to MMA

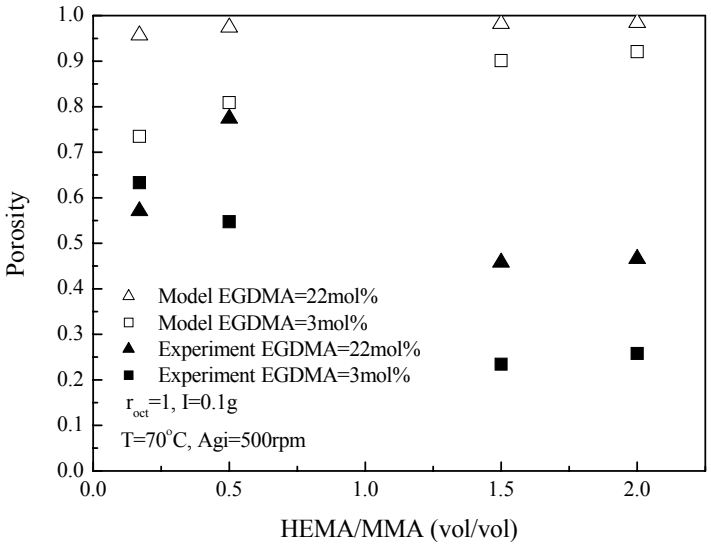

Figure 5-41 Changes of the porosity with various monomer ratios of HEMA to MMA

According to the experiments in the present study and other researchers' reports (Clayton et al, 1997), poly(HEMA) is very sticky and rubbery under swollen state which is like a 'sponge'. Although the gelation is earlier under higher HEMA content, the polymers are still softer than those having lower HEMA content according to the experiments. This means the primary polymer chains are more flexible under higher HEMA content so that the polymeric networks could be collapsed easily during porogen removal. The pore collapse or shrinkage results in the difference between experimental results and the simulation results. It can be seen that the difference is smaller under higher MMA

content because MMA polymeric chains are helpful in supporting the porous structures. The difference becomes bigger with an increase in the HEMA content because the porous collapse is much more serious under higher HEMA content. Therefore, the simulated porosity represents the highest porosity before porogen removal, and it proves that the shrinkage of the polymer networks does exist.

5.6 Summary

The porous poly(HEMA-MMA) particles were synthesized under various reaction conditions. The effect of the EGDMA molar concentrations, the porogen volume ratios and the monomer ratios of HEMA to MMA were studied.

Good particle morphology can be obtained at higher EGDMA concentration. The pore formation at various EGDMA concentrations can be explained by the different pore formation mechanisms, including χ-induced syneresis and ν-induced synerisis. The highest pore volume and porosity can be obtained at modest EGDMA concentration (~8mol%). At the highest EGDMA concentration, the pore size is the smallest and the porosity is decreased. But the porous surface area is increased with an increase in the EGDMA molar concentration. The porous structures become more heterogeneous with an increase in the EGDMA concentration because of the presence of more discrete microgels. The collapse or the shrinkage of the pores happens during solvent removal, especially at lower EGDMA concentration.

The increase in the HEMA content results in more particle aggregates or irregular particles. The porosity and the pore volume are reduced with an increase in the HEMA content. However, further increases in the HEMA content do not change the porous characteristics by much. The specific porous surface area increases with an increase in the monomer ratio. The average pore size is smaller under higher HEMA content.

At higher porogen volume ratios, shrinkage of the particles results and irregular particles are observed, especially at lower EGDMA molar concentration. With an increase in the porogen volume ratios, the maximum values of the porosity and the pore volume were observed and more pores are generated under higher porogen volume ratios.

By using the diagram of controllable pore size, the porous poly(HEMA-MMA) particles with the designed pore size and the favorable network properties could be made, which is very significant to real industrial use.

The gel formation and the porosity were simulated by the mathematical models. At higher EGDMA concentration, gelation occurs earlier. The gel points occur earlier under higher HEMA content as well. The non-solvents which have larger values of the Flory interaction parameter enhance the phase separation. At higher EGDMA concentration, the highly porous structures can be obtained whether in good solvents or in non-solvents. The simulation results show the real porosity or the maximum porosity during the formation of the pores. The shrinkage and the collapse of the pores are the main reasons resulting in the difference between the simulation and the experimental results. Since the model parameters were collected from different sources and the assumptions were made, there are errors between the model and the experiments. To get a better prediction, real reaction parameters have to be measured.

Chapter 6
Synthesis, Characterization and Modeling of Porous Poly(HEMA-Styrene) Particles

6.1 Introduction

Styrene was used as a hydrophobic comonomer of HEMA to synthesize highly porous poly(HEMA-St) particles in the present studies. Styrene already has been used in the preparation of the porous polymeric spheres, i.e., porous poly(styrene-DVB) particles. The porous poly(styrene-divinylbenzene) has been studied for decades including studies on the synthesis methods and the porous properties (Sederel et al, 1973; Okay et al, 1986; Okay, 1999; Howdle, et al, 2000; Viklund et al, 2001). In fact, poly(St-DVB), including porous particles and porous monolith, is one of the first types of the polymeric porous materials synthesized using porogens (Okay, 2000). Nowadays, porous poly(St-DVB) spheres have been widely used in chromatography as the sorbets. But these particles are not suitable for use in areas of biomedical and pharmaceutical application because the hydrophobic polymer lacks biocompatibility. However, biocompatible materials, such as poly(HEMA) particles, have weak mechanical strength and it is not easy to have a permanent porous structure inside. Therefore, the presence of styrene which is used as a comonomer with HEMA could improve the mechanical strength, control the pore structures and adjust the swelling capacity of poly(HEMA).

Styrene has been one of the comonomers used in copolymerization studies of HEMA. HEMA/ styrene copolymers have been used as model systems to study monomer reactivity in different solvents by free radical polymerization. However, it was found that the random HEMA-styrene copolymer made by conventional free radical initiation techniques had a surface composition that was similar to the bulk composition (Castner et al, 1992). The monomer pair was also studied in the emulsion polymerization (Sanchez-Chaves et al, 1999; Sanghvi et al, 2002). Chen et al (2002) proposed kinetic models for the emulsion copolymerization of HEMA and styrene. However, it was found that the results from the bulk polymerization of HEMA and St can be extended to explain the behaviors of other polymers in emulsion polymerization (Schnoobrood et al, 1995). The synthesis of the mono-sized macroporous PS-PHEMA particles has been reported using seeded polymerization (Tuncel et al, 2002; Ahmad et al, 2003). The PS latex or particles can be swollen by an organic

mixture including HEMA, crosslinker and initiator followed by the polymerization. Although the mono-sized macroporous particles can be obtained by this process, it takes a long time for the latex or the particles to be swollen by the organic mixtures and it takes a long time for the monomers to diffuse into the seeds to undergo reactions as well. In addition, the reported pore size was much bigger than 100 nm and the pore volume was low, and an increase in the HEMA feed concentration leads to the final particles with a non-porous surface and a crater-like porosity in the particle interior (Tuncel et al, 2002). Therefore, it tells us that high HEMA content is not good for the pore formation in the system. However, there is still insufficient research on the preparation of the highly porous poly(styrene-HEMA) particles using free radical suspension copolymerization.

Poly(HEMA-St) has been applied in many areas. For example, nonporous poly(HEMA-St) spheres and membrane have been used to immobilize enzymes (Liu et al, 1996; Tumturk et al, 2000) and it was found that the incorporation of styrene could control the amount of the immobilized enzymes and their activity. The non-porous poly(HEMA-St) particles reported by Uzun et al (2004) were used as specific sorbets in the dye affinity adsorption without any conformational changes. According to these applications, it can be seen that the presence of the styrene could have control over the properties of the poly(HEMA) polymers very well. Therefore, the highly porous poly(HEMA-St) particles will have better performance in more applications, such as absorbance, catalysis, controlled release, and so on.

However, studies on the porous structures and the particle morphology for the highly porous poly(HEMA-St) particles synthesized by free radical suspension polymerization are limited. How to have control over the polymers' nature in the presence of pores is still studied insufficiently. Accordingly, the objectives of this chapter were to synthesize the highly porous poly(HEMA-St) particles in the presence of an organic porogen (1-octanol), to characterize the particle morphology, to explore the porous structures and their formation mechanisms, and to simulate the gel formation and the porous characteristics.

6.2 FT-IR

Table 6-1 and Figure 6-1 show the possible spectral band assignments and FT-IR spectra (Gomez et al, 2004; Sanghvi et al, 2002) of monomer HEMA, St, EGDMA and one selected polymer sample. It can be seen that the peak of the C=C tends to dissappear in the resultant polymer, resulting from the copolymerization. However, there is still a small peak of C=C in the polymer because of non-equal

concentrations of C=C in the monomers. It also could be caused by the weakness of the monomer diffusion to the radicals since gelation. According to the peak for –OH, the HEMA unit structures are presented in the resultant polymers.

Table 6-1 Possible spectral band assignments of poly(HEMA-St) polymer

Wavenumbers (cm^{-1})	Spectral band assignments
3450-3500	Stretching vibration of O-H
2922, 2953, 3000	Stretching vibration of C-H
1724-1731	Stretching vibration of C=O
1635	Stretching vibration of C=C
3026	C=C from aromatic rings
1350-1500	In-plane bending or twist of C-H
1602	C-C from aromatic rings
1200-1350	Bending vibration of -OH
1000-1200	Stretching vibration of C-O
800-1000	Out-of-plane bending of C-H
700, 760	C-H bending from mono-substituted benzene
750	Out-of-plane bending of C-O

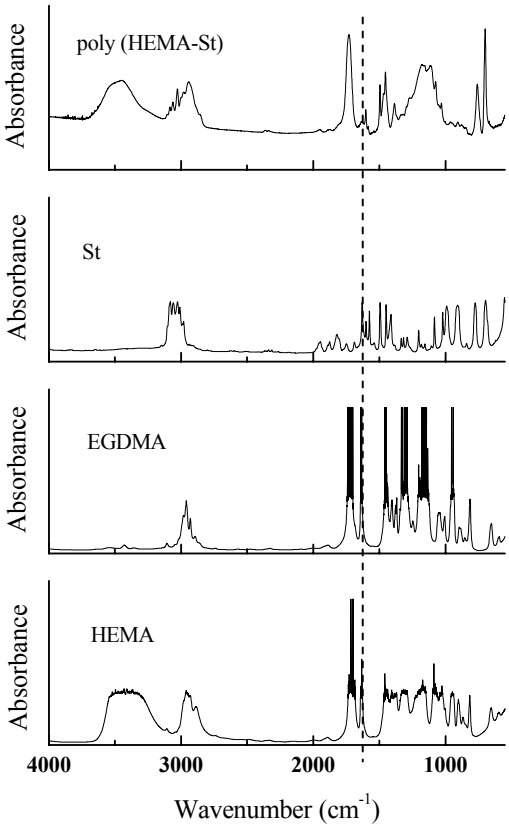

Figure 6-1 FT-IR spectra of poly(HEMA-St) polymer synthesized in the present studies; HEMA/St=2ml/12ml, EGDMA=2.9mol%

6.3 Glass Transition Temperature

Table 6-2 shows the estimated glass transition temperature of some selected samples synthesized under different monomer ratios and EGDMA molar concentration. It can be seen that the glass transition temperature is increased with an increase in the EGDMA concentration or styrene.

Table 6-2 Glass transition temperature of poly(HEMA-St)

HEMA (ml)	St (ml)	EGDMA (mol%)	T_g (K)
9.4	4.7	8.6	368.1
9.4	4.7	18.0	373.0
9.4	4.7	23.9	375.9
2	12	8.4	375.1
2	12	17.5	379.4
2	12	23.3	381.8

6.4 Characterization and Simulation of Porous Structures and Gel Formation

Table 6-3 Kinetic constants and parameters for the synthesis of the porous poly(HEMA-St) particle at 70°C using AIBN as an Initiator (1-HEMA; 2-St; 3-EGDMA)

Constants and Parameters	References
f=0.59	Li et al, 1989 (b)
$k_d(s^{-1})=8.5\times10^{-4}$	Naghash et al., 1995
k_{p1}=116.7 L/(mol·s)	
k_{p2}=480 L/(mol·s)	Tefera et al, 1994
k_{p3}=941.8 L/(mol·s)	Hild et al., 1985
$\overline{r_{43}}$ =0.1	Okay, 1999
k_{td}^0=0 L/(mol·s)	Naghash et al., 1995
$k_{tc}^0=2.9\times10^7$ L/(mol·s)	Naghash et al., 1995
k_{cyc}=0.3	Okay, 1999
d_1=1.073 g/ml	
d_2=0.909 g/ml	
d3=1.051 g/ml	
dp	equal to d_2
$\delta_1=23.2\ (Mpa)^{1/2}$	Okay, 2000
$\delta_2=19.0\ (Mpa)^{1/2}$	Barton, 1983
$\delta_3=18.2\ (Mpa)^{1/2}$	Okay, 2000
$\delta_{oct}=20.9\ (Mpa)^{1/2}$	Brandrup et al., 1999
$\delta_{PHEMA}=29.7\ (Mpa)^{1/2}$	Okay, 2000
$\delta_{PS}=19.7\ (Mpa)^{1/2}$	Barton, 1983
$\delta_{PEGDMA}=19.2\ (Mpa)^{1/2}$	Okay, 2000
M_{w1}=130.14 g/mol	
M_{w2}=104.15 g/mol	
M_{w3}=198.22 g/mol	
A	7

Compared to MMA, a slightly soluble comonomer, styrene is less water-soluble than MMA with a solubility of only 0.5wt% in water at 50°C. This will result in different behaviors of the formation of the porous structures. To study the gel formation and the porous characteristics of the porous poly(HEMA-St), the mathematical models introduced in Chapter 5 was used to simulate the gelation and the porous characteristics. Table 6-3 shows the model parameters which were collected from different sources or estimated from available data.

6.4.1 Effect of EGDMA Molar Concentration

Similar with HEMA-MMA system, the effect of the crosslinking in terms of the EGDMA molar concentration was studied at certain porogen volume ratio, and the high and low levels of the monomer ratios, HEMA/St=2ml/12ml and HEMA/St=9.4ml/4.7ml. Table 6-4 shows the reaction conditions and the experimental results.

Table 6-4 Reaction compositions and experimental results of the synthesis of the poly(HEMA-St) at various EGDMA molar concentrations; r_{oct}=1; T=70°C; Agi=500rpm

No.	HEMA (ml)	St (ml)	EGDMA (mol%)	Porosity (%)	d_2 (g/cm^3)	d_0 (g/cm^3)	Average Pore Size (nm)	Particle Size (μm)	Particle Morphology
HS1	2	12	0.6	56.1	1.08	0.60	406	12.1±2.6	p, a
HS2	2	12	2.9	59.7	1.13	0.46	243	12.7±5.6	p
HS3	2	12	8.4	82.9	1.11	0.39	82.6	5.8±2.9	p
HS4	2	12	17.5	82.0	1.25	0.39	40.4	8.3±3.9	p
HS5	2	12	23.3	79.9	1.15	0.57	20.8	11.4±4.9	p
HS6	9.4	4.7	0.6	41.7	1.58	1.23	-	-	i
HS7	9.4	4.7	3.0	46.5	1.22	0.73	10.7	5.7±1.1	p, a
HS8	9.4	4.7	8.6	70.8	1.21	0.76	77.4	10.5±6.8	p
HS9	9.4	4.7	18.0	80.4	1.18	0.60	39.5	18.8±6.1	p
HS10	9.4	4.7	23.9	68.7	1.24	0.93	19.3	14.3±4.0	p

p: particle; a: the presence of the aggregated particles; i: the presence of the irregular particles

6.4.1.1 Gel Formation

The change of the reaction conversion with the reaction time is shown in Figure 6-2 . The filled symbols represent the onset of the gelation which is the gel point. It can be seen that the reaction rate is much faster at higher EGDMA concentration than those at lower EGDMA concentration. Although there is no obvious explanation for the sudden decrease in reaction rate at higher conversions, some researchers pointed out that this is probably due to a combination of dffusion-controlled propagation

and a significant increase in initiator radical recombination in the 'cage' as the monomer/polymer mixture approaches a glass state (Li et al, 1989a).

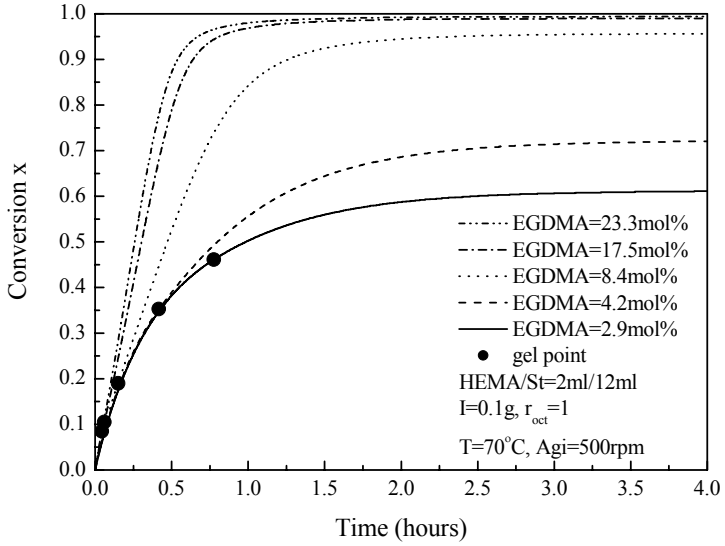

Figure 6-2 Reaction conversion and gel points under different EGDMA concentration

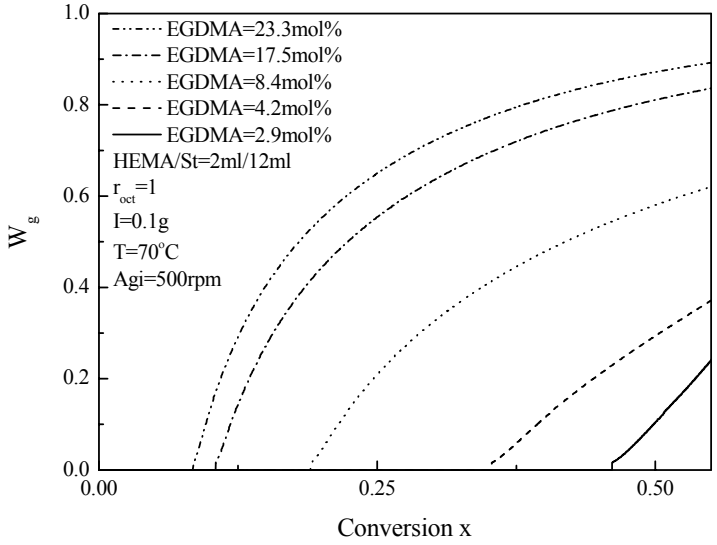

Figure 6-3 Changes of the gel fraction with reaction conversion at various EGDMA concentrations

Figure 6-3 shows the change of the gel fraction with the reaction conversion. The gel fraction grows faster at higher EGDMA concentration which is similar with that in the HEMA/MMA systems. The gelation occurs later at lower EGDMA concentration which implies that there are considerable fractions of the sol in the system when the reaction was stopped after 4 hours, which is consistent with the observation in the experiments. The polymers synthesized at higher EGDMA concentration

feels harder than those synthesized at lower EGDMA concentration, showing that the network formation and the crosslinking are greatly enhanced. Figure 6-4 compares the experimental results with the simulated values. The model predicts the gel formation pretty well, especially at the initial and the final stages of the gelation. The difference between the experimental results and the model prediction is probably resulted from the values of the selected reaction parameters and the model assumptions. To obtain more accurate simulation results, the real values of the reaction constants have to be measured based on the present reaction system. However, the present simulation results have illustrated the general gelation behaviors successfully. Furthermore, Figure 6-5 illustrates that these systems have a typical behavior at the gel point which is that the X_2 becomes infinite.

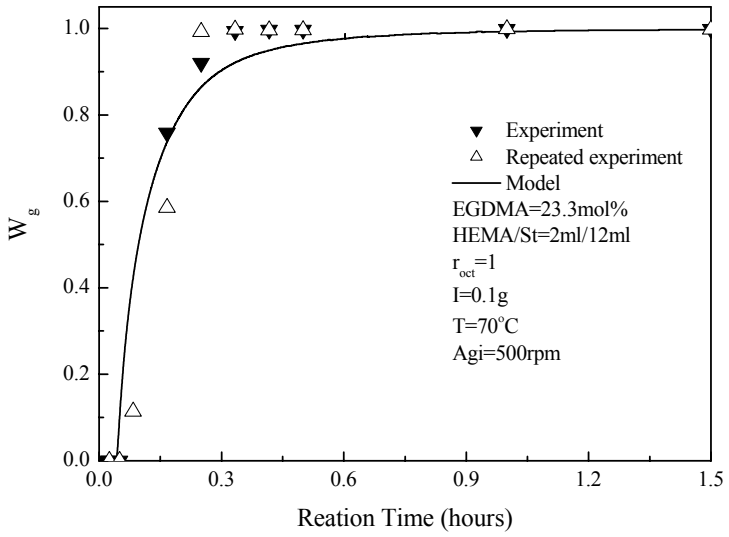

Figure 6-4 Comparison between the experimental results and the simulated values of the gel fraction

According to the discussion in Chapter 5, the crosslinking has a great effect on the average molecular weight between the successive crosslinks and the volume swelling ratio in the solvent. More importantly, it has been found that the different crosslinking density will change the values of the solubility parameters of the resultant polymers (Okay et al, 1992) so that the overall values of the Flory interaction parameter between the polymers and the solvent will be changed during the course of the reaction. This change could have a great impact on the particle morphology and the porous structures in the polymers. Based on this model, the average molecular weight between the successive crosslinks, the volume swelling ratio in the 1-octanol and the values of the Flory interaction parameters after 4 hours reaction were calculated as shown in Table 6-5. The values of M_c and q_v are decreased with an increase in the EGDMA molar concentration. With lower HEMA content, the solvent is a good solvent for the polymers (χ<0.5), whereas it is a poor one under higher HEMA

content (χ>0.5). It has been shown that 1-octanol is a non-solvent for the poly(HEMA) but it is a good one for PS according to the solubility parameters. However, under higher HEMA content, the higher EGMDA concentration enables the mixtures to be better solvents for the polymers (Okay, 2000). The highly crosslinked networks still result in a decrease in the values of q_v. Therefore, these values will be helpful to analyze the particle morphology and the porous structures.

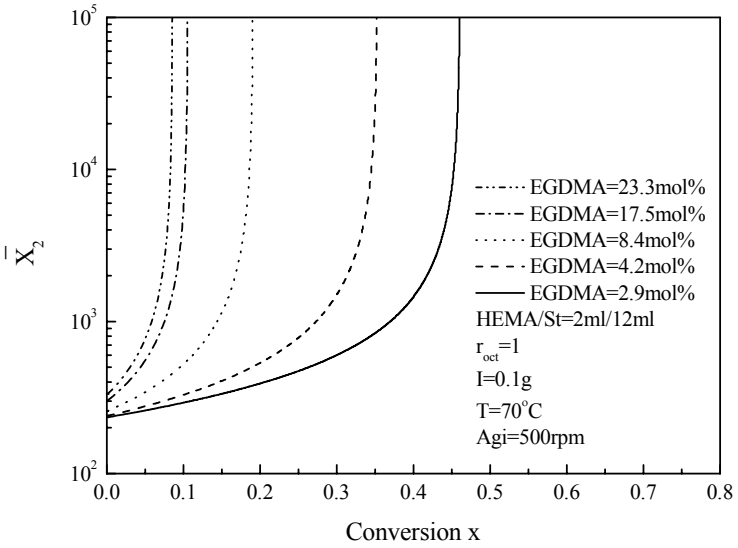

Figure 6-5 Changes of the average molecular weight of the branched polymers with reaction conversion in the *sol* until the gel point

Table 6-5 Average molecular weight between the successive crosslinks, the volume swelling ratio in 1-octanol and the Flory interaction parameters at different EGDMA molar concentrations; r_{oct}= 1

No.	HEMA (ml)	St (ml)	EGDMA (mol%)	χ	q_v (v/v)	M_c
HS2	2	12	2.9	0.341	23.8	63700
HS3	2	12	8.4	0.340	4.18	917
HS4	2	12	17.5	0.344	1.72	282
HS5	2	12	23.3	0.349	1.36	211
HS8	9.4	4.7	8.6	1.486	1.52	1272
HS9	9.4	4.7	18.0	1.069	1.40	349
HS10	9.4	4.7	23.9	0.871	1.26	241

6.4.1.2 Particle morphology

As stated in Chapter 5, the separated spherical particles with minimized aggregated particles of the irregular shapes are very important for the end use. As shown in Table 6-4, the resultant polymers have better particle morphology up to certain EGDMA concentration, such as 3.0mol%.

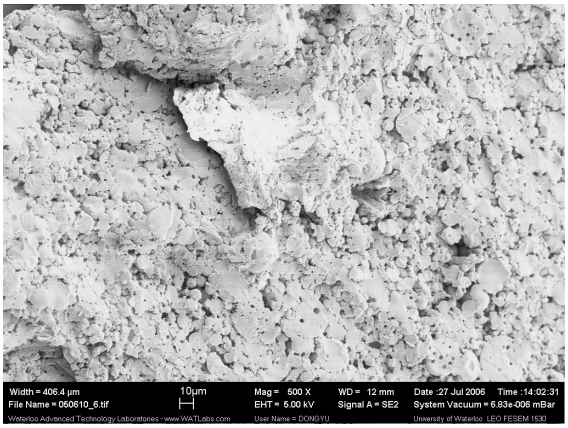

Figure 6-6 Particle morphology of Sample HS6; Scale bar=10µm; HEMA/St=9.4ml/4.7ml; [EGDMA]=0.6mol%; r_{oct}=1

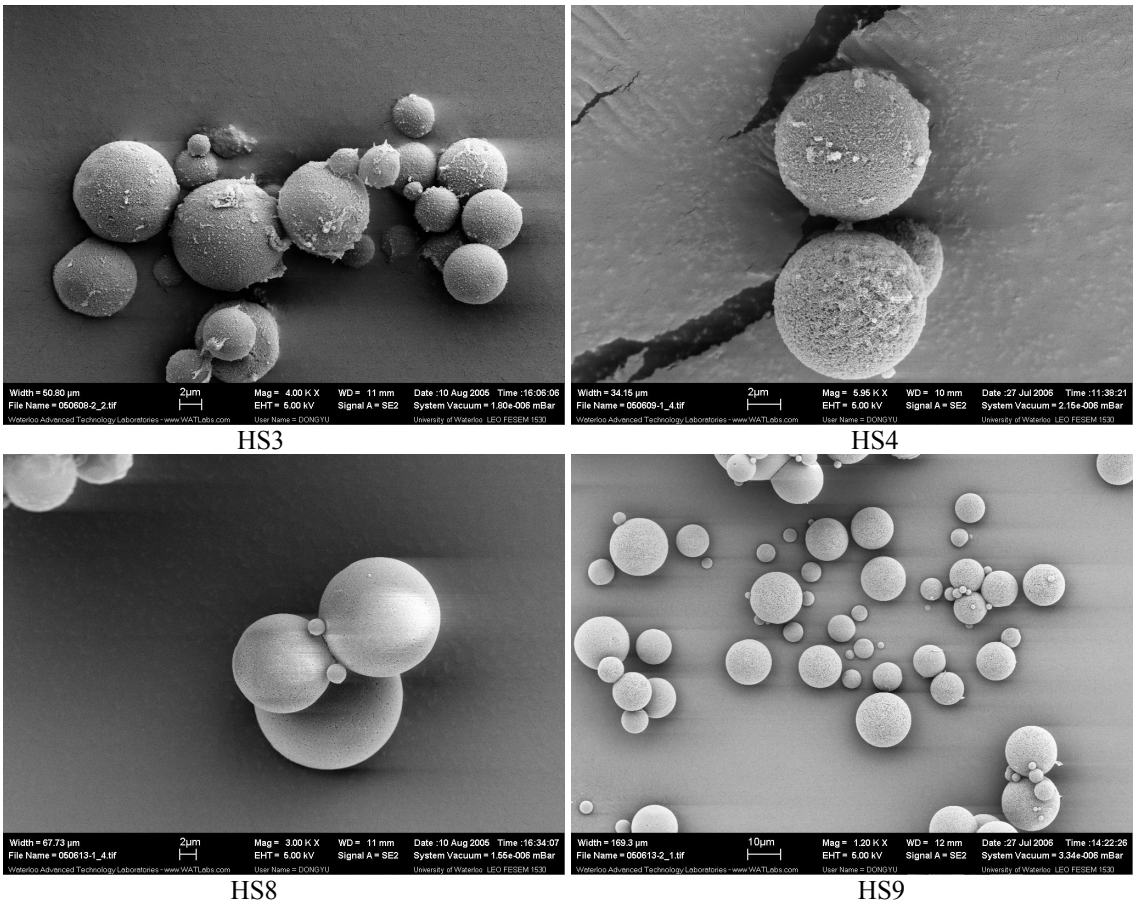

Figure 6-7 Particle morphology of selected particle samples; HS3: scale bar 2µm, r_H=2ml/12ml, [EGDMA]=8.4mol%; HS4: scale bar 2µm, r_H=2ml/12ml, [EGDMA]=17.5mol%; HM8: scale bar 2µm, r_H=9.4ml/4.7ml, [EGDMA]=8.6mol% and HM9: scale bar 10µm, r_H=9.4ml/4.7ml, [EGDMA]=18.0mol%; r_{oct}=1

The resultant polymers have less irregular particles or aggregates than poly(HEMA-MMA), which is probably because styrene is more hydrophobic than MMA. The average particle size of the poly(HEMA-St) porous particles show the fluctuation which could be caused by the errors of the calculation of particle size according to the SEM pictures. However, it still can be seen that the particle size distribution is more uniform than those of the poly(HEMA-MMA) particles. At higher EGDMA concentration, the crosslinking and the gel formation are faster so that it could be imagined that the 'hard' particles can be formed, preventing from the agglomeration.

On the other hand, the irregular particles formed by the agglomeration of small particles are found at lower EGDMA concentration as shown in Figure 6-6. It was found that there are some fused polymers between these agglomerated particles. This could be caused by the polymerization of HEMA lost in the aqueous phase. Under higher HEMA content, more HEMA will be lost in the aqueous phase to generate much smaller fine particles in water since water is a non-solvent for poly(HEMA) as well (Dušek et al, 1971). Therefore, the agglomeration of these fine particles and other small particles after reaction via pendent vinyl groups results in the irregular particles. The particle morphology of the selected samples is shown in Figure 6-7.

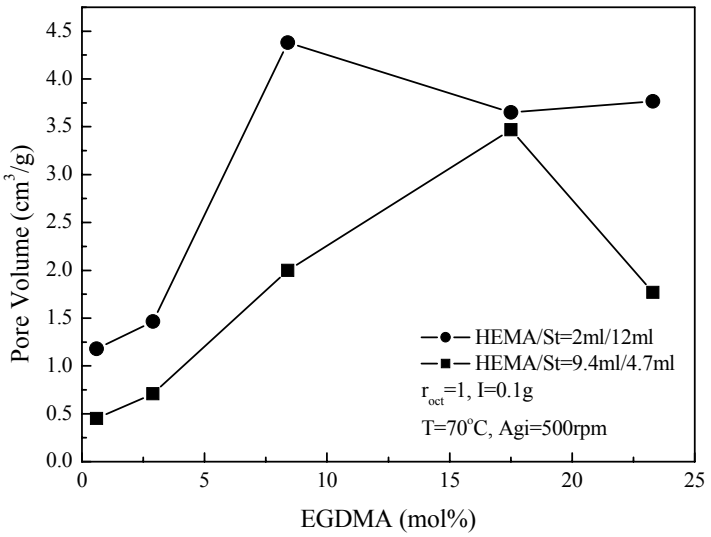

Figure 6-8 Changes of the pore volume of the porous poly(HEMA-St) particles at various EGDMA concentrations; the data are shown in Appendix I

6.4.1.3 Porous Structures

As shown in Table 6-4 and Figure 6-8, similar to the poly(HEMA-MMA) particles synthesized in the present studies, the change of the porosity and the pore volume demonstrates the maximums for the pore volume of poly(HEMA-St) particles over the range of the EGDMA concentration. According to the discussion in Chapter 5, this phenomenon implies the transformation from χ-induced syneresis (at low crosslinker concentration) to ν-induced synerisis (at higher crosslinker concentration). As shown in Table 6-5, the calculated q_v values are decreased rapidly at higher EGDMA concentration such that more porogen molecules are separated out of the network phase resulting in a higher pore volume and a higher porosity. However, at much higher EGDMA concentration, microgels are separated so that the porogen becomes a continuous phase. The agglomeration of these microgels generates smaller pores. The apparent density is decreased with an increase in the EGDMA concentration because of the presence of the highly porous strucuture; however, it increases again at the highest EGDMA concentration which implies that the porous structures are more compact resulting from the smaller pore size.

According to Okay (2000) and Dusek et al (1971), the reaction mixture is a poor solvent for the polymers at a lower crosslinker concentration and it becomes a good one at a higher crosslinker concentration. Therefore, at lower EGDMA concentration, the incompatibility between the polymers and the reaction mixtures will enhance the phase separation so that the porogen will be separated out of the network phase and dispersed in it. Further crosslinking will fix the spaces occupied by the porogen to form pores. Before the critical EGDMA concentration, the increase in the EGDMA concentration is helpful in fixing more spaces and protecting the pores from collapse so that the pore volume is increased. On the other hand, a further increase in the EGDMA concentration makes the reaction mixture a better solvent for the polymers under high HEMA, but the polymeric networks are hard to be swollen at higher EGDMA concentration as well. Therefore, highly crosslinked microgels will be separated and they agglomerate together to form porous structures. These porous structures are supported by the crosslinking so that they are retained during porogen removal. The agglomeration of these microgels results in lower pore volume because of the formation of much smaller pores. This implies again that the porous structures are even more compact at higher EGDMA concentration.

Generally, the pore volumes of poly(HEMA-St) synthesized at various EGDMA concentrations are higher than those of poly(HEMA-MMA). This probably results from inhomogeneity in crosslink distribution (Okay et al, 1986). Inhomogeneous crosslinking results in the formation of short chains in the beginning of the polymerization and long chains in the end so that the polymeric networks or the separated phase synthesized earlier have higher crosslink density, and they will not collapse on drying or solvent removal (Okay et al, 1986). Therefore, this procedure will probably retain some pores for poly(HEMA-St), resulting in higher pore volume than that of the porous poly(HEMA-MMA) particles. As stated above, it was also found that poly(HEMA-St) can be swollen by the monomer mixtures more easily. This means the separated polymers will be swollen by the monomer mixture to form slightly looser networks, resulting in more pores and higher pore volumes (Downey et al, 2001).

Figure 6-9 shows a comparison of the porosity between the model prediction and the experimental results. It can be seen that the model over-estimates the porosity because the polymeric networks are still collapsed or damaged during the porogen removal or the measurement. However, the difference between the simulation results and the experimental results is less for poly(HEMA-St) than that for poly(HEMA-MMA). This implies that the presence of styrene is better to support the whole networks.

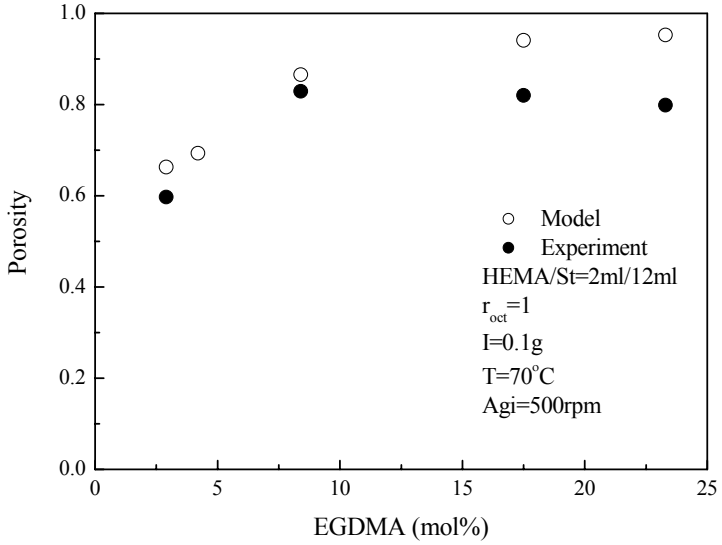

Figure 6-9 The comparison between the predicted porosity and the experimental results at different EGDMA molar concentration for the porous poly(HEMA-St) particles

Figure 6-10 shows the change of the specific porous surface area. It increases with an increase in the EGDMA molar concentration and deceases a little bit at the highest EGDMA concentration (such as 23mol%). According to the studies on the synthesis of porous poly(St-DVB) particles, an increase in

the crosslinking results in an increase in the specific surface area and a decrease in the pore size (Nyhus et al, 2000). However, in the present studies, this phenomenon was only observed up to a certain crosslinking density. The problem of Nyhus et al research is probably caused by the selection of the crosslinking range.

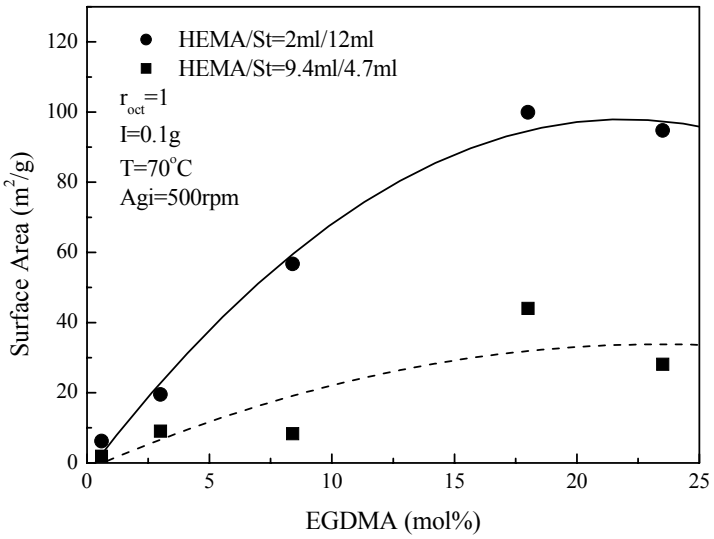

Figure 6-10 Change of the specific porous surface area with the various EGDMA concentrations; the data are shown in Appendix I

The decrease in the pore volume and the increase in the porous surface area imply that there are more pores of smaller size. However, if both the pore volume and the porous surface area are decreased, fewer pores or much smaller pores are generated at higher EGDMA concentration resulting from the formation of much more compact polymeric networks. According to the M_c values shown in Table 6-5, the polymeric networks are more compact at higher EGDMA concentration because the M_c values decrease rapidly with an increase in the EGDMA molar concentration, resulting in much smaller pores and compact networks. This could be verified by the porous morphology as shown in Figure 6-11. It can be seen that the pore size becomes smaller with an increase in the EGDMA molar concentration. In addition, the presence of higher styrene content and more EGDMA result in the more heterogeneous morphology of pores, which is similar to the poly(HEMA-MMA) particles.

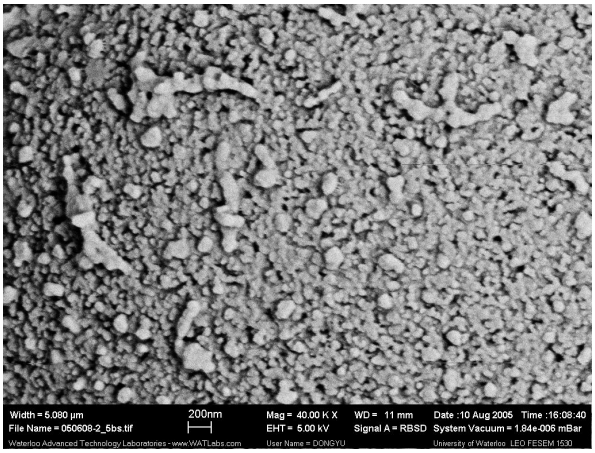

HS2

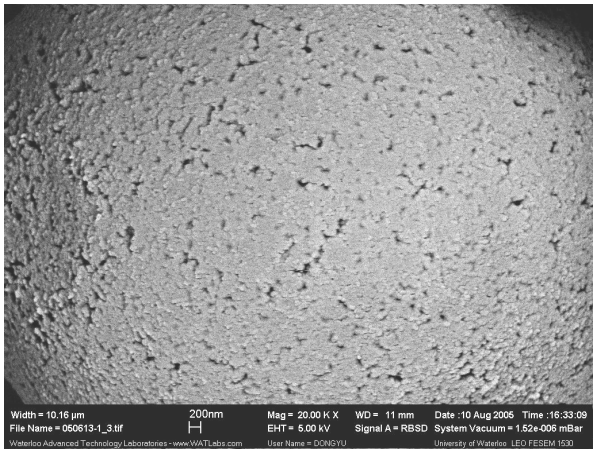

HS7

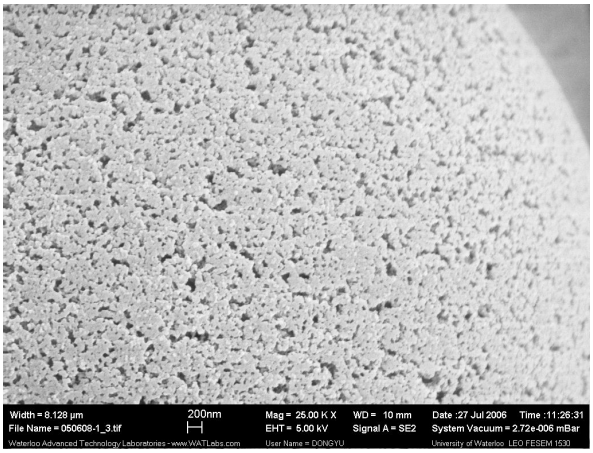

HS3

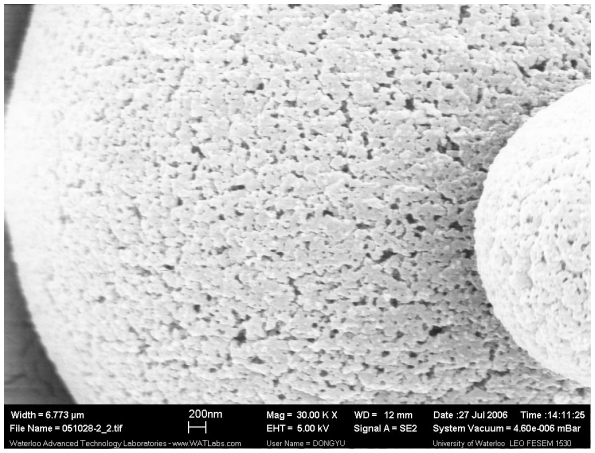

HS8

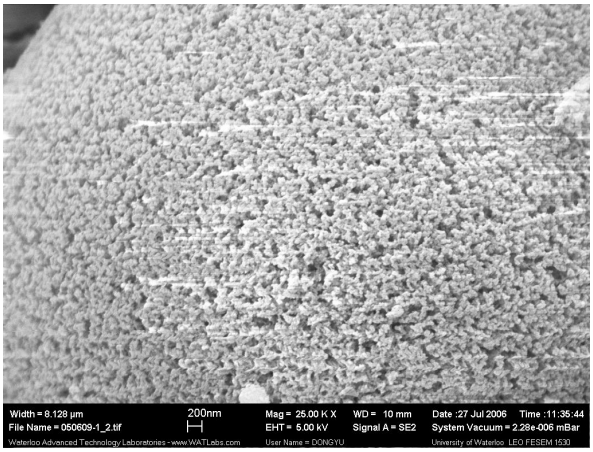

HS4

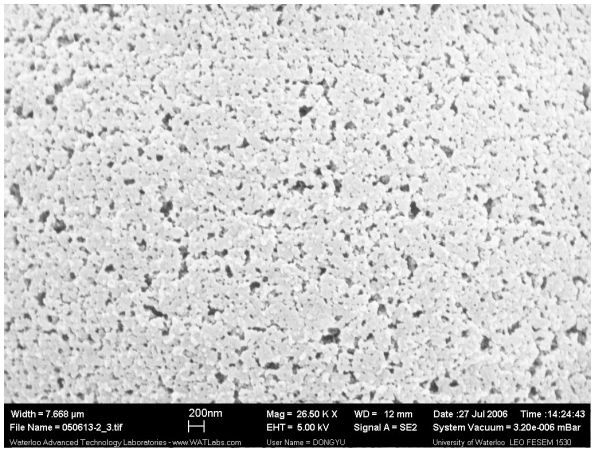

HS9

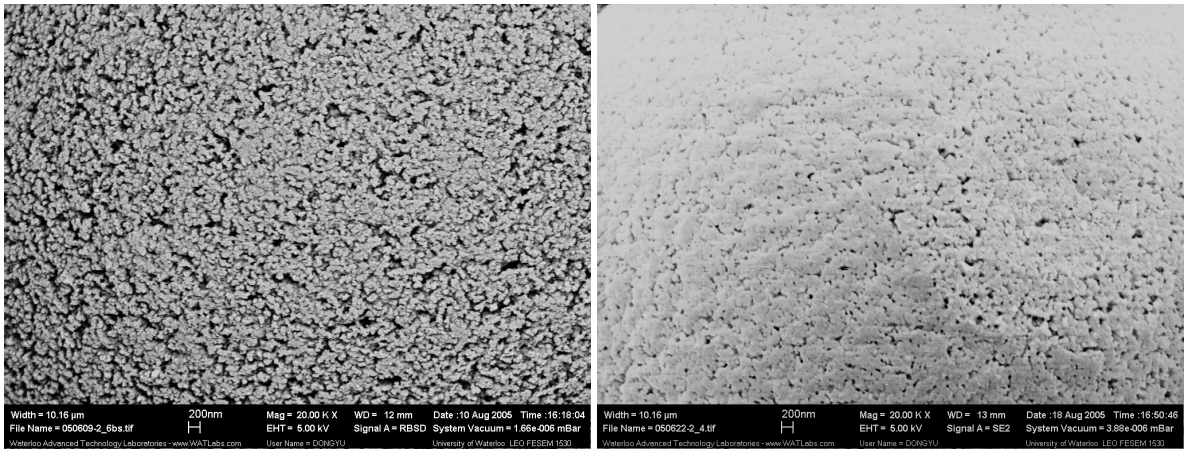

HS5 HS10

Figure 6-11 The porous structures of poly(HEMA-St) particles at various EGDMA concentrations; Scale bar: 200nm; HS2: r_H=2ml/12ml, [EGDMA]=2.9mol%; HS3: r_H=2ml/12ml, [EGDMA]=8.4mol%; HS4: r_H=2ml/12ml, [EGDMA]=17.5mol%; HS5: r_H=2ml/12ml, [EGDMA]=23.3mol%; HS7: r_H=9.4ml/4.7ml, [EGDMA]=3.0mol%; HS8: r_H=9.4ml/4.7ml, [EGDMA]=8.6mol%; HS9: r_H=9.4ml/4.7ml, [EGDMA]=18.0mol%; HS10: r_H=9.4ml/4.7ml, [EGDMA]=23.9mol%; r_{oct}=1

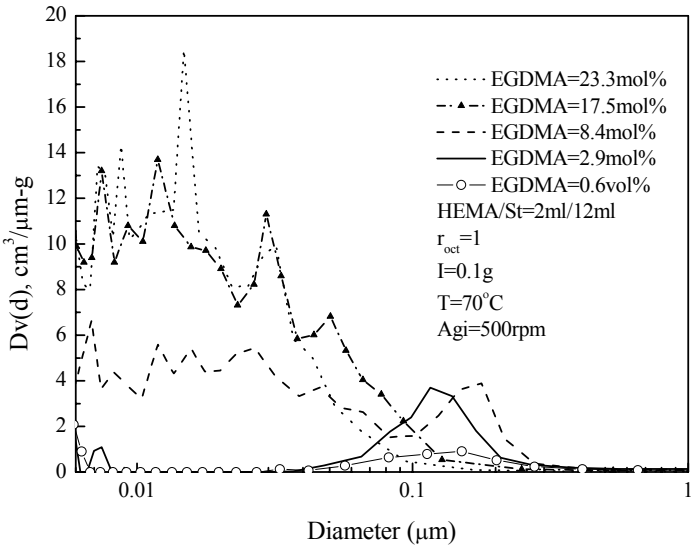

Figure 6-12 The pore size distribution of the porous poly(HEMA-St) particles prepared at various EGDMA molar concentration

To further understand the pore formation in the porous poly(HEMA-St) particles synthesized at various EGDMA concentrations, the pore size distribution, as shown in Figure 6-12 and Figure 6-13, was studied. According to Figure 6-12, under lower HEMA content, the pore size is larger at lower EGDMA concentration and the pore size distribution profiles are shifted toward smaller pores with an

increase in the EGDMA molar concentration. More pores with a pore size smaller than 100nm are generated with an increase in the EGDMA molar concentration. Pores larger than 100 nm tend to disappear.

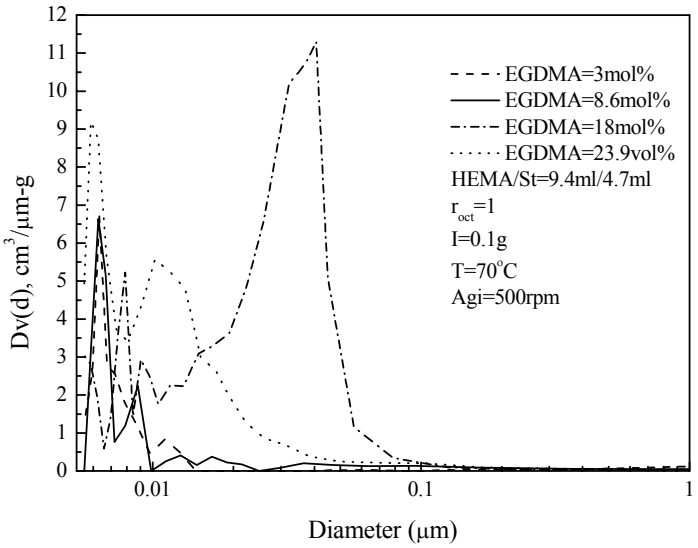

Figure 6-13 The pore size distribution of the porous poly(HEMA-St) particles prepared at various EGDMA molar concentration

If HEMA content is higher, as shown in Figure 6-13, the pore size is smaller and the pore size distribution is narrower. Under higher HEMA content and at lower EGDMA molar concentration, the pores are smaller and the pore size distribution shifts toward larger pores with an increase in the EGDMA molar concentration. When the EGDMA concentration is 17.5-18mol%, the distribution of smaller pores is similar to the cases under lower EGDMA concentration, but there are more pores between 30-80 nm resulting in the largest pore volume as shown in Figure 6-8. If the EGDMA concentration is increased further, it can be seen that the pore size distribution is shifted toward smaller pores again and there are fewer pores formed than for particles synthesized at moderate EGDMA molar concentration, 17.5-18.0mol%.

According to research carried out on poly(St-DVB) (Okay et al, 1985), at a low DVB concentration, the pores in the macromolecular network can collapse during the removal of the diluent or on drying, and no stable pores remain, resulting in the appearance of the individual microspheres and an increase in the randomness of the pore size distribution. However, high DVB concentration provides a narrower pore size distribution. However, in the present studies for poly(HEMA-St), the results are different. According to Figure 6-12 and Figure 6-13, the pore size distribution is narrower for the

polymers synthesized at lower EGDMA concentration. This implies that the polymeric networks are formed at lower EGDMA concentration and the presence of styrene is helpful in building up networks. The inhomogeneous distribution of crosslinking also contributes to a narrower distribution of pores at lower EGDMA concentration. At higher EGDMA concentration, the phase-separated microgels are agglomerated together. Obviously, this random agglomeration contributes to a broader and more random distribution. Therefore, the pore formation is determined by the properties of the different reaction systems. Generally speaking, the particles produced at 18mol% of EGDMA have better porous structures and porous characteristics.

6.4.2 Effect of Monomer Ratio

Table 6-6 Reaction compositions and experimental results of the synthesis of the porous poly (HEMA-St) particles under various monomer ratios; r_{oct}=1; T=70°C; Agi=500rpm

No.	HEMA (ml)	St (ml)	EGDMA (mol%)	Porosity (%)	d_2 (g/cm^3)	d_0 (g/cm^3)	Average Pore Size (nm)	Particle Size (μm)	Particle Morphology
HS2	2	12	2.9	59.7	1.13	0.46	243	12.7±5.6	p
HS11	4.7	9.4	3.0	49.4	1.10	0.76	45.6	14.6	p, a
HS12	7	7	3.0	40.3	1.12	0.77	48.6	-	i, a
HS13	8.4	5.6	3.1	34.6	1.22	0.88	27.4	9.1±4.1	p, a
HS7	9.4	4.7	3.0	46.5	1.22	0.73	10.7	5.7±1.1	p, a
HS5	2	12	23.3	79.9	1.15	0.57	20.8	11.4±4.9	p
HS14	4.7	9.4	23.4	77.0	0.95	0.55	23.7	17.0±2.8	p
HS15	7	7	23.8	79.6	1.30	0.68	13.2	9.8±5.1	p
HS16	8.4	5.6	23.9	73.9	1.18	0.73	15.3	8.6±4.8	p
HS10	9.4	4.7	23.9	68.7	1.24	0.93	19.3	14.3±4.0	p

p: particle; a: the presence of the aggregated particles; i: the presence of the irregular particles

The monomer volume ratios of HEMA to St have great effects on the particle morphology and the porous structures of the porous poly(HEMA-St) particles. Table 6-6 shows the reaction conditions and the experimental results. Figure 6-14 through Figure 6-17 illustrates the gel formation. Figure 6-18 through Figure 6-24 show the change of the particle morphology and the porous structures. It was found that the monomer ratios have more significant effects on the porous properties at higher EGDMA concentration than those at lower EGDMA concentration.

6.4.2.1 Gel Formation

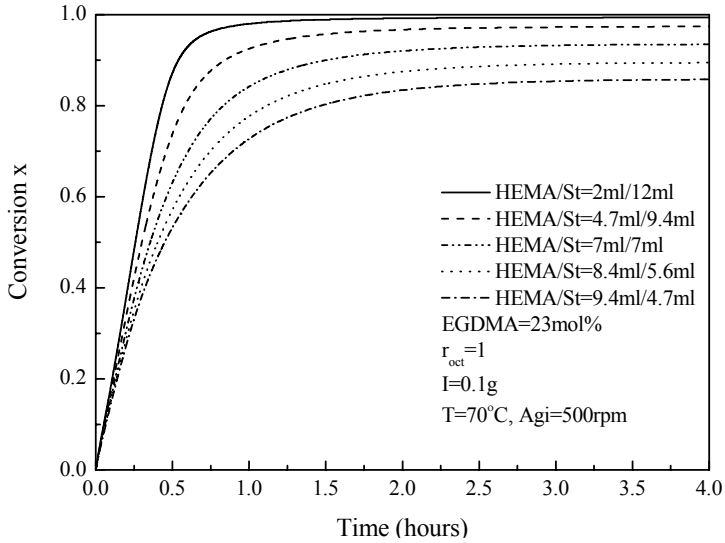

Figure 6-14 Changes of the reaction conversion with the reaction time under various monomer ratios

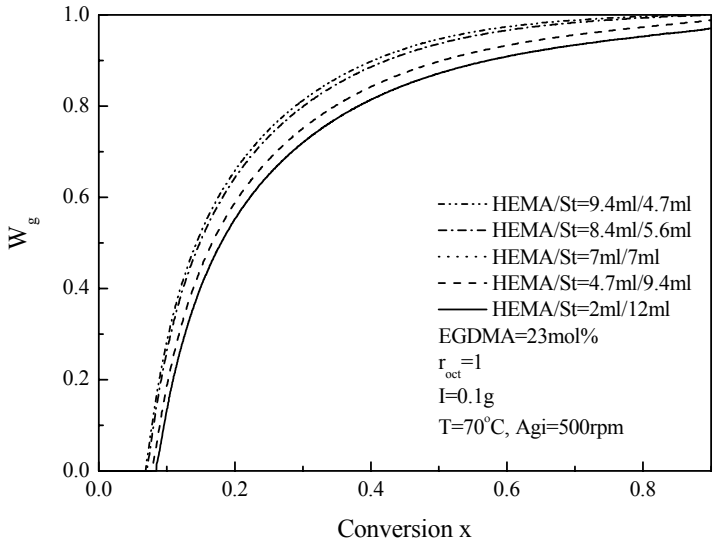

Figure 6-15 Changes of the gel fraction with the reaction conversion under various monomer ratios

Figure 6-14 shows the change of the reaction conversion with the reaction time under certain reaction conditions. Similar to the HEMA/MMA systems, the higher the hydrophobic contents, the faster the reaction rates are. However, the reaction conversion at 4 hours is lower under higher HEMA content than that under lower HEMA content. This is probably because HEMA and styrene are copolymerized in a alternating behavior according to the reactivity ratios of HEMA (r_1=0.62) and styrene (r_2=0.4) (Brar et al, 2006), and a higer HEMA content is favorable for the gel formation so

that the combination of diffusion controlled propagation and a significant increase in initiator radical recombination in the 'cage' as the monomer/polymer mixture approaches a glass state (Li et al, 1989b).

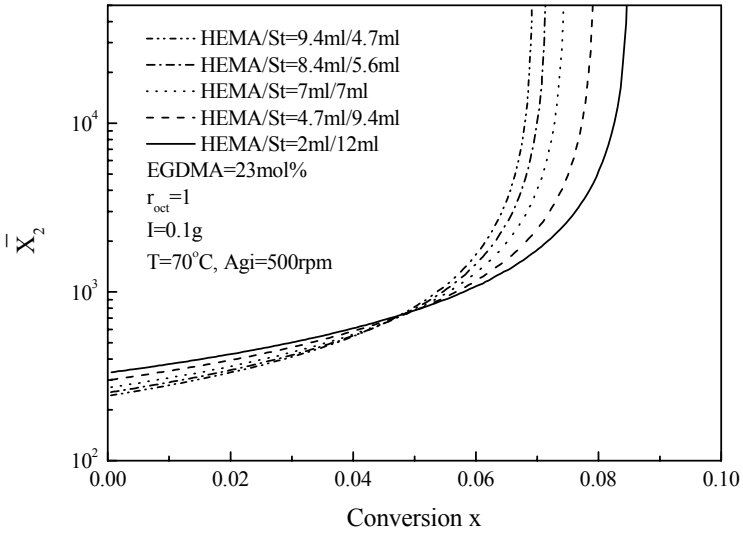

Figure 6-16 Changes of the average molecular weight with the reaction conversion under various monomer ratios

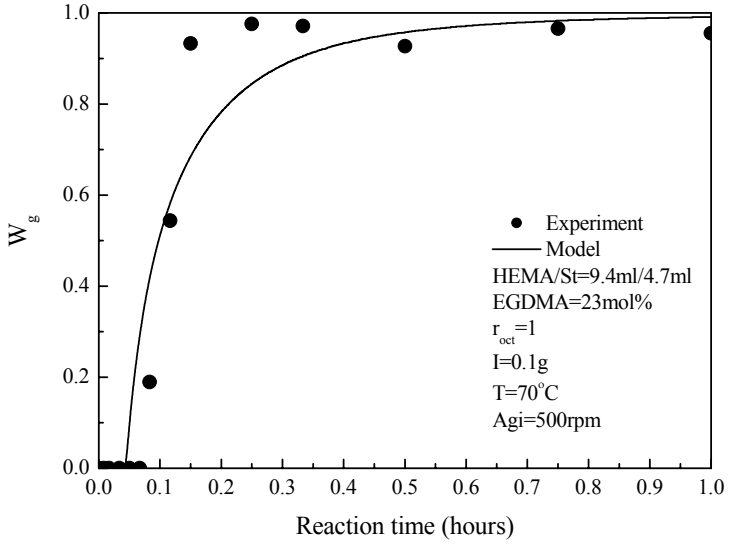

Figure 6-17 Comparison between the experimental results and the simulated values of the gel fraction

However, similar with the synthesis of the poly(HEMA-MMA), the time for the onset of the gelation are almost the same for each reaction system. But it still can be seen that the gel grows faster under higher HEMA content according to Figure 6-15. The reasons are the same as the discussion in the previous chapter according to Figure 6-16 about the average molecular weight of the branched

polymers. The average molecular weight of the branched polymers in the sol grows faster for the polymers synthesized under higher HEMA contents. One thing is that the molecular weight of HEMA monomer is higher than the styrene, and another thing is that the HEMA has a long side group with a hydroxyl group on it which contributes to hydrogen bonding. This side group could lead to the intermolecular crosslinking through the hydrogen bonding so that the gelation could be accelerated. Figure 6-17 shows a comparison of the experimental results and the simulated results. It can be seen that the model prediction is close to the experimental results, especially at the initial and the final stages of the gelation.

Table 6-7 Average molecular weight between the successive crosslinks, volume swelling ratio in 1-octanol and values of the Flory interaction parameters under different monomer ratios; r_{oct}=1

No.	HEMA (ml)	St (ml)	EGDMA (mol%)	χ	q_v (v/v)	M_c
HS2	2	12	2.9	0.341	23.8	63700
HS11	4.7	9.4	3.0	0.552	14.9	62200
HS12	7	7	3.0	1.037	2.53	56800
HS13	8.4	5.6	3.1	1.462	1.63	54000
HS7	9.4	4.7	3.0	1.804	1.39	53200
HS5	2	12	23.3	0.349	1.36	211
HS14	4.7	9.4	23.4	0.381	1.34	216
HS15	7	7	23.8	0.555	1.30	222
HS16	8.4	5.6	23.9	0.726	1.32	230
HS10	9.4	4.7	23.9	0.871	1.26	241

The number average molecular weight between successive crosslinks, the volume swelling ratio in 1-octanol and the Flory interaction parameters between 1-octanol and the polymers were calculated using the present model as shown in Table 6-7. No matter what the EGDMA concentration is, the values of the interaction parameter keep increasing and the volume swelling ratios keep decreasing. From the solubility parameter, 1-octanol is a non-solvent for poly(HEMA) but a good one for PS. So the higher HEMA content must lead to higher interaction parameter values showing that the solvent tends to be a non-solvent for the polymers. For the same reasons, the values of the volume swelling ratios are decreased. As to the values of M_c, they are decreased with an increase in the HEMA content at lower EGDMA concentration, whereas they are increased a little bit at higher EGDMA concentration. At lower EGDMA concentration, the flexibility of the polymeric chains are favored so that there are more opportunities for the polymeric chains to be crosslinked with each other under higher HEMA content to lower the M_c values. However, at higher EGDMA concentration, the values of M_c are much lower than those at lower EGDMA concentration, showing more compact networks. Because of this high crosslink density, the values of M_c do not change too much. However, it can be

seen that the effect of the monomer ratio on these parameter values are much greater at lower EGDMA concentration than those at higher EGDMA concentration.

6.4.2.2 Particle morphology

According to some researchers (Lebduska et al, 1986; Chen et al, 2002), styrene was used as a "hard" comonomer in their systems, which means the presence of styrene will be favorable for the formation of the hard spheres and it is helpful to support the polymer structures. Therefore, the particle morphology is better at higher styrene content, especially at a higher EGDMA concentration.

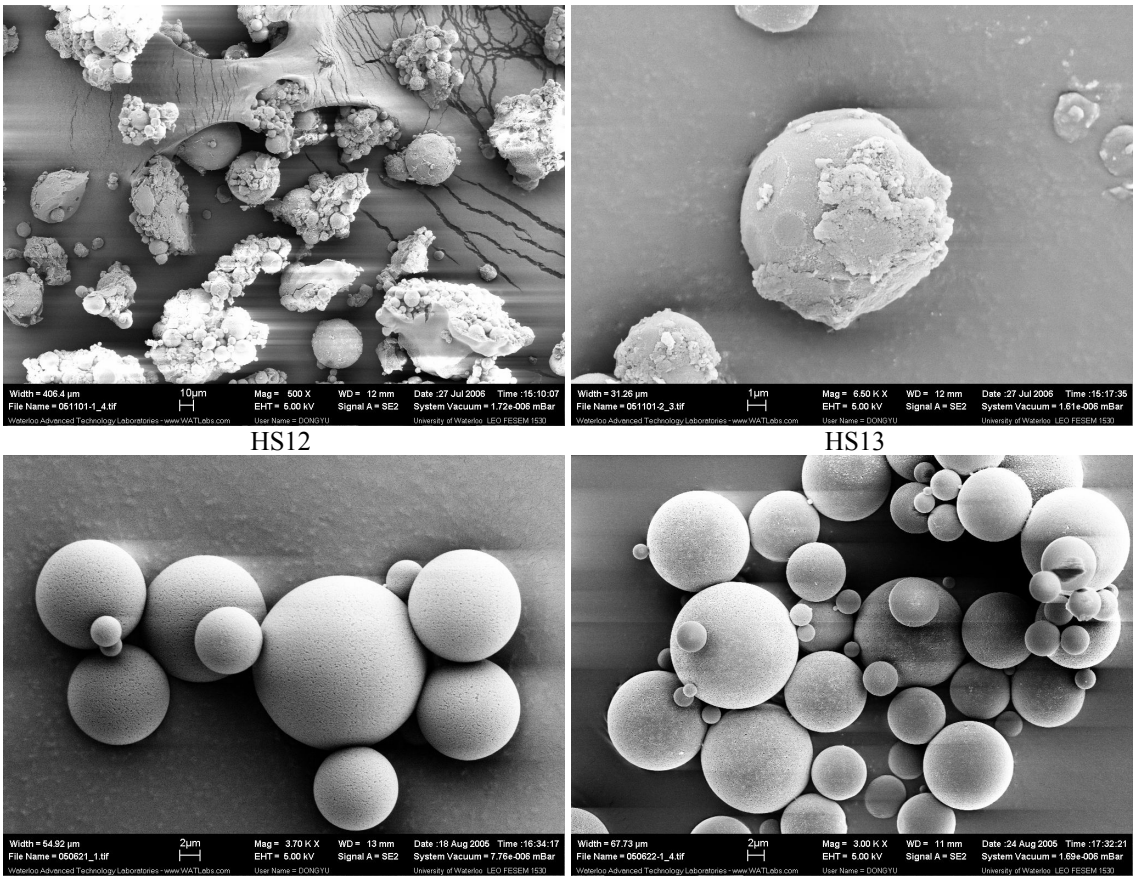

Figure 6-18 Particle morphology of selected particle samples; HS12: scale bar 10µm, r_H=7ml/7ml, [EGDMA]=3mol%; HS13: scale bar 1µm, r_H=8.4ml/5.6ml, [EGDMA]=3mol%; HS15: scale bar 2µm, r_H=7ml/7ml, [EGDMA]=23mol%; HS16: scale bar 2µm, r_H=8.4ml/5.6ml, [EGDMA]=23mol%

According to Table 6-6, there are more particle aggregates and irregular particles produced under higher HEMA content at lower EGDMA concentration. The average particle size tends to be smaller with an increase in the HEMA content which could be caused by the contraction of the particles under

higher HEMA content during drying. Since the HEMA is a hydrophilic monomer, to make spherical particles, the water-insoluble components must be used, such as hydrophobic monomers and solvents. For example, to make poly(HEMA) particles, cyclohexanol, a good solvent for the monomer and the polymer, should be used (Horak et al, 1993). According to the model studies, it is known that the whole reaction mixture determines the solubility of the whole reaction system. Therefore, if the solvent is a better solvent (with lower interaction parameter values less than 0.5) for the polymers, the particles have better morphology. So this is why the particle morphology is better at higher EGDMA concentration. The fluctuation of the average particle size is probably caused by the areas selected when the SEMs were taken. Figure 6-18 shows the particle morphology of selected polymer samples. The difference of the particle morphology under different HEMA content at high and low levels of the EGDMA concentration is clearly seen.

6.4.2.3 Porous Structures

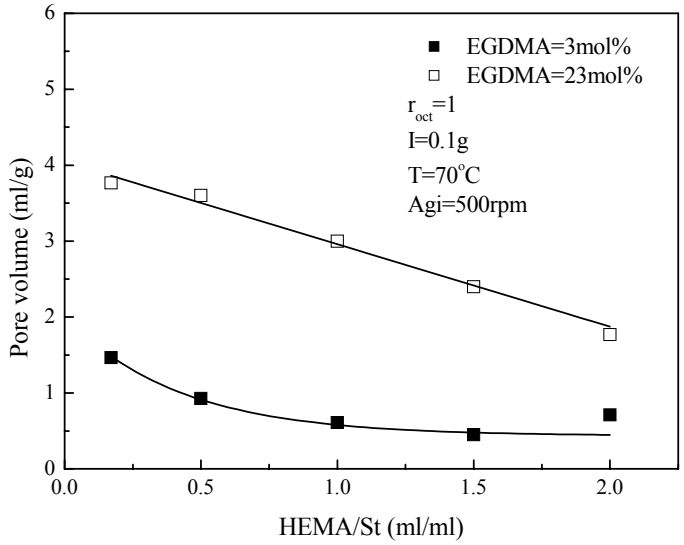

Figure 6-19 Change of the pore volume with monomer ratios for porous poly(HEMA-St) particles; the data are shown in Appendix I

The styrene, as a "hard" hydrophobic comonomer, enhances the formation of the pores. As shown in Table 6-6, Figure 6-19 and Figure 6-20, the pore volume, the porosity and the surface area are decreased over the range of the monomer ratio. The change of the surface area is different from that of the porous poly(HEMA-MMA) particles. At the same time, higher density as shown in Table 2 reveals that the compact porous structures exist.

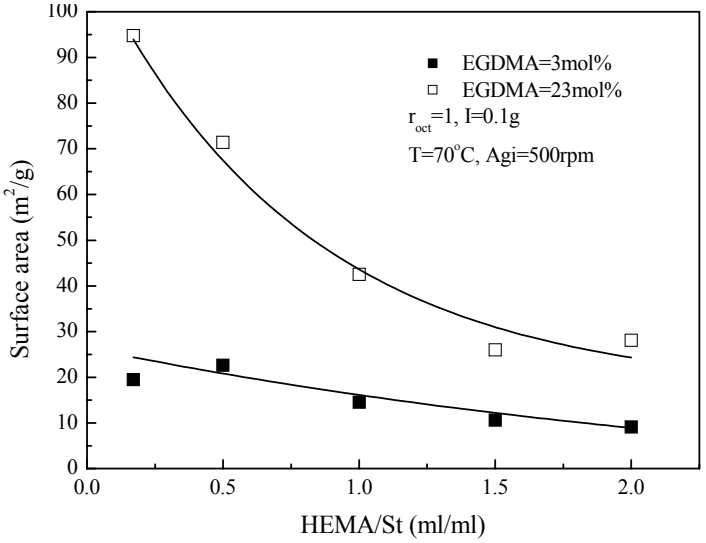

Figure 6-20 The change of the porous surface area with various monomer ratios for porous poly(HEMA-St) particles; the data are shown in Appendix I

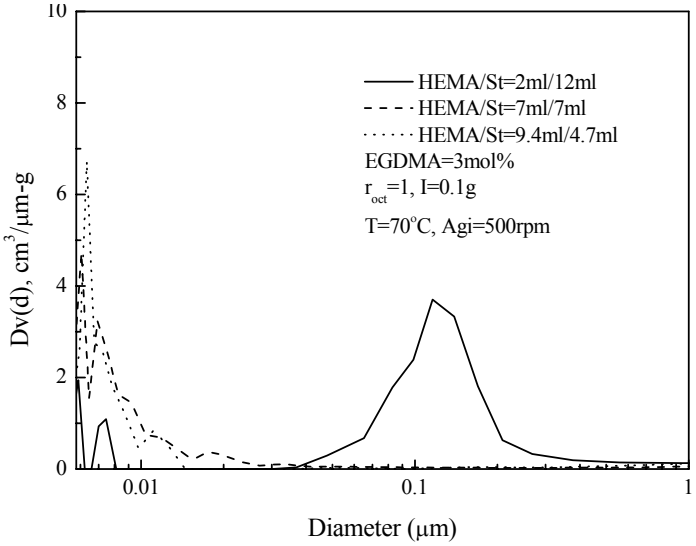

Figure 6-21 The pore size distribution of the porous poly(HEMA-St) particles synthesized under various monomer ratios at lower EGDMA molar concentration

As mentioned above, lower pore volume and lower specific porous surface area imply that there are less pores or the pore size becomes much smaller resulting in much more compact structures. This is verified by the pore size distribution profiles as shown in Figure 6-21 and Figure 6-22. The pore size distributions are shifted toward left (smaller pores) with an increase in the HEMA content for the porous poly(HEMA-St) particles. According to the height of the peaks, there are fewer pores for the particles synthesized at higher monomer ratios. Obviously, as a 'hard' comonomer, styrene is helpful to support the porous structures. Therefore, the decrease in the pore size and the amount of the pores

could be caused by the shrinkage or the collapse of the networks at higher HEMA content which was also observed in the porous poly(HEMA-MMA) particles. This can be seen according to the change of pore size distribution.

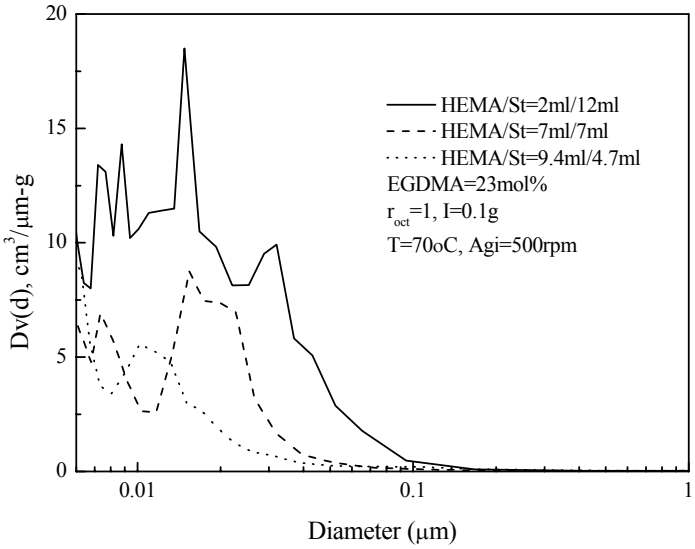

Figure 6-22 The pore size distribution of the porous poly(HEMA-St) particles synthesized under various monomer ratios at higher EGDMA molar concentration

At lower EGDMA concentration, the major pore size distributions under higher HEMA content are much smaller than 10 nm which could be very close to the mesh size between two crosslinks. Although HEMA is favorable for the formation of networks because of the presence of hydrogen bonding, if there is not enough crosslink to support the networks, the porous structures will collapse during the porogen removal. This means the shrinkage is much more serious at higher HEMA content and lower EGDMA concentration as shown in Figure 6-21. According to Figure 6-21, the pore size is larger for the polymers synthesized under higher styrene content. It has been mentioned that styrene could enhance the pore formation by supporting the networks and the monomer mixture is a good solvent for the polymer under higher styrene content according to Table 6-7 so that the polymeric networks could be swollen and expanded further to generate more pores. At higher EGDMA concentration, according to the pore size distribution shown in Figure 6-22, the pore size is smaller and there are fewer pores under higher HEMA content. This illustrates the same phenomenon as that at lower EGDMA concentration. However, there are more pores for the polymers synthesized at higher EGDMA concentration than those synthesized at lower EGDMA concentration.

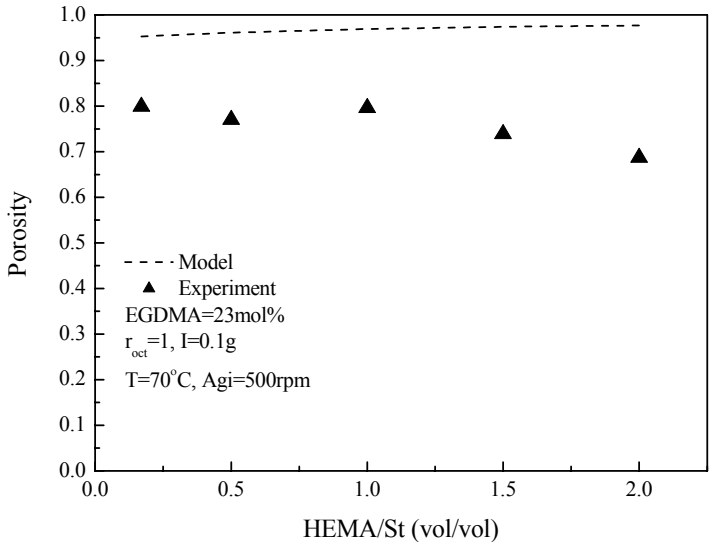

Figure 6-23 Comparison of the simulated values and the experimental results at various monomer ratios

The presence of the pore collapse could also be verified by a comparison of the simulated porosity and the experimental results as shown in Figure 6-23. The model predicts a similar trend for the change of the porosity except at higher monomer ratios. The model predicts the highest porosity for the polymers because of the collapse of the pores, especially at higher HEMA content. At higher styrene content, although there is a difference between the model and the experimental results, it is less than that under higher HEMA content.

The discussion about the porous structures can be verified by Figure 6-24 which shows the surface porous structures under various HEMA content at high and low levels of EGDMA molar concentration. Better porous structures can be seen at lower HEMA content or at higher EGDMA concentration. It can be seen that the amount of pores become less with an increase in HEMA content. And the polymeric networks show less heterogeneity at higher HEMA content. All in all, higher HEMA content is favorable for the formation of smaller pores. Therefore, the pore size could be well controlled by adjusting HEMA content at different EGDMA concentration.

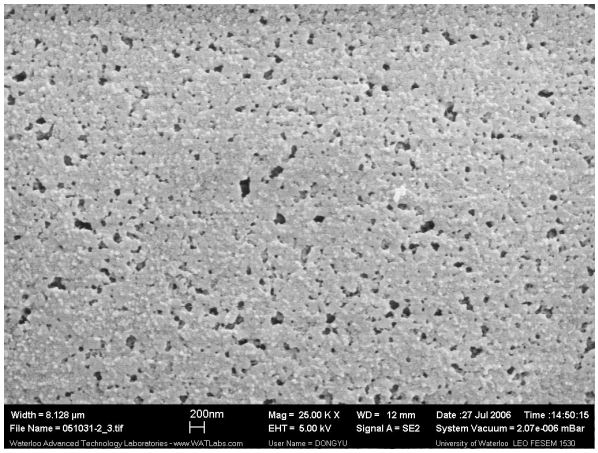

HS11

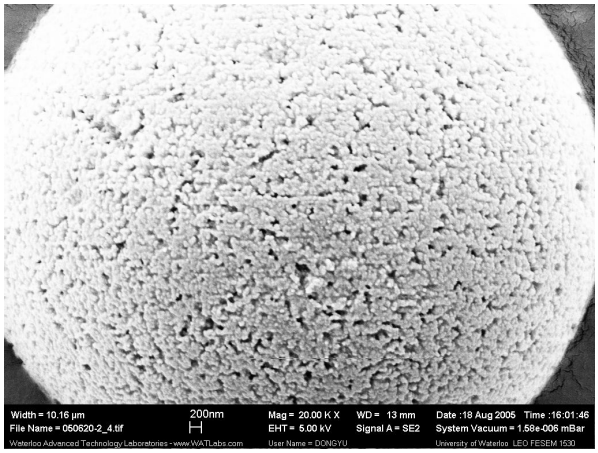

HS14

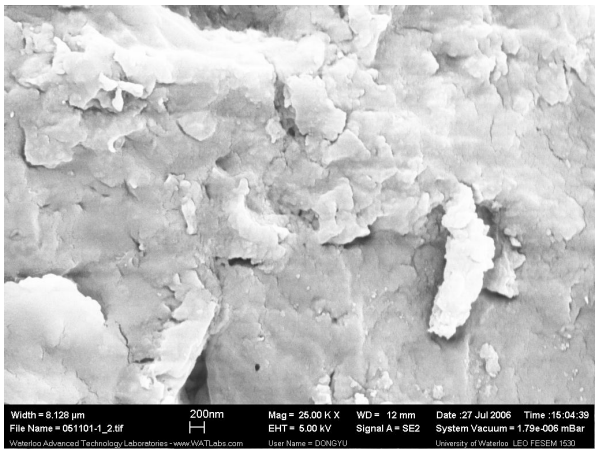

HS12

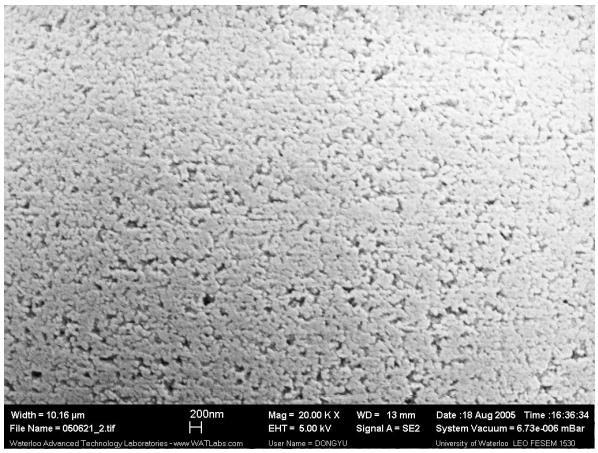

HS15

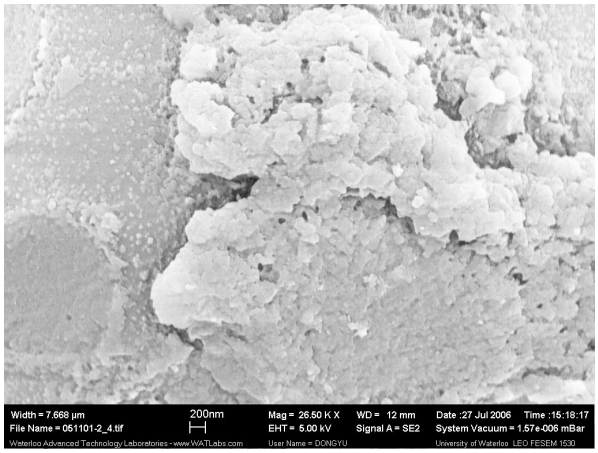

HS13

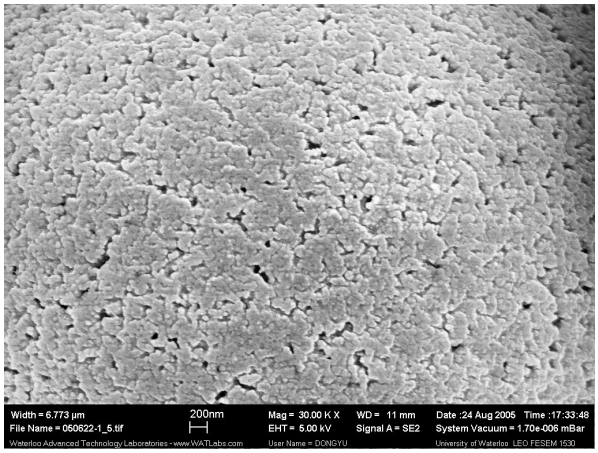

HS16

Figure 6-24 The porous structures of the selected samples for the porous poly(HEMA-St) particles; Scale bar: 200nm; HS11: r_H=0.5, [EGDMA]=3.0mol%; HS12: r_H=1, [EGDMA]=3.0mol%; HS13: r_H=1.5, [EGDMA]=3.0mol%; HS14: r_H=0.5, [EGDMA]=23.0mol%; HS15: r_H=1, [EGDMA]=23.0mol%; HS16: r_H=1.5, [EGDMA]=23.0mol%; r_{oct}=1

6.4.3 Effect of Porogen Volume Ratio

Table 6-8 shows the reaction systems used to study the effect of porogen volume ratio on the particle morphology and the porous characteristics at EGDMA mol%=3.0 mol% and at EGDMA mol%=23.9 mol%. Figure 6-26 through Figure 6-28 show the change of the pore volume and the specific porous surface area. The pore size distribution and the porous morphology were also studied. The effects of the thermodynamic quality of the solvent and the solvent volume ratio on the porous characteristics were studied using the mathematical model.

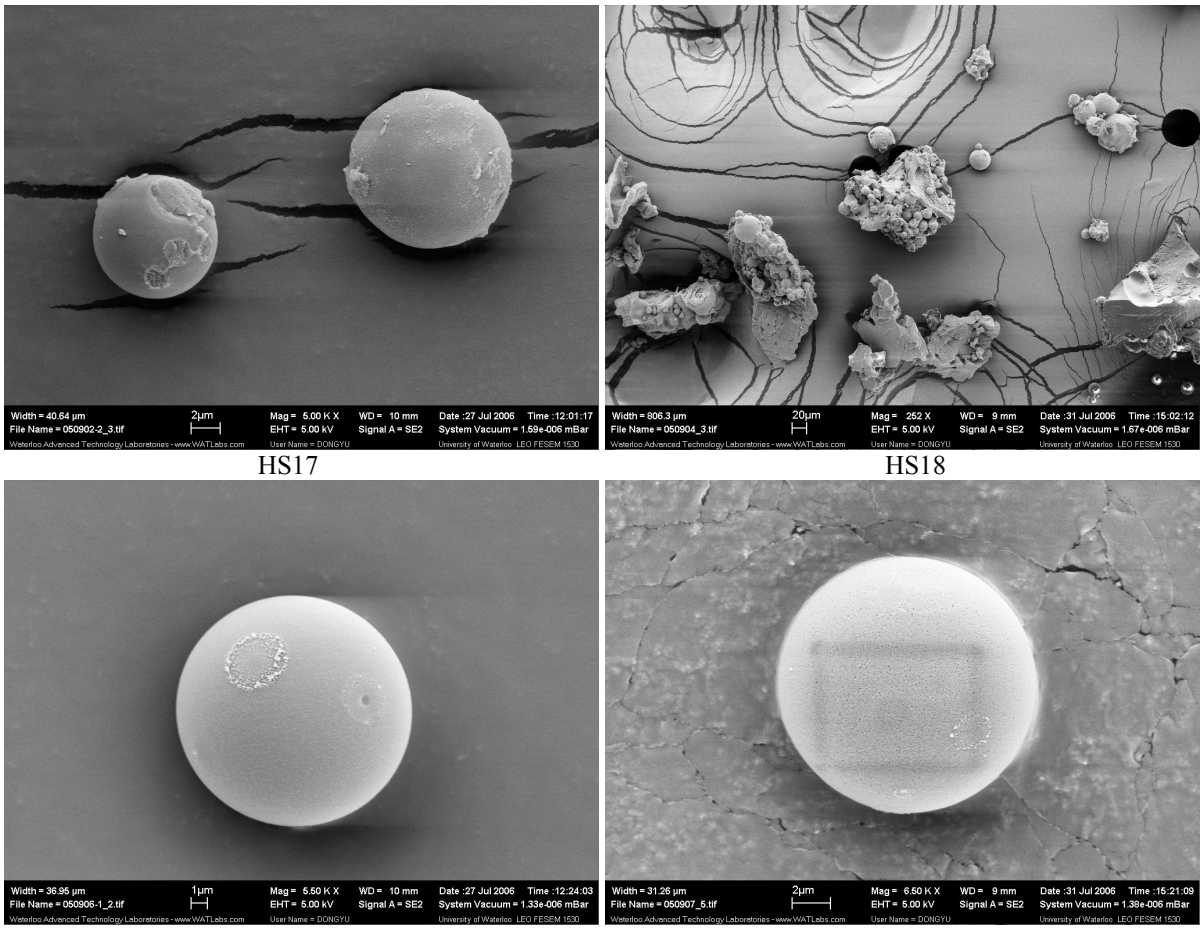

HS17 HS18

HS19 HS20

Figure 6-25 Particle morphology of the selected particle samples of the porous poly(HEMA-St); HS17: scale bar 2µm, r_{oct}=0.5, [EGDMA]=3mol%; HS18: scale bar 20µm, r_{oct}=0.8, [EGDMA]=3mol%; HS19: scale bar 1µm, r_{oct}=0.5, [EGDMA]=23.9mol%; HS20: scale bar 1µm, r_{oct}=0.8, [EGDMA]=23.9mol%; HEMA/St=9.4ml/4.7ml

Table 6-8 Reaction composition and experimental results of the synthesis of the porous poly (HEMA-St) particles at various porogen volume ratios; HEMA/St=9.4ml/4.7ml; T=70°C; Agi=500rpm

No.	EGDMA (mol%)	r_{oct} (ml/ml)	Porosity (%)	d_2 (g/cm^3)	d_0 (g/cm^3)	Average Pore Size (nm)	Particle Size (μm)	Particle Morphology
HS17	3.0	0.5	40.9	1.20	0.98	8.7	5.6±7.9	p, a
HS18	3.0	0.8	40.6	1.24	1.10	7.5	-	i, a
HS7	3.0	1	46.5	1.22	0.73	10.7	5.7±1.1	p, a
HS19	23.9	0.5	50.4	1.17	1.04	30.2	11.2±6.4	p
HS20	23.9	0.8	60.1	1.28	0.89	32.7	17.8±4.9	p, a
HS10	23.9	1	68.7	1.24	0.93	19.3	14.3±4.0	p

p: particle; a: the presence of the aggregated particles; i: the presence of the irregular particles

6.4.3.1 Particle morphology

According to Table 6-8, the particle size distribution is more uniform or narrower at higher porogen concentration according to the standard deviation of the average particle size. At lower porogen concentration, intramolecular reaction or cyclization is favored because of the low monomer concentration around C=C bonds resulting short polymer chains and smaller particles (Choi et al, 2002; Nyhus et al, 2000). The morphology of some particles' is shown in Figure 6-25. The rectangular shown in Figure 6-25 results from the electronic beam. The particles synthesized at a higher EGDMA concentration are used to study the effect of the porogen volume ratio on the porous structures in the following sections.

6.4.3.2 Porous Structures

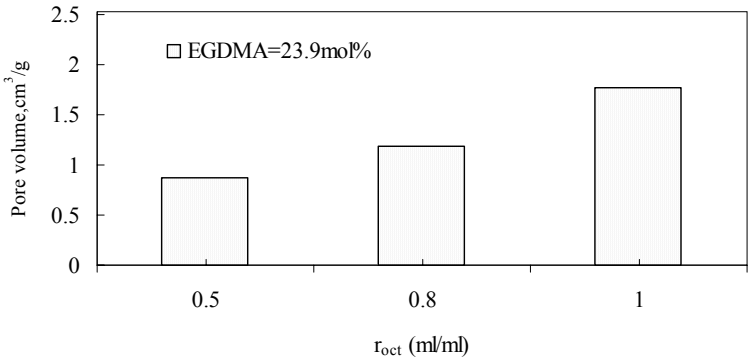

Figure 6-26 The pore volume of the porous poly(HEMA-St) particles prepared at various porogen volume ratios; HEMA/St=9.4ml/4.7ml; the data are shown in Appendix I

As shown in Table 6-8, Figure 6-26 and Figure 6-27, the pore volume, the porosity and the porous surface area are increased with an increase in the porogen volume ratio. This phenomenon is similar

to the observations in the synthesis of other porous polymers (Sederel et al, 1973; Vianna-Soares et al, 2003; Nyhus et al, 2000).

Compared to the porous structures formed in a large amount of good solvent for the polymers, larger pore volume is favored using a non-solvent for the resultant polymers (Sederel et al, 1973). Therefore, larger pore volume requires more non-solvent so that enhanced internal surface area is obtained (Sederel et al, 1973).

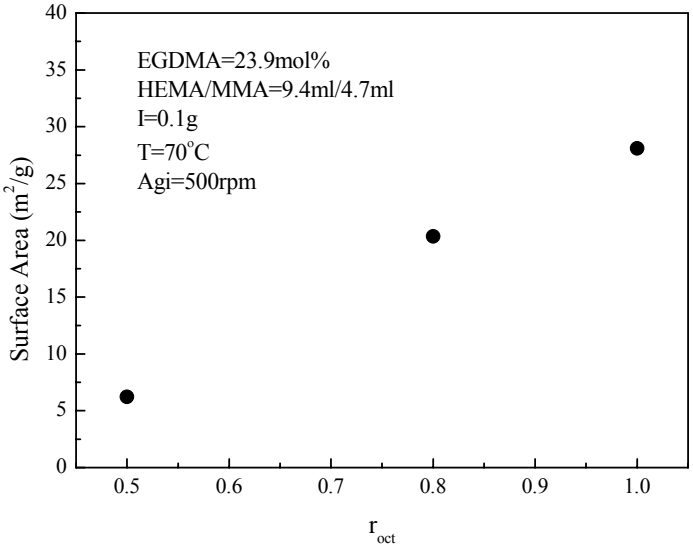

Figure 6-27 The specific porous surface area of the porous poly(HEMA-St) particles prepared at various porogen volume ratios and EGDMA molar concentrations; the data are shown in Appendix I

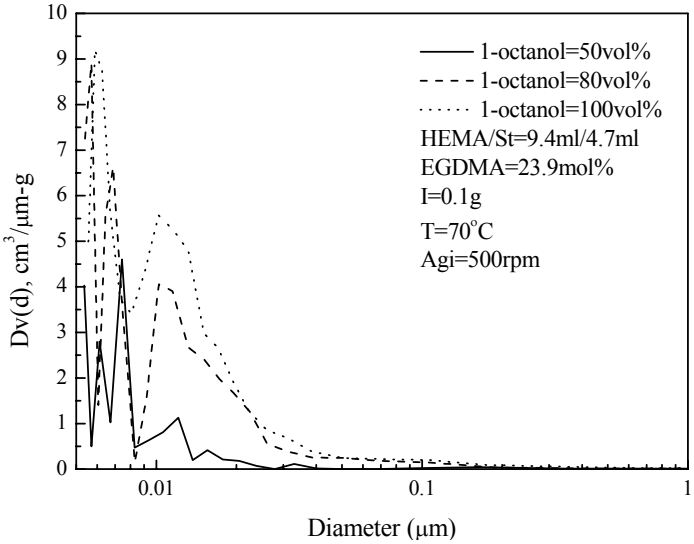

Figure 6-28 The pore size distribution of the porous poly(HEMA-St) particles at various porogen volume ratios at higher EGDMA concentration

To understand the porous characteristics, the pore size distribution profiles as shown in Figure 6-28 were studied. It can be seen that there are two types of pores in terms of the pore size in the particles according to the pore size distribution profiles. One type is the pores below 10 nm in diameters, and the other one is the pores larger than 10 nm in the diameters. With an increase in the porogen volume ratio, the fractions of pores which are larger than 10 nm are increased greatly. Although the fractions of the pores which are smaller than 10 nm are increased as well, this increase is not as great as those pores larger than 10 nm.

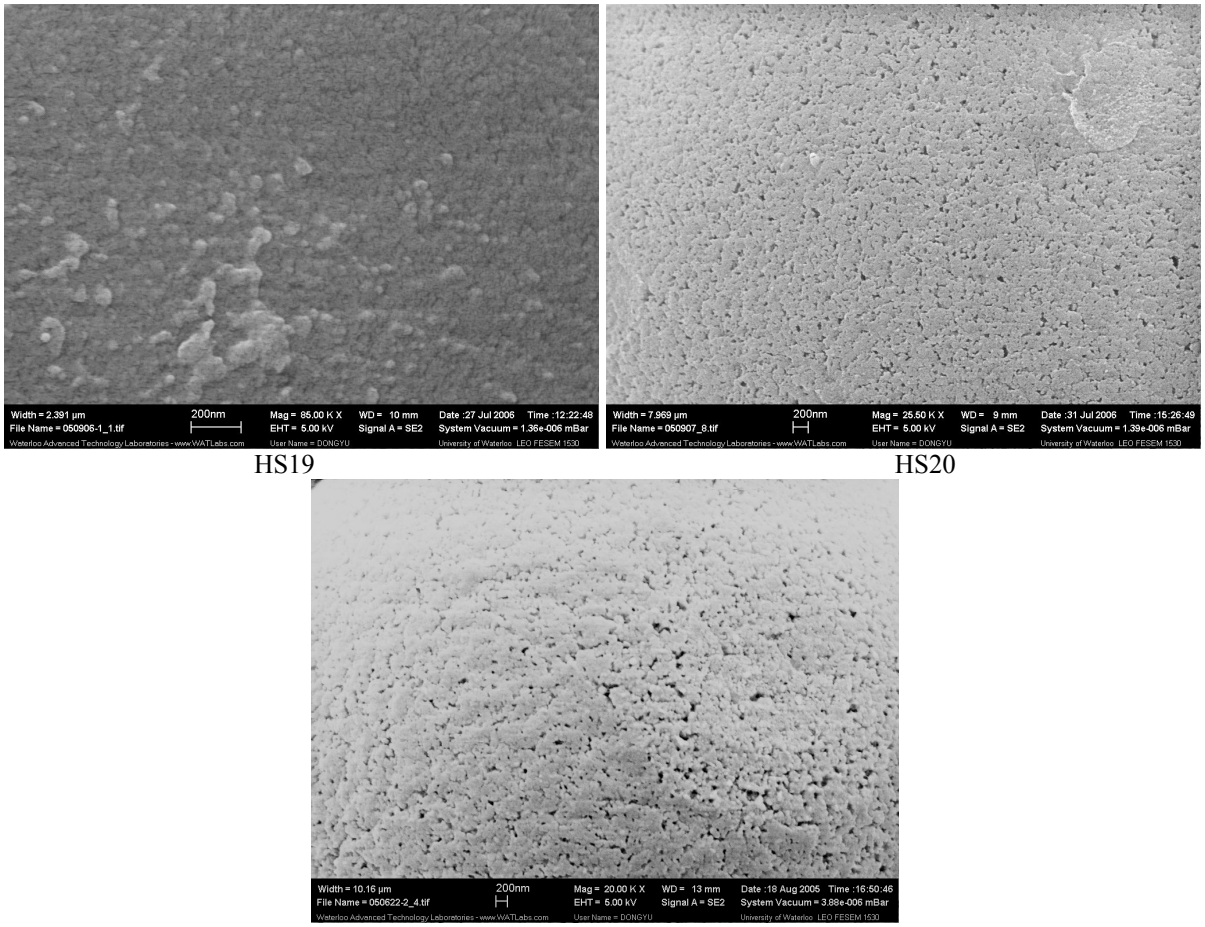

HS19 HS20

HS10

Figure 6-29 The porous structures of the porous poly(HEMA-St) particles. HEMA/St=9.4ml/4.7ml, [EGDMA]=23.9mol%; Scale bar: 200nm; HS19: r_{oct}=0.5; HS20: r_{oct}=0.8; HS10: r_{oct}=1

On the other hand, there are more pores in the particles synthesized at higher porogen volume ratio according to the height of the peaks. With an increase in the porogen volume ratio, although the peaks corresponding to the different pore sizes become higher, the shapes of the pore size distribution are

not changed very much. This means the increase in the porogen volume ratio does not change the structures but induce more pores and higher porous volume. After the phase separation, the agglomerated microspheres which are formed from the agglomeration of the nuclei can be swollen by the reaction mixture further and become less compact so that the particles will contain more pores in smaller size (Sederel et al, 1973).

However, according to Figure 6-28, the increase in the peak height becomes lesser at higher porogen volume ratio, and more pores in smaller size will not significantly give great contribution to the further increase in the porosity. As stated by Okay (2000), a higher solvent concentration results in the further dilution of monomer so that isochoric conditions can not be held. Therefore, the porosity can not increase greatly further if the porogen concentration reaches a certain level. According to the studies on the synthesis of poly(St-DVB) particles, Sederel et al (1973) also pointed out that an increasing amount of solvent will increase the pore volume within certain limits without changing the pore size distribution very much.

To verify the above discussion, the pore morphology of the porous poly(HEMA-St) particles synthesized at different porogen volume ratios is shown in Figure 6-29. The formation of the pores and the increase in the amount of the pores can be clearly seen. The porous structures look looser with an increase in the porogen volume ratio as well.

6.4.3.3 Modeling of the Porous Characteristics

Figure 6-30 illustrates the dependence of the porosity on the thermodynamic quality of the solvents. If a poor solvent (with higher χ values greater than 0.5) for the polymers is present, the system becomes discontinuous at the gel point. Since the pores are formed by the agglomeration of the microgels, as the reactions proceed, the volume fractions of these microgels are increased so that the porosity is decreased. When the conversion goes to 1, the porosity is increased a little bit because the crosslinking reaction causes the polymer volume to decrease at the highest conversion (Okay, 1999). According to Figure 6-30, the porosity is higher for the polymers synthesized in a non-solvent for the polymers. The onset of the phase separation occurs later with a decrease in the values of the interaction parameters because the polymers can be swollen much more in a good solvent as shown in Figure 6-31. Therefore, the good solvents result in lower porosity and the poor solvents result in higher porosity. At certain high crosslink density, the highly porous structures can be formed in both good solvents and poor solvents.

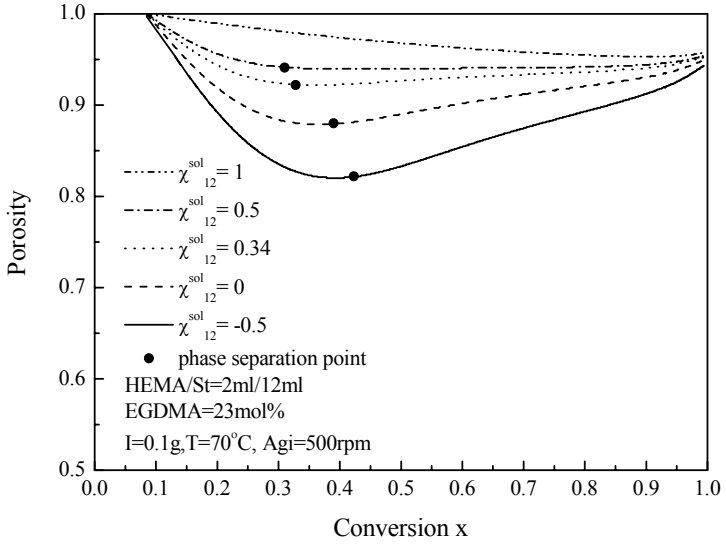

Figure 6-30 Variation of the total porosity of poly(HEMA-St) networks with the monomer conversion in the presence of various solvents

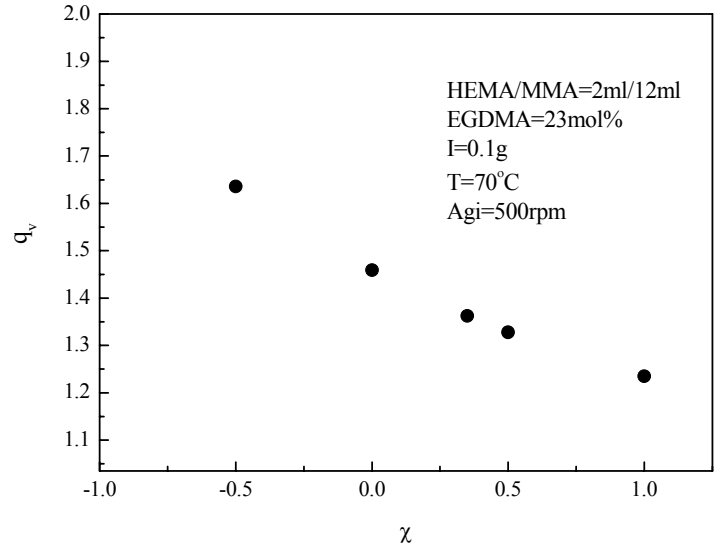

Figure 6-31 The change of the volume swelling ratio of the porous poly(HEMA-St) in the solvents with different thermodynamic quality

Figure 6-32 shows a comparison of the model prediction and the experimental results. Although the model over-estimates the experimental results, it still can be seen that the trend of the porosity change is identical between the model prediction and the experimental results. The value of the Flory interaction parameter is calculated as 1.8 for the reaction system shown in Figure 6-32. This means 1-octanol is a non-solvent for the polymer. Therefore, a large amount of solvent is separated but present

in the polymer networks, resulting in considerable porosity as estimated from the model. However, as discussed above, the polymeric network is too weak to support the porous structures so that the porous structures are collapsed drastically during porogen removal at lower crosslink density (Okay et al, 1985). Therefore, theoretically speaking, the model predicts the situation of the pore collapse.

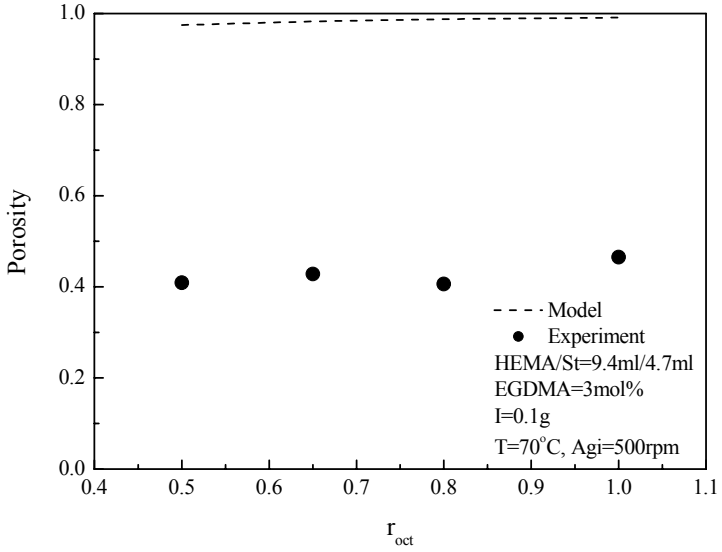

Figure 6-32 Comparison of the model prediction and the experimental results

6.4.4 Controllable Pore Size

According to Figure 6-33(A), the average pore size is smaller at lower porogen volume ratios and lower EGDMA concentration. The pore size is larger at lower EGDMA concentration and higher porogen volume ratios. Since styrene is good for support of the networks, the pore size is larger for polymers synthesized under higher styrene content at lower EGDMA concentration. However, the pore size is much smaller for polymers with higher HEMA content because of the pore shrinkage. According to Figure 6-33(B), at various monomer ratios, the pore size is larger at moderate EGDMA concentration and it is smaller at higher EGDMA concentraiton. If HEMA content is higher, under certain EGDMA concentration, the pore size is smaller. However, under higher styrene content, the pore size is the largest. Generally speaking, the pore size can be controlled in the present studies. By using the diagram about controllable pore size, the porous poly(HEMA-St) particles with the designed pore size and the favorable network properties could be made.

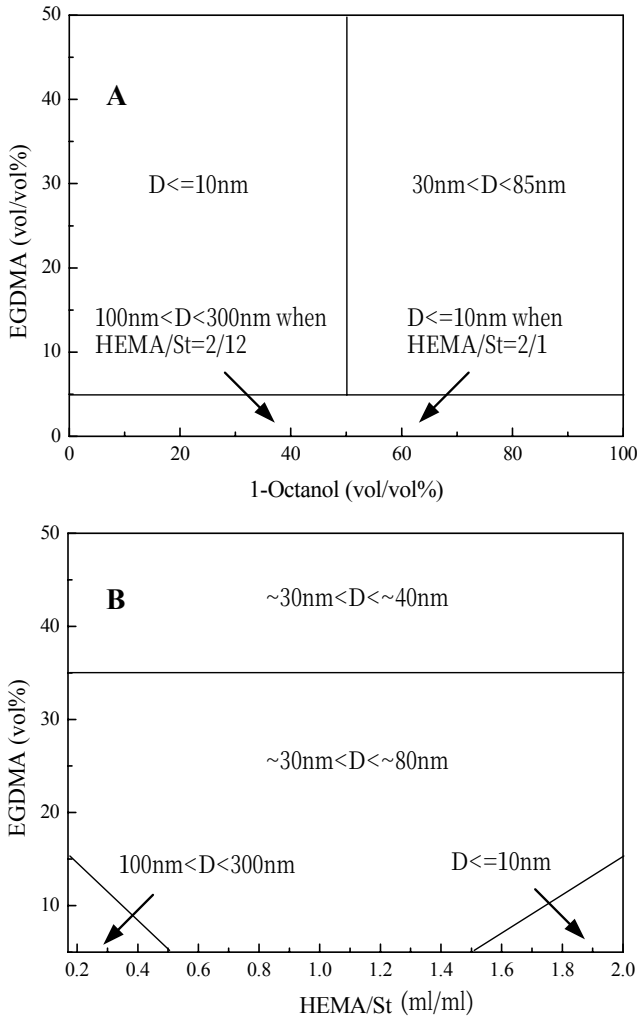

Figure 6-33 Controllable pore size of the porous poly(HEMA-St) particles synthesized under various reaction conditions in the present studies

6.5 Summary

The porous poly(HEMA-St) particles were synthesized at various EGDMA molar concentrations, porogen volume ratios and monomer ratios of HEMA to MMA in the present studies.

The reaction rate is much faster at higher EGDMA concentration than those at lower EGDMA concentration. The gelation occurs later at lower EGDMA concentration. The molecular weight between successive crosslinks and the volume swelling ratio of the polymers are decreased with an increase in the EGDMA concentration. The particle morphology is better at higher EGDMA concentration. With an increase in the EGDMA concentration, the change of the porosity and the pore volume demonstrates the maximum values. The specific porous surface area increases with an

increase in the EGDMA molar concentration at the beginning, and deceases a little bit at higher EGDMA concentration (such as 23mol%).

The monomer ratios of HEMA to St have great effects on the particle morphology and the porous structures of the porous poly(HEMA-St) particles. The higher the styrene content, the faster the reaction rates are. The time for the onset of the gelation is almost the same for each reaction system. But the gel fraction grows faster under higher HEMA content. There are more particle aggregates and irregular particles produced under higher HEMA content and at lower EGDMA concentration. The average particle size tends to be smaller with an increase in the HEMA contents at lower EGDMA concentration which could be caused by the contraction of the particles under higher HEMA content and lower EGDMA concentration. The pore volume and the porosity are decreased over the range of the monomer ratio. The specific porous surface area goes down with an increase in the HEMA content. At the lower EGDMA concentration, the major pore size distributions at higher HEMA content are much smaller than 10 nm which could be very close to the mesh size between two crosslinks. The pore size is larger for the polymers synthesized under higher styrene content. HEMA is favorable for the formation of networks because of the presence of the hydrogen bonding. If there is not enough crosslinks to support the networks, the porous structures will be collapsed during the porogen removal.

The particle size distribution is more uniform or narrower at higher porogen concentration. The pore volume does not change too much at various porogen volume ratios at lower EGDMA concentration. At higher EGDMA concentration, the pore volume and the porosity are increased with an increase in porogen concentration. There are more pores at higher porogen volume ratios. The specific surface area increases with an increase in the porogen volume ratio. It was also found that there are more pores of larger size after phase separation. An increasing amount of solvent will increase the pore volume within certain limits without changing the pore size distribution very much. The porosity change in different solvents with different thermodynamic quality was simulated using the model introduced in Chapter 5. The onset of the phase separation occurs later with a decrease in the values of the interaction parameters. Therefore, good solvents result in lower porosity and poor solvents result in higher porosity. At certain high crosslink densities, the highly porous structures can be formed in both good solvents and poor solvents.

The pore size can be controlled in the present studies. Higher styrene content or higher EGDMA concentration leads to better particle morphology. Higher HEMA content results in smaller pores. Higher EGDMA concentration results in smaller pores and higher 1-octanol volume ratio leads to more pores.

Chapter 7
Synthesis, Characterization, and Modeling of Porous Poly(HEMA-NVP) Particles

7.1 Introduction

Compared to MMA and styrene, NVP is a more hydrophilic monomer. The earliest patents about the synthesis of NVP date back to 1943 (Reppe et al, 1943). Nowadays, the homopolymers and the copolymers of NVP have been widely used in many applications such as pharmaceuticals, sorbents, biomedicals, textiles, fiber-glass treatments, adhesives, pigment, colloid stabilization in aqueous and nonaqueous dispersions, cosmetics, detergents, and flocculation agents in beverage clarification processes (Ng et al, 2005; Cizravi et al, 2000; Horak et al, 2000; Choi et al, 2005; Mark et al, 1989).

Copolymers of NVP and HEMA or other methacrylates have been prepared by thermal, photo- or irradiation polymerization using EGDMA or other dimethacrylates as the crosslinkers (Perera et al, 1996). Copolymers of HEMA/NVP or MMA/NVP are well-known for their applications in the soft contact lens (Lai, 1997). However, according to the published literature, most of the research on the synthesis of the copolymers of NVP and HEMA or other methacrylates was focused on the photo- or irradiation polymerizations without using solvents or porogens (Perera et al, 1996; Turner et al, 1986; Lai, 1997; Choi et al, 2005; El-Din et al, 2004). Therefore, these NVP copolymers are non-porous.

The reports on the synthesis of the spherical copolymeric particles of NVP and HEMA in the aqueous phase are hardly seen because this process is relatively difficult resulting from the great hydrophilicity of both HEMA and NVP. However, according to the most recent paper (Horak et al, 2000), macroporous poly(vinylpyrrolidone-co-ethylene dimethacrylate) beads were synthesized by suspension polymerization in the presence of cyclohexanol and 1-dodecanol. According to this report, the cyclohexanol was served as a good solvent of polymers to make spherical beads and the 1-dodecanol was used as a non-solvent which was responsible for inducing pores. The porogen used to induce pores should be a solvent with a moderate solubility parameter. So the porogen used in the synthesis of porous poly(HEMA-NVP) should be responsible for inducing pores and keeping the spherical shape. According to the solubility parameter and literature (Horak, 1993), 1-octanol could be a good candidate to be used as a porogen in the synthesis of porous poly(HEMA-NVP) particles

Accordingly, the objectives of this chapter were to synthesize the highly porous poly(HEMA-NVP) particles in the presence of an organic porogen (1-octanol), to characterize the particle morphology, to explore the porous structures and their formation mechanisms, and to simulate the gel formation and the porous characteristics of the porous poly(HEMA-NVP) particles. The model parameters in the simulation can be found in Appendix V.

7.2 FT-IR

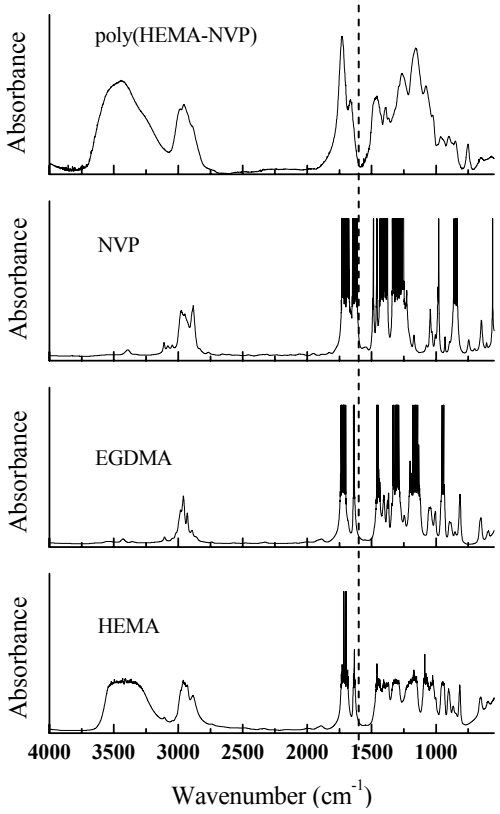

Figure 7-1 FT-IR spectra of poly (HEMA-NVP) polymer synthesized in the present studies; HEMA/NVP=9.4ml/4.7ml, EGDMA=23.5mol%.

Figure 7-1 shows the FT-IR spectra of monomer HEMA, comonomer NVP, crosslinker EGDMA and one selected polymer sample. Table 7-1 illustrates the possible spectral band assignments. The IR spectra of the crosslinked poly(HEMA-NVP) hydrogel show the same spectra as the original monomers except that the C=C absorption is greatly lowered. However, there is still an individual C=C peak in the polymer because of non-equal concentrations of C=C in the monomers. It also could

be caused by the weakened monomer diffusion to the radicals beyond the gelation. According to the –OH peak, the HEMA unit structures are present in the polymers.

Table 7-1 Possible Spectral Band Assignments of Poly(HEMA-NVP) Polymer

Wavenumbers (cm^{-1})	Spectral band assignments
3000-3500	Stretching vibration of O-H
2922, 2953, 3000	Stretching vibration of C-H
1724-1731	Stretching vibration of C=O
1635	Stretching vibration of C=C
1350-1500	In-plane bending or twist of C-H
1200-1350	Bending vibration of -OH
1000-1200	Stretching vibration of C-O
800-1000	Out-of-plane bending of C-H
750	Out-of-plane bending of C-O

7.3 Glass Transition Temperature

Table 7-2 Glass Transition Temperature of Poly(HEMA-NVP)

HEMA (ml)	NVP (ml)	EGDMA (mol%)	T_g (K)
9.4	4.7	8.6	358.4
9.4	4.7	18	364.3
9.4	4.7	23.9	367.9
2	12	8.4	349.6
2	12	17.5	356.6
2	12	23.3	360.8

Table 7-2 shows the estimated glass transition temperature of some selected samples synthesized at different monomer ratios and EGDMA concentration. It can be seen that the glass transition temperature is increased with an increase in the HEMA content or the EGDMA concentration.

7.4 Characterization and Simulation of Porous Structures and Gel Formation

7.4.1 Effect of EGDMA Molar Concentration

Without a crosslinker, the copolymers of HEMA and NVP are very soft and very difficult to be handled because of the presence of a high fraction of soluble components in the resultant copolymers. If a crosslinker is introduced, the soluble fraction decreases significantly and it continuously decreases with an increase in the crosslinker concentration (Perera et al, 1996). According to the research on the copolymerization of HEMA and NVP (Perera et al, 1996; Horak et al, 2000), it was found that HEMA and EGDMA are more reactive than NVP so that they enter the polymeric chains more quickly than NVP. This implies that the polymers will have a composition of PNVP

homopolymer in the later stage of the reaction (Perera et al, 1996). Therefore, the soluble fractions could mainly consist of PNVP. However, significant decrease of these fractions in the presence of the crosslinker implies that a majority of NVP are still reacted, which is consistent with Lai's investigation (Lai, 1997) that EGDMA is a good crosslinker for the copolymerization of HEMA and NVP. In the present work, the effect of the EGDMA concentration on the porous structures and the gel formation was studied at a certain porogen volume ratio, and at high and low levels of the monomer ratios, HEMA/NVP=2ml/12ml and HEMA/NVP=9.4ml/4.7ml. Table 7-3 shows the reaction conditions used to study the effect of the EGDMA concentration and the experimental results obtained.

Table 7-3 Reaction compositions and experimental results of the synthesis of the poly (HEMA-NVP) at various EGDMA molar concentrations; r_{oct}=1; T=70°C; Agi=500rpm

No.	HEMA (ml)	NVP (ml)	EGDMA (mol%)	Porosity (%)	d_2 (g/cm^3)	d_0 (g/cm^3)	Average Pore Size (nm)	Particle Size (μm)	Particle Morphology
HN1	2	12	8.4	43.4	1.27	1.20	269	101.5±15.6	p, a
HN2	2	12	17.5	74.5	1.22	0.68	86.4	10.2±0.7	p, a
HN3	2	12	23.3	62.6	1.15	0.69	-	-	i, a
HN4	9.4	4.7	3.0	19.3	1.23	1.21	-	-	i
HN5	9.4	4.7	8.6	73.3	1.60	0.63	92.1	14.7±3.6	p, a
HN6	9.4	4.7	18.0	68.1	1.38	0.73	81.7	268.7±71	p
HN7	9.4	4.7	23.5	68.5	1.24	0.72	44.9	65.2±55.6	p

p: particle; a: the presence of the aggregated particles; i: the presence of the irregular particles

7.4.1.1 Gel Formation

The gel formation was simulated using the mathematical models discussed in the previous chapter. It has been shown that HEMA, EGDMA and MMA are much more reactive than NVP in the copolymerization (Lai, 1997; Ahmad et al, 2004). For instance, the reactivity ratios of HEMA and NVP are 3.07 and 0.045, respectively (Ahmad et al, 2004). Figure 7-2 and Figure 7-3 show the change of the reaction conversion of HEMA, EGDMA and NVP with the reaction time. It can be seen that the reaction rates for HEMA and EGDMA are very fast, and they are faster at higher EGDMA molar concentration. The reaction curves of HEMA and EGDMA show a little s shape because of gel effect. However, in Figure 7-3, the reaction rate of NVP is slow at the beginning, but it becomes faster after a certain reaction time when the conversion of HEMA and EGDMA reaches a certain level. This implies that the reactions between HEMA and EGDMA mainly undergo at the beginning of the reactions, and then more NVP starts to be reacted after that. This verifies the statement about

that the polymers will have a composition of PNVP homopolymer in the later stage of the reaction (Perera et al, 1996). Therefore, the formations of the polymeric networks are mainly due to the reaction of HEMA and EGDMA.

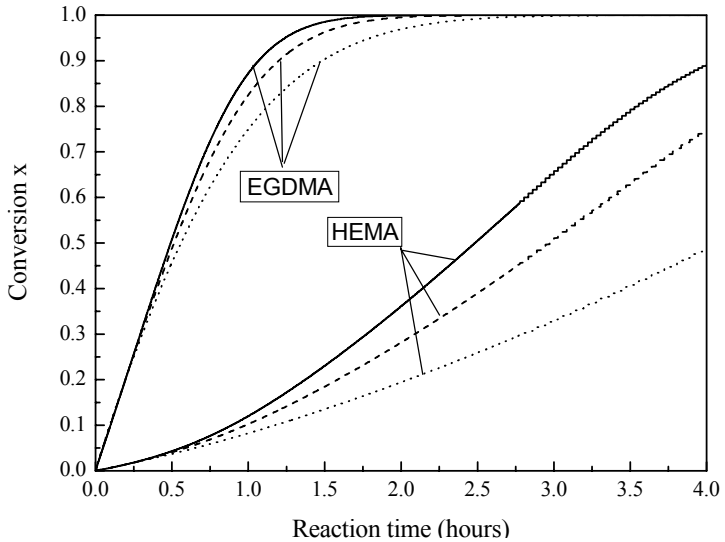

Figure 7-2 Reaction conversion of the monomers HEMA and EGDMA; — EGDMA=23.9mol%, ---- EGDMA=18mol%; ·····EGDMA=8.6mol%; HEMA/NVP=9.4ml/4.7ml; r_{oct}=1; I=0.1g; T=70°C; Agi=500rpm

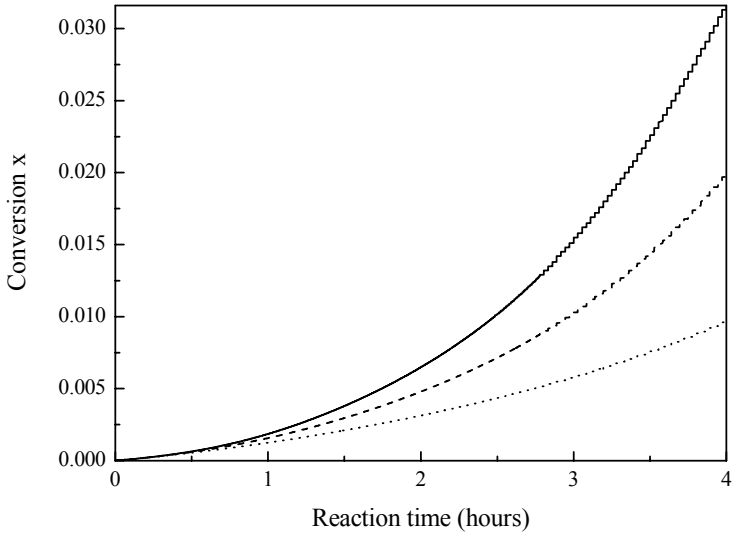

Figure 7-3 Reaction conversion of the monomer NVP; — EGDMA=23.9mol%, ---- EGDMA=18mol%; ·····EGDMA=8.6mol%; HEMA/NVP=9.4ml/4.7ml; r_{oct}=1; I=0.1g; T=70°C; Agi=500rpm

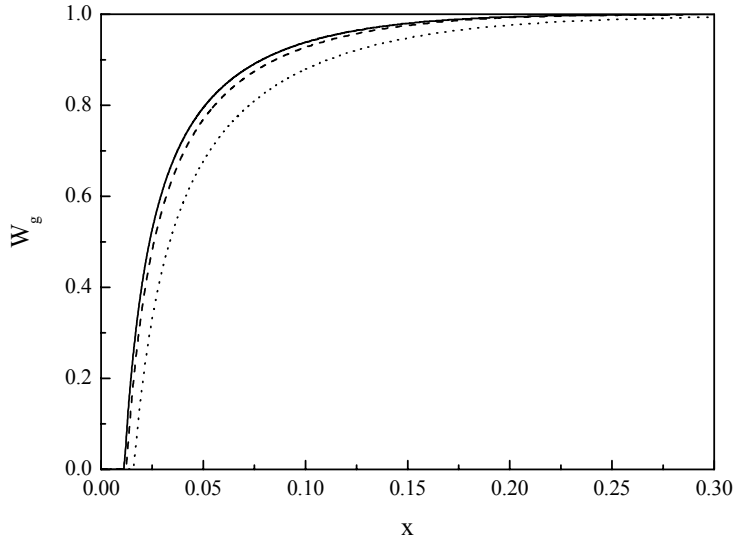

Figure 7-4 Change of the gel fraction with the reaction conversion at various EGDMA concentrations; — EGDMA=23.9mol%, ----EGDMA=18mol%; ·····EGDMA=8.6mol%; HEMA/NVP=9.4ml/4.7ml; r_{oct}=1; I=0.1g; T=70°C; Agi=500rpm

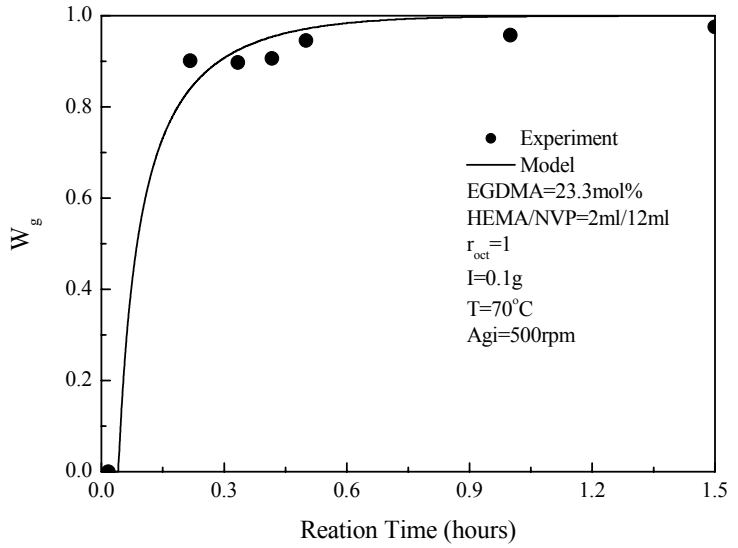

Figure 7-5 Comparison between the model and the experimental results of the gel fraction under certain reaction conditions

Figure 7-4 shows the change of the gel fraction with the reaction conversion at various EGDMA concentrations. The gelation occurs earlier and the gel fraction grows faster at higher EGDMA concentration than those at lower EGDMA concentration because of the rapid network formation at higher EGDMA concentration. Figure 7-5 compares the experimental results with the simulated values. The difference between the models and the experimental results is probably caused by the

accuracy of the model parameters. Furthermore, Figure 7-6 illustrates the change of the average molecular weight of the branched polymers in the sol with respect to the reaction conversion. At the gel points, the average molecular weight becomes infinite.

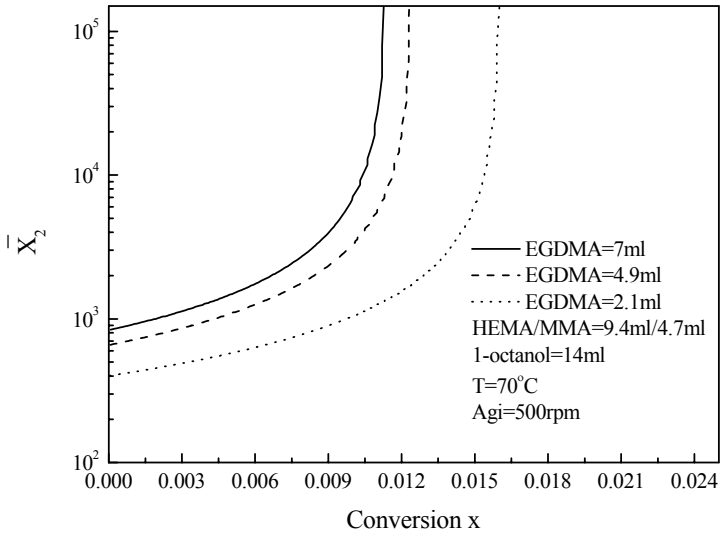

Figure 7-6 Change of the average molecular weight of the branched polymers in the sol at various EGDMA concentrations; — EGDMA=23.9mol%, ----EGDMA=18mol%; ·····EGDMA=8.6mol%; HEMA/NVP=9.4ml/4.7ml; r_{oct}=1; I=0.1g; T=70°C; Agi=500rpm

Table 7-4 Average molecular weight between the successive crosslinks, the volume swelling ratio in the 1-octanol and the values of the interaction parameters at various EGDMA concentrations; r_{oct}=1

No.	HEMA (ml)	NVP (ml)	EGDMA (mol%)	χ	M_c	q_v (v/v)
HN1	2	12	8.4	2.558	1440	1.09
HN2	2	12	17.5	1.802	1050	1.03
HN3	2	12	23.3	1.439	884	1.01
HN4	9.4	4.7	3.0	3.750	5044	1.07
HN5	9.4	4.7	8.6	3.070	1290	1.07
HN6	9.4	4.7	18.0	2.162	579	1.01
HN7	9.4	4.7	23.5	1.722	395	1.00

7.4.1.2 Particle morphology

Almost no research has been carried out regarding the particle morphology of poly(HEMA-NVP) particles synthesized by free radical suspension polymerization. The main reason might be the difficulties to synthesize this type of particles in the aqueous phase. The particle morphology and the calculated system parameters, including χ, M_c, and q_v, are shown in Table 7-3 and Table 7-4. The particle morphology of some selected samples is shown in Figure 7-7.

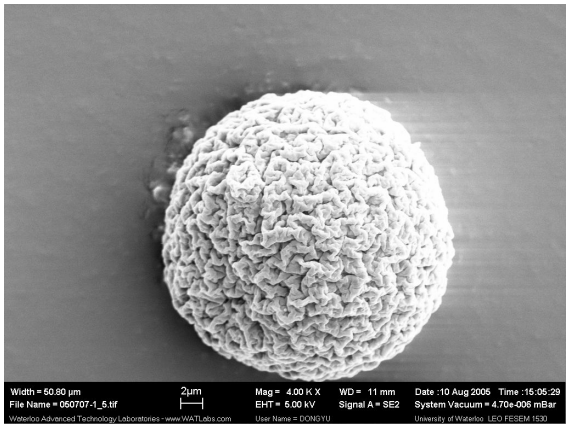

HN1

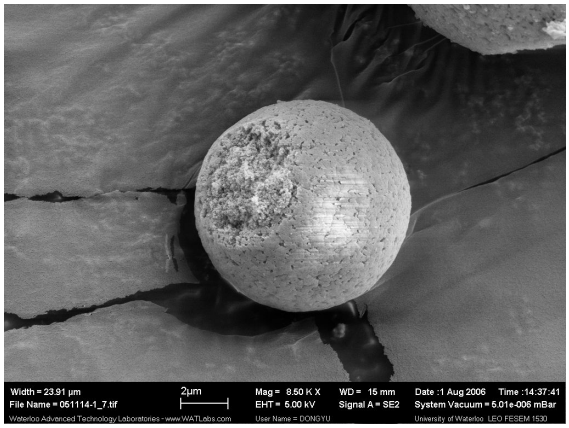

HN2

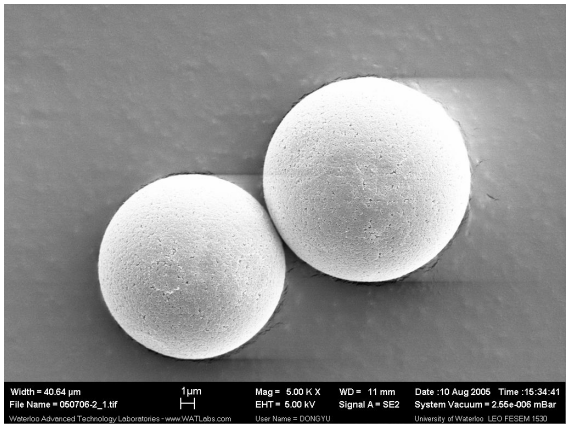

HN5

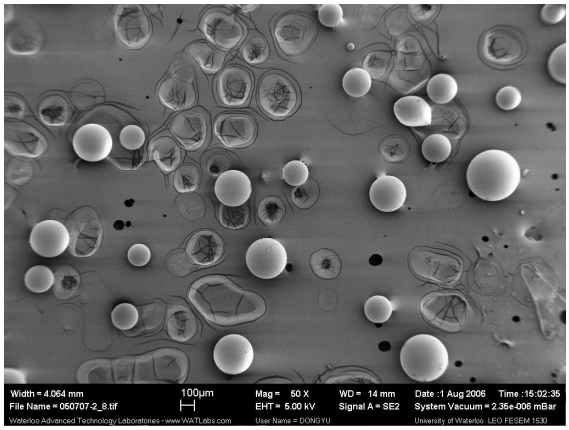

HN6

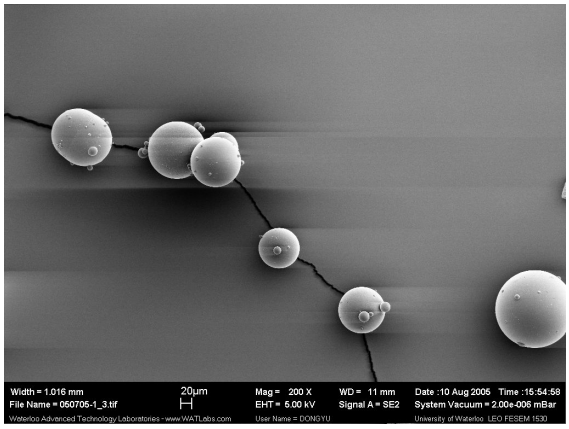

HN7

Figure 7-7 Particle morphology of selected particle samples; HN1: scale bar 2µm, r_H=2ml/12ml, [EGDMA]=8.4mol%; HN2: scale bar 2µm, r_H=2ml/12ml, [EGDMA]=17.5mol%; HN5: scale bar 1µm, r_H=9.4ml/4.7ml, [EGDMA]=8.6mol%; HN6: scale bar 100µm, r_H=9.4ml/4.7ml, [EGDMA]=18.0mol%; HN7: scale bar 20µm, r_H=9.4ml/4.7ml, [EGDMA]=23.5mol%; r_{oct}=1

According to Table 7-3, the particle morphology becomes better, changing from the irregular particles or the particle aggregates to the spherical particles, with an increase in the EGDMA concentration at a

higher level of HEMA content; whereas the particle morphology becomes worse with an increase in the EGDMA concentraiotn at lower HEMA content. This is probably caused by the natures of NVP and its polymer. As stated by Searaz et al (2000), the hydrogen bonds in PVP are mainly passing from intramolecular to intermolecular bonds in water. Therefore, under higher NVP content, the stronger intermolecular hydrogen bonding and the high concentration of pendent vinyl groups at higher EGDMA concentration could result in the agglomeration of the particles.

The particles tend to be 'hard' balls at a higher EGDMA concentration resulting from compact networks because of the higher crosslink density so that the particles are more spherical and not easily agglomerated. Therefore, a higher EGDMA molar concentration under higher HEMA content is favorable to produce the porous particles with better morphology. Although high crosslinker concentration is always required to produce this type of particles in the presence of NVP, the poly(HEMA-NVP) particles with better morphology were prepared using the crosslinker concentration between 15wt%~50wt% in the present work, which is far less than the crosslinker concentration, 67wt%, reported by Horak et al (2000) in poly(HEMA-EDMA). All in all, the spherical poly(HEMA-NVP) particles can be produced using the procedure described in the present studies. Certain high HEMA content is required. Higher HEMA content and higher EGDMA concentration is favorable to the formation of particles. With regard to the discussion on the porous structures in the following sections, the monomer ratio of 2 (HEMA/NVP=9.4ml/4.7ml) is used.

7.4.1.3 Porous Structures

According to Table 7-4, the values of M_c and q_v are decreased with an increase in the EGDMA concentration because of the formation of more rigid polymeric networks in the presence of more crosslinks at higher EGDMA concentration. The values of χ are decreased with an increase in the EGDMA concentration as well because the solvent becomes better for the polymers at higher EGDMA concentration (Okay, 2000). Therefore, the profiles of the pore volume change at various EGDMA concentrations are a little similar with those shown in HEMA-MMA and HMEA-St system.

Figure 7-8 shows the change of the pore volume and the porous surface area with the EGDMA molar concentration. With an increase in the EGDMA concentration, a maximum pore volume can be found. The porosity shown in Table 7-3 illustrates the same manner. However, the porous surface area keeps increasing and the average pore size is decreased with an increase in the EGDMA concentration. In addition, the apparent density of the particles decreases first and then increases

again. These phenomena were also observed in the copolymerization of HEMA and EGDMA (Okay, 2000). According to Okay (2000), the reaction mixture is a non-solvent for the polymers at a lower EGDMA concentration, whereas it becomes a better one at a higher EGDMA concentration. However, at lower EGDMA concentration, the polymer chains could be more extended when the phase separation is enhanced in a poor solvent of the polymers so that the porogen will be separated and present in the polymers like dispersed droplets (Cizravi et al, 2000). The further crosslinking will fix these spaces occupied by the porogen. The pores will be induced if the porogen is removed from the polymers. However, at a low crosslink density, the mechanical strength of poly(HEMA-NVP) is pretty low in the swollen state (Turner et al, 1986) so that the porous structures could collapse or even disappeare during the porogen removal, generating smaller pore volume, smaller surface area and higher density because of fewer pores. If the EGDMA molar concentration is high enough, such as 8mol%, the permanent porous structures are resulted because the pores are fixed by the sufficient crosslinking density. If the EGDMA concentration is further increased, the phase separation is induced by the crosslinking. The pores will be formed because of the agglomeration of these microgels which can be seen in Figure 7-9. The size of the microgels is smaller at higher EGDMA concentration so that the pore size is smaller. Thus, the surface area is higher because of the contribution of more discrete structures of smaller size. These findings are very similar to the HEMA/MMA systems in the present study.

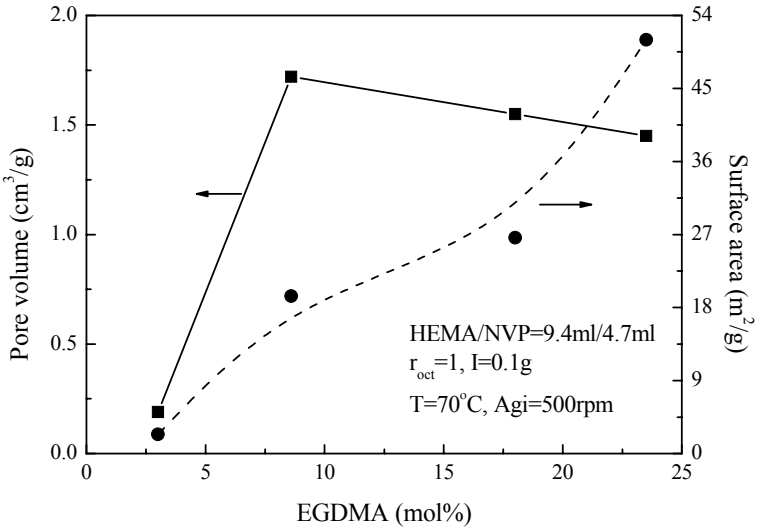

Figure 7-8 Change of the pore volume and the surface area with the EGDMA molar concentration; the data are shown in Appendix I

Clear porous structures and the interior structures are also shown in Figure 7-9. It can be seen that the interior structures are resulted from the agglomeration of the nuclei and become compact at the higher EGDMA concentration. However, the surface becomes smoother at a higher EGDMA concentration because the pores are fused. However, according to the interior structures and the pore size distribution profiles, the porous structures should exist on surface but they are too small to be seen under SEM.

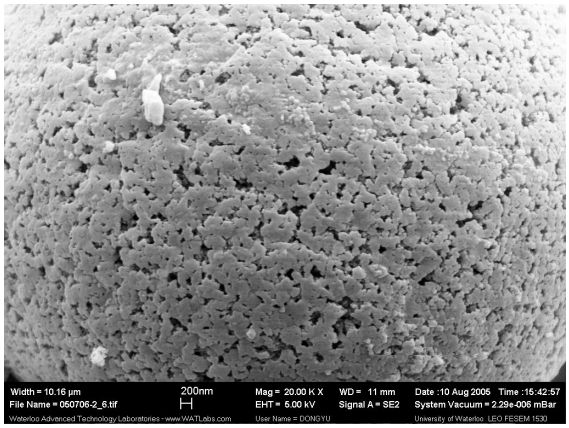

HN5

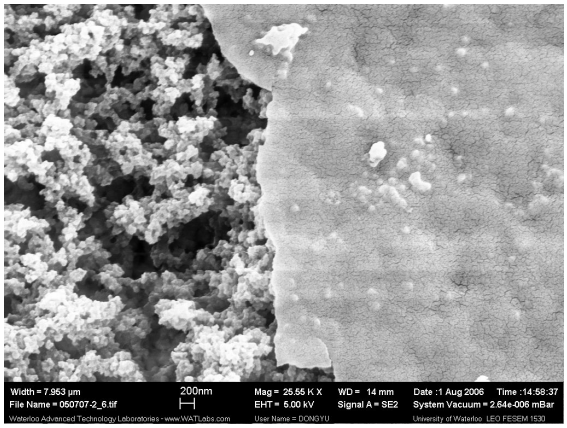

HN6

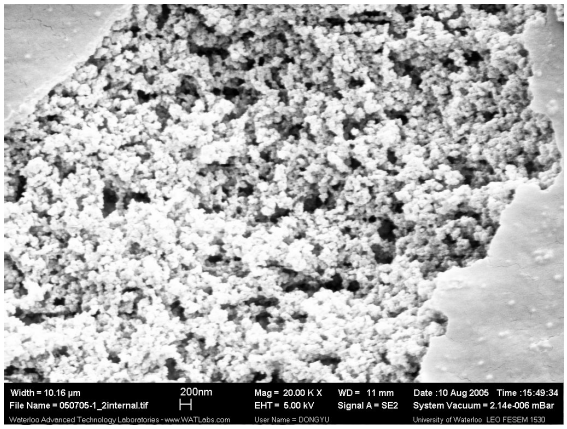

HN7

Figure 7-9 The porous structures of the porous poly(HEMA-NVP) particles at various EGDMA concentrations; Scale bar: 200nm; HN5: [EGDMA]=8.6mol%; HN6: [EGDMA]=18mol%; HN7: [EGDMA]=23.5mol%; HEMA/NVP=9.4ml/4.7ml

The change of the pores can also be described quantitatively by the pore size distribution as shown in Figure 7-10. The pore size distribution is shifted toward smaller pores and the peaks become higher (more pores) with an increase in the EGDMA concentration because of the formation of more compact networks at higher EGDMA concentration. The particles synthesized at the EGDMA concentration of 8.6mol% have a broad pore size distribution. There are a few peaks below 10 nm, which could be as a result of the shrinkage or collapse of the networks.

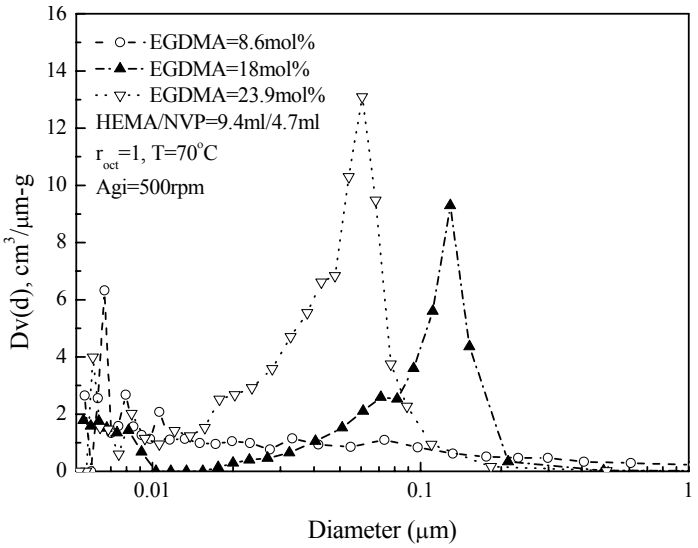

Figure 7-10 The pore size distribution of the porous poly(HEMA-NVP) synthesized at various EGDMA concentrations and under higher HEMA contents

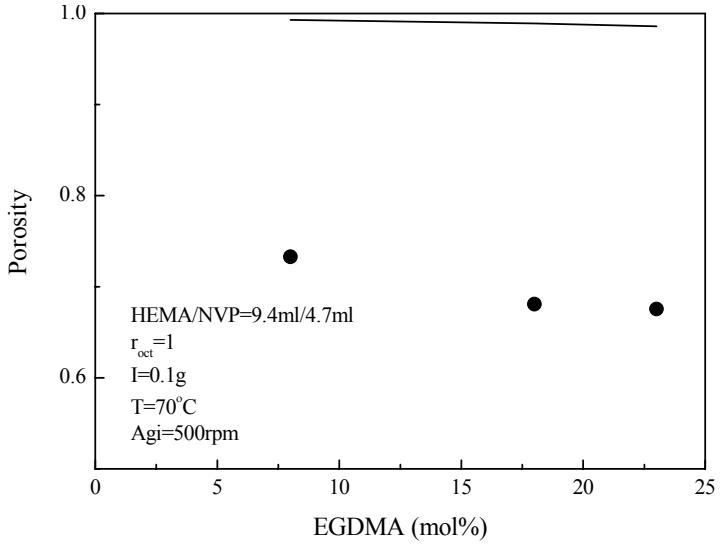

Figure 7-11 Comparison of the simulated porosity and the experimental results

Figure 7-11 compares the simulated porosity and the experimental results. According to the simulated results, the porosity is decreased with an increase in the EGDMA concentration because the reaction mixture is a good solvent for the polymer in this case. Although there are differences between the simulated results and the experimental results, the trend of the porosity change is similar. As stated in the previous chapters, this difference is caused by the pore collapse or the pore shrinkage during porogen removal or measurement.

In a word, the porous poly(HEMA-NVP) particles can be prepared by adjusting the EGDMA concentration. In the present studies, it is shown that the EGDMA concentration should be at least 8mol% under higher HEMA content in order to produce permanent porous structures of good particle morphology.

7.4.2 Effect of Monomer Ratio

Since NVP is a more hydrophilic comonomer, the change of the porous structures of the porous poly(HEMA-NVP) particles show different behavior compared to the porous poly(HEMA-St) and poly(HEMA-MMA). The effect of the monomer ratio is studied at a lower and a higher EGDMA concentration as shown in Table 7-5. However, the good morphology can not be achieved at lower EGDMA concentration at various monomer ratios. Therefore, the following discussion will focus on the porous particles synthesized at higher EGDMA concentration.

Table 7-5 Reaction compositions and experimental results of the synthesis of the poly (HEMA-NVP) at various monomer ratios; r_{oct}=1; T=70°C; Agi=500rpm

No.	HEMA (ml)	NVP (ml)	EGDMA (mol%)	Porosity (%)	d_2 (g/cm^3)	d_0 (g/cm^3)	Average Pore Size (nm)	Particle Size (μm)	Particle Morphology
HN8	4.7	9.4	2.8	5.6	1.24	1.19	10.0	-	i
HN9	8.4	5.6	3.0	53.9	0.89	0.78	17.9	-	i
HN4	9.4	4.7	3.0	19.3	1.23	1.21	9.11	-	i
HN3	2	12	23.3	62.6	1.15	0.69	53.4	-	i
HN10	4.7	9.4	22.6	71.7	1.07	0.61	38.6	19.4±11.1	p, a
HN11	7	7	23.1	68.3	1.07	0.63	41.7	103.8±38.8	p
HN12	8.4	5.6	23.4	67.3	1.21	0.97	37.4	82.4±27.4	p
HN7	9.4	4.7	23.5	68.5	1.24	0.72	44.9	65.2±55.6	P

p: particle; a: the presence of the aggregated particles; i: the presence of the irregular particles

7.4.2.1 Gel Formation

Figure 7-12 and Figure 7-13 show the change of the reaction conversion of HEMA, EGDMA and NVP with the reaction time at various monomer ratios. It can be seen that the reaction rates are faster and the reaction conversions are higher for each monomer at higher monomer ratios of HEMA to NVP after 4 hours reaction. Obviously, higher HEMA content is helpful for the conversion of NVP. As shown in Figure 7-14, the time for the occurrence of the gelation is almost the same at various monomer ratios. However, it still can be seen that the gelation is a little faster at lower HEMA contents. According to Figure 7-15, the increase in rate for the average molecular weight of the branched polymers is a little faster under lower HEMA contents as well. As stated in the previous

section, the hydrogen bonds in the homopolymer of NVP (PVP) are mainly passing from intramolecular to intermolecular bonds in polar solvent (Searaz et al, 2000). Thefore, under higher NVP content, coupled with HEMA, the stronger intermolecular hydrogen bonding could result in a little fast gelation. However, the presence of more HEMA favors the consumption of NVP so that more NVP enters the networks or the polymeric chains, lowering the network formation and increasing the soluble fractions.

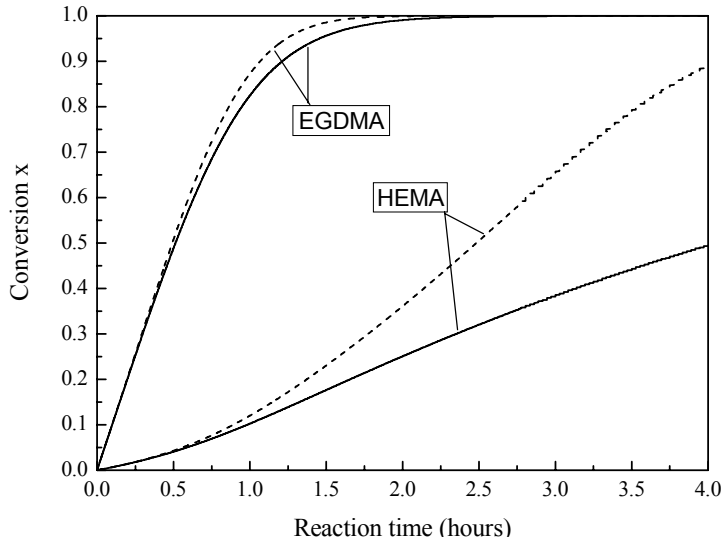

Figure 7-12 Change of the reaction conversion of HEMA and EGDMA with the reaction time at different monomer ratios of HEMA to NVP; ----: HEMA/NVP=9.4ml/4.7ml, —: HEMA/NVP=2ml/12ml; EGDMA=23mol%; I=0.1g; T=70°C; Agi=500rpm

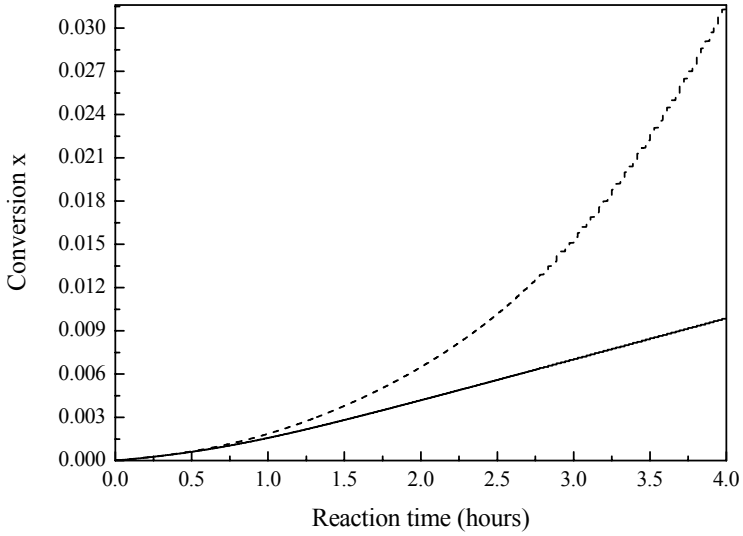

Figure 7-13 Change of the reaction conversion of NVP with reaction time under different monomer ratios of HEMA to NVP; ----: HEMA/NVP=9.4ml/4.7ml, —: HEMA/NVP=2ml/12ml; EGDMA=23mol%; I=0.1g; T=70°C; Agi=500rpm

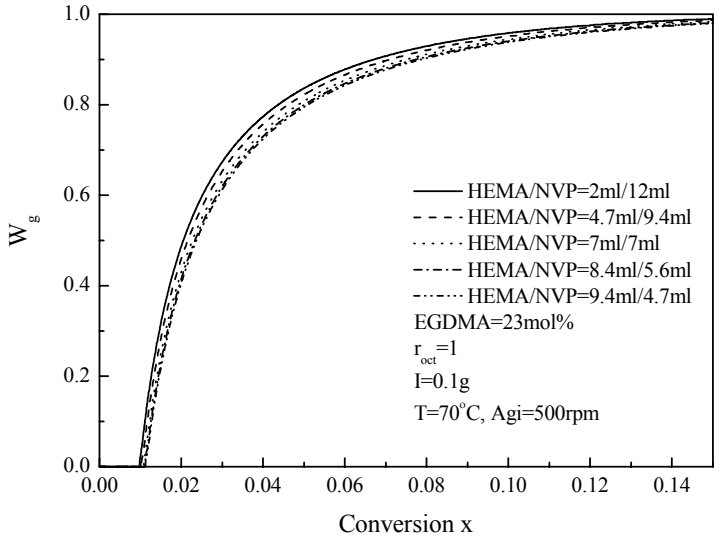

Figure 7-14 Change of the gel fraction with the reaction conversion at various monomer ratios of HEMA to NVP

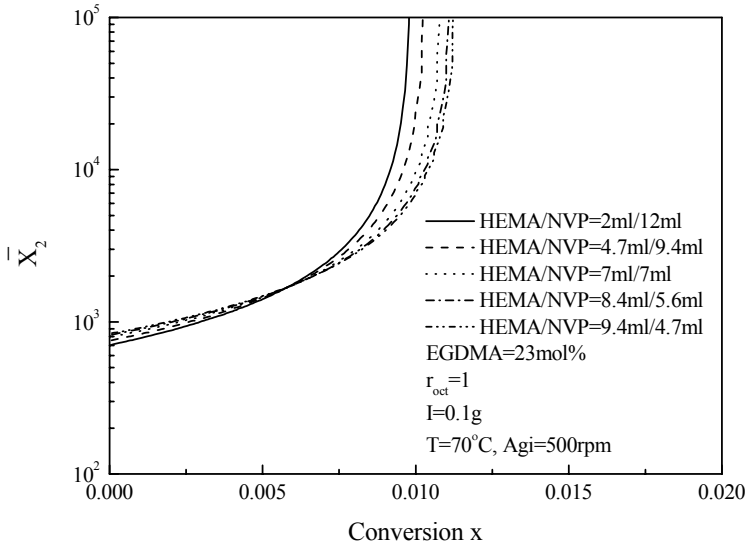

Figure 7-15 Change of the average molecular weight of the branched polymers in the sol at various monomer ratios of HEMA to NVP

Table 7-6 Average molecular weight between the successive crosslinks, the volume swelling ratio in the 1-octanol and the values of the Flory interaction parameters at different monomer ratios; r_{oct}=1

No.	HEMA (ml)	NVP (ml)	EGDMA (mol%)	χ	M_c	q_v (v/v)
HN3	2	12	23.3	1.439	884	1.01
HN10	4.7	9.4	22.6	1.543	756	1.01
HN11	7	7	23.1	1.623	595	1.00
HN12	8.4	5.6	23.4	1.677	482	1.00
HN7	9.4	4.7	23.5	1.722	395	1.00

The calculated values of χ, M_c and q_v are shown in Table 7-6. At a certain EGDMA concentration, the values of M_c keep decreasing with an increase in the monomer ratios. Therefore, higher HEMA content enhances the formation of the more compact networks. In addition, the higher the monomer ratios, the higher the interaction parameters are. Since 1-octanol is a non-solvent for poly(HEMA), higher HEMA content will increase the values of the interaction parameter. However, the values are not that much different because 1-octanol is a poor solvent for PNVP as well according to the solubility parameter shown in Appendix V. Therefore, it could say that the reason for the similar volume swelling ratio is probably because 1-octanol is a non-solvent for both poly(HEMA) and poly(NVP).

7.4.2.2 Particle morphology

Particle morphology is changed with an increase in the HEMA content as shown in Table 7-5.

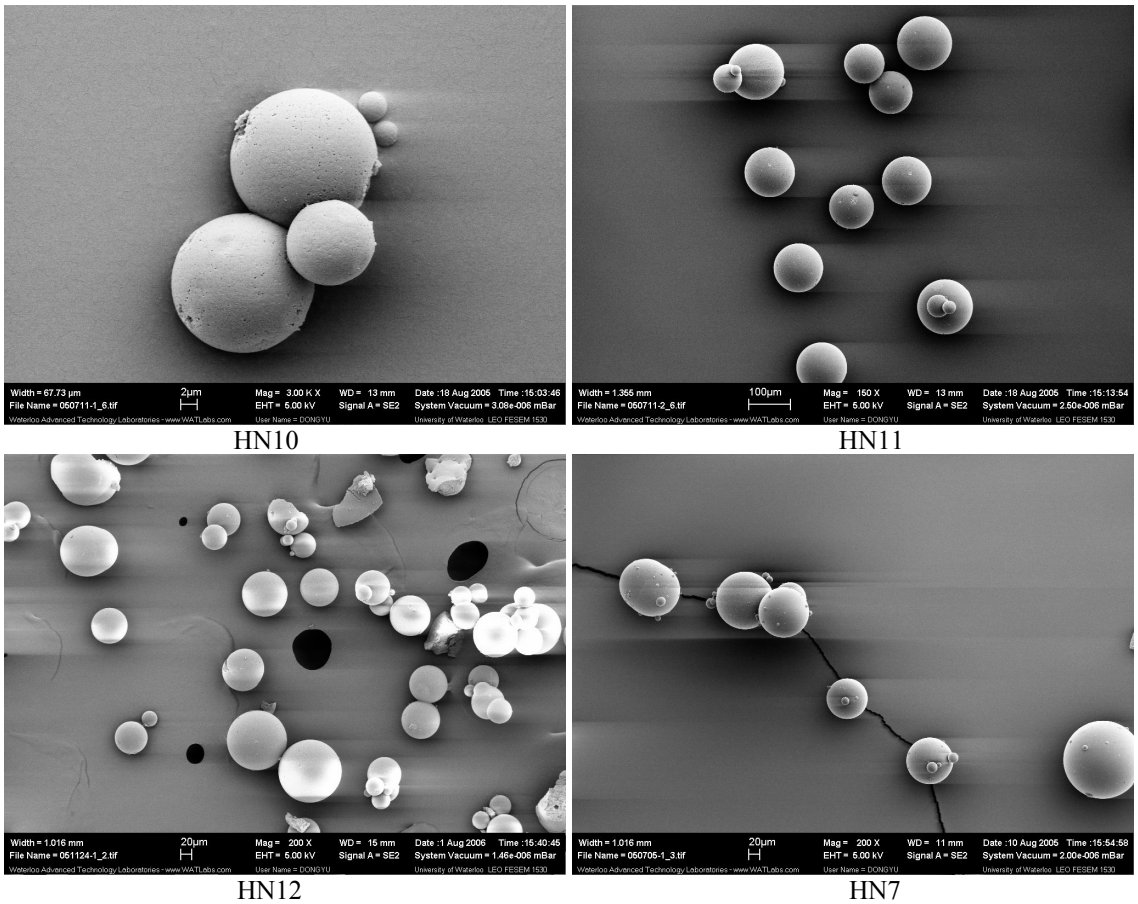

HN10 HN11

HN12 HN7

Figure 7-16 Particle morphology of selected particle samples; HN10: scale bar 2µm, r_H=0.5, [EGDMA]=22.6mol%; HN11: scale bar 100µm, r_H=1, [EGDMA]=23.1mol%; HN12: scale bar 20µm, r_H=1.5, [EGDMA]=23.4mol%; HN7: scale bar 20µm, r_H=2, [EGDMA]=23.5mol%

At higher EGDMA concentration, the particle morphology becomes better with an increase in HEMA content. But at lower EGDMA concentration, the increase in the HEMA content does not improve the particle morphology very much. As stated in the previous chapters, crosslinking is the most important factor for the particle morphology of poly(HEMA-NVP) particles. Therefore, at lower EGDMA concentration, a large amount of soluble fractions in the particles which could consist of PNVP mainly make the polymer soft and sticky so that the irregular particles are easily formed. At higher EGDMA concentration, soluble fractions drop significantly and the presence of HEMA is helpful for forming the networks so that better particle morphology is obtained. The particle morphology of selected samples is shown in Figure 7-16. Therefore, the particle morphology is determined by a combination of monomer ratios and crosslinking.

7.4.2.3 Porous Structures

According to Table 7-5 and Figure 7-17, the porosity and the pore volume are reduced with an increase in the HEMA content. As shown in Figure 7-18, the specific porous surface area decreases with an increase in the HEMA content. This could result from the decrease in the pore volume. The much lower porosity for HN3 in Table 7-5 is probably caused by the formation of the irregular particles by the agglomeration of fine particles.

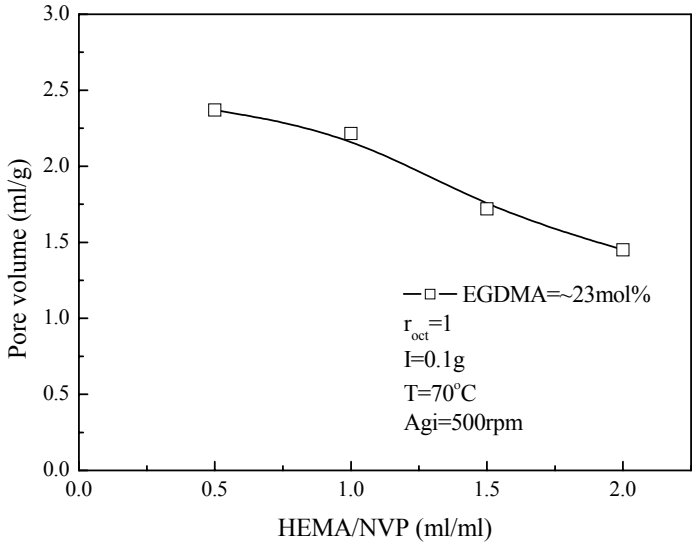

Figure 7-17 The change of the pore volume at various monomer ratios of poly(HEMA-NVP) particles; the data are shown in Appendix I

Compared to NVP, HEMA is relatively less hydrophilic and is favorable for the network formation so that a higher amount of HEMA helps generate more discrete structures (microspheres) and promote a

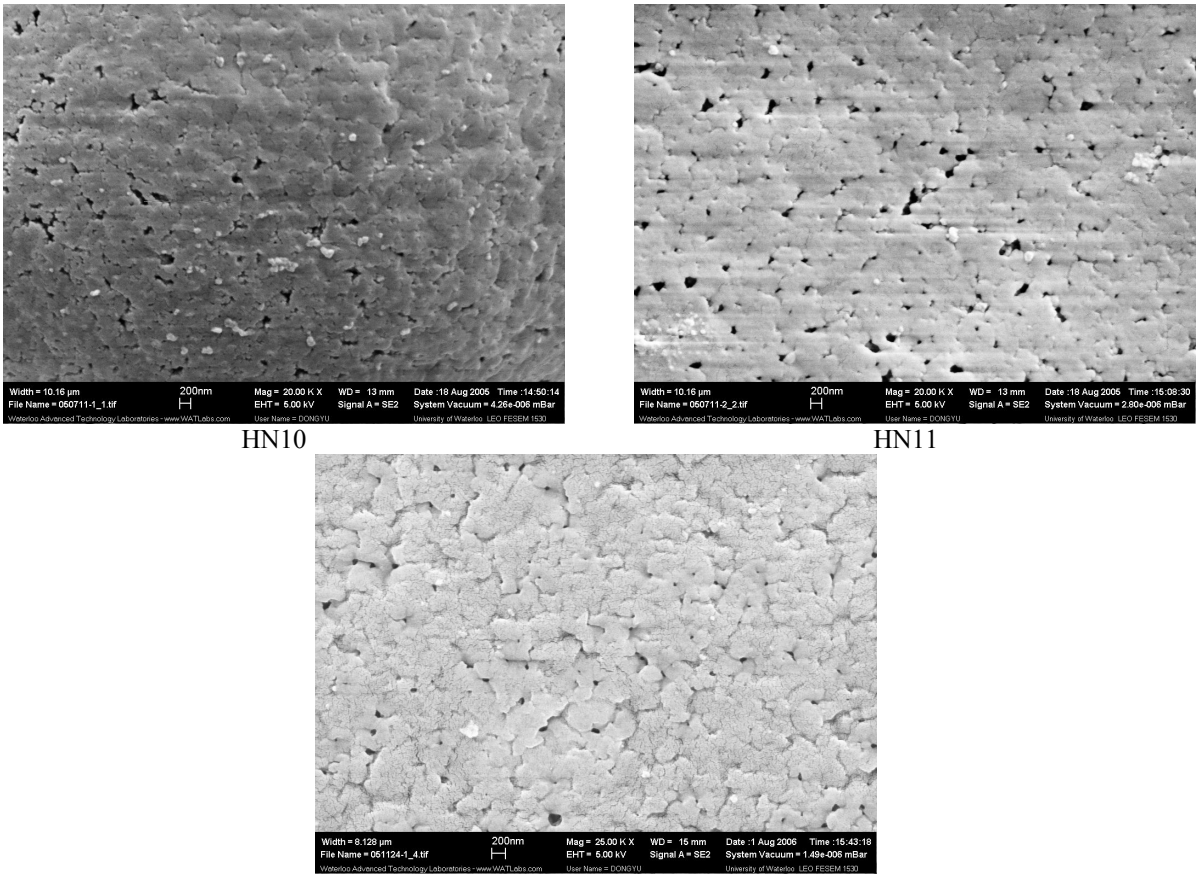

Figure 7-20 The porous structures of the porous poly(HEMA-NVP) particles. Scale bar: 200nm; HN10: r_H=0.5; HN11: r_H=1; HN12: r_H=1.5; [EGDMA]=~23mol%

Figure 7-22 shows a comparison between the simulated porosity and the experimental results. The difference between them should result from the porogen removal and the drying procedure after the synthesis of the porous polymers. However, the trend of the porosity change is very close between the simulated porosity and the experimental results. At very low HEMA content, the presence of more soluble polymers in the system results in more serious network collapse so that the experimental porosity is smaller. Generally speaking, the particles synthesized by adjusting HEMA content have larger pores than those of poly(HEMA-MMA) and poly(HEMA-St) because of the hydrophilic nature of NVP.

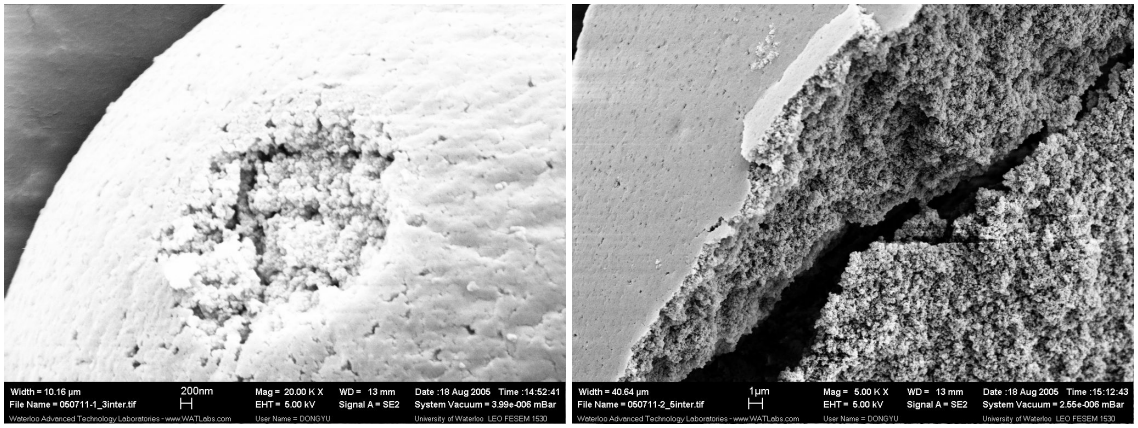

HN10, scale bar 200nm HN11, scale bar 1µm

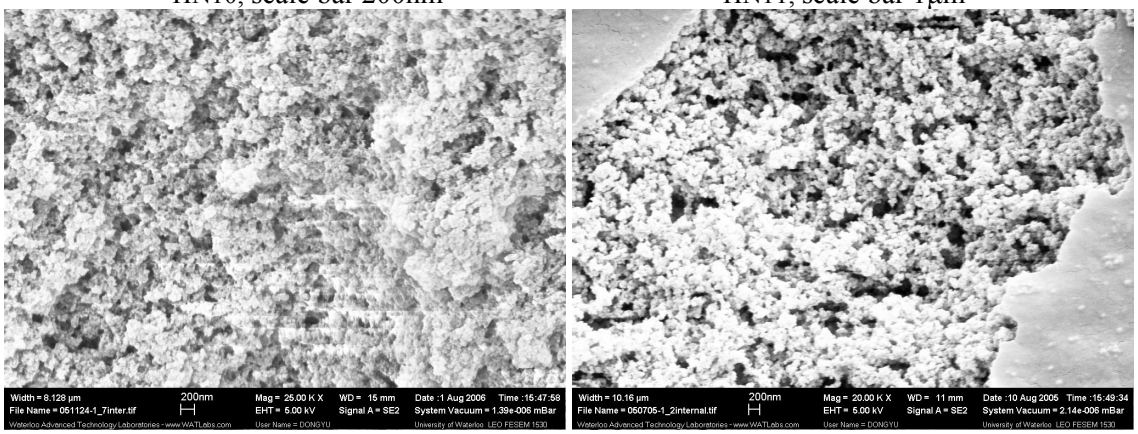

HN12, scale bar 200nm HN7, scale bar 200nm

Figure 7-21 The interior porous structures of the porous poly(HEMA-NVP) particles; HN10: r_H=0.5; HN11: r_H=1; HN12: r_H=1.5; HN7: r_H=2; [EGDMA]=~23mol%

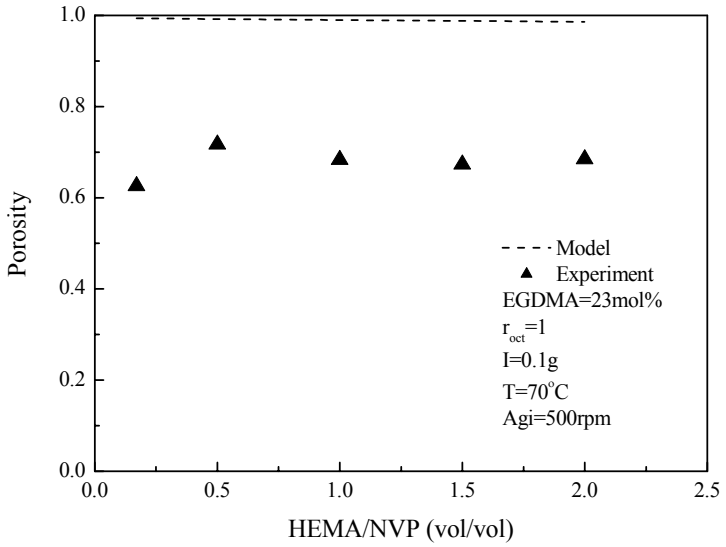

Figure 7-22 Comparison between simulated porosity and the experimental results

7.4.3 Effect of Porogen Volume Ratio

According to the discussion above, the EGDMA molar concentration is very crucial for the nature of the particle morphology and the porous formation of porous poly(HEMA-NVP) particles. It implies that considerable EGDMA concentration must be present in the reaction composition to obtain the porous particles with good particle morphology. Therefore, to study the effect of porogen volume ratio, the particles were synthesized at higher EGDMA concentration at various porogen volume ratios as shown in Table 7-7.

Table 7-7 Reaction composition and experimental results of the synthesis of the poly (HEMA-St) at various porogen volume ratios; HEMA/NVP=9.4ml/4.7ml; [EGDMA]=23.5mol%; T=70°C; Agi=500rpm

No.	r_{oct} (ml/ml)	Surface area (m^2/g)	Pore volume (cm^3/g)	Porosity (%)	d_2 (g/cm^3)	d_0 (g/cm^3)	Average Pore Size (nm)	Particle Size (μm)	Particle Morphology
HN13	0.5	49.2	0.89	52.0	1.21	0.95	14	92.5±19.7	p
HN14	0.8	50.2	1.04	57.1	1.27	0.87	35.6	90.9±21.4	p
HN7	1	51.0	1.45	68.5	1.24	0.72	44.9	65.2±55.6	p

p: particle; a: the presence of the aggregated particles; i: the presence of the irregular particles

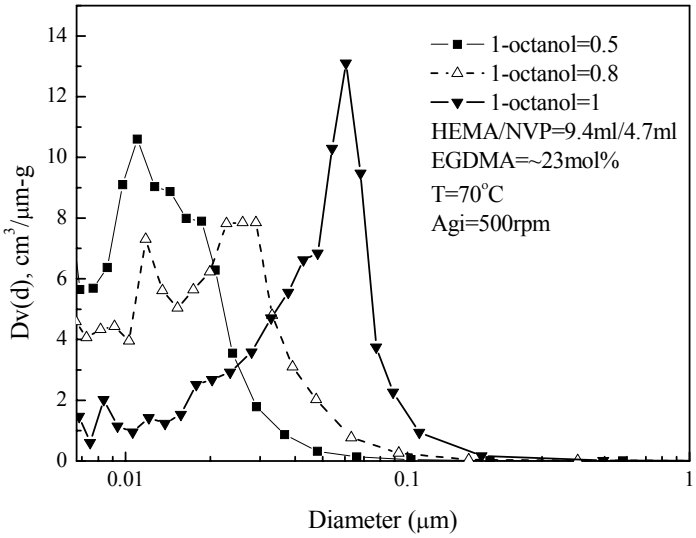

Figure 7-23 The pore size distribution of the porous poly(HEMA-NVP) particle at various porogen volume ratios and at higher monomer ratio

According to Table 7-7, the porosity and the pore volume increase with an increase in the porogen volume ratio. The average pore size is larger and the apparent density is smaller at higher porogen volume ratio. However, the porous surface area does not have much difference. It has been known that, for the porous polymers, the agglomeration of microspheres formed in the poor solvents

contributes to the surface area mainly, and the sizes of these microspheres determine the internal surface area (Nyhus et al, 2000). However, in the present study, it was found that the pore volume increases with an increase in the porogen volume ratio, whereas the porous surface area does not change too much. This implies that even though the internal volume is increased, the sizes of the agglomerated microspheres are not changed greatly. If the decreased apparent density and the increased pore size are taken into account, it suggests that the porous structures are looser at a higher porogen volume ratio, which is consistent with the pore size distribution as shown in Figure 7-23.

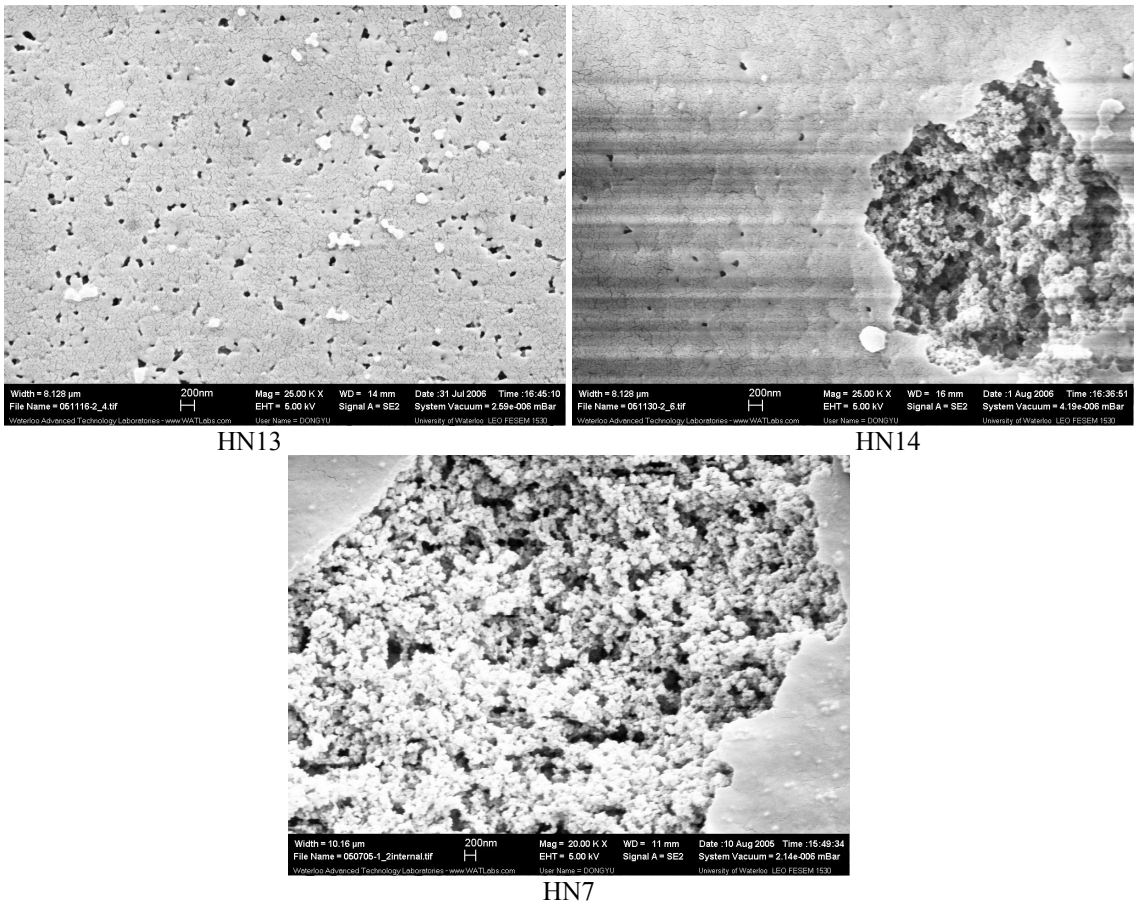

HN13 HN14

HN7

Figure 7-24 The porous structures of poly(HEMA-NVP) particles synthesized at different porogen volume ratios; Scale bar: 200nm; HN13: r_{oct}=0.5; HN14: r_{oct}=0.8; r_H=2, [EGDMA]=~23mol%

As shown in Figure 7-23, the pore size distribution is shifted toward larger pores when the porogen volume ratio is increased. Smaller pores become less and larger pores become more with the increase in the porogen volume ratio. This verifies that the porous structures are looser at a higher porogen volume ratio. On the other hand, the values of d_2 (skeletal density) as shown in Table 7-7 are close to each other, which implies that the properties of the polymer phase for the particle are similar at

different porogen volume ratios under identical monomer ratios and EGDMA molar concentrations. Therefore, it could be concluded that most of the porogen is separated out of the networks during the reaction so that the whole porous structures are looser and more pores are generated because porogen molecules occupy more spaces at higher porogen volume ratios.

Figure 7-24 shows the porous structures of selected samples. The porous structures can be clearly seen. Since higher dilution of the monomers, the pores on surface tend to fuse together. However, accoding to the interior structures shown in HN13 and HN7, it verifies that the porous structures are looser at a higher porogen volume ratio.

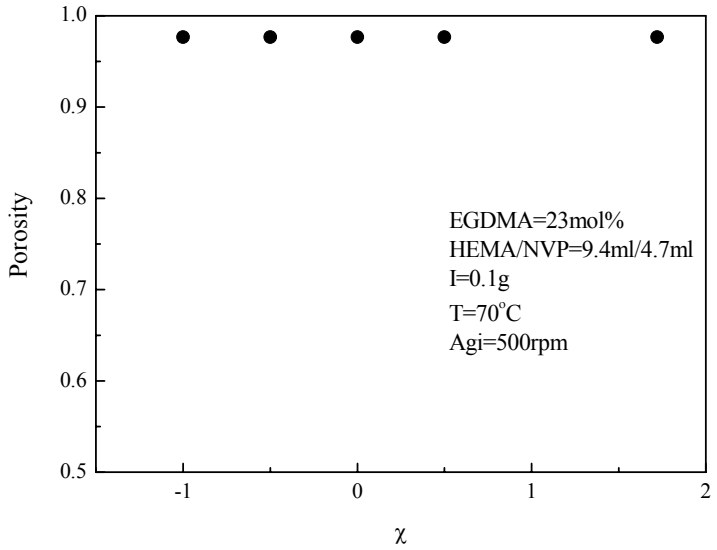

Figure 7-25 Simulated porosity in various solvents with different thermodynamic quality

At higher EGDMA concentration, the different solvents with different interaction parameter values do not have a great effect on the porosity of the polymer as shown from the simulated results in Figure 7-25. This result is the similar to those for the porous poly(HEMA-St) and poly(HEMA-MMA). Since the compact networks are formed at higher EGDMA concentration, the relaxation of the polymer chains is difficult so that the volume swelling ratio of the polymers in a different solvent is almost the same as shown in Figure 7-26 although it still becomes a little smaller in a non-solvent with higher interaction parameter values. Figure 7-27 shows the simulated porosity at various porogen volume ratios. It can be seen that the porosity is increased with an increase in the porogen volume ratio which is consistent with the experimental results. The difference between the

experimental results and the simulated ones should result from the pore collapse during the porogen removal and the drying procedure in the real experiments.

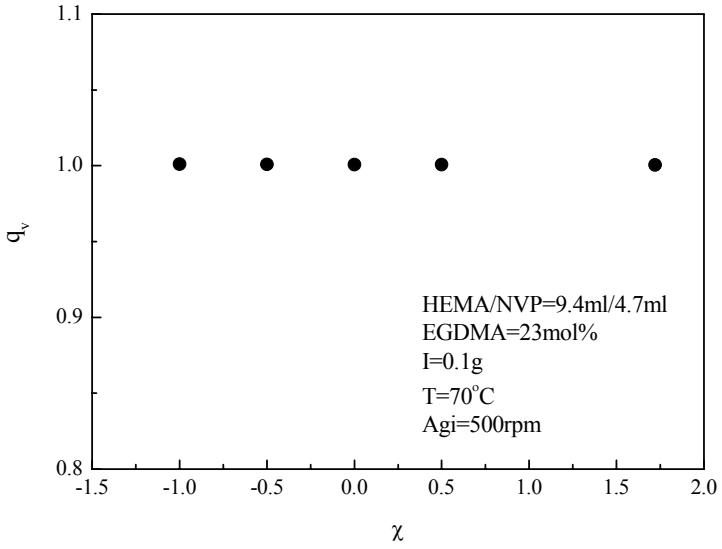

Figure 7-26 Change of the volume swelling ratio with the interaction parameter values

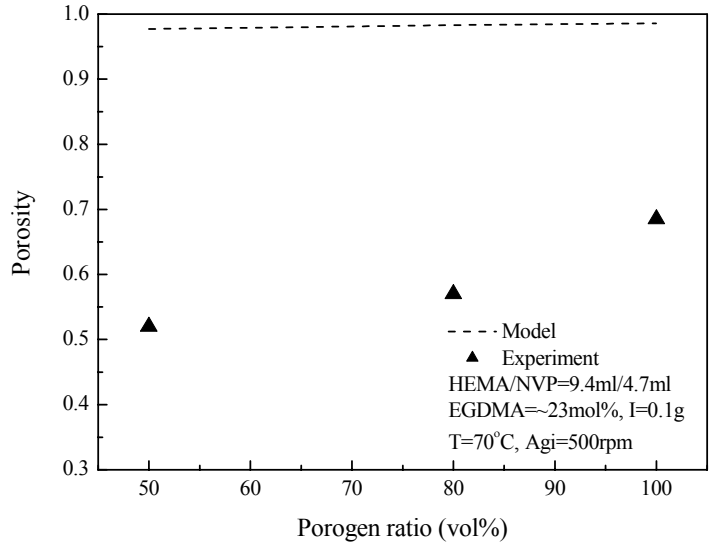

Figure 7-27 Comparison of the simulated porosity and the experimental results at various porogen volume ratios

7.4.4 Controllable Pore Size

The average pore size can be calculated to illustrate the controllable pore size of the porous poly (HEMA-NVP) particles. The pore size changes over a wider range for the particles produced under lower HEMA content. Accoring to the above discussion, to have control over the pore size of the

porous poly(HEMA-NVP) particles, higher HEMA content and higher EGDMA content will be required. The porous morphology is also better under these conditions according to the discussion above. Figure 7-28 through Figure 7-30 show the change of average pore size under various reaction conditions.

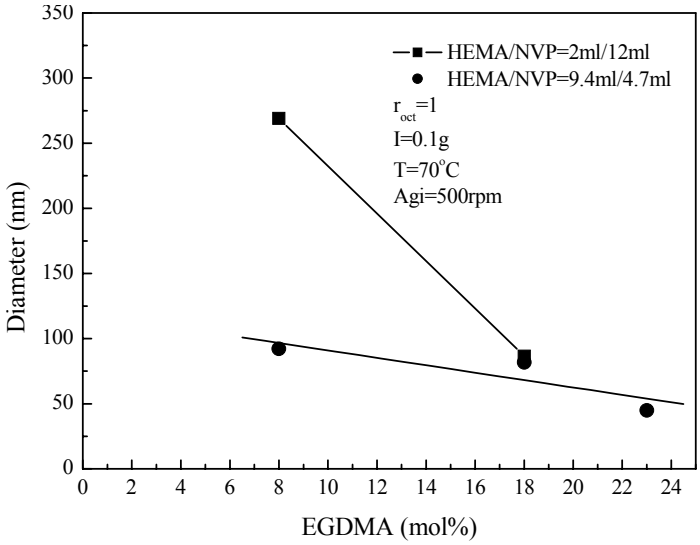

Figure 7-28 The change of the average pore size under various EGDMA concentration for the porous poly(HEMA-NVP) particles; the data are shown in Appendix I

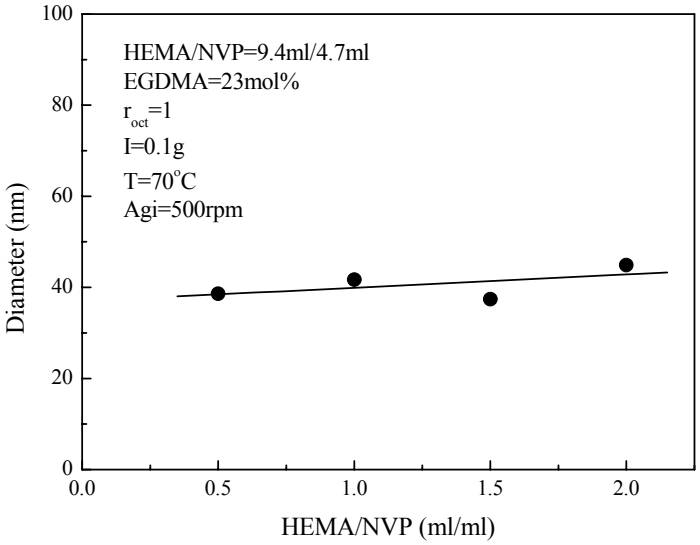

Figure 7-29 The change of the average pore size at various monomer ratios for the porous poly(HEMA-NVP) particles; the data are shown in Appendix I

Figure 7-28 shows the change of the average pore size with respect to the EGDMA concentration. With an increase in the EGDMA concentration, the average pore size is decreased. However, under

faster phase separation in a non-solvent. The further increase in the monomer ratio (ml/ml) will also reduce the pore volume because of the formation of the more compact networks. Thus the density is increased. According to the pore size distribution shown in Figure 7-19, there are more pores at higher NVP content, resulting in higher pore volume and higher surface area. If taking into account the soluble polymers, the soluble fractions in reaction systems become less at a higher HEMA content, which induces fewer pores, i.e. lower pore volume and lower surface area.

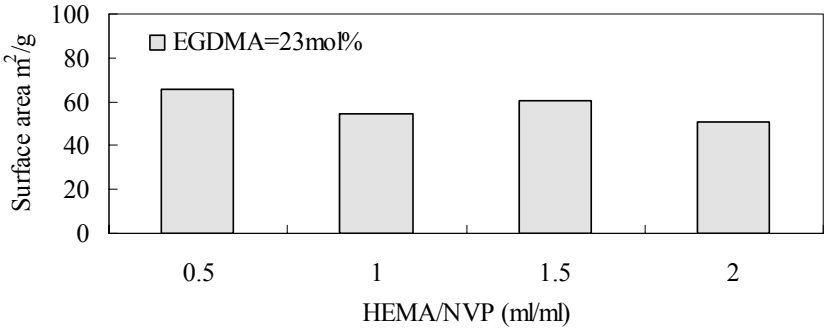

Figure 7-18 The change of the porous surface area with the monomer ratio for the porous poly(HEMA-NVP) particles; the data are shown in Appendix I

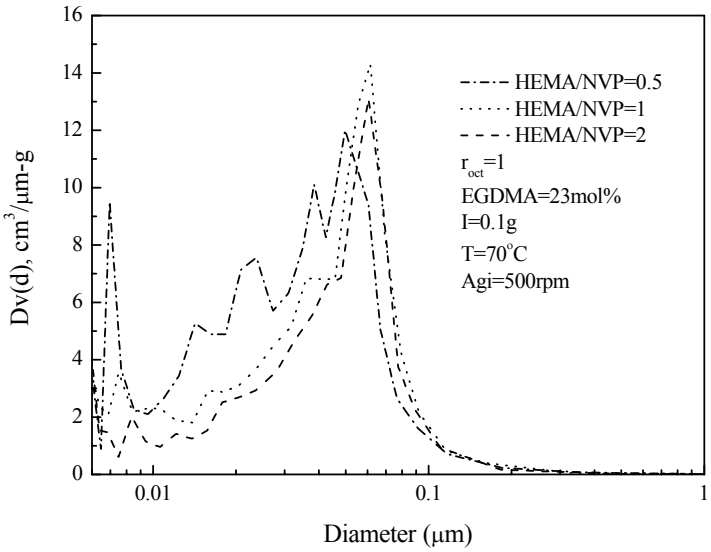

Figure 7-19 Pore size distribution of porous poly(HEMA-NVP) particles at various monomer ratios

SEMs shown in Figure 7-20 illustrate the change in the nature of the pores. Figure 7-21 shows the interior structures of these particles. It can be seen that the pores are formed by the agglomeration of many discrete structures.

lower HEMA content, the change of the pore size is greater, whereas the pore size change is not that drastic under higher HEMA content. The change of the average pore size with the monomer ratio for the particles which have good particle morphology is shown in Figure 7-29. The pore size is slightly increased with an increase in the monomer ratios and the pore size is below 100nm. Figure 7-30 shows the change of the average pore size at various porogen volume ratios. The average pore size increases with an increase in the porogen volume ratio, which is consistent with the common phenomenon in the preparation of the porous polymers by taking advantage of the phase separation in the presence of certain solvents (Kiefer et al, 1999). All in all, the pore size could be controlled by adjusting different reaction parameters including the EGDMA concentration, the monomer ratios and the porogen volume ratio.

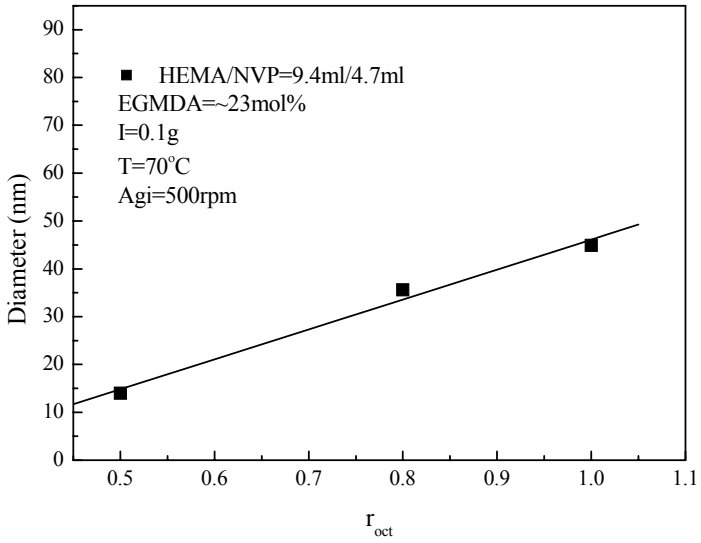

Figure 7-30 The change of the average pore size under various porogen volume ratios for the porous poly(HEMA-NVP) particles; the data are shown in Appendix I

7.5 Summary

According to the studies on the synthesis of porous poly(HEMA-NVP) particles, the EGDMA concentration, the monomer ratio and the porogen volume ratio can control the porous properties and the particle morphology of poly(HEMA-NVP) efficiently.

The porous poly(HEMA-NVP) particles can be prepared by adjusting the EGDMA molar concentration. The reaction rates for HEMA and EGDMA are faster at higher concentration. The reaction rate of NVP is slow at the beginning, but it becomes faster after certain reaction time when HEMA and EGDMA reach certain high conversions. The gelation occurs earlier and the gel fraction

grows faster at higher EGDMA concentration than those at lower EGDMA concentration. The particle morphology becomes better with an increase in the EGDMA concentration under a high level of HEMA. To produce permanent porous structures and generate good particle morphology, the EGDMA concentration must be at least 8mol%.

The reaction rates are faster and the reaction conversions are higher for each monomer at higher monomer ratios of HEMA to NVP. Higher HEMA content is helpful in the conversion of NVP. However, the time for the occurrence of the gelation is almost the same at various monomer ratios. The porosity, the pore volume and the surface area are reduced with an increase in the HEMA content. The particle morphology becomes better with an increase in HEMA content. But at lower EGDMA concentration, the increase in the HEMA content does not improve the particle morphology very much.

The porosity and the pore volume increase with an increase in the porogen volume ratio. The values of the porous surface area are mainly in the range of 50-70 m^2/g. The pore size could be controlled by adjusting different reaction parameters including the EGDMA concentration, the monomer ratios and the porogen volume ratio.

Chapter 8
Swelling Properties of Porous Copolymeric Particles of HEMA

8.1 Introduction

One of the most important properties of poly(HEMA) is that it can be swollen by taking up a large amount of water which can be characterized by the equilibrium weight swelling ratio (q_w) and the equilibrium volume swelling ratio (q_v). Poly(HEMA) homopolymer has been found to follow a Fickian model for water uptake with a diffusion coefficient at 37°C in the range between $1.55\times10^{-11}m^2/s$~$2.00\times10^{-11}m^2/s$ in the absence of any added crosslinker (Hill et al, 1999). However, in the presence of a crosslinker, such as EGDMA, the diffusion coefficient has been reported to decrease depending on the extent of the crosslinking (Hill et al, 1999). The high crosslink density leads to a higher glass transition temperature. The presence of water, which acts as a plasticizer to make the glassy polymer become rubbery (Luperano et al, 1996), can reduce the glass transition temperature of the poly(HEMA) polymers during the swelling. However, the higher crosslink density deteriorates the swelling capacity of the polymers because the polymeric networks are hard to be relaxed at higher crosslink density. Therefore, as reported in the literatures, the swelling properties of poly(HEMA) are greatly affected by the crosslink density of the polymers (Hill et al, 1999; Wu et al, 2004; Sun et al, 1997; Shieh et al, 1991).

However, due to the poor mechanical properties of swollen PHEMA, its use has been limited to applications where good mechanical properties of the material are not required, such as soft contact lens (Migliaresi et al, 1984). Nevertheless, it is possible to control the swelling degree and mechanical properties by changing the composition of poly(HEMA) in the copolymer systems prepared with the appropriate amount of a second comonomer (Migliaresi et al, 1984; Peniche et al, 1994; Barcellos et al, 2000). In most cases, a hydrophobic comonomer is used, but sometimes a hydrophilic comonomer of HEMA is used as well if the mechanical strength is not the most important issue. The change of the swelling capacity of some copolymers of HEMA have been studied, such as poly(HEMA-MMA) (Migliaresi et al, 1984; Migliaresi et al 1984), poly(HEMA-NVP) (Korsmeyer, et al, 1986), poly(HEMA-FA) (Peniche et al, 1994), poly(HEMA-DHPMA) (Tsai et al, 2004), and so on. In these HEMA copolymers, the copolymer composition is responsible for the different swelling behaviors.

Therefore, the right balance of the copolymer compositions leads to hydrogels with tailor-made swelling properties and other related properties (Barcellos et al, 2000).

However, most of the studies on the swelling of the HEMA copolymers were focused on the polymers which are non-porous. According to Brazel et al (1999), the q_w values of the non-porous poly(HEMA-NVP) containing 25mol% and 75mol% of NVP are about 1.90~1.98 at 37°C, whereas they are ~1.60 for crosslinked poly(HEMA) with 1mol% EGDMA at 37°C and they are 1~1.3 for nonporous poly(HEMA-MMA) containing 0mol% to 75mol% HEMA at 37°C. Although the effects of the crosslinking density and the copolymer composition were studied, the effect of the porous structures, together with the crosslinking and copolymer composition, was never studied carefully before. The swelling process of the porous polymer particles in water includes two main steps: i) water fills in to the pores; ii) the polymeric networks are swollen by the water. Therefore, the presence of pores must have a great effect on the swelling properties of the porous HEMA copolymers.

In the present work, the swelling properties of the porous copolymer particles of HEMA were studied. The water uptake was much higher than the reported data in the literature. According to the previous chapters, the reaction parameters, including EGDMA molar concentration, monomer ratios and the types of the comonomers determine the characteristics of the porous structures and the polymeric networks. So the effects of the above factors on the swelling properties were studied. The effect of the environment temperature on the swelling properties was studied as well. The effect of the pH on the swelling properties was not studied. However, it was found that the swelling capacity of poly(HEMA) reaches a maximum at pH=7 and does not change at higher pH values under different ionic strength (Li et al, 2005). Therefore, experiments were carried out in water at pH=7. The experimental method has been introduced in the previous chapter. In addition, the values of q_w and q_v are average values for each sample because the particle size distribution was not considered in the swelling studies.

8.2 Experimental Reproducibility

The experimental methods have been introduced in Chapter 4. Each experiment was repeated three times to calculate the average values. The errors shown in this chapter were calculated using statistical tools in Microsoft Excel at a 95% confidence interval. According to the errors, the reproducibility of the experimental method is acceptable.

8.3 Results and Discussion

8.3.1 Effect of EGDMA Molar Concentration

Figure 8-1 and Figure 8-2 show the effect of the EGDMA concentration on q_w and q_v of the porous copolymer particles synthesized with certain HEMA content and at certain porogen volume ratio. It can be seen that the values of q_v and q_w decrease with an increase in the EGDMA concentration. However, different comonomers show different behaviors at various EGDMA molar concentrations. It has been mentioned that the swelling process consists of two steps which are that water fills in the pores and that water swells the polymeric networks. Therefore, the porous structures mainly determine the values of q_w if the highly porous structures are present and the properties of polymeric networks determine the volume swelling ratio q_v.

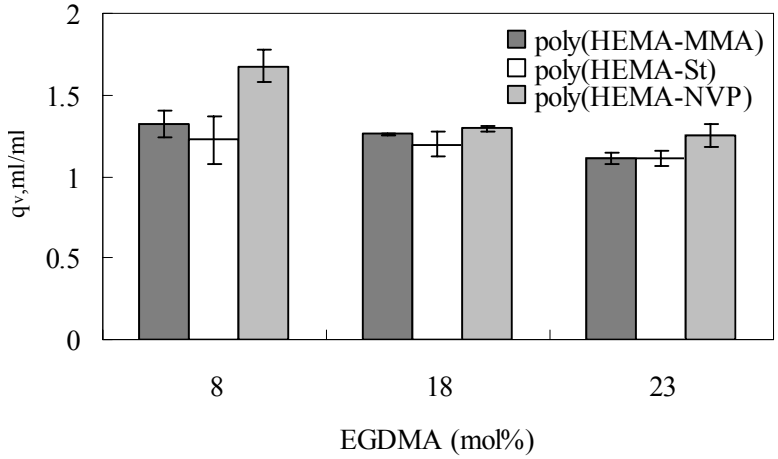

Figure 8-1 Change of the equilibrium weight swelling ratio with an increase in the EGDMA concentration; HEMA/comonomer=9.4ml/4.7ml; r_{oct}=1; the data are shown in Appendix I

As shown in Figure 8-1, poly(HEMA-NVP) particles have the highest q_v values, whereas poly(HEMA-St) have the lowest ones. In the poly(HEMA) hydrogels, the –OH and C=O groups are responsible for polar intermolecular bonds determining the cohesion of polymer chains. Thus, the water absorbed in the glassy polymer, causes the loosening of intermolecular bonds and the lowering of the rotational energy barriers, which is responsible for the glass-rubber transition (Luprano et al, 1996), resulting in the change of the volumes. With an increase in the EGDMA concentration, more crosslinks are generated in the polymeric networks as shown by the decrease in the M_c for these three types of particles presented in the previous chapters. Thus the polymeric networks are more compact and the stretching and dilation of the polymer chains become more difficult (Sun et al, 1997).

Therefore, the polymer chains need to conquer higher rotation energy to enhance mobility so that the volume swelling is weakened at higher EGDMA molar concentration. In addition, it can be seen that the EGDMA concentration has the least effect on the q_v values of the poly(HEMA-St) particles, whereas it has the greatest effect on q_v of the poly(HEMA-NVP) particles. Styrene is the most hydrophobic comonomer in these three comonomers and the presence of the aromatic groups greatly hinders the absorption of water already. Therefore, at higher EGDMA concentration, the q_v values do not show much difference. For the poly(HEMA-NVP) particles, the presence of NVP enhances the hydrophilicity of the polymer chains resulting in stronger intermolecular interactions between the polymer chains and water so that the relaxation of the polymers is accelerated. The presence of more crosslinks restrains the relaxation of the poly(HEMA-NVP) networks. Therefore, the more hydrophilic the comonomer, the greater effect the EGDMA molar concentration has.

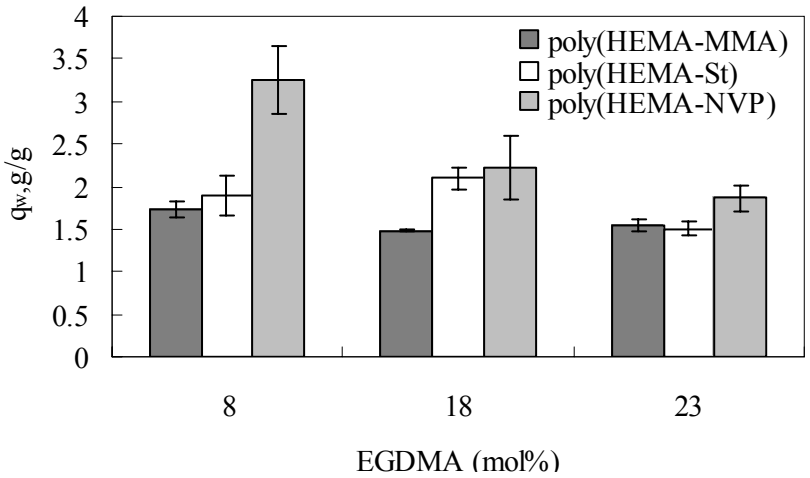

Figure 8-2 Change of the equilibrium volume swelling ratio with an increase in the EGDMA concentration; HEMA/comonomer=9.4ml/4.7ml; r_{oct}=1; the data are shown in Appendix I

With regard to the equilibrium weight swelling ratio q_w, it decreases with an increase in the EGDMA molar concentration as well. It can be said that the increasing crosslinks reduces the free volumes between the macromolecular chains which lowers the degree of swelling of the hydrogel (Bajpai et al, 2002). But the presence of the pores provides more volume for the water to enter the particles. With an increase in the EGDMA concentration, the pore volume becomes less and the average pore size becomes smaller. Coupling with the change of the network properties, the water uptake process is weakened at higher EGDMA concentration. The poly(HEMA-NVP) particles have the highest q_w values although the pore volume is lower than that of poly(HEMA-St). But poly(HEMA-NVP) particles have the largest average pore size which is helpful for the diffusion of the water molecules,

coupling with its strong hydrophilic properties. However, the interesting thing is that the poly(HEMA-St) has a little higher or close q_w values compared to those of poly(HEMA-MMA) particles which could be caused by the higher pore volume of poly(HEMA-St). This implies that a large amount of water is present in the pores for the poly(HEMA-St) particles. Therefore, to a certain extent, the changes of q_w values correspond to the change of the porosity or the pore volume for each porous polymeric particle, which means a higher porosity or a higher pore volume could lead to higher water uptake for the same polymer.

8.3.2 Effect of Monomer Ratio

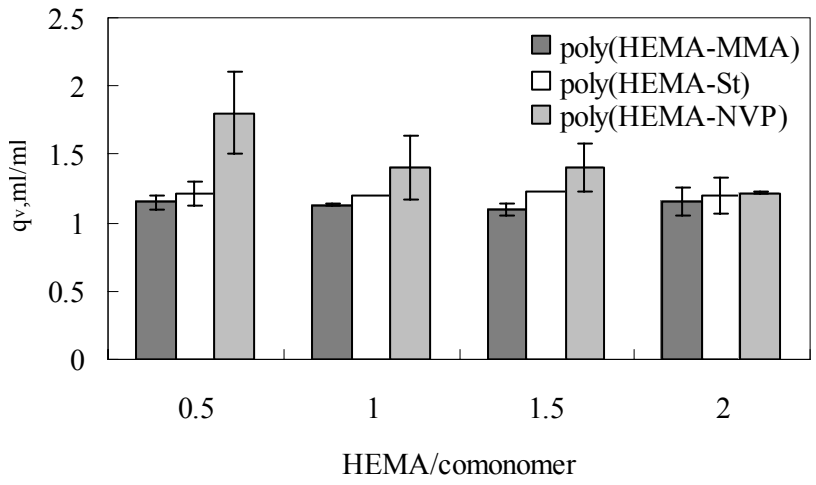

Figure 8-3 Change of the equilibrium volume swelling ratio with an increase in the monomer ratios; EGDMA=23mol%; r_{oct}=1; the data are shown in Appendix I

Figure 8-3 and Figure 8-4 show the effect of HEMA content on the swelling properties of the resultant copolymer particles. With an increase in the HEMA content, the values of q_w and q_v of the porous poly(HEMA-NVP) particles are reduced. Compared to NVP, HEMA is relatively less hydrophilic and its presence decreases the free volume between the polymer chains because it enhances the crosslinking in the polymers. Therefore, this implies that the hydrophilicity of the poly(HEMA-NVP) is weakened with an increase in the HEMA contents so that the q_v and the q_w values are decreased.

For the poly(HEMA-St) and the poly(HEMA-MMA), the q_v and the q_w show different behaviors. With an increase in the HEMA content, basically, the q_v values are increased a little bit for

poly(HEMA-MMA) and poly(HEMA-St) because of the presence of the more hydrophilic HEMA. However, the q_v values do not change that much at higher EGDMA molar concentration. This phenomenon was also observed in other copolymers including hydrophilic and hydrophobic monomers (Bajpai et al, 2002). In addition, some swelling ratios of the poly(HEMA-St) particles are a little higher than those of the poly(HEMA-MMA) particles. This could be caused by the hydrophobicity of the styrene. Some hydrophobic PS segments could move into the particles further to form some cores whereas poly(HEMA) segments are on the outside. This would help the particles swell much easier. Generally speaking, the different swelling behaviors of these particles are determined by the porous structures and the properties of the polymer networks.

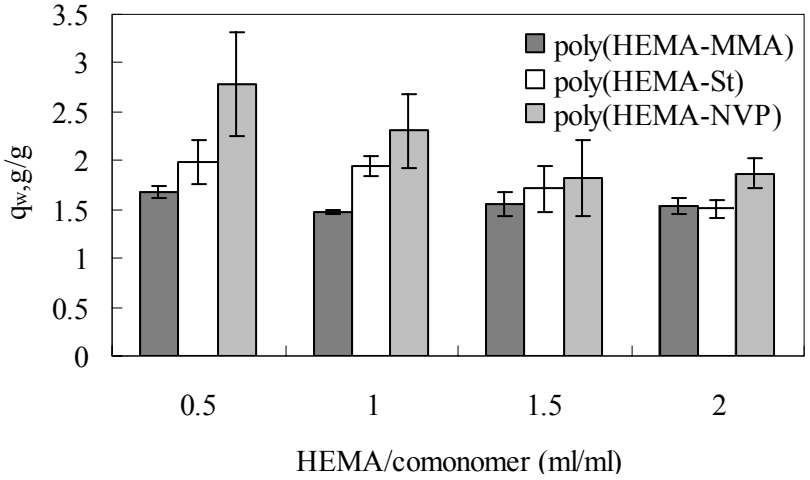

Figure 8-4 The change of the equilibrium weight swelling ratio with an increase in the monomer ratios; EGDMA=23mol%; r_{oct}=1; the data are shown in Appendix I

8.3.3 Effect of Temperature

Table 8-1 shows the effect of the temperature on the swelling properties of the poly(HEMA-MMA), poly(HEMA-St) and poly(HEMA-NVP) particles. It can be seen that the swelling capacity is strengthened at higher temperature. The presence of water, acting as a plasticizer, lowers the glass transition temperature of the polymer chains through the interactions between water and polymer chains so that the rotation energy of the intermolecular chains can be overcome (Bajpai et al, 2002). This implies that the relaxation of the polymer chains is enhanced at higher temperature. Therefore, higher values of q_v and q_w were observed.

Table 8-1 Effect of Temperature on the swelling properties

HEMA (ml)	Comonomer (ml)	EGDMA (mol%)	r_{oct}	q_w		q_v	
				25°C	37°C	25°C	37°C
9.4	4.7, MMA	8	1	1.73±0.09	2.21	1.32±0.08	1.44
		23	1	1.54±0.08	1.69	1.16±0.10	1.22
9.4	4.7, St	8	1	1.89±0.23	2.20	1.23±0.15	1.25
		23	1	1.51±0.09	1.54	1.16±0.11	1.18
9.4	4.7, NVP	8	1	3.24±0.40	3.92	1.68±0.10	2.74
		23	1	1.87±0.15	2.13	1.25±0.07	1.33

8.4 Summary

According to the study, the porous structures mainly determine the values of q_w if the highly porous structures are present and the properties of polymeric networks determine the volume swelling ratio q_v.

The values of q_v and q_w decrease with an increase in the EGDMA concentration. However, different comonomers show different behaviors at various EGDMA molar concentrations. The more hydrophilic the comonomer, the greater effect the EGDMA molar concentration has. The EGDMA concentration has the least effect on the q_v values of the poly(HEMA-St) particles, whereas it has the greatest effect on it of the poly(HEMA-NVP) particles. With regard to the equilibrium weight swelling ratio q_w, it decreases with an increase in the EGDMA concentration as well. However, the presence of pores provides larger volume for the water to enter the particles. Coupling with the change of the network properties, the water uptake process is weakened at higher EGDMA concentration. Therefore, to a certain extent, the changes of q_w values correspond to the change of the porosity or the pore volume for each porous polymeric particle, which means higher porosity or pore volume could lead to higher water uptake for the same polymer.

With an increase in the monomer ratio (HEMA content), the values of q_w and q_v for the porous poly(HEMA-NVP) particles are reduced. Compared to NVP, HEMA is relatively less hydrophilic and its presence decreases the free volume between the polymer chains because it enhances the crosslinking in the polymers. With an increase in the HEMA contents, the q_v values are increased for poly(HEMA-MMA) and poly(HEMA-St) because of the presence of more hydrophilic HEMA. The q_w values increase to certain HEMA content, and then decrease a little bit, which implies that the pore volume or the porosity play a more important role under higher HEMA content at higher EGDMA concentration in the presence of a hydrophobic comonomer.

The swelling capacity is strengthened at higher temperature because the relaxation of the polymer chains is enhanced at higher temperature. Therefore, higher values of q_v and q_w were observed.

Generally speaking, the different swelling behaviors could be controlled successfully by the porous structures and the properties of the polymer networks in the present studies. The water uptake properties are better than those reported for non-porous HEMA copolymers.

Chapter 9
Application of the Porous Copolymer Particles of HEMA in Controlled Release

9.1 Introduction

Controlled release of bioactive agents or other chemicals has been studied for several decades. A variety of methods have been studied. Traditionally, polymeric delivery systems for controlled release include monolithic and reservoir systems in which the released materials are just simply dispersed throughout polymer matrix (Korsmeyer et al, 1984). Therefore, the materials leach out slowly when the systems are placed in the target sites. However, the most important requirement for a polymeric delivery system is that the release is continuous and the release rate could stay constant during a certain course of the release process. The above two types of the systems can not satisfy these requirements very well.

However, the swelling-controlled release systems can be used to overcome the above stated difficulties. The swelling-controlled release systems are able to deliver drugs at constant rates over an extended period of time (Peppas et al, 1993). Basically, a swelling-controlled release system consists of a hydrophilic polymer that undergoes swelling more or less continuously throughout the matrix so that the glass-to-gel transition loosens the polymeric matrix and the drugs are able to diffuse out (Fan et al, 1989). Therefore, the release rate is controlled by the balance between drug diffusion across a concentration gradient, the polymer relaxation occurring as the crosslinked polymer imbibes water, and the osmotic pressure occurring during the swelling process (Brazel et al, 1999).

A swelling-controlled release system can be produced by copolymering the monomers in the presence of a bioactive agent or by loading the bioactive agent into a copolymer sample in its saturated solution (Fan et al, 1989). For the former, the system preparation is more convenient. However, the compositions of the copolymers and the reaction conditions have to be carefully controlled so that the drugs' molecular structures can not be destroyed and there are no trace chemicals left behind. Therefore, this technique is not widely applied. For the latter, the polymer can be synthesized first, eliminating any unreated chemicals. Then the drugs are loaded by immersing the polymers into the

saturated drug solutions. Most of the studies on the swelling-controlled release systems use this technique.

Although many HEMA polymeric swelling-controlled release systems have been synthesized and studied (Brazel et al, 1999), a majority of them are focused on non-porous polymers. In addition, the morphologies of the polymers are mainly slabs. However, the swelling of porous poly(HEMA) particles in water makes them suitable for close obliteration of vessels (Montheard et al, 1992) and deliver drugs as well. Furthermore, the presence of the pores could result in a constant release rate which is very important in the drug delivery. In the present studies, the applications of three types of the porous HEMA copolymeric particles, poly(HEMA-MMA), poly(HEMA-St) and poly(HEMA-NVP), in the drug delivery of the model drug theophylline were studied. The effects of the particle size, the network properties and the polymer composition were explored.

9.2 Experimental

9.2.1 Model Drug—Theophylline

Theophylline has been widely used as a model drug in studies on the various hydrophilic controlled release systems (Shozo et al, 2000; Katime et al, 2001; Coviello et al, 2003; Liu et al, 2005). It has moderate water solubility and is one of the most effective drugs being used in the treatment of asthma, bronchial asthma and chronic obstructive pulmonary disease (Brazel et al, 1999; Liu et al, 2005). The drug has a very narrow therapeutic margin, and therapeutic plasma concentrations range from 10 to 20μg/mL with severe toxicities associated with higher concentrations (Saez et al, 1993). Hence, plasmatic concentrations of theophylline lower than 10μg/mL do not have therapeutic effects and higher than 20μg/mL produces secondary effects in patients (Saez et al, 1993). For non-smoking adults between 18-73 years old, it takes about 8 hours for the body to clear the drug (Jackson et al, 1985). Some physical properties of theophylline are shown in Table 9-1.

Table 9-1 Physical properties of theophylline (Brazel et al, 1999)

Drug	Molecular weight	UV wavelength	Diffusion coefficient in water ($10^7 cm^2 s^{-1}$)	Hydrodynamic radius, r_h (Å)	Water solubility (g/L)
Theophylline	180	273nm	117.6 (37°C)	3.7	8.3 (37°C)

9.2.2 Drug Loading

The drug loading experiments were carried out in concentrated aqueous solution of theophylline at room temperature. The polymer samples were dispersed in the solution. The vials containing the polymers and the solution were put into an Eviron-Shaker which was kept at a low shaking speed. At each predetermined time interval, a very small amount of solution sample (~75μL) was taken to be characterized using Varian Cary 300 Bio UV/Vis Spectrophotometer to obtain the drug concentration (C_t). The loading experiments were stopped until the drug concentration stays constant. The polymers were then filtrated, dried at 40°C in a vacuum centrifuge for half an hour and put into a vacuum desiccator at room temperature for three days. The Drug Loading Capacity (DLC) can be calculated using the equation (9-1) as follows,

$$DLC = \frac{(C_0 - C_\infty) \cdot V \cdot M_W \cdot 1000}{m_p} (mgDrug / gPolymer) \qquad (9\text{-}1)$$

where C_0 is the initial drug concentration (mol/L), C_∞ is the drug concentration at the equilibrium state (mol/L), M_w is the molecular weight of the theophylline (g/mol), V is the volume of the drug loading solution (L), and m_p is the weight of the polymers used in the drug loading experiment (g), respectively. Each loading experiment was repeated three times and the experimental errors were calculated at a 95% confidence interval.

9.2.3 Drug Release

Controlled release experiments of the theophylline were carried out in water at 37°C. The polymers dried after drug loading were merged into a large amount of water kept at 37°C and stirred using a magnetic bar. The drug concentration change was characterized using Varian Cary 300 Bio UV/Vis Spectrophotometer to obtain drug concentration (C_t). The release experiments were stopped until the drug concentration stays constant (C_∞).The power law as shown in the equation (9-2) was widely used to characterize the release mechanism (Brazel et al, 1999).

$$\frac{M_t}{M_\infty} = \frac{C_t V}{C_\infty V} = kt^n \qquad (9\text{-}2)$$

where M_t and M_∞ are the amount of the drug released at time *t* and at the equilibrium state, respectively. The *k* and *n* are the constants. For a sphere, the diffusion coefficient of the theophylline from the polymer into water can be calculated using equation (9-3) (Brannon-Peppas et al, 1990).

$$\frac{M_t}{M_\infty} = 6\left(\frac{Dt}{\pi \cdot r_p^{\,2}}\right)^{1/2} - 3\frac{Dt}{r^2} \qquad (9\text{-}3)$$

where D is the diffusion coefficient and r_p is the initial average radius of the particles. However, the equations (9-2) and (9-3) are only valid when $M_t/M_\infty<0.6$ (Peppas et al, 2000; Brannon-Peppas et al, 1990; Korsmeyer et al, 1984)

9.2.4 Calibration

To quantify the concentration of the drug solutions, the calibration curves of the theophylline in the aqueous solution was obtained and the values of the extinction coefficient (ε) were calculated using Beer's law as shown in the equation (9-4).

$$A = \varepsilon L C \qquad (9\text{-}4)$$

where A is the absorbance (no units, $A = \log_{10} I_0 / I$, I_0: intensity of incoming light; I: intensity of out coming light), ε is the extinction coefficient (mol $l^{-1}cm^{-1}$), L is the length of light path (cm), and C is the concentration of the solution (mol/l), respectively. The length of the light path L of the cuvette used in the present studies was 1 cm.

The calibration curve of the theophylline in the water is shown in Figure 9-1, and the value of the extinction coefficient was obtained from the slope as shown in the figure. With the extinction coefficient, the concentration of the drug solution can be quantitatively measured.

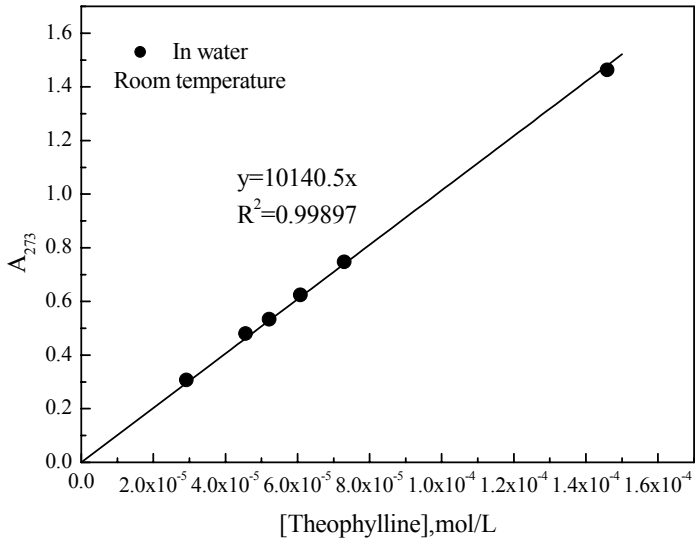

Figure 9-1 Calibration curves of theophylline in water

9.3 Results and Discussion

9.3.1 Drug Loading Capacity

The model drug theophylline was loaded into the highly porous poly(HEMA-MMA), poly(HEMA-St) and poly(HEMA-NVP) particles using concentrated aqueous solution at room temperature. The solubility of the theophylline in water at 25°C is about 6.3g/L as measured in the present studies. It was found that the loading capacity is affected by the network properties, comonomer properties, porous structures and the particle size.

Table 9-2 shows the effect of the particle size on the loading capacity. Two ranges of the particle size were studied. One is the particle size between 75-150μm, and the other one is in the range of 150-180μm. According to Table 9-2, the porous poly(HEMA-MMA) and poly(HEMA-St) have lower loading capacity of the theophylline when using larger particles than when using smaller particles. This is probably because the polymeric networks of the smaller particles can be relaxed faster so that the drugs can diffuse into them faster and more easily. On the other hand, smaller particles give higher specific surface areas so that more drugs could be adsorbed than bigger particles. The loading capacity does not have much difference for the poly(HEMA-St) of different particle size since the polymers are more hydrophobic compared to other polymer particles. Another interesting thing is that the loading capacity is higher for the poly(HEMA-NVP) particles of larger size than those of smaller size. This could be caused by higher NVP content in the larger particles resulting in more efficient absorption of the theophylline.

Table 9-2 Drug loading results using the particles in different size

HEMA (ml)	Comonomer (ml)	EGDMA (mol%)	r_{oct} (ml/ml)	Drug loading (mg/g polymer)	
				75-150 μm	150-180 μm
2	MMA: 12	23	1	105.9±16.0	41.7±5.0
2	St: 12	23	1	47.2±18.6	46.8±11.3
9.4	NVP: 4.7	23	1	20.3±1.9	62.3±15.3

Tables 9-3 through 9-5 show the effect of the crosslinking on the drug loading using different porous polymer particles for particle size of 150-180 μm. Under higher HEMA content, for poly(HEMA-MMA) and poly(HEMA-St), the drug loading is lowered at higher EGDMA concentration because the pore volume is lowered and the polymeric networks are hard to be relaxed. It seems that the presence of the pores have great effects on the drug loading because higher drug loading was observed at higher EGDMA concentration and lower HEMA contents for the poly(HEMA-MMA)

and poly(HEMA-St). The pore volume is higher and there are more pores under these conditions. The porous poly(HEMA-NVP), with higher EGDMA concentration results in higher drug loading. The pore volume for these two polymer samples as shown in Table 9-5 are similar, however, the porous surface area is much higher at higher EGDMA concentration because of the presence of more discrete structures. This is helpful to enhance the absorption of the drugs into the networks. In addition, NVP conversion is higher at higher EGDMA concentration so that the hydrophilic content is higher in polymers which are good for absorbing hydrophilic drugs like theophylline.

Table 9-3 Drug loading results using porous poly(HEMA-MMA) particles at different EGDMA molar concentration

HEMA(ml)	MMA(ml)	EGDMA(mol%)	r_{oct}	Drug loading (mg/g polymer)
9.4	4.7	8	1	41.5±9.5
9.4	4.7	18	1	22.4±1.0
2	12	3	1	14.1±5.2
2	12	23	1	41.7±5.0

Table 9-4 Drug loading results using porous poly(HEMA-St) particles at different EGDMA molar concentration

HEMA(ml)	St(ml)	EGDMA(mol%)	r_{oct}	Drug loading (mg/g polymer)
9.4	4.7	18	1	39.0±5.7
9.4	4.7	23	1	34.6±1.3
2	12	3	1	40.0±5.7
2	12	23	1	46.8±11.3

Table 9-5 Drug loading results using porous poly(HEMA-NVP) particles at different EGDMA molar concentration

HEMA(ml)	NVP(ml)	EGDMA(mol%)	r_{oct}	Drug loading (mg/100g polymer)
9.4	4.7	18	1	15.9±2.5
9.4	4.7	23	1	62.3±15.3

The effect of the monomer ratio on the drug loading was studied as shown in Tables 9-6 through 9-8. According to Table 9-6 and Table 9-7, although HEMA is a hydrophilic monomer, its presence does not mean that the drug loading must be higher. These results are very different from those reported by Brazel et al (1999). For the porous poly(HEMA-MMA) and poly(HEMA-St), the pore volume keeps deceasing greatly with an increase in the HEMA contents. The effect of the porous structures is even greater than the effect of the polymer compositions so that the drug loading is lowered at higher HEMA contents in the presence of the highly porous structures even though hydrophilic HEMA is favorable to absorb theophylline. However, this is the same if a more hydrophilic component is

present, such as NVP. Therefore, it can be concluded that the porous structures have greater effect on the drug loading of the porous HEMA copolymer particles.

Table 9-6 Drug loading results using porous poly(HEMA-MMA) particles at different monomer ratios

HEMA(ml)	MMA(ml)	EGDMA(mol%)	r_{oct}	Drug loading (mg/g polymer)
2	12	23	1	41.7±5.0
7	7	23	1	32.4±5.5

Table 9-7 Drug loading results using porous poly(HEMA-St) particles at different monomer ratios

HEMA(ml)	St(ml)	EGDMA(mol%)	r_{oct}	Drug loading (mg/g polymer)
2	12	23	1	46.8±11.3
9.4	4.7	23	1	34.6±1.3

Table 9-8 Drug loading results using porous poly(HEMA-NVP) particles at different monomer ratios

HEMA(ml)	NVP(ml)	EGDMA(mol%)	r_{oct}	Drug loading (mg/g polymer)
7	7	23	1	101.4±29.5
9.4	4.7	23	1	62.3±15.3

However, for the polymers having identical compositions, the different pore volume leads to different drug loading results. This could be seen from Table 9-9 which shows the effect of the porogen volume ratio on the drug loading capacity of these three polymer particles. Higher porogen volume ratio means higher pore volume or more pores as reported in the previous chapters, resulting in higher drug loading as a result of the presence of more pores.

Table 9-9 Drug loading results using porous HEMA copolymeric particles synthesized at different porogen volume ratios; HEMA/Comonomer=9.4ml/4.7ml; EGDMA=23mol%

Comonomer(ml)	r_{oct}	Drug loading (mg/g polymer)
MMA	0.5	13.5±3.5
	1	27.3±1.0
St	0.5	29.4±1.4
	1	34.6±1.3
NVP	0.5	27.2±5.8
	1	62.3±15.3

All in all, the drug loading capacity of the polymers can be controlled by the introduction of the different compositions and porous characteristics. The comonomer of HEMA makes the polymers' drug loading capacity sensitive to the porous structures, whereas the more hydrophilic one, NVP, is sensitive to the hydrophilic content. For these three polymers, poly(HEMA-NVP) has relatively higher loading capacity and poly(HEMA-MMA) has relatively lower drug loading capacity. Poly(HEMA-St) has relatively higher loading capacity than poly(HEMA-MMA) because of the

presence of higher pore volume. On the other hand, according to the reported drug loading capacity of theophyllline using non-porous poly(HEMA) (3mg/g polymer) (Kim et al, 1992), poly(HEMA-MMA) (0.8mg/g polymer) (Brazel et al, 1999) and poly(HEMA-NVP) (50-60mg/g polymer) (Korsmeyer et al, 1984), the drug loading capacity of the porous polymeric particles can be controlled by the pores over a wide range from lower loading capacity to much higher loading capacity. This is very significant for the drug controlled release.

9.3.2 Drug Release

The drug release kinetics was studied under different conditions, including different particle size, different network properties and different porous characteristics. The power law shown in the equation (9-2) was used to study the diffusion mechanisms. The diffusion coefficient was estimated using the equation (9-3). The average particle size in the range of 75-150μm and 150-180μm was used in the calculation. It is well known that the swelling-controlled release system exhibits the release behaviors ranging from Fickian to Case II diffusion characterized by the values of *n* in the equation (9-2) (Fan et al, 1989). The values of n are different for the release systems with the various geometries as shown in Table 9-10 .

Table 9-10 Values of *n* for the release systems with the various geometries

	Thin Film	Cylinder	Sphere	Diffusion Mechanism	References
n	0.5	0.45	0.43	Fickian diffusion	Siepmann et al, 2001
	0.5<n<1	0.45<n<0.89	0.43<n<0.85	Anomalous diffusion	Siepmann et al, 2001
	1	0.89	0.85	Pseudo-case II diffusion	Siepmann et al, 2001
	n>1			Pseudo-super-case II diffusion	Fan et al, 1989

The meanings of the different diffusion mechanisms are (Alfrey et al, 1966),

- Fickian diffusion: diffusion rate << relaxation rate
- Case II (relaxation-balanced diffusion): diffusion rate >> relaxation rate
- Anomalous diffusion: diffusion and relaxation rates are comparable.

9.3.2.1 Effect of Particle Size

Different average particle size has an effect on the controlled release of the model drug. Figure 9-2 through Figure 9-4 show the effect of the particle size on the drug release using the three highly

porous copolymer particles. It can be seen that the presence of the comonomers with different properties results in different release behaviors using the particles of various sizes. Some repeated experiments were also shown.

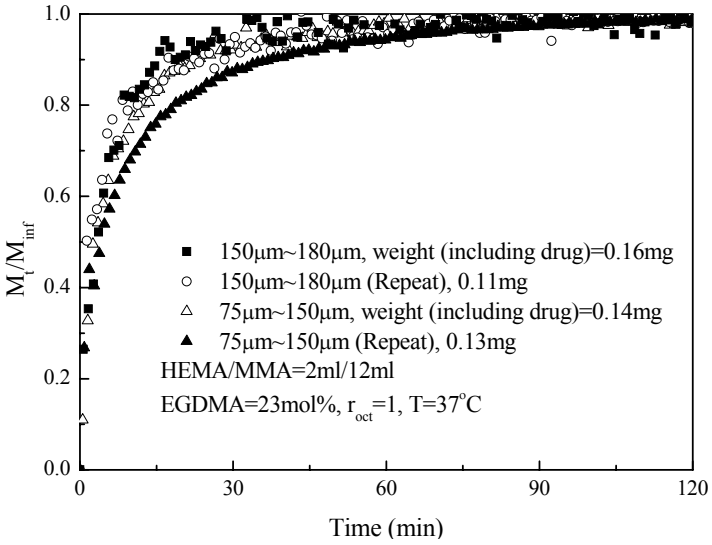

Figure 9-2 The effect of the particle size on the controlled release of theophylline from the highly porous poly(HEMA-MMA) particles

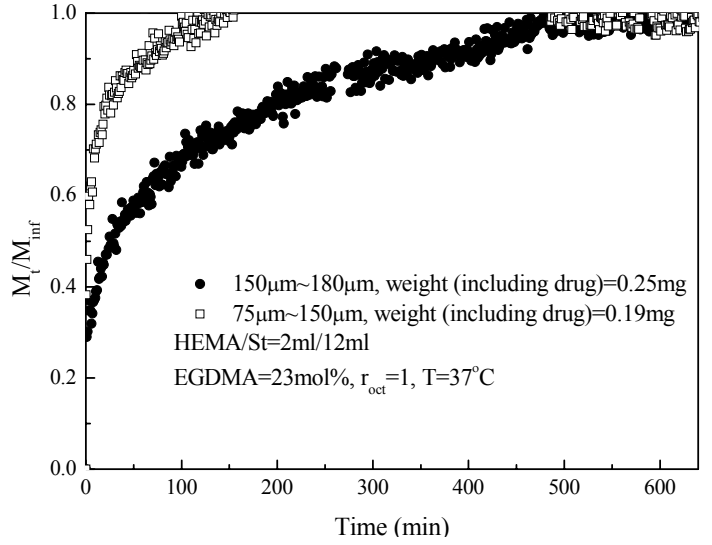

Figure 9-3 The effect of the particle size on the controlled release of theophylline from the highly porous poly(HEMA-St) particles

According to Figure 9-2 through Figure 9-4, the drug release shows similar behaviors for different particle size for each type of the polymer particles. For poly(HEMA-MMA) and poly(HEMA-NVP),

it can be seen that smaller particles show a little faster release at the beginning of the release process. Then the release is a little faster for larger particles. This is probably caused by the presence of the pores. The smaller particles can be swollen by water more quickly, but larger ones have higher pore volume so that more drugs will be released quicker once the networks are relaxed. However, poly(HEMA-St) shows much faster release for smaller particles than for larger particles because poly(HEMA-St) chains take a longer time to be relaxed and the pore size is small. The exponent *n*, the diffusion coefficient *D*, as well as R^2 and fitting errors are shown in Table 9-11.

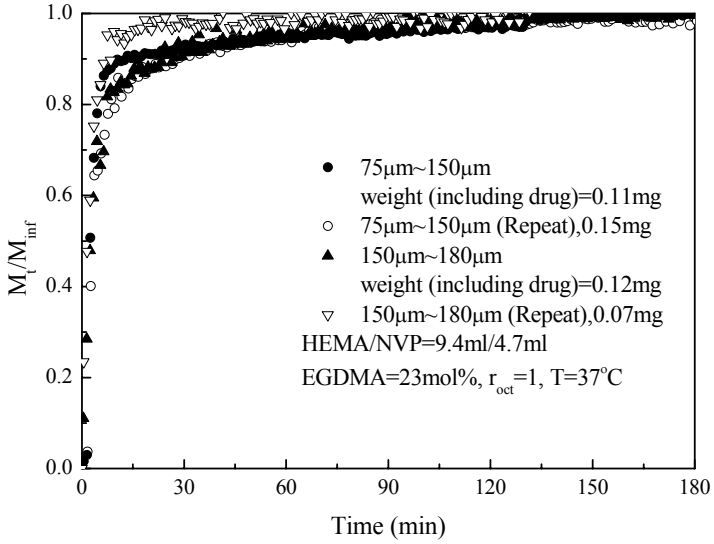

Figure 9-4 The effect of the particle size on the controlled release of theophylline from the highly porous poly(HEMA-NVP) particles

Table 9-11 Diffusional exponents n, drug diffusion coefficients D and initial normalized drug release rate of the particles in different sizes, EGDMA=23mol%

Sample	poly(HEMA-MMA)[a]		poly(HEMA-St)[a]		poly(HEMA-NVP)[b]	
Particle size, μm	75-150	150-180	75-150	150-180	75-150	150-180
n	0.57±0.08 (R^2=0.970)	0.56±0.06 (R^2=0.994)	0.24±0.03 (R^2=0.999)	0.22±0.01 (R^2=0.964)	0.81±0.05 (R^2=0.997)	0.88±0.01 (R^2=0.987)
k	0.25±0.03 (R^2=0.970)	0.25±0.02 (R^2=0.994)	0.45±0.01 (R^2=0.999)	0.25±0.01 (R^2=0.964)	0.22±0.01 (R^2=0.997)	0.23±0.01 (R^2=0.987)
D ($\times 10^9 cm^2/min$)	8.68±1.22 (R^2=0.943)	17.5±0.32 (R^2=0.992)	15.3±1.93 (R^2=0.955)	3.75±0.20 (R^2=0.940)	9.54±1.37 (R^2=0.944)	28.5±2.53 (R^2=0.989)

a: HEMA/comonomer=2ml/12ml; b: HEMA/NVP=9.4ml/4.7ml

According to Table 9-11, the drug diffusion coefficients are higher for the particles of larger size which implies that the diffusion rate of theophylline is higher for larger particles because of the

higher pore volume. The constants *k* and *n* are dependent on the systems and geometries. Therefore, *k* shows a little difference resulting from the different polymer systems and the particle size. The constant *n* is very important to characterize the different release mechanisms. Basically, the values of *n* are independent of the particle size. This means the diffusion mechanisms are not related to the particle size.

For the same particle size, different polymeric particles show different diffusion mechanisms. For poly(HEMA-MMA), the diffusion is an anomalous diffusion according to the *n* values. This implies that the diffusion rate and the relaxation rate are comparable. This is different from the diffusion of theophylline from a non-porous poly(HEMA-MMA) film (Brazel et al, 1999). For poly(HEMA-St) particles, the values of *n* are even less. Since the pore size of poly(HEMA-St) is much smaller and the networks take a longer time to become relaxed, the diffusion rate is lowered for larger particles. The diffusion of the drug from poly(HEMA-NVP) follows an anomalous or case II diffusion according to the values of *n*. Poly(HEMA-NVP) is more hydrophilic so that the swelling of the polymer is faster. The faster swelling and the presence of the pores increase the diffusion rate greatly.

Generally speaking, different particle size results in a little different diffusion rate at the beginning of the release process. However, the diffusion mechanisms are independent of the particle size. In the following sections, in order to examine the different reaction parameters for the drug release, an identical particle size range, 150-180μm, was used.

9.3.2.2 Effect of EGDMA Concentration

Figure 9-5 through Figure 9-7 show the effect of the EGDMA concentration on the drug release from these three types of the highly porous polymer particles. It can be seen that a lower EGDMA molar concentration results in a faster release rate because the networks could undertake relaxation faster at lower crosslink density. On the other hand, the pore size is smaller at higher EGDMA concentration according to the previous chapters. This will slow down the drug release as well. Since NVP is very hydrophilic, the poly(HEMA-NVP) relaxes much faster than the other two polymers. Therefore, the release lasts longer for poly(HEMA-MMA) and poly(HEMA-St). Some repeated experiments can be found in the figures. To understand the drug diffusion process, the diffusional exponent *n* and the drug diffusion coefficients *D* were calculated as shown in Table 9-12.

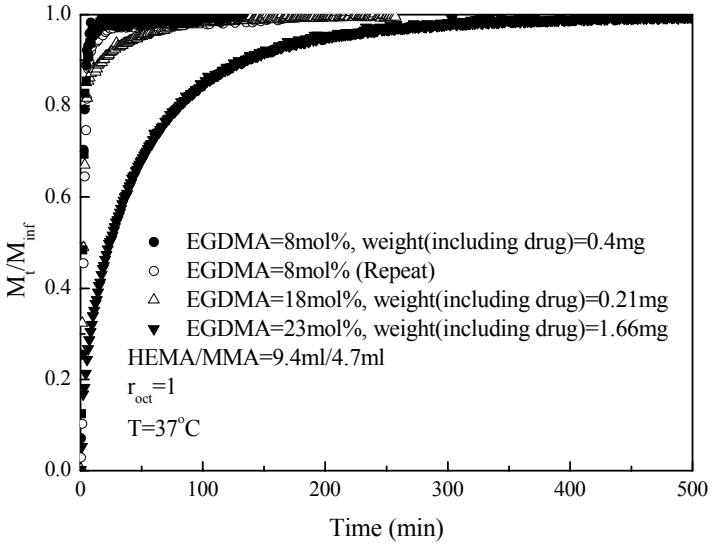

Figure 9-5 The effect of the EGDMA concentration on the controlled release of theophylline from the highly porous poly(HEMA-MMA) particles

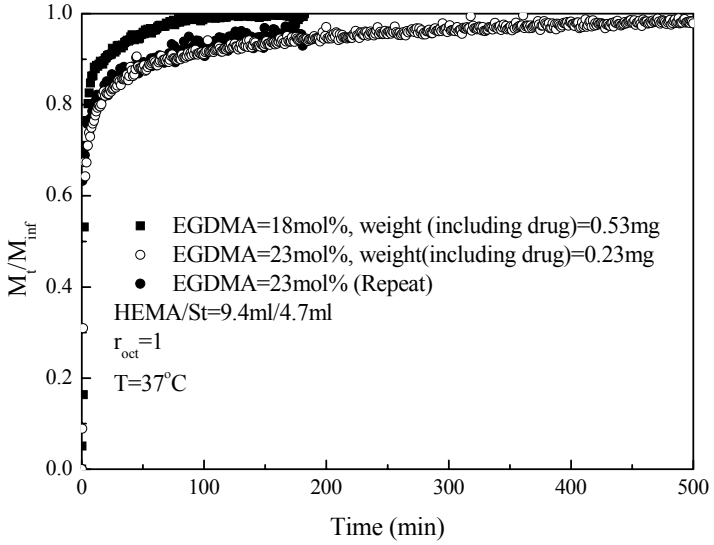

Figure 9-6 The effect of the EGDMA concentration on the controlled release of theophylline from the highly porous poly(HEMA-St) particles

According to Table 9-12, the diffusion mechanism for the porous particles synthesized at lower EGDMA concentration is close to the case II diffusion according to the values of *n*. It can be seen that some values of *n* are greater than 1 which is a behavior characteristic of super case II diffusion. However, some researchers pointed out that this is the result of the spherical geometry and not super case II diffusion (Lee et al, 1992). At lower EGDMA concentration, the rapid network relaxation and the presence of the pores greatly enhance the drug release. At higher EGDMA concentration, the

diffusion becomes anomalous diffusion or Fickian diffusion because of the presence of much smaller pores, the decreased pore volume and the higher crosslink density. It is well known that the constant velocity of an advancing front forms the boundary between a swollen shell and a glassy core in case II diffusion (Kuipers et al, 1993). Therefore, at lower EGDMA concentration, the drug is released constantly as the boundary moves inside at a constant velocity. However, the release is pretty fast occurring with the first several minutes. Except for the burst effect, a critical solvent concentration must be reached before case II diffusion occurs (Lasky et al, 1988). At higher EGDMA concentration, the diffusion tends to be anomalous diffusion as shown in Table 9-12. The pore size and the pore volume are much smaller at higher EGDMA concentration than those at moderate EGDMA concentration. The smaller mesh size and pore size will slow down the diffusion of the drug (Brazel et al, 1999) and the network relaxation is slowed down as well so that the diffusion tends to be anomalous diffusion or Fickian diffusion.

Table 9-12 Diffusional exponents n and drug diffusion coefficients D at different EGDMA concentration, r_H=9.4ml/4.7ml, particle size 150-180μm, r_{oct}=1

Sample	poly(HEMA-MMA)			poly(HEMA-St)		poly(HEMA-NVP)	
EGDMA, mol%	8	18	23 (250μm)	18	23	18	23
n	1.87±0.20 (R^2=0.995)	0.81±0.04 (R^2=0.999)	0.48±0.004 (R^2=0.999)	1.22±0.27 (R^2=0.974)	0.82±0.13 (R^2=0.982)	0.87±0.22 (R^2=0.967)	0.77±0.29 (R^2=0.954)
k	0.13±0.02 (R^2=0.995)	0.23±0.07 (R^2=0.999)	0.11±0.001 (R^2=0.99)	0.18±0.05 (R^2=0.974)	0.27±0.04 (R^2=0.982)	0.32±0.05 (R^2=0.967)	0.30±0.10 (R^2=0.954)
D ($\times10^9$cm^2/min)	77.4±2.83 (R^2=0.873)	20.3±2.18 (R^2=0.983)	5.80±0.03 (R^2=0.998)	27.8±8.54 (R^2=0.833)	26.4±6.61 (R^2=0.906)	35.8±7.81 (R^2=0.915)	36.4±6.15 (R^2=0.932)

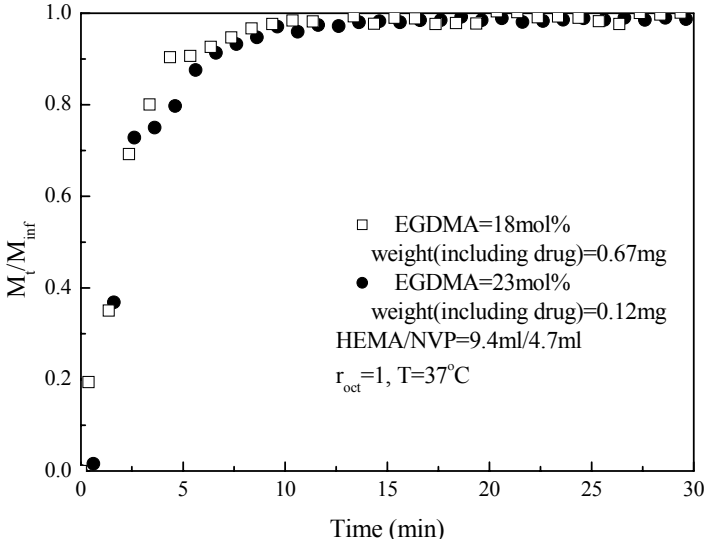

Figure 9-7 The effect of the EGDMA concentration on the controlled release of theophylline from the highly porous poly(HEMA-NVP) particles

Generally speaking, in the controlled release, a kinetic zero-order release (Case II) is preferred because the release rate is constant for a zero-order release. According to the above discussion, the particles synthesized at moderate EGDMA concentration under a monomer ratio of 2 can generate case II diffusion.

9.3.2.3 Effect of Monomer Ratio

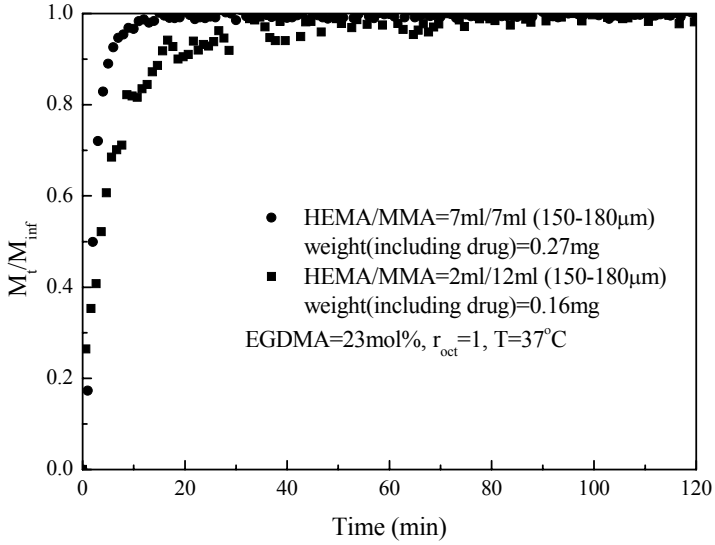

Figure 9-8 The effect of the monomer ratio on the controlled release of theophylline from the highly porous poly(HEMA-MMA) particles

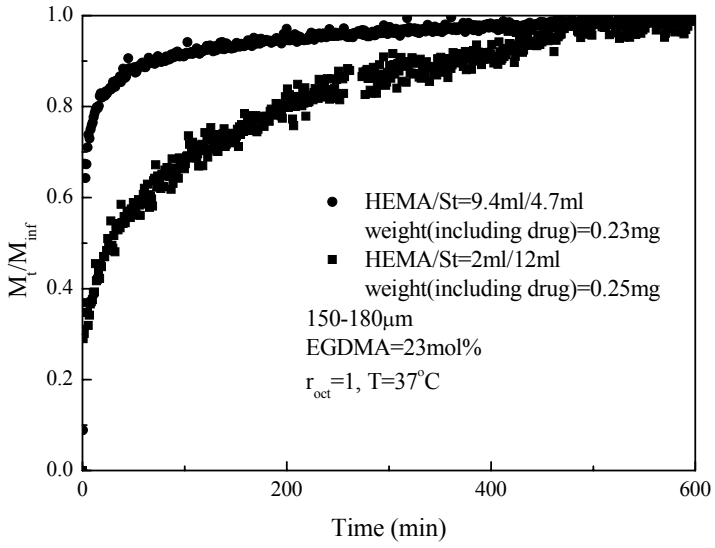

Figure 9-9 The effect of the monomer ratio on the controlled release of theophylline from the highly porous poly(HEMA-St) particles

At different monomer ratios, the controlled release behaviors for the polymers are different since the properties of MMA, St and NVP are different. The drug release is faster for the polymers synthesized at a higher monomer ratio (higher HEMA content) for poly(HEMA-MMA) and poly(HEMA-St). As a hydrophilic monomer, higher HEMA content increases the interaction between the polymer chains and the water so that the relaxation of the networks is faster to accelerate the diffusion rate. Due to the presence of the pores, the diffusion rate is much faster. Therefore, the diffusion mechanism changes from Fickian diffusion to Non-Fickian diffusion according to the values of *n* as shown in Table 9-13. The results are similar to those obtained when using nonporous poly(HEMA-MMA) polymers (Brazel et al, 1999).

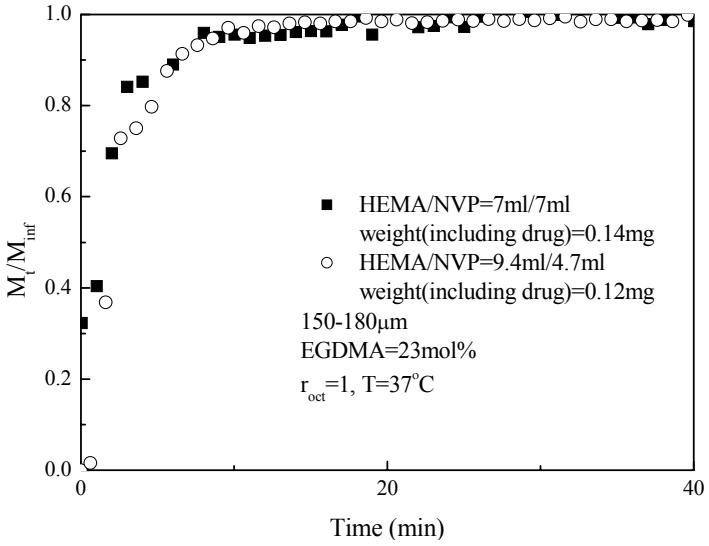

Figure 9-10 The effect of the monomer ratio on the controlled release of theophylline from the highly porous poly(HEMA-St) particles

Poly(HEMA-NVP) shows a little different behavior. At the beginning of the release, the release rate seems faster for the polymer synthesized with higher NVP content. According to Chapter 7, higher HEMA content result in higher conversion of NVP. Higher NVP content makes the relaxation of the polymer faster which enhances the drug diffusion. If NVP content is higher, more PNVP is polymerized during the later stage of the reaction. Therefore, a glassy core could be formed consisting mainly of HEMA and EGDMA. During the release, PNVP segments will be relaxed earlier to release drugs first and then the glassy core will be relaxed slowly. Table 9-13 shows the calculated results of the diffusional exponent *n* and drug diffusion coefficient *D*. Diffusion mechanisms for the drug release in poly(HEMA-NVP) exhibits anomalous diffusion. Therefore, although the pore volume is decreased with an increase in the HEMA content, the hydrophilic content has a greater effect on the

drug release than the porous structures in the presence of a hydrophilic comonomer. Generally speaking, higher HEMA content could make a better drug release system which performs close to zero-order release behavior.

Table 9-13 Diffusional exponents n and drug diffusion coefficients D at different monomer ratios, EGDMA=23mol%, r_{oct}=1

Sample	poly(HEMA-MMA)		poly(HEMA-St)		poly(HEMA-NVP)	
Monomer ratio, ml/ml	2/12	7/7	2/12	9.4/4.7	7/7	9.4/4.7
n	0.47±0.06 (R^2=0.986)	1.16±0.15 (R^2=0.991)	0.22±0.01 (R^2=0.964)	0.69±0.13 (R^2=0.971)	0.66±0.07 (R^2=0.995)	0.77±0.29 (R^2=0.954)
k	0.28±0.02 (R^2=0.986)	0.21±0.03 (R^2=0.991)	0.25±0.01 (R^2=0.964)	0.27±0.04 (R^2=0.971)	0.42±0.02 (R^2=0.995)	0.30±0.10 (R^2=0.954)
D ($\times 10^9 cm^2/min$)	17.8±9.22 (R^2=0.985)	29.8±8.35 (R^2=0.859)	3.75±0.20 (R^2=0.940)	26.7±4.17 (R^2=0.940)	52.5±4.28 (R^2=0.984)	36.4±6.15 (R^2=0.932)

9.3.2.4 Effect of Porogen Volume Ratio

As discussed in the previous chapters, the polymers synthesized at higher porogen volume ratios show higher porosity and more pores. Therefore, the presence of more pores must have a significant effect on the drug release.

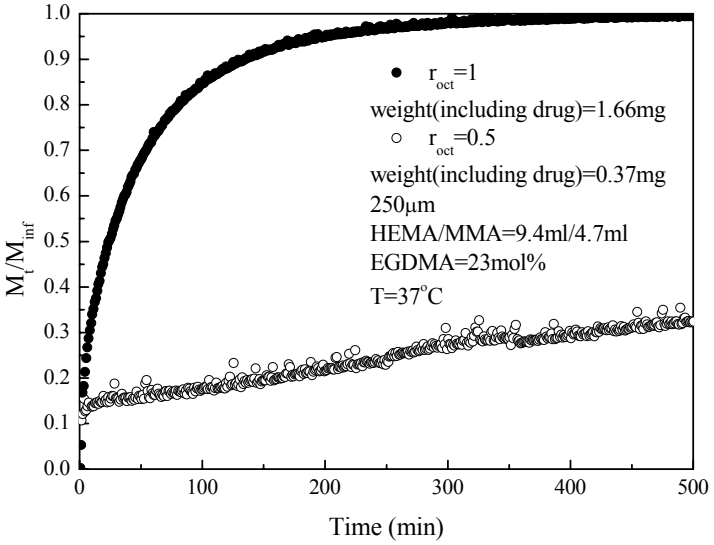

Figure 9-11 The effect of the porogen volume ratio on the controlled release of theophylline from the highly porous poly(HEMA-MMA) particles

Figure 9-11 through Figure 9-13 show the theophylline release behaviors using these porous particles synthesized at different porogen volume ratios. It can be seen that the porous particles synthesized at higher porogen volume ratio have faster drug release rate than those synthesized at lower porogen

volume ratio, especially for the porous poly(HEMA-MMA) and poly(HEMA-St). Therefore, the presence of more pores can accelerate the diffusion of the drug into the water. However, it seems that the porogen volume ratio does not have a very significant effect on the drug release using porous poly(HEMA-NVP) particles. This is probably caused by the strong hydrophilicity of the comonomer NVP. To understand the diffusion mechanisms, the exponent *n* was calculated as shown in Table 9-14. Poly(HEMA-MMA) shows a slower release rate than the others since the particle size of poly(HEMA-MMA) synthesized under the reaction conditions is over 250μm.

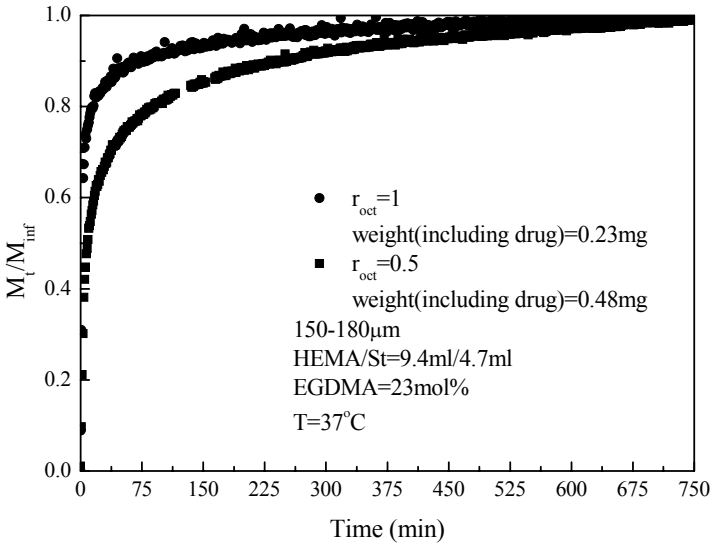

Figure 9-12 The effect of the porogen volume ratio on the controlled release of theophylline from the highly porous poly(HEMA-St) particles

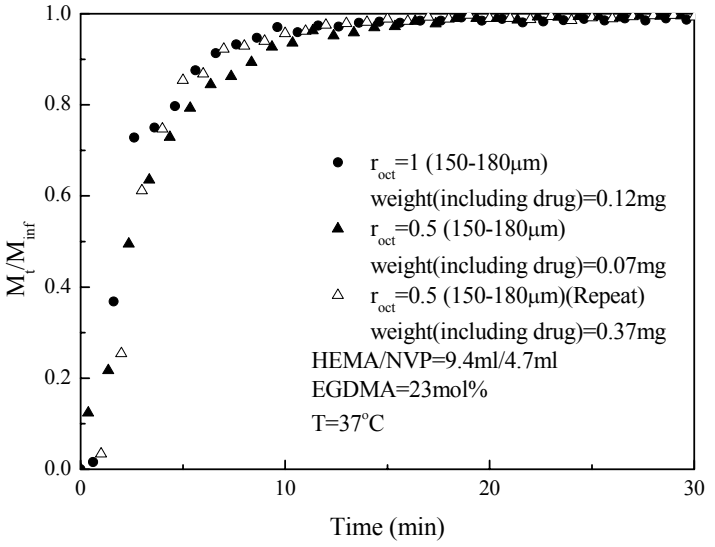

Figure 9-13 The effect of the porogen volume ratio on the controlled release of theophylline from the highly porous poly(HEMA-NVP) particles

Table 9-14 Diffusional exponents n, drug diffusion coefficients D and initial normalized drug release rate (mg/mg/h) at different porogen volume ratios, r_H=9.4ml/4.7ml, EGDMA=23mol%

Sample	poly(HEMA-MMA)[a]		poly(HEMA-St)[b]		poly(HEMA-NVP)[b]	
r_{oct}	0.5	1	0.5	1	0.5	1
n	0.47±0.001 (R^2=0.996)	0.48±0.004 (R^2=0.999)	0.62±0.06 (R^2=0.980)	0.69±0.13 (R^2=0.971)	0.75±0.09 (R^2=0.978)	0.77±0.29 (R^2=0.954)
k	0.02±0.001 (R^2=0.996)	0.11±0.001 (R^2=0.999)	0.14±0.02 (R^2=0.980)	0.27±0.04 (R^2=0.971)	0.24±0.03 (R^2=0.978)	0.30±0.10 (R^2=0.954)
D ($\times 10^9 cm^2/min$)	0.12±0.02 (R^2=0.992)	5.80±0.03 (R^2=0.998)	7.35±0.48 (R^2=0.967)	26.7±4.17 (R^2=0.940)	27.8±0.72 (R^2=0.997)	36.4±6.15 (R^2=0.932)

a: 250μm; b: 165μm

According to Table 9-14, the diffusion behaviors are similar for each polymer synthesized at different porogen volume ratios. The only difference is in the diffusion coefficients. This suggests again that the porogen volume ratio has effects on the diffusion rate instead of changing diffusion mechanism. Therefore, through adjusting the porogen volume ratio, the diffusion rate could be controlled for these polymers.

9.4 Summary

The model drug theophylline was used to study the nature of controlled release from porous poly(HEMA-MMA), poly(HEMA-St) and poly(HEMA-NVP) particles in the present studies. It was found that the network properties and the presence of the pores play an important role on the controlled release process.

The drug loading capacity of the polymers can be controlled by the introduction of the different comonomer of HEMA and porous structures. A hydrophobic comonomer of HEMA, such as MMA and St, makes the polymers' drug loading capacity sensitive to the porous structures, whereas the stronger hydrophilic one than HEMA, such as NVP, is sensitive to the polymer compositions. Poly(HEMA-St) has higher loading capacity than poly(HEMA-MMA) because of the higher pore volume. The porous poly(HEMA-MMA) and poly(HEMA-St) have lower loading capacity of the theophylline in the larger particles than those for the smaller particles. The loading capacity is higher for the poly(HEMA-NVP) particles of larger size than those of smaller size. For poly(HEMA-MMA) and poly(HEMA-St), the drug loading is lowered at higher EGDMA concentration. However, for the porous poly(HEMA-NVP), higher EGDMA concentration results in higher drug loading. The highly porous particles synthesized at higher porogen volume ratio have higher drug loading.

Different average particle size has little effect on the diffusion mechanisms of the controlled release of the model drug, but smaller particles result in a little faster release at the beginning. Larger particles have a higher diffusion coefficient because of a higher pore volume. The particles synthesized at moderate EGDMA concentration under a monomer ratio of 2 are good for the controlled release. Although the pore volume is decreased with an increase in the HEMA content, the hydrophilic contents have a greater effect on the drug release than for the porous structures. Generally speaking, higher HEMA contents could provide a better drug release system which performs close to zero-order release behavior. Through adjusting the porogen volume ratio, the diffusion rate could be controlled for these polymers.

Chapter 10
Conclusions and Recommendations

10.1 Conclusions

HEMA was copolymerized with MMA, St and NVP using EGDMA as a crosslinker and using 1-octanol as porogen to synthesize highly porous polymeric particles by free radical suspension copolymerization initiated by the oil-soluble initiator AIBN. The resultant polymers show good porous structures and good particle morphology under certain reaction conditions. It was found that the porous characteristics and the swelling properties can be well controlled by the various reaction parameters. The gel formation and the porous characteristics were simulated using mathematical models combined with the reaction kinetics and the thermodynamics. The model can be used to predict the gel fraction in the reaction systems of HEMA and the comonomers. The model also can predict the maximum porosity after the porous particle preparation. Furthermore, it proves that the porous structures are collapsed or shrunk to a certain level during porogen removal. In the application part, the synthesized porous particles were used in the controlled release of the model drug, theophylline. The drug loading dose can be controlled over a wide range with the help of the porous structures, which is much better than previously reported results. The release process shows different behaviors for the different porous particles synthesized under different conditions. Zero-order release behavior can be obtained using some porous particles. Therefore, this work shows good connectivity from the polymer synthesis to the applications. Major conclusions are made as follows:

1) Synthesis technique

- Through the literature survey, the suspension copolymerization was regarded as a relativly good technique to synthesize the highly porous polymeric particles, especially for the porous particles used in medical or pharmaceutical areas. Even though hydrophilic components were used in the reactions, such as HEMA and NVP, suspension copolymerization were still applicable in the presence of the hydrophobic comonomer and the water-insoluble solvent because they decrease the solubility of HEMA and NVP in the aqueous phase greatly according to the present studies.

2) Porous poly(HEMA-MMA) particles

- The porous poly(HEMA-MMA) particles have good particle morphology under higher MMA content or at higher EGDMA concentration. The average particle size is larger at

higher EGDMA concentration. However, further increase in the EGDMA concentration results in more particle aggregates.

- The porous structures of the porous poly(HEMA-MMA) particles can be controlled at various EGDMA molar concentrations, porogen volume ratios and monomer ratios of HEMA to MMA in the present studies. The pores in a diameter which is less than 100nm were obtained. The specific porous surface area was between 5-100m^2/g. The pore formation shows the mechanisms of χ-induced syneresis and ν-induced synerisis. The maximum pore volume and porosity were observed over the range of the EGDMA monomer concentration (3mol%~23mol%) at lower (2ml/12ml) and higher (9.4ml/4.7ml) monomer ratios. The highest pore volume and porosity occurred at a modest EGDMA concentration (8mol%). At the highest EGDMA concentration, there are more pores and the particle surface is more heterogeneous as a result of the more discrete structures. In the present studies, the porous surface area varies between 10-100m^2/g with an increase in the EGDMA molar concentration. The collapse or the shrinkage of the pores occurs during solvent removal, especially at lower EGDMA concentration. The porosity and the pore volume are reduced with an increase in the HEMA contents. The specific porous surface area increases with an increase in the monomer ratio. The average pore size does not change too much at various monomer ratios. With an increase in the porogen volume ratios, the maximum values of the porosity and the pore volume were observed and more pores are generated at higher porogen volume ratios. The average pore size is smaller at lower porogen volume ratio. At higher porogen volume ratios, shrinkage of the particles and irregular particles were observed.

- Gel formation and porosity were simulated using mathematical models. The gel point occurs earlier at higher EGDMA concentration or under higher HEMA contents. The non-solvents which have larger values of the Flory interaction parameter could enhance the phase separation. The highly porous structures can be obtained no matter whether in good solvents or in non-solvents at certain high crosslinking. The simulation results show the real porosity or the maximum porosity during the formation of the pores so that the simulation results over-estimated the experimental results. In the real experiments, the shrinkage and the collapse of the pores are the main reasons resulting in the difference between the simulation results and the experimental results.

3) Porous poly(HEMA-St) particles

- The porous poly(HEMA-St) particles have better particle morphology than poly(HEMA-MMA) and poly(HEMA-NVP). Good particle morphology can be obtained at higher EGDMA concentration or under higher styrene content. The average particle size tends to be smaller with an increase in the HEMA contents at lower EGDMA concentration. The particle size distribution is more uniform or narrower under higher porogen concentration.

- The porous structures of the porous poly(HEMA-St) particles can be controlled at various EGDMA molar concentrations, porogen volume ratios and the monomer ratios of HEMA to St in the present studies. Pores with a diameter which is less than 100nm were obtained. The specific porous surface area was between 5-100m^2/g. Generally speaking, higher styrene content or higher EGDMA concentration leads to better particle morphology. Lower HEMA content gives larger pores. Higher EGDMA concentration results in smaller pores and higher 1-octanol volume ratio leads to more pores.

- According to the simulation and kinetic experiments, the reaction rate is much faster and the reaction conversion is higher at higher EGDMA concentration than those at lower EGDMA concentration for the poly(HEMA-St) system. The gel point occurs later at lower EGDMA concentration. The molecular weight between the successive crosslinks and the volume swelling ratio of the polymers in 1-octanol are decreased with an increase in the EGDMA molar concentration. For the porous structures, similar to that of poly(HEMA-MMA), the change of the porosity and the pore volume demonstrates the maximum values in the range of the EGDMA concentration. The specific porous surface area, between 1-100m^2/g, increases with an increase in the EGDMA molar concentration although it deceases a little bit under higher EGDMA concentration (such as 23mol%). Higher EGDMA concentration results in more heterogeneous structures. The average pore size becomes smaller with an increase in the EGDMA concentration.

- At lower monomer ratios (higher styrene content), the reaction rates are faster for the poly(HEMA-St) system. However, the reaction conversion at 4 hours is lower under higher HEMA content than that under lower HEMA content. The time for the onset of the gelation has little difference at various monomer ratios. But the gel fraction grows faster under higher HEMA content. Styrene, as a hydrophobic comonomer, enhances the

formation of the pores so that there are more heterogeneous structures under higher styrene content. The pore volume and the porosity are decreased over the range of the monomer ratio. The specific porous surface area, between 5-100m^2/g, goes down with an increase in the HEMA contents, which is different from the porous poly(HEMA-MMA) particles. At the lower EGDMA concentration, the major pore size distributions at higher HEMA content are much smaller than 10 nm which could be very close to the mesh size between two crosslinks. The average pore size is larger for the polymers synthesized under lower styrene content because the porous structures are collapsed during the porogen removal.

- For the poly(HEMA-St) system, the pore volume does not change too much at various porogen volume ratios at lower EGDMA concentration. At higher EGDMA concentration, the pore volume and the porosity are increased with an increase in the porogen volume ratio. There are more pores at higher porogen volume ratios so that the specific surface area increases with an increase in the porogen volume. Increasing the amount of solvent will increase the pore volume within certain limits without changing the pore size distribution very much. The porosity change in different solvents with different thermodynamic quality under certain reaction conditions was simulated. The onset of the phase separation occurs later with a decrease in the values of the interaction parameters because the polymers can be swollen much more in a good solvent. Therefore, good solvents result in lower porosity and poor solvents results in higher porosity. At certain high crosslink density, the highly porous structures can be formed in both good solvents and poor solvents.

4) Porous poly(HEMA-NVP) particles

- Porous poly(HEMA-NVP) particles have good particle morphology at higher EGDMA concentration or under higher HEMA content. The average particle size tends to be larger with an increase in the HEMA content at higher EGDMA concentration. The average particle size is smaller at a higher porogen volume ratio.

- According to the studies on the synthesis of the porous poly(HEMA-NVP) particles, the EGDMA molar concentration, the monomer ratio and the porogen volume ratio can control the porous properties and the particle morphology of poly(HEMA-NVP) efficiently. Pores below 100nm were obtained. Since HEMA and EGDMA are much

more reactive than NVP, the HEMA and EGDMA enter into the copolymer much faster than NVP and thus the resultant polymers have a composition very close to that of a PNVP homopolymer in the latter stages of the conversion. The reaction rates for HEMA and EGDMA are very fast, and they are faster under higher concentration. The reaction rate of NVP is slow at the beginning, but it becomes faster after a certain reaction time when the conversion of HEMA and EGDMA reaches certain high levels. The gel point occurs earlier and the gel fraction grows faster at higher EGDMA concentration than those at lower EGDMA concentration. For the porous structures, the transformation of χ-induced syneresis (at low crosslinker concentration) and ν-induced synerisis (at higher crosslinker concentration) can be observed. To produce permanent porous structures and generate good particle morphology, the EGDMA concentration must be at least 8mol%. The porous specific surface area is in the range of 1-50m^2/g. The pore size becomes smaller at higher EGDMA concentration. The reaction rates are faster and the reaction conversions are higher for each monomer at higher monomer ratios of HEMA to NVP. Higher HEMA content is helpful for the conversion of NVP. However, the onset for the occurrence of the gelation is almost the same at various monomer ratios. The porosity and the pore volume are reduced with an increase in the HEMA content. The porosity and the pore volume increase with an increase in the porogen volume ratio. The values of the porous specific surface area are mainly in the range of 50-60 m^2/g. The average pore size becomes larger at higher porogen volume ratios.

5) Swelling

- The swelling process consists of two steps: water fills in the pores and the water swells the polymeric networks. Therefore, the porous structures mainly determine the values of q_w if highly porous structures are present and the properties of polymeric networks determine the volume swelling ratio q_v. The values of q_v and q_w decrease with an increase in the EGDMA molar concentration. The more hydrophilic the comonomer, the greater effect the EGDMA molar concentration has. The EGDMA concentration has the least effect on the q_v values of the poly(HEMA-St) particles, whereas it has the greatest effect on the poly(HEMA-NVP) particles. With regard to the equilibrium weight swelling ratio q_w, generally, it decreases with an increase in the EGDMA concentration as well. But the presence of pores provides more volume for the water to enter the particles. Coupled with

the change of the network properties, the water uptake process is weakened at higher EGDMA concentration. The changes of q_w values correspond to the changes of the porosity or the pore volume for each porous polymeric particle, which means higher porosity or pore volume could lead to higher water uptake for the same polymer. With an increase in the HEMA content, basically, the q_v values are increased for poly(HEMA-MMA) and poly(HEMA-St) because of the presence of more hydrophilic HEMA. The q_w values increase to certain HEMA content, and then decrease a little bit, which implies that the pore volume or the porosity play a more important role under higher HEMA content at higher EGDMA concentration in the presence of a hydrophobic comonomer. However, with an increase in the monomer ratio, the values of q_w and q_v for the porous poly(HEMA-NVP) particles are reduced because NVP is more hydrophilic. The swelling capacity is strengthened at higher temperature because the relaxation of the polymer chains is enhanced at higher temperature.

6) Controlled release

- The drug loading capacity of the polymers can be controlled by the introduction of the different compositions and porous characteristics. Different average particle size has little effect on the diffusion mechanisms of the controlled release of the model drug, but smaller particles result in a little faster release at the beginning. Larger particles have a higher diffusion coefficient because of a higher pore volume. The particles synthesized at moderate EGDMA concentration under a monomer ratio of 2 are good for use in the controlled release. Although the pore volume is decreased with an increase in the HEMA content, the hydrophilic content has greater effect on the drug release than the porous structures. Through adjusting the porogen volume ratio, the diffusion rate could be controlled for these polymers. Generally speaking, higher HEMA content could provide a better drug release system which shows close to zero-order release behavior.

10.2 Recommendations

1) The suspension copolymerization of HEMA copolymeric particles needs to be improved further to make porous particles with good morphology over a wide range of the reaction conditions. First of all, different stabilizers except for PVP could be used in the studies. Differernt ways to minimize the water solubility of the HEMA and other comonomers could

be applied, such as the addition of NaCl into the aqueous phase. In addition, the effect of the agitation speed should be studied to find out better agiation speed to make separated particles. Furthermore, detailed process should be studied to make uniform particles with tailor-made particle size and pore size.

2) Different organic solvents (porogen) can be used in the synthesis to study the most suitable porogen for each type of HEMA copolymeric particles. Different crosslinkers could be used in the synthesis. Further studies could also include the synthesis of the environment-sensitive porous HEMA copolymeric particles.
3) To simulate the gel formation and the porous structures more accurately, real reaction constants must be measured. Mathematical models are needed to simulate the pore size distribution of the porous polymeric materials.
4) More detailed application studies are still needed for controlled release of drugs from the copolymer systems reported in this thesis. It is very important to search for more suitable applications for these porous particles, especially in biomedical and pharmaceutical areas, environmental protection, water treatment as well as separations and uses in the food industry. In the controlled release applications, more hydrophilic drugs with different molecular size should be studied further to find the most suitable hydrophilic drugs for which the present systems could be used.

Appendix I

Experimental Data Shown in Figures

Table I-1 Experimental data of the synthesis of the porous poly (HEMA-MMA) particles at various EGDMA molar concentrations; r_{oct}=1; T=70°C; Agi=500rpm

No.	HEMA (ml)	MMA (ml)	EGDMA (mol%)	Porosity (%)	Pore volume (cm^3/g)	d_2 (g/cm^3)	d_0 (g/cm^3)	S_v (m^2/g)	Average Pore Size (nm)
HM1	2	12	0.6	50.3	0.87	1.17	0.86	10.4	7.0
HM2	2	12	2.8	67.4	1.51	1.15	0.74	22.1	9.4
HM3	2	12	7.9	73.4	2.25	1.22	0.67	56.8	32.2
HM4	2	12	16.7	61.8	1.48	1.24	0.81	65.4	23.2
HM5	2	12	22.3	57.1	1.27	1.24	0.71	57.7	18.8
HM6	9.4	4.7	0.6	8.9	0.08	-	-	-	-
HM7	9.4	4.7	3.0	25.8	0.29	-	-	-	-
HM8	9.4	4.7	8.4	64.5	1.46	1.25	0.85	22.7	46.7
HM9	9.4	4.7	17.7	52.8	0.85	1.32	1.03	42.3	53.1
HM10	9.4	4.7	23.5	46.6	0.50	1.76	0.97	98.3	17.3

Table I-2 Experimental data of the synthesis of the porous poly (HEMA-MMA) particles at various monomer ratios; r_{oct}=1; T=70°C; Agi=500rpm

No.	HEMA (ml)	MMA (ml)	EGDMA (mol%)	Porosity (%)	Pore volume (cm^3/g)	d_2 (g/cm^3)	d_0 (g/cm^3)	S_v (m^2/g)	Average Pore Size (nm)
HM2	2	12	2.8	67.4	1.51	1.15	0.74	22.1	9.4
HM11	4.7	9.4	2.8	54.7	0.95	1.39	1.32	8.7	11.6
HM12	8.4	5.6	2.9	23.4	0.22	1.25	1.04	12.6	16.3
HM7	9.4	4.7	3.0	25.8	0.29	-	-	-	-
HM5	2	12	22.3	57.1	1.27	1.24	0.71	57.7	18.8
HM13	4.7	9.4	22.6	77.4	2.85	1.28	0.67	72.4	19.7
HM14	8.4	5.6	23.4	45.8	0.49	1.71	0.99	80.9	16.5
HM10	9.4	4.7	23.5	46.6	0.50	1.76	0.97	98.3	17.3

Table I-3 Experimental data of the synthesis of the porous poly (HEMA-MMA) particles at various porogen volume ratios; HEMA/MMA=9.4ml/4.7ml; T=70°C; Agi=500rpm

No.	EGDMA (mol%)	r_{oct}	Porosity (%)	Pore volume (cm^3/g)	d_2 (g/cm^3)	d_0 (g/cm^3)	S_v (m^2/g)	Average Pore Size (nm)
HM18	23.5	0.5	20.7	0.21	1.29	1.11	32.3	12.2
HM19	23.5	0.65	66.4	1.23	1.60	1.21	30.5	17.1
HM20	23.5	0.8	53.1	0.91	1.24	0.94	61.0	12.1
HM10	23.5	1	46.6	0.50	1.76	0.97	98.3	17.3

Table I-4 Experimental data of the synthesis of the poly(HEMA-St) at various EGDMA molar concentrations; r_{oct}=1; T=70°C; Agi=500rpm

No.	HEMA (ml)	St (ml)	EGDMA (mol%)	Porosity (%)	Pore volume (cm^3/g)	d_2 (g/cm^3)	d_0 (g/cm^3)	S_v (m^2/g)	Average Pore Size (nm)
HS1	2	12	0.6	56.1	1.18	1.08	0.60	6.19	406
HS2	2	12	2.9	59.7	1.47	1.13	0.46	19.5	243
HS3	2	12	8.4	82.9	4.38	1.11	0.39	56.7	82.6
HS4	2	12	17.5	82.0	3.65	1.25	0.39	99.9	40.4
HS5	2	12	23.3	79.9	3.77	1.15	0.57	94.8	20.8
HS6	9.4	4.7	0.6	41.7	0.45	1.58	1.23	1.93	-
HS7	9.4	4.7	3.0	46.5	0.71	1.22	0.73	9.11	10.7
HS8	9.4	4.7	8.6	70.8	2.01	1.21	0.76	8.30	77.4
HS9	9.4	4.7	18.0	80.4	3.47	1.18	0.60	44.0	39.5
HS10	9.4	4.7	23.9	68.7	1.77	1.24	0.93	28.1	19.3

Table I-5 Experimental data of the synthesis of the porous poly (HEMA-St) particles under various monomer ratios; r_{oct}=1; T=70°C; Agi=500rpm

No.	HEMA (ml)	St (ml)	EGDMA (mol%)	Porosity (%)	Pore volume (cm^3/g)	d_2 (g/cm^3)	d_0 (g/cm^3)	S_v (m^2/g)	Average Pore Size (nm)
HS2	2	12	2.9	59.7	1.47	1.13	0.46	19.5	243
HS11	4.7	9.4	3.0	49.4	0.93	1.10	0.76	22.6	45.6
HS12	7	7	3.0	40.3	0.61	1.12	0.77	14.5	48.6
HS13	8.4	5.6	3.1	34.6	0.45	1.22	0.88	10.6	27.4
HS7	9.4	4.7	3.0	46.5	0.71	1.22	0.73	9.11	10.7
HS5	2	12	23.3	79.9	3.77	1.15	0.57	94.8	20.8
HS14	4.7	9.4	23.4	77.0	3.60	0.95	0.55	71.4	23.7
HS15	7	7	23.8	79.6	3.00	1.30	0.68	42.5	13.2
HS16	8.4	5.6	23.9	73.9	2.40	1.18	0.73	26.0	15.3
HS10	9.4	4.7	23.9	68.7	1.77	1.24	0.93	28.1	19.3

Table I-6 Experimental data of the synthesis of the porous poly (HEMA-St) particles at various porogen volume ratios; HEMA/St=9.4ml/4.7ml; T=70°C; Agi=500rpm

No.	EGDMA (mol%)	r_{oct} (ml/ml)	Porosity (%)	Pore volume (cm^3/g)	d_2 (g/cm^3)	d_0 (g/cm^3)	S_v (m^2/g)	Average Pore Size (nm)
HS19	23.9	0.5	50.4	0.87	1.17	1.04	6.23	30.2
HS20	23.9	0.8	60.1	1.18	1.28	0.89	20.3	32.7
HS10	23.9	1	68.7	1.77	1.24	0.93	28.1	19.3

Table I-7 Experimental data of the synthesis of the poly (HEMA-NVP) at various EGDMA molar concentrations; r_{oct}=1; T=70°C; Agi=500rpm

No.	HEMA (ml)	NVP (ml)	EGDMA (mol%)	Porosity (%)	Pore volume (cm^3/g)	d_2 (g/cm^3)	d_0 (g/cm^3)	S_v (m^2/g)	Average Pore Size (nm)
HN4	9.4	4.7	3.0	19.3	0.19	1.23	1.21	2.38	-
HN5	9.4	4.7	8.6	73.3	1.72	1.60	0.63	19.4	92.1
HN6	9.4	4.7	18.0	68.1	1.55	1.38	0.73	26.6	81.7
HN7	9.4	4.7	23.5	68.5	1.45	1.24	0.72	51.0	44.9

Table I-8 Experimental data of the synthesis of the poly (HEMA-NVP) at various monomer ratios; r_{oct}=1; T=70°C; Agi=500rpm

No.	HEMA (ml)	NVP (ml)	EGDMA (mol%)	Porosity (%)	Pore volume (cm^3/g)	d_2 (g/cm^3)	d_0 (g/cm^3)	S_v (m^2/g)	Average Pore Size (nm)
HN10	4.7	9.4	22.6	71.7	2.37	1.07	0.61	65.4	38.6
HN11	7	7	23.1	68.3	2.22	1.07	0.63	54.2	41.7
HN12	8.4	5.6	23.4	67.3	1.72	1.21	0.97	60.4	37.4
HN7	9.4	4.7	23.5	68.5	1.45	1.24	0.72	51.0	44.9

Table I-9 Experimental data of the synthesis of the poly (HEMA-St) at various porogen volume ratios; HEMA/NVP=9.4ml/4.7ml; [EGDMA]=23.5mol%; T=70°C; Agi=500rpm

No.	r_{oct} (ml/ml)	Porosity (%)	Pore volume (cm^3/g)	d_2 (g/cm^3)	d_0 (g/cm^3)	S_v (m^2/g)	Average Pore Size (nm)
HN13	0.5	52.0	0.89	1.21	0.95	49.2	14
HN14	0.8	57.1	1.04	1.27	0.87	50.2	35.6
HN7	1	68.5	1.45	1.24	0.72	51.0	44.9

Table I-10 Experimental data of the q_v and q_w for the poly(HEMA-MMA) at various EGDMA molar concentration; HEMA/MMA=9.4ml/4.7ml; r_{oct}=1; T=25°C

EGDMA mol%	q_v	q_w
8	1.32±0.08	1.73±0.09
18	1.26±0.01	1.48±0.01
23	1.16±0.10	1.54±0.08

Table I-11 Experimental data of the q_v and q_w for the poly(HEMA-MMA) at various monomer ratios; [EGDMA]=23mol%; r_{oct}=1; T=25°C

r_H (ml/ml)	q_v	q_w
0.5	1.15±0.05	1.68±0.07
1	1.13±0.01	1.47±0.01
1.5	1.09±0.05	1.55±0.13
2	1.16±0.10	1.54±0.08

Table I-12 Experimental data of the q_v and q_w for the poly(HEMA-St) at various EGDMA molar concentration; HEMA/St=9.4ml/4.7ml; r_{oct}=1; T=25°C

EGDMA mol%	q_v	q_w
8	1.23±0.15	1.89±0.23
18	1.20±0.08	2.10±0.12
23	1.16±0.11	1.51±0.09

Table I-13 Experimental data of the q_v and q_w for the poly(HEMA-St) at various monomer ratios; [EGDMA]=23mol%; r_{oct}=1; T=25°C

r_H (ml/ml)	q_v	q_w
0.5	1.22±0.09	1.98±0.22
1	1.20	1.94±0.10
1.5	1.22	1.71±0.23
2	1.16±0.11	1.51±0.09

Table I-14 Experimental data of the q_v and q_w for the poly(HEMA-NVP) at various EGDMA molar concentration; HEMA/NVP=9.4ml/4.7ml; r_{oct}=1; T=25°C

EGDMA mol%	q_v	q_w
8	1.68±0.10	3.24±0.40
18	1.29±0.02	2.23±0.37
23	1.25±0.07	1.87±0.15

Table I-15 Experimental data of the q_v and q_w for the poly(HEMA-NVP) at various monomer ratios; [EGDMA]=23mol%; r_{oct}=1; T=25°C

r_H (ml/ml)	q_v	q_w
0.5	1.80±0.30	2.78±0.54
1	1.41±0.23	2.30±0.37
1.5	1.40±0.18	1.82±0.40
2	1.25±0.07	1.87±0.15

Appendix II

Derivation of Equation (5-7) and Equation (5-8)

According to the equation (5-2)

$$\Delta G_m = RT(n_1 \ln v_1 + n_2 \ln v_2 + n_3 \ln v_3 + n_1 v_2 \chi_{12} + n_2 v_3 \chi_{23} + n_1 v_3 \chi_{13}) \qquad \text{(II-1)}$$

For the network phase, differentiating the equation (II-1) with respect to n_1,

$$\frac{\Delta \mu_{1m}}{RT} = \ln v_1 + n_1 \frac{1}{v_1}(\frac{\partial v_1}{\partial n_1}) + \frac{\partial n_2}{\partial n_1} \ln v_2 + n_2 \frac{1}{v_2} \frac{\partial v_2}{\partial n_1} + \frac{\partial n_3}{\partial n_1} \ln v_3 + n_3 \frac{1}{v_3} \frac{\partial v_3}{\partial n_1} + v_2 \chi_{12} + n_1 \frac{\partial v_2}{\partial n_1} \chi_{12}$$
$$+ v_3 \chi_{13} + n_1 \frac{\partial v_3}{\partial n_1} \chi_{13} + \frac{\partial n_2}{\partial n_1} v_3 \chi_{23} + n_2 \frac{\partial v_3}{\partial n_1} \chi_{23} \qquad \text{(II-2)}$$

According to the definition of v_i,

$$v_1 = \frac{X_1 n_1}{X_1 n_1 + X_2 n_2 + X_3 n_3} \qquad \text{(II-3)}$$

$$v_2 = \frac{X_2 n_2}{X_1 n_1 + X_2 n_2 + X_3 n_3} \qquad \text{(II-4)}$$

$$v_3 = \frac{X_3 n_3}{X_1 n_1 + X_2 n_2 + X_3 n_3} \qquad \text{(II-5)}$$

where X_1, X_2, X_3 are the number of segments in the components 1, 2 and 3, respectively. Each segment occupies one lattice according to the Flory-Huggins theory (Flory, 1953). Therefore, for the pure solvent, it occupies one single lattice (X_1=1). Differentiating the equations (II-3)-(II-5) with respect to n_1 obtains,

$$\frac{\partial v_1}{\partial n_1} = \frac{v_1(v_2 + v_3)}{n_1} = \frac{v_1(1 - v_1)}{n_1} \qquad \text{(II-6)}$$

$$\frac{\partial v_2}{\partial n_1} = -\frac{v_1 v_2}{n_1} \qquad \text{(II-7)}$$

$$\frac{\partial v_1}{\partial n_1} = -\frac{v_1 v_3}{n_1} \qquad \text{(II-8)}$$

Substitution the equations (II-6)-(II-8) into the equation (II-2) and define,

$$y = \frac{X_3}{X_1} \qquad \text{(II-9)}$$

$$\chi_{23} = \chi_{23}\frac{X_1}{X_2} \qquad \text{(II-10)}$$

The equation (II-11) is obtained,

$$\frac{\Delta\mu_{1m}}{RT} = \ln v_1 + (1-v_1) - \frac{v_3}{y} + (v_2\chi_{12} + v_3\chi_{13})(1-v_1) - \chi_{23}v_2v_3 \qquad \text{(II-11)}$$

Differentiating the equation (5-3) with respect to n_1 and multiplying ($V_s \times X_2 \times n_2$) on the both sides obtain the equation (II-12) for the whole network phase,

$$\frac{\Delta\mu_{1el}}{RT} = \frac{1}{N}(v_2^{0\frac{2}{3}}v_2^{\frac{1}{3}} - \frac{v_2}{2}) \qquad \text{(II-12)}$$

Adding the equations (II-11) and (II-12) together obtains the chemical potential equation (II-13) with respect to n_1 in the network phase,

$$\frac{\Delta\mu_1}{RT} = \frac{1}{N}(v_2^{0\frac{2}{3}}v_2^{\frac{1}{3}} - \frac{v_2}{2}) + \ln v_1 + (1-v_1) - \frac{v_3}{y} + (v_2\chi_{12} + v_3\chi_{13})(1-v_1) - \chi_{23}v_2v_3 \qquad \text{(II-13)}$$

Similarly, the chemical potential with respect to n_1 in the network phase, the chemical potential with respect to n_3 in the separated phase and the chemical potential with respect to n_3 in the network phase are obtained as shown in the equations (II-14)-(II-16),

$$\frac{\Delta\mu_1'}{RT} = \ln v_1' + v_3'(1-1/y) + \chi_{13}v_3'^2 \qquad \text{(II-14)}$$

$$\frac{\Delta\mu_3}{yRT} = \frac{1}{N}(v_2^{0\frac{2}{3}}v_2^{\frac{1}{3}} - \frac{v_2}{2}) + \frac{1}{y}\ln v_3 + \frac{1}{y}(1-v_3) - v_1 + (\chi_{13}v_1 + \chi_{23}v_2)(1-v_3) - \chi_{12}v_1v_2 \qquad \text{(I-15)}$$

$$\frac{\Delta\mu_3'}{yRT} = \frac{1}{y}\ln v_3' - v_1'(1-1/y) + \chi_{13}v_1'^2 \qquad \text{(II-16)}$$

Finally, substitution the equations (II-13), (II-14), (II-15) and (II-16) into the equations (5-4) and (5-5) obtains the equations (5-7) and (5-8).

Appendix III

Derivation of Equation (5-11) and Equation (5-12)

1) Derivation of the Equation (5-11)

According to the definition of v_g, W_g, and $\bar{v}_p$,

$$v_g = \frac{V_{nw}}{V_{sys}} \qquad \text{(III-1)}$$

$$W_g = \frac{m_g}{m_g + m_s} \qquad \text{(III-2)}$$

$$\bar{v}_p = \frac{V_{sg}}{V_{sys}} \qquad \text{(III-3)}$$

where V_{nw} is the volume of the network phase in the whole systems, V_{sys} is the volume of the whole systems, V_{sg} is the volume of the polymers including sol polymers and gel polymers, m_g is the mass of gel polymers and m_s is the mass of the sol polymers. Since v_2 is the polymer fraction in the network phase, it can be calculated from the equations (III-1) through (III-3) assuming the densities of the gel polymers and the sol polymers are identical,

$$v_2 = \frac{(\bar{v}_p V_{sys})W_g}{V_{nw}} = \frac{\bar{v}_p W_g}{v_g} \qquad \text{(III-4)}$$

At the incipient of the phase separation, the equation (5-6) is given so that the equation (5-11) is obtained.

2) Derivation of the Equation (5-12)

Assume at a certain stage of the reaction,

$$V_{sg} = \frac{\alpha V_{mon} d_M}{d_p} \qquad \text{(III-5)}$$

$$V_{sys} = V_0 - \alpha V_{mon} + \alpha V_{mon} \frac{d_M}{d_p} \qquad \text{(III-6)}$$

where V_{mon} is the initial volume of monomers, V_0 is the initial volume of the whole system, α is the volume conversion, d_M is the density of the monomer mixtures and d_p is the density of the resultant polymers. Therefore, according to the definition of $\bar{v}_p$, substitution the equations (III-5) and (III-6)

into the equation (III-3), defining $1\text{-}d_M/d_p$ as the contract factor ε and V_{mon}/V_0 as v_2^{00}, and dividing V_{sg} and V_{sys} by V_0 obtains the equastion (5-12).

Appendix IV

Derivation of Equation (5-64) and Equation (5-65)

1) Derivation of the Equation (5-64)

At the gel point, every component is assumed in the sol, so the equation (IV-1) is given,

$$\frac{[\mu_1^g]}{Q_1^{g\bullet}} = \frac{[\mu_1^s]}{Q_{1,\varphi_s=1}^{s\bullet}} \qquad \text{(IV-1)}$$

According to the equations (5-58) and (5-59),

$$\frac{[\mu_1^s]}{Q_{1,\varphi_s=1}^{s\bullet}} = \frac{\overline{\varepsilon}^s}{2\overline{X}_{2,\varphi_s=1}^{s\bullet}} \qquad \text{(IV-2)}$$

At the gel point, $\overline{\varepsilon}^s = 1$, so that the equation (5-64) is figured out.

2) Derivation of the Equation (5-65)

According to the Flory (1953), the ratio of the crosslink densities in the gel and in the entire system is,

$$\frac{\rho^g}{\overline{\rho}} = 1 + W_s \qquad \text{(IV-3)}$$

Also, the ratio of the crosslink densities in the gel and in the entire system can be derived from the kinetic point of view (Okay, 1994),

$$\frac{\rho^g}{\overline{\rho}} = \frac{[\mu^g]}{[\mu]W_g} \qquad \text{(IV-4)}$$

Therefore,

$$\frac{[\mu^g]}{Q_1^{g\bullet}} = \frac{[\mu^g]}{W_g Q_{1,\varphi_s=1}^{s\bullet}} = \frac{[\mu]W_g(1+W_s)}{W_g Q_{1,\varphi_s=1}^{s\bullet}} = \frac{[\mu](1+W_s)}{Q_{1,\varphi_s=1}^{s\bullet}} \qquad \text{(IV-5)}$$

Appendix V

Simulation Parameters for the Porous Poly(HEMA-NVP) Particles

Table V-1 Kinetic Constants and Parameters for the Porous poly(HEMA-NVP) Particle Synthesis at 70°C Using AIBN as an Initiator (1-HEMA; 2-NVP; 3-EGDMA)

Constants and Parameters	References
f=0.59	Li et al, 1989
$k_d(s^{-1})=1.95^{19}\exp(-1.91\times10^4/T)$	Ajzenberg et al, 2001
k_{p1}=1000 L/(mol·s)	Goodner et al., 1997
k_{p2}=15 L/(mol·s)	Estimated from reactivity ratios
k_{p3}=8073 L/(mol·s)	Estimated from reactivity ratios
$\overline{r}_{43}$ =0.1	Okay, 1999
$k_{td}^0=1.01\times10^7$ L/(mol·s)	Li et al, 1989 (2)
$k_{tc}^0=1.06\times10^7$ L/(mol·s)	Li et al, 1989 (2)
k_{cyc}=0.3	Okay, 1999
r_{12}=3.07	Ahmad et al, 2004
r_{21}=0.045	Ahmad et al, 2004
r_{13}=0.811	Ajzenberg et al, 2001
r_{31}=6.548	Ajzenberg et al, 2001
d_1=1.073 g/ml	
d_2=1.04 g/ml	
d3=1.051 g/ml	
dp, g/ml	Obtained by measurements
$\delta_1=23.2$ (Mpa)$^{1/2}$	Okay, 2000
$\delta_2=23$ (Mpa)$^{1/2}$	Brandrup et al., 1999
$\delta_3=18.2$ (Mpa)$^{1/2}$	Okay, 2000
$\delta_{oct}=20.9$ (Mpa)$^{1/2}$	Brandrup et al., 1999
$\delta_{PHEMA}=29.7$ (Mpa)$^{1/2}$	Okay, 2000
$\delta_{PNVP}=28.2$ (Mpa)$^{1/2}$	Barton, 1983
$\delta_{PEGDMA}=19.2$ (Mpa)$^{1/2}$	Okay, 2000
M_{w1}=130.14 g/mol	
M_{w2}=111.14 g/mol	
M_{w3}=198.22 g/mol	
A	9

The solubility parameter of a polymer could be estimated from the cohesive energy (-U) and the molar volume (V) of each group using the equation (IV-1) (Barton, 1983).

$$\delta = \left(\frac{\sum_{i=1}^{n} (-jU)}{\sum_{i}^{n} jV} \right)^{\frac{1}{2}} \qquad \text{(V-1)}$$

Where δ ($Mpa^{1/2}$) is the solubility parameter, and n is the number of different individual groups, and j is the number of one group. The available groups of PNVP and their cohesive energy and molar volume are shown in Table V-2. The calculated solubility parameter is shown in Table V-1.

Table V-2 Group Molar Cohesive Energies and Molar Volumes in Poly(vinyl pyrrolidone)

Groups	Numbers	-U/kJ mol-1	V/cm^3mol-1
-CH2-	3	4.94	16.1
>C=	1	4.31	-5.5
-CO-	1	21.4	22.3
-N<	1	4.2	-9.0

Bibliography

Ahmad, B.; Bashir, S.; Nisa, S.; Huglin, M. G. *Turk. J. Chem.* 28, 279-285, 2004.

Ahmad, H.; Miah, M. A. J.; Rahman, M. M. *Coll. Polym. Sci.* 281 (10), 988-992, 2003.

Ajzenberg, N.; Ricard, A. *J. Appl. Polym. Sci.* 80, 1220-1228, 2001.

Albright, R. L. Porous polymers as an anchor for catalysis. *React. Polym*., 4, 155-174, 1986.

Alfrey, T. and Goldfinger, G. *J. Chem. Phys.* 12, 205, 1944.

Alfrey, T. and Goldfinger, G. *J. Chem. Phys.* 14, 115, 1946.

Alfrey, T.; Gurnee, E. T.; Lloyd, W. G. *J. Polym. Sci.* C12, 249, 1966

Almog, Y.; Reich, S.; Levy, M. *Brit. Polym. J.* 14, 131-137, 1982.

Arrua, R. D.; Serrano, D.; Pastrana, G.; Strumia, M.; Igarzabal, C. I. A. *J. Polym. Sci. Part A: Polym. Chem*. 44, 6616-6623, 2006.

Bajpai, A. K.; Shrivastava, M. *J. Appl. Polym. Sci.* 85, 1419-1428, 2002.

Barcellos, I. O.; Pires, A. T. N.; Katime, I. *Polym. Int.* 49, 825-830, 2000.

Barton, A. F. M. *Handbook of Solubility Parameters and Other Cohesion Parameters*, CRC Press Inc., Boca Raton, Florida, 1983.

Bennett, D. J.; Burford, R. P.; Davis, T. P.; Tilley, H. J. *Polym. Int.* 36, 219-226, 1995.

Benson, J. R. Highly porous polymers. American Laboratory, 44-52, May, 2003.

Beranova, H.; Dusek, K. *Collection Czech. Chem. Commun.* 34, 2932, 1969.

Bhawal, S.; Reddy, H.; Murthy, R. S. R.; Devi, S. *J. Appl. Polym. Sci.*, 92, 402-409, 2004.

Bodhibukkana, C.; Srichana, T.; Kaewnopparat, S.; Tangthong, N.; Bouking, P.; Martin, G. P.; Suedee, R. *J. Control. Release* 113, 43-56, 2006.

Brandrup, J.; Immergut, E. H.; Grulke, E. A. Polymer Handbook, 4th ed. John Wiley & Sons, New York, Chapter 7, 1999.

Brannon-Peppas, L.; Harland, R. S. Absorbent Polymer Technology, Edited by Brannon-Peppas, L. and Harland, R. S., Elsevier Science Publishing Company Inc., New York, p45-66, 1990.

Brar, A. S.; Hooda, S.; Goyal, A. K. Ind. *J. Chem. Section A: Inor. Bio-Inor. Phys.Theo. Analy. Chem.* 45(9), 1981-1987, 2006.

Brazel, C. S.; Peppas, N. A. *Polymer* 40, 3383-3398, 1999.

Brown, J. F.; Krajnc, P.; Cameron, N. R. *Ind. Eng. Chem. Res.* 44, 8565-8572, 2005.

Buera, M. P.; Levi, G.; Karel, M. *Biotechnol. Prog.* 8, 144-148, 1992.

Castner, D. G.; Ratner, B. D.; Grainger, D. W.; Kim, S. W.; Okano, T.; Suzuki, K.; Briggs, D.; Nakahama, S. *J. Biomater. Sci. Polym. Ed.* 3(6), 463-480, 1992.

Chen, Z.; Pruess, J.; Flechtner, U.; Warnecke, H. *Chem. Eng. Technol.* 25, 1115-1119, 2002.

Cheng, C. M., Micale, F. J., Vanderhoff, J. W. and EI-Aasser, M. S. *J. Polym. Sci., Part A: Polym. Chem.* 30, 235-244, 1992.

Chew, C. H.; Li, T. D.; Gan, L. H.; Quek, C. H.; Gan, L. M. *Langmuir* 14, 6068-6076, 1998.

Chiellini, F.; Petrucci, F.; Ranucci, E.; Solaro, R. J. *J. Appl. Polym. Sci*. 85, 2729-2741, 2002.

Chirila, T. V. *Biomaterials* 22, 3311-3317, 2001.

Chirila, T. V.; Constable, I. J.; Crawford, G. J.; Vi-Jayasekaran, S.; Thompson, D. E.; Chen, Y. C.; Fletcher, W. A.; Griffin, B. J. *Biomaterials* 14, 26-38, 1993.

Choi, J.; Kwak, S. Y.; Kang, S.; Lee, S. S.; Park, M.; Lim, S.; Kim, J.; Choe, C. R.; Hong, S. I. *J. Polym. Sci., Part A: Polym. Chem.* 40, 4368-4377, 2002.

Choi, S.; Christensen, M. B.; Fredin, N.; Pitt, W. G. *J. Biomater. Appl.* 20, 123-135, 2005.

Cizravi, J. C.; Tay, T. Y.; Pon, E. C. *J. Appl. Polym. Sci.* 75, 239-246, 2000.

Clayton, A. B.; Chirila, T. V.; Lou, X. *Polym. Int.*, 44, 201-207, 1997.

Coviello, T.; Grassi, M.; Lapasin, R.; Marino, A.; Alhaique, F. *Biomaterials* 24, 2789-2798, 2003.

Dalton, P. D.; Flynn, L.; Shoichet, M. S. *Biomaterials*, 23, 3843-3851, 2002.

Dowding, P. J., Goodwin, J. W. and Vincent, B. *Colloids and Surfaces A: Physicochemical and Engineering Aspects* 145, 263-270, 1998.

Dowding, P. J. and Vincent, B. *Colloids and Surfaces A: Physicochemical and Engineering Aspects* 161, 259-269, 2000.

Downey, J. S.; McIsaac, G.; Frank, R. S.; Stover, H. D. H. *Macromolecules* 34, 4534-4541, 2001.

Dušek, K. *Polymer Letters* 3, 209-212, 1965.

Dušek, K. *J. Polym. Sci.: Part C* 16, 1289-1299, 1967.

Dušek K, Polymer networks, structure and mechanical properties, edited by Chompff AJ and Newman S, Plenum Press, New York, p245-260, 1970.

Dušek, K.; Sedláček, B. *Euro Polym J* 7, 1275-1285, 1971.

Dušek, K. Developments in Polymerization, Vol 3, Edited by Haward, R. N., Applied Science, London, p143, 1982.

Dziubla, T. D.; Torjman, M. C.; Joseph, J. I.; Murphy-Tatum, M.; Lowman, A. M. *Biomaterials* 22, 2893-2899, 2001.

El-Din, H. M. M. N.; Maziad, N. A.; El-Naggar, A. W. M. *J. Appl. Polym. Sci.* 91, 3274-3280, 2004.

Elliott, J. E.; Bowman, C. N. *Macromolecules* 32, 8621-8628, 1999.

Elliott, J. E.; Bowman, C. N. *Chem. Eng. Sci.* 56, 3173-3184, 2001.

Fan, L. T.; Singh, S. K. Controlled Release-A Quantitative Treatment, Springer-Verlag, New York, pp.110, 1989.

Flory, P. J. *J. Am. Chem. Soc.* 63, 3083, 1941.

Flory, P. J. *J. Am. Chem. Soc.* 63, 3091, 1941.

Flory, P. J. *J. Am. Chem. Soc.* 63, 3096, 1941.

Flory, P. J.; Rehner, J. *J. Chem. Phys.* 11, 521, 1943.

Flory, P. J. Principles of Polymer Chemistry, Cornell University Press, Ithaca, NY, Chapter 9, 1953.

Franson, N. M.; Peppas, N. A. *J. Appl. Polym. Sci.* 28, 1299, 1983.

Galina, H.; Kolarz, B. N. *Polym. Bull.* 2, 235, 1980.

Gan, L. M.; Chieng, T. H.; Chew, C. H.; Ng, S. C. *Langmuir* 10, 4022-4026, 1994.

Gao, C. Y.; Mhowald, H.; Shen, J. C. *Polymer* 46, 4088-4097, 2005.

Gates, G.; Harmon, J. P. Polymer 44, 215-222, 2003.

Goh, E. C. C.; Stőver, D.H. *Macromolecules* 35, 9983-9989, 2002.

Gomez, C. G.; Alvarez, C. I.; Strumia, M. C.; Rivas, B. L.; Reyes, P. *J. Appl. Polym. Sci.* 79, 920-927, 2000.

Gomez, C. G.; Alvarez, C. I.; Strumia, M. C. *Polymer* 45, 6189-6194, 2004.

Goodner, M. D.; Lee, H. R.; Bowman, C. N. *Ind. Eng. Chem. Res.* 36, 1247-1252, 1997.

Hild, G.; Rempp, P. *Pure Appl. Chem.* 53, 1541, 1981.

Hild, G.; Okasha, R.; Rempp, P. *Makromol. Chem.* 186, 407, 1985.

Hill, D. J. T.; Lim, M. C. H.; Whittaker, A. K. *Polym. Int.* 48, 1046-1052, 1999.

Hocking, M. B.; Klimchuk, K. A. *J. Polym. Sci.: Part A: Polym. Chem.* 34, 2481-2497, 1996.

Horak, D.; Lednicky, F.; Bleha, M. *Polymer* 37, 4243-4249, 1996.

Horak, D.; Lednichy, F.; Rehak, V.; Svec, F. *J. Appl. Polym. Sci.*, 49, 2041-2050, 1993.

Horak, D.; Benes, M. *J. React. Func. Polym.* 45, 189-195, 2000.

Horak, D.; Svec, F.; Kalal, J.; Gumargalieve, K. Z.; Adamyan, A. A.; Skuba, N.; Titova, M. I.; Trostenyuk, N. V. *Biomaterials* 7, 188-192, 1986.

Howdle, S. M.; Jerabek, K.; Leocorbo, V.; Marr, P. C.; Sherrington, D. C. *Polymer* 41, 7273-7277, 2000.

Hradil, J.; Plichta, Z.; Benes, M. J. *React. Funct. Polym.* 44, 259-272, 2000.

Hsu, C. P.; Lee, L. J. *Polymer* 34, 4496-4505, 1993.

Ishizaki, K.; Komarneni, S.; Nanko, M. Porous Materials-Process Technology and Applications, Kluwer Academic Publishers, Dordrecht, Netherlands, pp204, 1998.

Jackson, S. H. D.; Wiffen, J. K.; Johnston, A.; Peverel-Cooper, C. A. *Eur. J. Clin. Pharmacol.* 29, 177-179, 1985.

Jose, A. J.; Ogawa, S.; Bradley, M. *Polymer* 46, 2880-2888, 2005.

Katime, I.; Novoa, R.; Zuluaga, F. *Eur. Polym. J.* 37, 1465-1471, 2001.

Kiefer, J.; Hedrick, J. L.; Hilborn, J. G. *Adv. Polym. Sci.* 147, 163-247, 1999.

Kim, S. W.; Bae, Y. H.; Okano, T. *Pharm. Res.* 9, 283-290, 1992.

Korsmeyer, R. W.; Peppas, N. A. *J. Contr. Rel.* 1, 89-98, 1984.

Korsmeyer, R. W.; Peppas, N. A. *J. Polym. Sci. Polym. Phys. Ed.* 24, 409-434, 1986.

Krajnc, P.; Leber, N.; Brown, J. F.; Cameron, N. R. *React. Funct. Polym*. 66, 81-91, 2006.

Kuipers, N. J. M.; Beenackers, A. A. C. M. *Chem. Eng. Sci.* 48, 2957-2971, 1993.

Kumar, M. N. V. R.; Kumar, N.; Domb, A. J.; Arora, M. Adv. Polym. Sci. 160, 45-117, 2002.

Kwok, A. Y.; Neo, S. A.; Qiao, G. G.; Solomon, D. H. *J. Appl. Polym. Sci.* 98, 1462-1468, 2005.

Lai, Y. *J. Appl. Polym. Sci.* 66, 1475-1484, 1997.

Lasky, R. C.; Kramer, E. J.; Hui, C. Y. *Polymer* 29, 1131-1136, 1988.

Lebduska, J.; Snuparek, J. J.; Kaspar, K. *J. Polym. Sci., Part A: Polym. Chem. Ed.* 24, 777, 1986.

Lee, P. I.; Kim, C. J. *J. Membrane Sci.* 65, 77-92, 1992.

Li, D.; Zhu, S.; Hamielec, A. E. *Polymer* 34 (7), 1383-1387, 1993.

Li, H.; Ng, T.Y.; Yew, Y. K.; Lam, K. Y. *Biomacro*. 6, 109-120, 2005.

Li, W. H.; Hamielec, A. E., Crowe, C. M. *Polymer* 30, 1513-1517, 1989 (a).

Li, W. H.; Hamielec, A. E., Crowe, C. M. *Polymer* 30, 1518-1523, 1989 (b).

Li, Y. et al. Hydrogels and methods of making and using the same. U.S. Patent 6,268,405, 2001.

Liu, J.; Chung, Y.; Liu, H. *Die Ang. Makromol. Chem.* 234, 133-143, 1996.

Liu, J., Gan, L. M., Chew, C. H., Teo, W. K. and Gan, L. H. *Langmuir* 13, 6421-6426, 1997.

Liu, J.; Lin, S.; Li, L.; Liu, E. *Inter. J. Pharm.* 298 117-125, 2005.

Liu, Q.; Hedberg, E. L.; Liu, Z.; Bahulekar, R.; Meszlenyi, R. K.; Mikos, A. G. *Biomaterials* 21, 2163-2169, 2000.

Luprano, V. A. M.; Montagna, G.; Maffezzoli, A. IEEE Trans. Ultra. Ferro. Frequ. Contr. 43, 948-955, 1996.

Lustig, S. R.; Rochen, U.; Peppas, N. A. *Symp. Contr. Rel. Bioact. Mater.* 13, 210, 1986.

Mabilleau, G.; Stancu, I. C.; Honore, T.; Legeay, G.; Cincu, C.; Basle, M. F.; Chappard, D. *J. Biomed. Mater. Res.*, 77A, 35-42, 2006.

Macintyre, F. S.; Sherrington, D. C.; Tetley, L. *Macromolecules* 39, 5381-5384, 2006.

Marin Saez, R.; Llobat Estelles, M.; San Martin Ciges, M. D.; Mauri Aucejo, A. R. *Analy. Lett.* 26, 641-655, 1993.

Mark, H. F.; Bikales, N. M.; Overberger, C. G.; Menges, G. *Encyclopedia of Polymer Science and Engineering*, John Wiley and Sons, New York, 1989.

Martin, P.; Petr, L.; Jindrich, F.; Jiri, V.; Miroslav, S.; Jiri, M.; Eva, S. Collect. Czech. Chem. Commun., 68, 812-822, 2003.

Mayo, F. R.; Lewis, F. M. *J. Am. Chem. Soc.* 66, 1594, 1944.

Menner, A.; Bismarck, A. *Macromol. Sym.* 242, 19-24, 2006.

Migliaresi, C.; Nicodemo, L.; Nicolais, L.; Passerini, P. *Polymer* 25, 686-689, 1984.

Migliaresi, C.; Nicodemo, L.; Nicolais, L.; Passerini, P. Stol, M.; Hrouz, J.; Cefelin, P. *J. Biomed. Mater. Res.* 18, 137-146, 1984.

Mikos, A. G.; Takoudis, C. G.; Peppas, N. A. *Macromolecules* 19, 2174-2182, 1986.

Mikos, A. G.; Takoudis, C. G.; Peppas, N. A. *Polymer* 28, 998-1004, 1987.

Ming, W.; Jones, F. N.; Fu, S. *Polym. Bull.* 40, 749-756, 1998.

Montheard, J.; Chatzopoulos, M.; Chappard, D. *J. M. S.-Rev. Macromol. Chem. Phys.*, C32 (1), 1-34, 1992.

Mueller, K. F.; Heiber, S. J.; Plankl, W. L. Process for preparing hydrogels as spherical beads of large size. U. S. Patent 4, 224, 427, 1978.

Murphy, S. M.; Hamilton, C. J.; Tighe, B. J. *Polymer* 29, 1887-1893, 1988.

Naghash, H. J.; Okay, O; Yildirim, H. *J. Appl. Polym. Sci.* 56, 477-483, 1995.

Ng, L. T.; Swami, S. *Carbohydrate Polymers* 60, 523-528, 2005.

Nyhus, A. K.; Hagen, S.; Berge, A. *J. Appl. Polym. Sci.* 76, 152-169, 2000.

Odian, G. Principles of Polymerization, 4th Ed, Wiely-Interscience, Chapter 3, 2004.

Olah, L.; Filipczak, K.; Jaegermann, Z.; Czigany, T.; Borbas, L.; Sosnawski, S.; Uianski, P.; Rosiak, J. M. *Polym. Adv. Tech.* 17, 889-897, 2006.

Okay, O.; Balkas, T. I. *J. Appl. Polym. Sci.* 31, 1785-1795, 1986.

Okay, O.; Gürün, Ç. *J. Appl. Polym. Sci.* 46, 401-410, 1992.

Okay, O.; Soner, E.; Gungor, A.; Balkas, T. I. *J. Appl. Polym. Sci.* 30, 2065-2074, 1985.

Okay, O. *J. Appl. Polym. Sci.* 32, 5533, 1986.

Okay, O. *Angew. Makromol. Chem.* 157, 1, 1988.

Okay, O. *Polymer* 35, 796-807, 1994.

Okay, O. *Polymer* 35, 2613-2618, 1994.

Okay, O. *Polymer* 40, 4117-4129, 1999.

Okay, O. *J. Appl. Polym. Sci.* 74, 2181-2195, 1999.

Okay, O. *Prog. Polym. Sci.* 25, 711-779, 2000.

Ozer, F.; Beskardes, M. O.; Zareie, H.; Piskin, E. *J. Appl. Polym. Sci.* 82, 237-242, 2001.

Park, K. et al. Hydrogel composites and superporous hydrogel composites having fast swelling, high mechanical strength, and superabsorbent properties. U. S. Patent 6,271,278, 2001.

Peniche, C.; Zaldivar, D.; Gallardo, A.; Roman, J. S. *J. Appl. Polym. Sci.* 54, 959-968, 1994.

Peppas, N. A.; Bures, P.; Leobandung, W. L.; Ichikawa, H. *Euro. J. Pharm. Biopharm.* 50, 27-46, 2000.

Peppas, N. A.; Khare, A. R. *Adv. Drug. Deliv. Rev.* 11, 1, 1993.

Perera, D. I.; Shanks, R. A. *Polym. Int.* 39, 121-127, 1996.

Perova, T. S.; Vij, J. K.; Xu, H. *Colloid. Polym. Sci.* 275, 323-332, 1997.

Portsmouth, R. L.; Gladden, L. F. *Chem. Eng. Sci.* 46, 3023-3036, 1991.

Rabelo, D.; Coutinho, F. M. B. *Polym. Bull.* 33, 487-491, 1994.

Reppe, W.; Krzikalla, H.; Dornheim, O.; Ranerbler, R. *U. S. Patent 2317804*, 1943.

Reverchon, E.; Cardea, S. Rappo, E. S. *J. Membr. Sci.* 273, 97-105, 2006.

Sanchez-Chaves, M.; Martinez, G.; Madruga, E. L. *J. Polym. Sci.: Part A: Polym. Chem.* 37, 2941-2948, 1999.

Sang, E. S.; Sunhye, Y.; Myung-Jong, J.; Yoon, C. H. *Colloid Polym. Sci.* 283, 41-48, 2004.

Sanghi, P. G.; Pokhriyal, N. K.; Devi, S. *Polym. Int.* 51, 721-728, 2002.

Sannino, A.; Netti, P. A.; Madaghiele, M.; Coccoli, V.; Luciani, A.; Maffezzoli, A.; Nicolais, L. *J. Biomed. Mater. Res, Part A* 79A, 229-236, 2006.

Sasthav, M.; Raj, W. R. P.; Cheung, H. M. *J. Colloid. Interface Sci.* 152, 376-385, 1992.

Schoonbroad, H. A. S.; Aerdts, A. M.; Germar, A. L.; Der Velden, G. P. M. *Macromolecules* 28, 5518, 1995.

Scranton, A. B.; Peppas, N. A. *J. Polym. Sci., Polym. Chem. Ed.*, 28, 39-57, 1990.

Scranton, A. B.; Mikos, A. G.; Scranton, L. C.; Peppas, N. A. *J. Appl. Polym. Sci.* 40, 997-1004, 1990.

Sederel, W. L.; De Jong, G. J. *J. Appl. Polym. Sci.* 17, 2835-2846, 1973.

Seidl, J.; Malinsky, J.; Dusek, K.; Heitz, W. *Adv. Polym. Sci.* 5, 113-213, 1967.

Sergeyeva, T. A.; Brovko, O. O.; Piletska, E. V.; Piletsky, S. A.; Goncharova, L. A.; Karabanova, L. V.; Sergeyeva, L. M.; El'skaya, A. V. *Analy. Chim. ACTA* 582, 311-319, 2007.

Shapiro, L. and Cohen, S. *Biomaterials* 8, 583-590, 1997.

Shen, M. C.; Strong, J. D.; Matusik, F. J. *J. Macromol. Sci.* B1, 15-27, 1967.

Shen, S.; El-Aasser, M. S.; Dimonie, V. L.; Vanderhoff, J. W.; Sudol, E. D. *J. Polym. Sci. Part A: Polym. Chem.* 29, 557, 1991.

Sherrington, D. C. *Makromol. Chem. Macromol. Symp.* 70/71, 303-314, 1993.

Sherrington, D. C. *Chem. Commun.* 2275-2286, 1998.

Shieh, L. Y.; Peppas, N. A. *J. Appl. Polym. Sci.* 42, 1579-1587, 1991.

Shozo, M.; Wataru, K.; David, A. *J. Control. Release* 67, 275-280, 2000.

Siepmann, J.; Peppas, N. A. Adv. *Drug Deliv. Rev.* 48, 139, 2001

Sivakumar, M.; Rao, K. P. *J. Appl. Polym. Sci.* 83, 3045-3054, 2002.

Stefanec, D.; Krajnc, P. *React. Funct. Polym*. 65, 37-45, 2005.

Stockmayer, W. H. *J. Chem. Phys.* 11, 45, 1943.

Stockmayer, W. H. *J. Chem. Phys.* 12, 125, 1944.

Sun, Y.; Huang, J.; Lin, F.; Lai, J. *Biomaterials* 18, 527-533, 1997.

Svec, F.; Rechet, J. M. J. *Macromolecules* 28, 7580-7582, 1995.

Szaraz, I.; Forsling, W. *Polymer* 41, 4831-4839, 2000.

Tefera, N.; Weickert, G.; Bloodworth, R.; Schweer, J. *Macromol. Chem. Phys.*, 195, 3067-3085, 1994

Tefera, N.; Weickert, G.; Westerterp, K. R. *J. Appl. Polym. Sci.* 63, 1649-1661, 1997.

Tobita, H.; Hamielec, A. E. *Macromolecules* 22, 3098-3105, 1989.

Tsai, C.; Lee, S. *J. Mater. Res.* 19, 3359-3363, 2004.

Tumturk, H.; Aksoy, S.; Hasirci, N. *Food Chem.* 68, 259-266, 2000.

Tuncel, A.; Tuncel, M.; Cicek, H.; Fidanboy, O. *Polym. Int.* 51(1), 75-84, 2002.

Turner, D. T. *Polymer* 28, 293, 1987.

Turner, D. T.; Abell, A. K. Polymer, 28, 297-302, 1987.

Turner, D. T.; Schwartz, A.; Graper, J.; Sugg, H.; Williams, J. L. *Polymer* 27, 1619-1625, 1986.

Uzun, L.; Odabasi, M.; Arica, Y.; Denizli, A. *Separ. Sci. Tech.* 39 (10), 2401-2418, 2004.

Vianna-Soares, C. D.; Kim, C. J.; Borenstein, M. R. *J. Poro. Mater.* 10, 123-130, 2003.

Vianna-Soares, C. D.; Kim, C. J.; Borenstein, M. R. *Mater.Res.* 8(1), 15-21, 2005.

Viklund, C.; Nordstrom, A.; Irgum, K.; Svec, F.; Frechet, J. M. J. *Macromolecules* 34, 4361-4369, 2001.

Walling, C.; Briggs, E. R. *J. Am. Chem. Soc.* 67, 1774, 1945.

Ward, J. H.; Peppas, N. A. *Macromolecules* 33, 5137-5142, 2000.

Wichterle, O. *Nature*, 185, 117-118, 1961.

Wieczorek, P. P.; Kolarz, B. N.; Galina, H. *Angew. Makromol. Chem.* 126, 39, 1984.

Wood, C. D.; Cooper, A. I. *Macromolecules* 34, 5-8, 2001.

Woodhouse, J. C. Esters of methacrylic acid, US Patent 2129722, 1938.

Wu, S.; Li, H.; Chen, J. P. *J. Macro. Sci. Part C: Polym. Rev.* 44, 113-130, 2004.

Yan, X. H.; Liu, G. J.; Dickey, M.; Willson, C. G. *Polymer* 45, 8469-8474, 2004.

Zhang, C. F.; Zhu, B. K.; Ji, G. L.; Xu, Y. Y. *J. Appl. Polym. Sci.* 103, 1632-1639, 2007.